The Occurrence, Impacts and Dynamics of Debris Flows in Brazil

Dissertation

der Mathematisch-Naturwissenschaftlichen Fakultät

der Eberhard Karls Universität Tübingen

zur Erlangung des Grades eines

Doktors der Naturwissenschaften

(Dr. rer. nat.)

vorgelegt von

Victor Carvalho Cabral

aus Bodoquena, Brasilien

Tübingen

2023

Gedruckt mit Genehmigung der Mathematisch-Naturwissenschaftlichen Fakultät der Eberhard Karls Universität Tübingen.

Tag der mündlichen Qualifikation:	17.04.2023
Dekan:	Prof. Dr. Thilo Stehle
1. Berichterstatter/-in:	Prof. Dr. Todd Alan Ehlers
2. Berichterstatter/-in:	Prof. Dr. Tiago Damas Martins

Acknowledgments

This study was financed in part by the Coordenação de Aperfeiçoamento de Pessoal de Nível Superior - Brasil (CAPES) - Finance Code 001.

First of all, I would like to thank my supervisors Christiane Zarfl and Fábio Reis for their support, advices and friendship during the development of the research. They allowed me to follow my ideas and provided all the resources needed to making the thesis possible. I am thankful to Fernando Mazzo D'Affonseca, for supporting my first research visit in the University of Tübingen, and to Prof. Peter Grathwohl, for supervising me during this time.

I am also thankful to all my friends and colleagues in Brazil and Germany, who collaborated with me and encouraged me during the PhD. I am especially thankful to Ran, Ana, Gaëlle, Clarissa, Timm, Anh and Marco, who made my time in Germany very special and joyful. In Brazil, I am especially thankful to Vinicius and Claudia, for the scientific exchanges that were really insightful, and to Raquel, André, Vanessa, Thamiris, Michele and Gabriela, who made these four years lighter and more fun.

I would like to express my deepest gratitude to my parents, Sirlei and Carlos, who encouraged me during my academic career, as well as my sister, Carla. Finally, I would like to thank my partner, Rodrigo, for the friendship and all the support.

Abstract

Among the landslide types, debris flows represent a greater hazard to society due to their high destruction potential. In Brazil, debris-flow studies are still incipient when compared to other hydrogeomorphic processes and a good understanding of their dynamics is fundamental to supporting hazard and risk assessment studies. In particular, determining the spatialization of events and the extent of the impacts that the phenomenon represents in the country is crucial to supporting targeted and more in-depth studies. In this context, the main objectives of this thesis are to assess the societal impact of debris flows in Brazil and to propose a methodology that aims at reducing the potential damage that future events can cause in susceptible regions. A detailed post-event characterization of a debris-flow event is also conducted, as it is a fundamental step to understanding the phenomenon's dynamics and can further support the proposal of the hazard assessment methodology. To determine the societal impact of debris flows, a catalogue of events that have caused fatalities and/or economic losses between 1920 and 2021 was created, which supported the debris-flow Mortality Rate (MR) calculation and the application of the so-called F-N Curves (Frequency of events vs. Number of Fatalities). In total, 45 debris-flow events were documented in the considered period, having caused more than 5,773 fatalities and 5.4 billion USD in economic losses. The city of Cubatão (state of São Paulo) shows the highest number of recorded events in the considered period (9), consolidating the status as the most debris-flow prone region in the country. A multi-step hazard assessment is, then, proposed using Cubatão as the test-site, based on the combination of Logistic Regression (LR) analysis, numerical simulation and rainfall back-analysis. The LR results highlight that rainfall is the main influencing factor in debris-flow initiation in the region and indicate the catchments more susceptible to the phenomenon. The simulation results, performed in the catchments indicated by the LR, show that the average runout distance in the region is 470 m, with an average peak flow height of 5 m and a peak velocity of 23 m s^{-1}, according to the calibration based on two past debris-flow events. These results are comparable to the debris-flow event of February 2017 that occurred in the Pedra Branca catchment (Guaratuba, state of Paraná), in which a detailed post-event geomorphological characterization was conducted to estimate the event's magnitude. The Guaratuba event was of a large-sized stony debris flow, with a total magnitude of 120,195 m^3, a peak flow heigh of 7 m and a peak velocity of 26.5 m s^{-1}. Debris-flow events both in Cubatão and Guaratuba are generally triggered by short duration (<48 h), high-intensity (>200 mm) precipitation, with return periods that vary from 3 to 15 years. Five levels of hazard (very low to very high) are, then, proposed

in our hazard assessment method, based mainly on the 48-h accumulated rainfall, flow properties (height, velocity) and the spatial analysis of the elements (infrastructures, houses, etc.) at hazard. In Cubatão, industrial and residential areas in the projected debris-flow route generally exhibit the highest overall hazard levels, as many were developed in the depositional area of the phenomenon and near fluvial courses, where associated floods and flash floods may occur. As pointed out by recent studies, an increase in the frequency of extreme precipitation events is projected in the Serra do Mar region and when the general short return period of the debris-flow triggering rainfall is considered (< 20 years), large magnitude (>10^5 m^3) events are likely to occur in the next decade in the portions of the mountain range located in the states of São Paulo and Paraná. This thesis, therefore, is a contribution to better understanding the dynamics of debris flows in Brazil and is a step towards the prevention of future disasters.

Keywords: Landslides, Geological hazards, Multivariate statistics, Natural disasters.

Zusammenfassung

Unter den Rutschungsarten stellen Murgänge aufgrund ihres hohen Zerstörungspotentials eine größere Gefahr für die Gesellschaft dar. In Brasilien sind Murgangstudien im Vergleich zu anderen hydrogeomorphen Prozessen noch am Anfang und ein gutes Verständnis ihrer Dynamik ist essentiell für die Erstellung von Gefahren- und Risikobewertungsstudien. Insbesondere ist die Bestimmung des Ausmaßes der Auswirkungen, die das Phänomen in einer Region oder einem Land darstellt, von wesentlicher Bedeutungfür gezielte und eingehendere Studien. In diesem Zusammenhang besteht das Hauptziel dieser Arbeit darin, die gesellschaftlichen Auswirkungen von Murgängen in Brasilien zu bewerten und eine Methodik vorzuschlagen, die darauf abzielt, den potenziellen Schaden zu verringern, den zukünftige Ereignisse in anfälligen Regionen verursachen können. Eine detaillierte Nachuntersuchung eines Murgangereignisses wird ebenfalls durchgeführt, da dies ein grundlegender Schritt zum Verständnis der Dynamik des Phänomens ist und den Vorschlag der Gefahrenbewertungsmethodik weiter unterstützen kann. Um die gesellschaftlichen Auswirkungen von Murgängen zu bestimmen, wurde ein Katalog von Ereignissen erstellt, die zwischen 1920 und 2021 Todesopfer und/oder wirtschaftliche Schäden verursacht haben, was die Berechnung der Murgangmortalitätsrate (MR) und die Anwendung der sogenannten F-N unterstützten Kurven (Häufigkeit von Ereignissen vs. Anzahl Todesfälle) ermöglicht. Insgesamt wurden im betrachteten Zeitraum 45 Murgangereignisse dokumentiert, die mehr als 5.773 Todesopfer und 5,4 Milliarden US-Dollar an wirtschaftlichen Schäden verursachten. Die Stadt Cubatão (Bundesstaat São Paulo) weist die meisten Ereignisse auf und festigt damit ihren Status als die am stärksten von Murgängen bedrohte Region des Landes. Daher wird eine mehrstufige Gefährdungsbeurteilung vorgeschlagen und am Beispiel von Cubatão getestet, basierend auf einer Kombination von logistischer Regressionsanalyse (LR), numerischer Simulation und Niederschlagsrückanalyse. Die LR-Ergebnisse verdeutlichen, dass Niederschlag der Haupteinflussfaktor bei der Entstehung von Murgängen in der Region ist und zeigen die Einzugsgebiete, die für das Phänomen in der Region anfälliger sind. Die Simulationsergebnisse von zwei Murgangereignissen, die in diesen Einzugsgebieten durchgeführt wurden, zeigen, dass die durchschnittliche Auslaufstrecke in der Region 470 m beträgt, mit einer durchschnittlichen Fließhöhe von 5 m und einer Spitzengeschwindigkeit von 23 m s-1. Diese Ergebnisse sind vergleichbar mit dem Murgangereignis vom Februar 2017 im Einzugsgebiet von Pedra Branca (Guaratuba, Bundesstaat Paraná), bei dem eine detaillierte geomorphologische Charakterisierung nach dem Ereignis durchgeführt wurde, um das Ausmaß

des Ereignisses abzuschätzen. Bei dem Guaratuba-Ereignis handelte es sich um einen großen steinigen Schuttstrom mit einer Gesamtgröße von 120.195 m3, einem Spitzenabfluss von 2.146,7 m3 s-1 und einer Spitzengeschwindigkeit von 26,5 m s-1. Murgangereignisse in Cubatão und Guaratuba wurden durch Niederschläge von kurzer Dauer (< 48 h) und hoher Intensität (> 200 mm) mit Wiederkehrperioden von 3 bis 15 Jahren ausgelöst. Fünf Gefahrenstufen (sehr gering bis sehr hoch) werden dann in unserer Gefahrenbewertungsmethode vorgeschlagen, die hauptsächlich auf den Niederschlägen über 48 Stunden und Strömungseigenschaften basiert. In Cubatão weisen Industrie- und Wohngebiete in der prognostizierten Murgangroute im Allgemeinen die höchsten Gesamtgefahrenstufen auf, da diese sich überwiegend im Ablagerungsgebiet des Phänomens und in der Nähe von Flussläufen befinden, wo damit verbundene Überschwemmungen und Sturzfluten auftreten können. Wie neuere Studien zeigen, wird in der Region Serra do Mar eine Zunahme der Häufigkeit extremer Niederschlagsereignisse prognostiziert; unter Berücksichtigung der allgemein kurzen Wiederkehrperiode (< 20 Jahre) von Murgang auslösenden Niederschlägen, können Ereignisse großen Ausmaßes (> 105 m3) im nächsten Jahrzehnt in Teilen der Bergkette in den Bundesstaaten São Paulo und Paraná auftreten. Diese Arbeit trägt daher zum besseren Verständnis der Dynamik von Murgängen in Brasilien bei und ist ein Schritt zur Vermeidung zukünftiger Katastrophen.

Keywords: Erdrutsche, Geologische Gefahren, Multivariate Statistik, Naturkatastrophen.

Resumo

Entre os tipos de movimentos de massa, os fluxos de detritos representam um risco maior à sociedade devido ao seu alto potencial de destruição. No Brasil, os estudos de fluxos de detritos ainda são incipientes quando comparados a outros processos hidrogeomorfológicos e uma melhor compreensão da sua dinâmica é fundamental para subsidiar estudos de avaliação de perigos e riscos. A estimativa da extensão dos impactos que o fenômeno representa no país é, particularmente, fundamental para subsidiar estudos direcionados e mais aprofundados. Nesse contexto, os principais objetivos desta tese são de espacializar os eventos de fluxos de detritos e avaliar o impacto socioeconômico do fenômeno no Brasil, além de propor uma metodologia que tem como objetivo reduzir os danos potenciais que eventos futuros podem causar nas regiões mais suscetíveis. A caracterização detalhada pós-evento de um fluxo de detritos também é conduzida, uma vez que é um passo fundamental na compreensão da dinâmica do fenômeno e dá suporte à proposta de metodologia de avaliação de perigo. Para determinar o impacto socioeconômico dos fluxos de detritos, foi criado um banco de dados dos eventos que causaram fatalidades e/ou perdas econômicas entre 1920 e 2021, que serviu de base para o cálculo da Taxa de Mortalidade (TM) e a aplicação de Curvas F-N (Frequência de eventos vs. Número de Fatalidades). No total, 45 eventos de fluxo de detritos foram documentados no período considerado, causando mais de 5.773 mortes e US$ 5,4 bilhões em perdas econômicas. A cidade de Cubatão (SP) apresenta o maior número de eventos, consolidando-se como a região mais propensa a fluxos de detritos no país. Consequentemente, a proposta de uma metodologia de avaliação de perigo a fluxos de detritos em várias etapas é feita utilizando Cubatão como área piloto, que tem como base a combinação de análise de Regressão Logística (LR), simulação numérica e retro análise de eventos de chuva. Os resultados da LR destacam que a chuva é o principal fator de influência no início do fluxo de detritos na região, além de também indicarem as bacias mais suscetíveis ao fenômeno no local de estudo. Os resultados da simulação de fluxos de detritos nas bacias indicadas pelo LR mostram que a distância média de *runout* na região é de 470 m, com altura média do pico do fluxo de 5 m e velocidade de pico de 23 m s^{-1}. Esses resultados são comparáveis ao evento de fluxo de detritos de fevereiro de 2017 que ocorreu na bacia hidrográfica de Pedra Branca (Guaratuba, estado do Paraná), no qual uma caracterização geomorfológica pós-evento detalhada foi realizada com o objetivo de estimar a magnitude do evento. O evento de Guaratuba foi um fluxo de detritos "rochoso" (*stony debris flow*) de grande porte, com magnitude total de 120.195 m^3, altura do pico de vazão de 7 m e pico de velocidade de 26,5 m s^{-1}. Os eventos de fluxo de detritos em Cubatão e

Guaratuba são, de uma forma geral, desencadeados por precipitação de curta duração (<48 h), alta intensidade (>200 mm), com períodos de retorno que variam de 3 a 15 anos. Cinco níveis de risco (muito baixo a muito alto) foram, então, propostos em nosso método de avaliação de perigo, baseado principalmente na chuva acumulada em 48 horas, propriedades cinemáticas do fluxo (altura de vazão, velocidade) e nos elementos no raio de perigo (infraestruturas, casas, etc.). As áreas industriais e residenciais na rota estimada de fluxo de detritos geralmente exibem os mais altos níveis de perigo geral na área piloto, uma vez que se desenvolveram na área de deposição do fenômeno e perto de cursos fluviais, onde podem ocorrer inundações e enxurradas associadas. Conforme apontado por estudos recentes, projeta-se um aumento na frequência de eventos extremos de precipitação na região da Serra do Mar e, quando se considera o curto período geral de retorno das chuvas desencadeadoras do fenômeno (< 20 anos), eventos de fluxos de detritos de alta magnitude (> 10^5 m^3) podem ocorrer na próxima década nas áreas consideradas nesta tese, localizadas na região da Serra do Mar paulista e paranaense. Esta tese, portanto, contribui para a melhor compreensão da dinâmica dos fluxos de detritos no Brasil e para a prevenção de futuros desastres.

Palavras-chave: Movimentos de Massa, Perigos geológicos, Estatística multivariada, Desastres naturais.

List of Figures

List of Tables

Table of Contents

List of accepted publications

I. **Cabral VC,** Reis FAV, Veloso V, Corrêa CV, Kuhn C, Zarfl C (2022) The consequences of debris flows in Brazil: a historical analysis based on recorded events in the last 100 years. *Landslides.* Doi: https://doi.org/10.1007/s10346-022-01984-7.

Individual contributions: ***Victor Cabral*** *designed the concept of this study with the support of Fábio Reis.* ***Victor Cabral*** *reviewed literature and wrote the manuscript with the support of Christiane Zarfl. Vinicius Veloso, Christiane Zarfl, Claudia dos Santos Corrêa and Caiubi Kuhn supported the analysis of the data.*

II. **Cabral VC,** Reis FAV, D'Affonseca FM, Lucía A, ..., Zarfl C (2021) Characterization of a landslide-triggered debris flow at a rainforest-covered mountain region in Brazil. *Natural Hazards* 108: 3021 – 3043. Doi: https://doi.org/10.1007/s11069-021-04811-9.

Individual contributions: ***Victor Cabral*** *and Fábio Reis designed the concept of this study.* ***Victor Cabral*** *reviewed literature and wrote the manuscript with the support of Ana Lucía, Christiane Zarfl and Fernando D'Affonseca.* ***Victor Cabral****, Claudia Corrêa, Vinicius Veloso, Marcelo Gramani, Agostinho Ogura, Andrea Lazaretti, Felipe Vemado, Augusto José Pereira Filho, Claudia Santos, Eymar Lopes, Lis Rabado and Lucília Giordano supported the collection of the data that sourced the manuscript.*

III. **Cabral VC,** Reis FAV, Veloso V, Ogura AT, Zarfl C (*2023*) A multi-step hazard assessment for debris-flow prone areas influenced by hydroclimatic events. *Engineering Geology.* Doi: https://doi.org/10.1016/j.enggeo.2022.106961

Individual contributions: ***Victor Cabral*** *designed the concept of this study.* ***Victor Cabral*** *reviewed literature and wrote the manuscript with the support of Christiane Zarfl. Fábio Reis, Christiane Zarfl, Vinicius Veloso and Agostinho Ogura supported the analysis of the data and the final review.*

Acknowledgments

This study was financed in part by the Coordenação de Aperfeiçoamento de Pessoal de Nível Superior - Brasil (CAPES) - Finance Code 001.

First of all, I would like to thank my supervisors Christiane Zarfl and Fábio Reis for their support, advices and friendship during the development of the research. They allowed me to follow my ideas and provided all the resources needed to making the thesis possible. I am thankful to Fernando Mazzo D'Affonseca, for supporting my first research visit in the University of Tübingen, and to Prof. Peter Grathwohl, for supervising me during this time.
I am also thankful to all my friends and colleagues in Brazil and Germany, who collaborated with me and encouraged me during the PhD. I am especially thankful to Ran, Ana, Gaëlle, Clarissa, Timm, Anh and Marco, who made my time in Germany very special and joyful. In Brazil, I am especially thankful to Vinicius and Claudia, for the scientific exchanges that were really insightful, and to Raquel, André, Vanessa, Thamiris, Michele and Gabriela, who made these four years lighter and more fun.
I would like to express my deepest gratitude to my parents, Sirlei and Carlos, who encouraged me during my academic career, as well as my sister, Carla. Finally, I would like to thank my partner, Rodrigo, for the friendship and all the support.

1. Introduction

Debris flows represent great threat to humans and infrastructures in mountain regions worldwide, due mainly to their sudden occurrence and high impact energy that can cause great damage along their path (IVERSON, 2000; BEGUERIA *et al*., 2009; LUNA *et al*., 2012). The phenomenon occurs when a mixture of earth material, water and air very rapidly surges down steep drainage paths (VARNES, 1978; TAKAHASHI, 2006; HUNGR *et al*., 2014), with high-intensity rainfall as the primary triggering factor (MILNE *et al*., 2008). The increasing frequency of extreme rainfall events on a global scale (BENISTON 2009; GIORGI *et al*., 2011; BORGA *et al*., 2014; WESTRA *et al*., 2014) has been associated to an observed increase in the frequency and magnitude of debris-flow events (STOFFEL; HUGGEL, 2012; WINTER; SHEARER, 2014; BORGA *et al*., 2014), which, combined with landslides, were responsible for more than 32,000 fatalities between 2004 and 2010 worldwide (PETLEY, 2012; BORGA *et al*., 2014).

In Brazil, debris flows are mainly initiated by rainfall-triggered landslides (WOLLE; HACHICH, 1989; LACERDA, 2007) and the Serra do Mar Mountain Range is the main site of occurrence, due to its steep slopes and high rainfall rates (VIEIRA *et al*., 2010; VIEIRA; GRAMANI, 2015). Recent projections in the context of global warming have indicated that the Serra do Mar region may experience a surge in the frequency and magnitude of hydrogeomorphic processes, particularly in scenarios with a 2.0º C increase in Global Warming Levels (GWLs) (MARENGO *et al*., 2021). More frequent debris-flow events can lead to significant socioeconomic losses, especially in the Global South[1] where little investment is made to prevent natural disasters (PETLEY, 2012; COROMINAS *et al*., 2013; MARENGO *et al*., 2021).

According to Bastos *et al*. (2015), landslides and debris flows were responsible for approximately 1,700 deaths in Brazil between 2000 and 2010, affecting almost 8 million people and causing economic losses of 1.5 billion USD (United States Dollar). The increasing urbanization towards mountain regions, especially in south and southeast Brazil, has been highlighted by recent studies (GUERRA *et al*., 2007; PATEL; BURKE, 2009; LONDE *et al*., 2018), which can further increase the humanitarian losses that the debris flows can cause, as changes in society and economic development are the main driving forces that can magnify associated damage (ANDRES; BADOUX, 2018).

[1] According to the definition of the United Nations Finance Center for South-South Cooperation (UN FCSSC, 2022)

Despite this extensive history of damage and destruction related to debris flows, quantitative studies about the phenomenon in Brazil are still scarce when compared to other hydrogeomorphic processes. As a result, a reliable estimative of the damage that the phenomenon represents to the society is not yet determined, mostly due to the poor monitoring and documentation of events, which can further be linked to the irregular occurrence of debris flows (KEAN *et al*., 2013; GREGORETTI *et al*., 2018; DESTRO *et al*., 2018). Moreover, the difficult access to debris-flow prone catchments also represents a challenge for the acquisition of good-quality data, which is a prerequisite for reliable risk and hazard studies, as well as for understanding the dynamics and mechanisms of the phenomenon (ÁLVALA *et al*., 2019).

In Geosciences, hazard can be defined as a process or phenomenon that may cause negative impacts to the society, such as loss of life, injuries, property damages, social and economic disruption or environmental degradation (UNDRR, 2015). Hazard incorporates the concepts of *magnitude* (the intensity), *geographical location* (the place the phenomenon occurred) and *time recurrence* (temporal frequency) (GUZZETTI *et al*., 1999). Risk considers the probability of the negative effects to occur, as a function of the *hazard*, *exposure* (human assets in the hazard zone), *vulnerability* (the social, physical, economic and environmental conditions) and *capacity* (resources to cope with the consequences) (UNDRR, 2015). Risk assessment studies, therefore, require a more multidisciplinary approach.

The foundation of a hazard assessment that focuses on landslide-triggered debris flows commonly relies on a comprehensive landslide inventory, knowledge of the main controlling and triggering factors that influence their occurrence, as well as the consideration of the elements at hazard (SOETERS; VAN WESTEN, 1996; VAN WESTEN *et al*., 2008; COROMINAS *et al*., 2013). Landslide inventories are a critical first step, as they are applied in the investigation of their distribution patterns in relation to environmental variables, as well as in the validation of hazard scenarios (CARDINALI *et al*., 2002; VAN WESTEN *et al*., 2008; BĂLTEANU *et al*., 2010; GUZZETTI *et al*., 2012; STEGER *et al*., 2021). The creation of landslide inventories is often dependent on the availability of aerial imagery both prior and after an event, which can represent a serious limiting factor in most regions of Brazil.

The influencing factors are associated to the triggering and controlling parameters that lead to debris-flow occurrence, which can vary according to the characteristics of a region (COROMINAS *et al*.; 2013; NIKOLOVA *et al*., 2020). Since the study of Melton (1958), several attempts have been made at identifying the critical morphometric variables that control debris-flow initiation in a catchment (e.g., ZHOU *et al*., 1991; LIN *et al*., 1993; CHEN; SHIEH, 1993; BOVIS; JAKOB, 1999; LIN *et al*., 2002; WILFORD *et al*., 2004; KOVANEN;

SLAYMAKER, 2008; BERTRAND *et al*., 2013; MEYER *et al*., 2014; HEISER *et al*., 2015; LAY *et al*., 2019; NIKOLOVA *et al*., 2020), including in Brazil (e.g., DIAS *et al*., 2016; CERRI *et al*., 2018; GABELINI *et al*., 2019, CABRAL *et al*., 2019; among others). Multivariate statistics analyses have traditionally been applied in this regard, due to their objective evaluation of the relationship between a dependent variable (occurrence or not of an event) and a series of independent variables (i.e., the influencing factors) (SÜZEN; KAYA, 2011; COROMINAS *et al*., 2013; BUDIMIR *et al*., 2015).

More recently, numerical and physically-based models have been developed to support hazard and risk analysis, due to their ability to represent important features of the debris-flow dynamics (CROSTA *et al*., 2003; MEDINA *et al*. 2008; HUSSIN *et al*., 2012; CASTELLI *et al*., 2017). These models can predict runout path and distance, velocity, flow height and impact pressure, as well as entrainment rate (FRANK *et al*., 2017), which are fundamental to estimating hazard intensity and to supporting the dimensioning of protective structures and measures (TAN *et al*., 2020). Some examples of dynamic models include DAN-3D (HUNGR; MCDOUGALL, 2009; SALVATICI *et al*., 2017), FLO-2D (MUIR *et al*., 2006; QUAN LUNA *et al*., 2011) and RAMMS (FRANK *et al*., 2015; 2017).

Furthermore, direct field investigations are essential to better understanding the debris-flow dynamics in a catchment (GAUME; BORGA, 2008; BORGA *et al*., 2014; LUCÍA *et al*., 2018). Field investigations can also provide a sound knowledge of the magnitude of a debris-flow event (i.e., the total volume of transported debris), which is a prerequisite for quantifying associated hazards (JAKOB, 2005a). Magnitude estimations are more commonly carried out by statistical and empirical methods (e.g., TAKAHASHI, 1992; BIANCO; FRANZI, 2000; MASSAD, 2002; TAKAHASHI, 2006; KANJI *et al*., 2007; CHANG *et al*., 2011) or by post-event (forensic) geomorphological investigation of the debris-flow route in a catchment (e.g., MARCHI; D'AGOSTINO, 2004; LIU *et al*., 2009; GREGORETTI *et al*., 2018).

Geomorphology-based estimations are considered one of the most accurate, since they are based on direct field evidences (LIU *et al*., 2009; GREGORETTI *et al.*, 2018) and do not necessarily require information about previous events (MARCHI; D'AGOSTINO, 2004), which can be especially rare in Brazil. By estimating the magnitude, important kinematic parameters such as peak discharge and flow velocity can also be obtained (RICKENMANN, 1999; PAK; LEE, 2008; SANTI *et al*., 2008; REID *et al*., 2016), which can greatly support debris-flow hazard assessments (KANJI *et al*., 2007; SANTI, 2014; GREGORETTI *et al*., 2018).

In this brief context, the following questions arise:

- What are the societal consequences of debris flows in Brazil?
- What are the most affected regions in the country?
- What are the main characteristics of debris flows in Brazilian catchments and in what way their kinematic parameters influence hazard levels?
- What are the differences and similarities between the dynamics and mechanisms of the phenomenon in different Brazilian catchments?
- What methods can more successfully be applied to mitigate and prevent new losses in the most affected areas?

Three papers have been developed during this research, in the attempt to answering these questions and which results are integrated and discussed in this thesis. Paper I, entitled "*The consequences of debris flows in Brazil: a historical analysis based on recorded events in the last 100 years*", provides an overview of the damage and losses that the phenomenon has caused so far, based on a comprehensive compilation of recorded events between 1920 and 2021. Paper I also highlights the areas in Brazil where debris flows are more common and have historically caused more negative consequences.

A detailed characterization of a debris-flow event is conducted in Paper II, entitled "*Characterization of a landslide-triggered debris flow at a rainforest-covered mountain range in Brazil*", to describe the dynamics of the phenomenon in a Brazilian catchment and to contribute to better understanding the hazard that debris flows can represent to the society. A more in-depth analysis and comparison of debris-flow dynamics in different Brazilian catchments is conducted in this thesis.

Furthermore, Paper III proposes a "*multi-step hazard assessment for debris-flow prone areas influenced by hydroclimatic events*", which is also the title of the study, based on the combination of Logistic Regression analysis, numerical simulation and rainfall back-analysis. The method was developed mainly for tropical and subtropical areas and the region of Cubatão (São Paulo State) is chosen as test site for the study, as it is identified by Paper I as one of the regions most affected by debris flows in Brazil. The results of Paper II are also compared and incorporated in the development of the hazard assessment presented in Paper III. The three papers are available in Appendix A.

2. Objectives

The main objectives are to assess the societal impact of debris flows in Brazil and to propose a methodology that aims at reducing the potential damage that future events can cause in susceptible regions. Another objective is to conduct a detailed post-event characterization of a debris flow, as it is a fundamental step to understanding the phenomenon and can further support the proposal of the hazard assessment methodology. As for the specific objectives, they include:

- To create a comprehensive catalogue of debris-flow events that have caused fatalities and/or economic losses in the last 100 years in Brazil;
- To quantify the social and economic consequences that the phenomenon represents in the country;
- To identify the main factors that influence debris-flow initiation in a catchment;
- To conduct a rainfall back-analysis aimed at identifying precipitation patterns that lead to the phenomenon;
- To correlate rainfall with the magnitude and consequences of a debris-flow event;
- To characterize the dynamics and to estimate the magnitude of a recent debris-flow event, to better comprehend the development of the phenomenon in a Brazilian catchment, which can also further aid the implementation of preventive measures and support hazard assessments;
- To propose a hazard zonation matrix that can be applied in hazard assessment studies of debris-flow prone areas.

The thesis contributes to the effort of better understanding the dynamics of debris flows in Brazil and is a step towards the prevention of future disasters.

3. Results and discussions

3.1. The impact of debris flows in Brazil

According to the catalogue compiled in our research and presented in Paper I, 45 debris-flow events have occurred in Brazil between 1920 and 2021, which have caused fatalities and/or economic losses. Figure 3.1 shows the spatial distribution of these events, responsible for at least 5.5 billion USD in direct economic losses and over 5,771 fatalities (Table 3.1). According to our estimates, the average fatality rate per event is around 128 (total number of deaths/total number of debris-flow events) and the average economic loss per event is of ca. 122 million USD (total sum of economic losses/total number of debris-flow events).

In total, 64.5% of the recorded debris-flow events occur at the Serra do Mar Mountain range, followed by Serra da Mantiqueira (13.3%) and Serra Geral (13.3%). Southeast Brazil is the most affected region by the phenomenon, both in terms of number of events and socioeconomic losses. This can be related to the highest population density in the southeast (especially in the states of Rio de Janeiro and São Paulo), the intense urbanization of the coast, where the mountain ranges "Serra do Mar" is located.

Table 3-1: Analysis of debris-flow related damages according to state. Fatalities include missing people. Avg. = average, N/A = not available.

State	Number of events	Economic losses (USD)	Fatalities	Avg. Fatality/event	Avg. Economic loss/event (USD)
Bahia (BA)	2	34,884,425	173	87	17,442,212
Ceará (CE)	1	N/A	91	91	N/A
Minas Gerais (MG)	3	718,275	286	95	359,138
Paraná (PR)	2	76,095,510	4	2	38,047,755
Rio de Janeiro (RJ)	13	3,517,256,731	4,353	335	270,558,210
São Paulo (SP)	18	168,802,604	621	35	9,377,922
Santa Catarina (SC)	5	1,693,749,577	243	49	338,749,915
Rio Grande do Sul (RS)	1	24,683,356	0	0	24,683,356
Total:	45	5,516,190,478	5,771	128	122,582,011

São Paulo is the state with the highest number of reported debris-flow events, followed by Rio de Janeiro and Santa Catarina (Table 3.1). The state of Rio de Janeiro is, by far, the most impacted by the phenomenon, with 4,353 fatalities in the last 100 years and ca. 3.5 billion USD in economic losses, which corresponds to approximately 75% of all reported fatalities and 64% of the economic losses reported in the whole country. Among the cities most affected by debris flows, Cubatão (São Paulo) and Petrópolis (Rio de Janeiro) stand out with the highest numbers of events in the considered period (9 and 6 events, respectively).

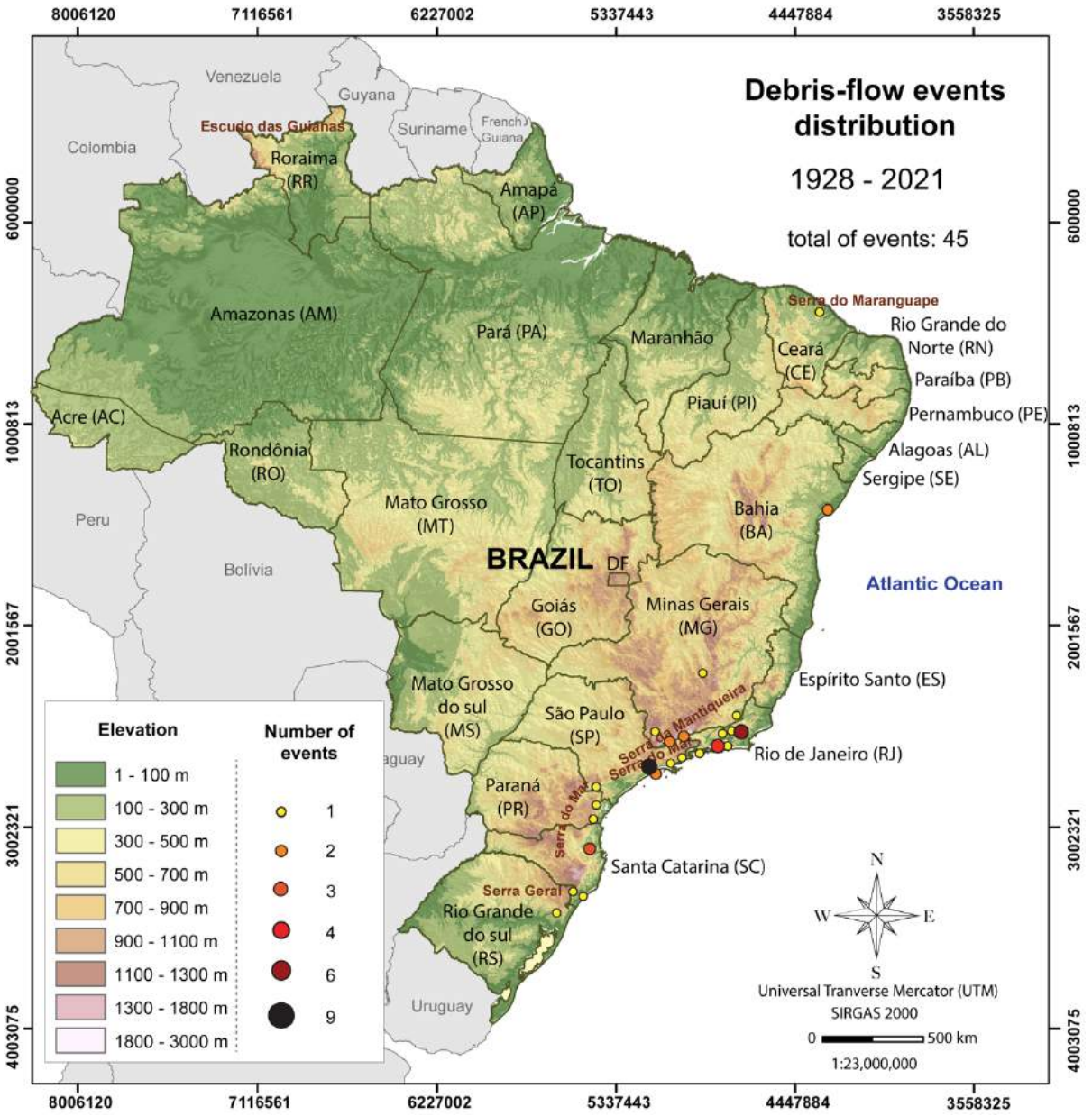

Figure 3-1. Geographic distribution of reported debris-flow events in Brazil. The reported events are more often associated to the mountain ranges of Serra do Mar, Serra da Mantiqueira and Serra Geral. The underlying Digital Elevation Model (DEM) is created using GTOPO30 data retrieved from Earth Explorer (USGS, 2021).

To assess the impact that debris-flows have caused in Brazil in the considered period, we calculated the Mortality Rate (MR) of the phenomenon and we applied the relationship between the frequency of events and their consequences, using the so-called F-N plots. Calculating the MR is a direct method of estimating the debris-flow impact in a country and is expressed as the number of deaths by debris flows per a specified population size in a defined period of time, e.g., a specific year (GUZZETTI, 2000). Here, the MR is calculated per 100,000 people. F-N plots provide the likelihood of multiple fatalities due to a debris-flow event, by plotting the cumulative frequency of events that have cause N or more fatalities (F) with the number of fatalities (N), in a log-log scale (FELL; HARTFORD, 1997).

Table 3-2: Analysis of debris-flow related damages according to municipality. Fatalities include reported cases of dead and missing people. N/A = not available.

Municipality/Region	Number of events	Economic losses (USD)	Fatalities	Material losses (unit)
Além Paraiba (MG) and Volta Grande (MG) region	1	N/A	250	63
Antonina, Morretes (PR)	1	76,095,510	25	223
Bom repouso (MG)	1	718,275	0	11
Campos do Jordão (SP)	2	N/A	27	381
Caraguatatuba (SP)	1	63,449,964	436	400
Contagem (MG)	1	N/A	36	300
Cubatão (SP)	9	73,332,253	11	40
Guaratuba (PR)	1	N/A	0	1
Ilha Grande (RJ)	1	180,668,819	31	8
Itaóca (SP)	1	5,578,975	23	123
Lavrinhas (SP)	2	2,329,412	11	N/A
Maranguape (CE)	1	N/A	91	N/A
Niterói (RJ)	1	146,587,2770	269	62
Nova Friburgo (RJ)	1	1,932,584,390*	392**	N/A
Petrópolis (RJ)	6	322,416,245 + 1,932,584,390*	428**	1,929
Rio de Janeiro (RJ)	4	1,010,547,344	804	> 1,500
Rolante (RS)	1	24,683,356	0	400
Salvador (BA)	2	34,884,425	173	1,401
Santos (SP)	2	24,112,000	102	67
Serra das Araras – Piraí (RJ)	1	N/A	1700	> 100
Teresópolis (RJ)	1	1,932,584,390*	429**	N/A
Timbé do Sul (SC)	1	71,311,286	16	N/A
Tubarão (SC)	1	666,840,081	40	N/A
Ubatuba (SP)	1	N/A	11	30
Vale do Itajaí region (SC)	3	946,442,920	187	5158

* Economic losses associated to the 2011 debris flow event, undistinguished between cities

** +300 missing people, undistinguished between cities

Figure 3.2a shows the average Mortality Rate (MR) of debris flows per 100,000 habitants in Brazil for every decade between 1920 and 2020, whereas the average national MR (combining all death causes) is shown in Figure 3.2b, plotted against the population growth. The results indicate that while the average national MR has been going down since 1920, the national MR of debris flows has been fairly steady through the decades. The comparison between the declining average national MR with the steady debris-flow MR suggests that while

there have been several advances in public health and public security policies in Brazil since 1920, the same is not observed for debris-flow prevention and mitigation measures.

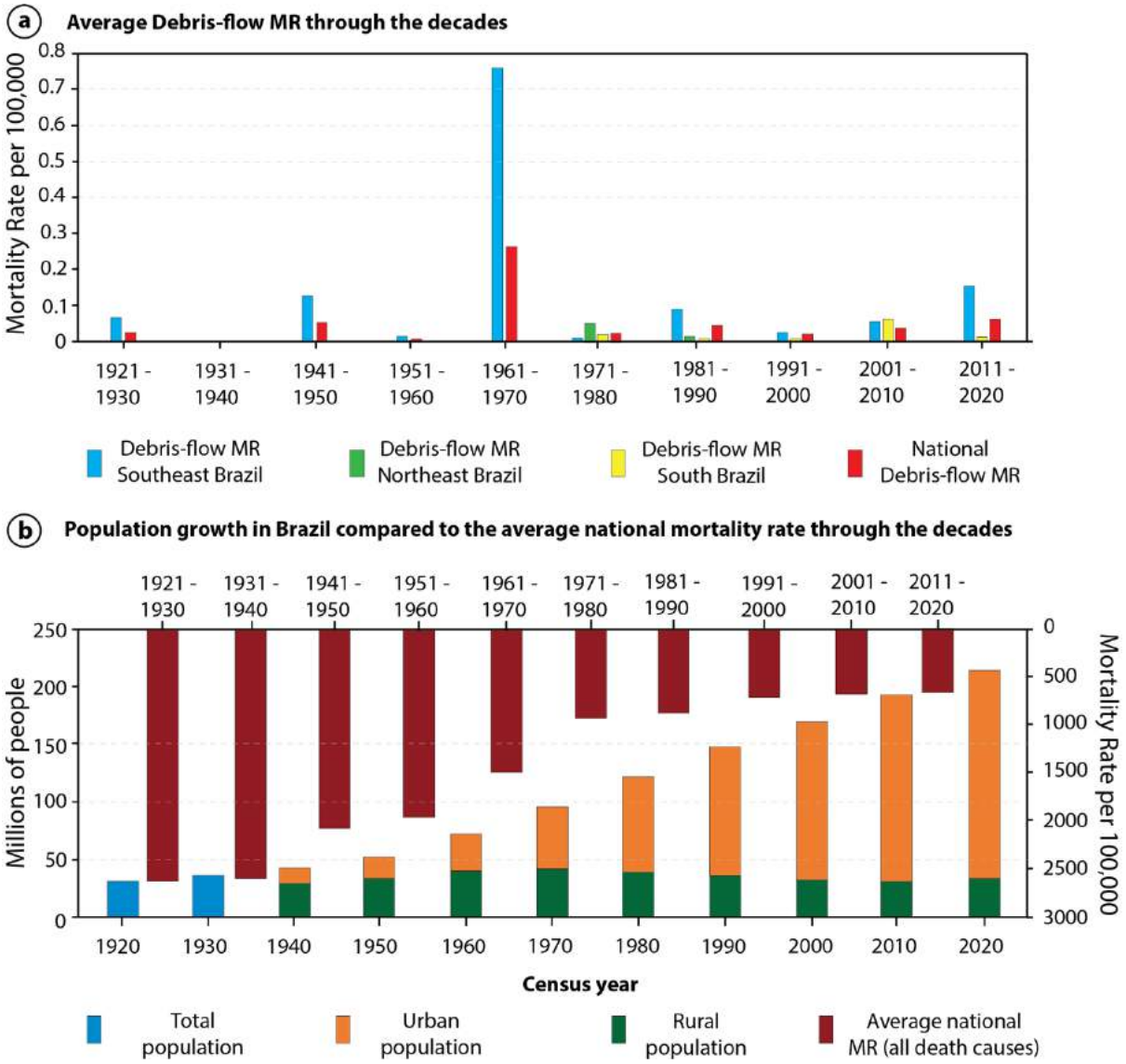

Figure 3-2. Mortality rate (MR) and demographic analysis. A) Average national debris-flow MR (red bar) through the decades, compared to the debris-flow MR of the Southeastern (blue), Northeastern (green), and Southern (yellow) region. B) Populational growth of Brazil according to census year, compared to the average mortality rate through the decades comprising all death causes (dark red bar). The number of people living in urban areas has been steadly increasing since 1960. The Demographic and average MR data for Brazil is retrieved from IBGE (2019; 2021).

Southeast Brazil exhibits the highest debris-flow MR, with debris-flow related fatalities reported in all decades since 1920, except for the 1930s (Figure 3.2a). The average MR in the Southeast ranged from 0.06 in 1920s to 0.76 in the 1960s, decreasing in the 1970s (0.004) and increasing again in the last decade (0.15). In South Brazil, debris-flow related fatalities are recorded every decade since the 1970s, with the highest average debris-flow MR in the 2000s (0.06), due to the debris-flow event in the Itajaí river basin in 2008. In Northeast Brazil, only

in the 1970s and 1980s the region reported debris-flow related deaths, with the highest debris-flow MR in the 1970s (0.05).

The debris-flow MR in the country compared to the MR of other diseases and human-induced causes is shown in Figure 3.3, considering the average MR values for the last decade (2011-2020) according to the Global Burden of Diseases (VOS *et al*., 2020). Fatalities related to debris flows are rather rare in Brazil when compared to other death causes, with approximately 127 deaths per year during the last decade, while homicides and drowning cause each year approximately 61,000 and 6,380 deaths per year, respectively (Figure 3.3). The primary cause of death in Brazil are diseases, followed by public violence, with COVID-19 related deaths representing the leading cause of fatalities between 2020-2021.

However, when we analyze the plots that considers the Frequency of Events with N or more fatalities (F) and the number fatalities (N) (Figure 3.4), we can observe the high probability of fatal events in the country, which can be directly related to the lack of preparedness and preventive programs to natural disasters. For instance, a debris-flow event with a fatality number of 1,200 or more, such as the one in 2011 in Rio de Janeiro (we refer Paper I, annex A), has a probability of occurring every 50 years, if no preventive measures are adopted, and one with 10 or more fatalities has a probability of occurring every 3 years.

When the fatal consequences of debris flows in Brazil is compared to other countries, the country stands out showing a higher societal impact than in China (TIANCHI *et al*., 1989), Japan (CASCINI *et al*., 2008), and Hong Kong (HO; KO, 2009), and a similar societal impact to that of Italy (GUZZETTI, 2000) (Figure 3.4). It is important to point out, however, that our analysis focuses only on debris-flow events, which tend to cause higher number of fatalities and are less frequent than localized fatal landslides (COROMINAS *et al*., 2013), which is also considered in the other international studies and can potentially impact the slope of the F-N curve. Moreover, Japan, Italy and Hong Kong are much smaller in territorial area than Brazil, which can also potentially affect the probability of fatal events due to scale effect.

F-N plots are commonly applied in landslide studies worldwide (e.g., MACCIOTTA *et al*., 2015; KELLER, 2017; ZHANG *et al*., 2019; STROUTH; MCDOUGALL, 2021; among others), even though they are not universally acknowledged as a good indicator of risk (EVANS; VERLANDER, 1997; STROUTH; MCDOUGALL, 2021). F-N plots have also been applied in the establishment of thresholds of what is deemed as an acceptable risk by society for different types of natural hazards, including specifically for landslides (MALONE, 2005; STROUTH; MCDOUGALL, 2021). Hong Kong, through the country's Geotechnical Engineering Office (GEO), established landslide risk thresholds (ERM, 1998) (**Figure 3.6**),

which have been adopted by some countries (e.g., Australia, AGS, 2007; Western Canada, PORTER; MORGENSTERN, 2013), though, as pointed out by Strouth and McDougall (2021), to no great success taking Canada as an example.

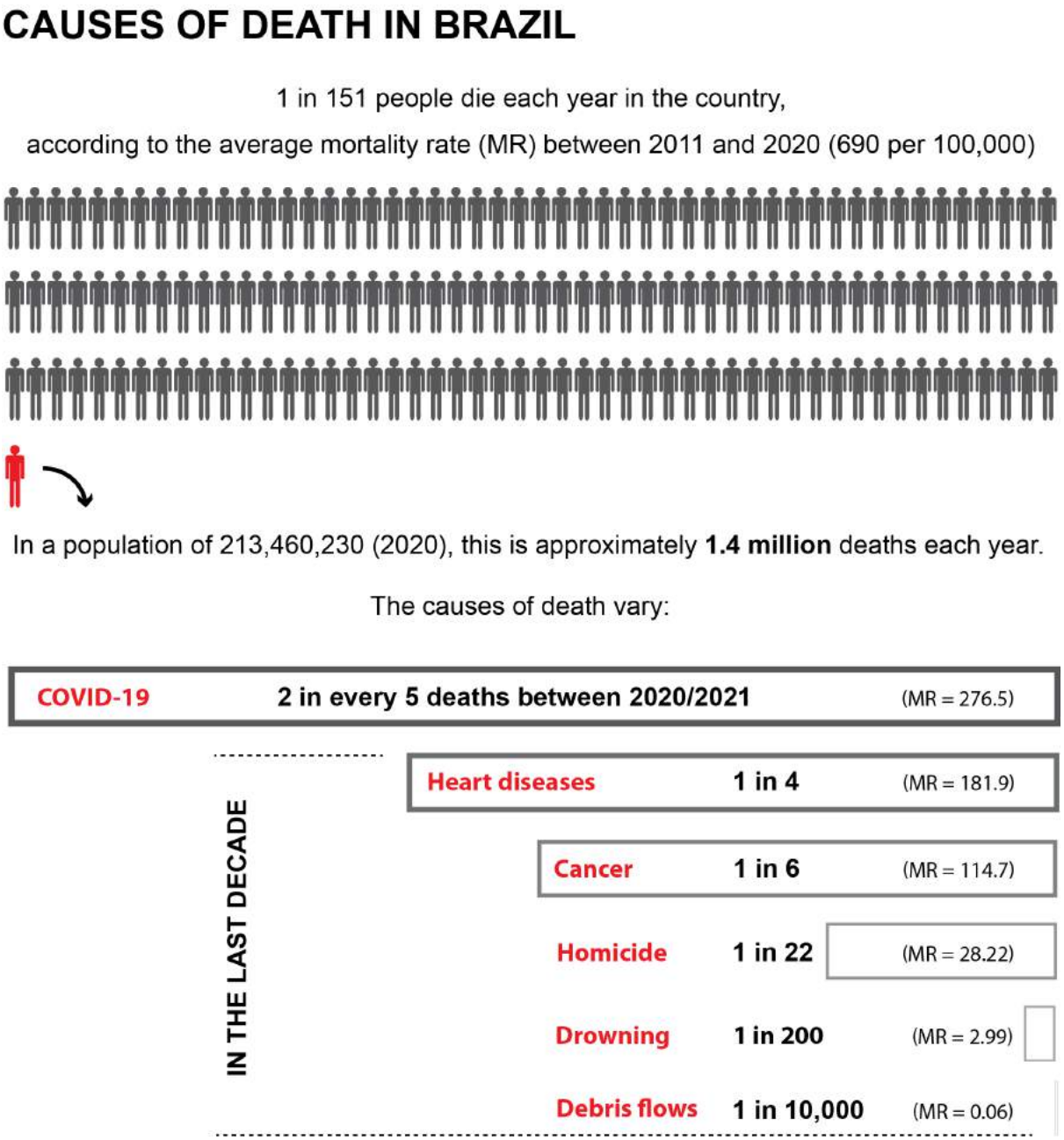

Figure 3-3. Mortality Rate (MR) per 100,000 people per year of different death causes in Brazil. The average mortality rates for the last decade (2011-2020) are based on data from the Global Burden of Diseases (VOS et al., 2020). The MR of coronavirus in Brazil is based on data from data from the Brazilian Health Ministry (BRASIL, 2021c). The figure is based on Strouth and McDougall (2021).

F-N curves can potentially be applied in risk analysis studies at cities with extensive historical incidence of debris-flow events in Brazil, such as Petrópolis and Cubatão, providing a good estimation of the probability of fatal events occurrence, which can later support

decisions about preventive measures. While F-N curves can be useful, the adoption of risk thresholds, such as the one from GEO (ERM, 1998), can be more challenging. Despite similar climate and hydrogeomorphic process dynamics (HO; KO, 2009; LACERDA, 2007), especially in the southeast region of Brazil (sub-tropical climate), economic and cultural differences about the perception of landslide and debris-flow risk are some of the factors that are not easily transferable (STROUTH; MCDOUGALL, 2021).

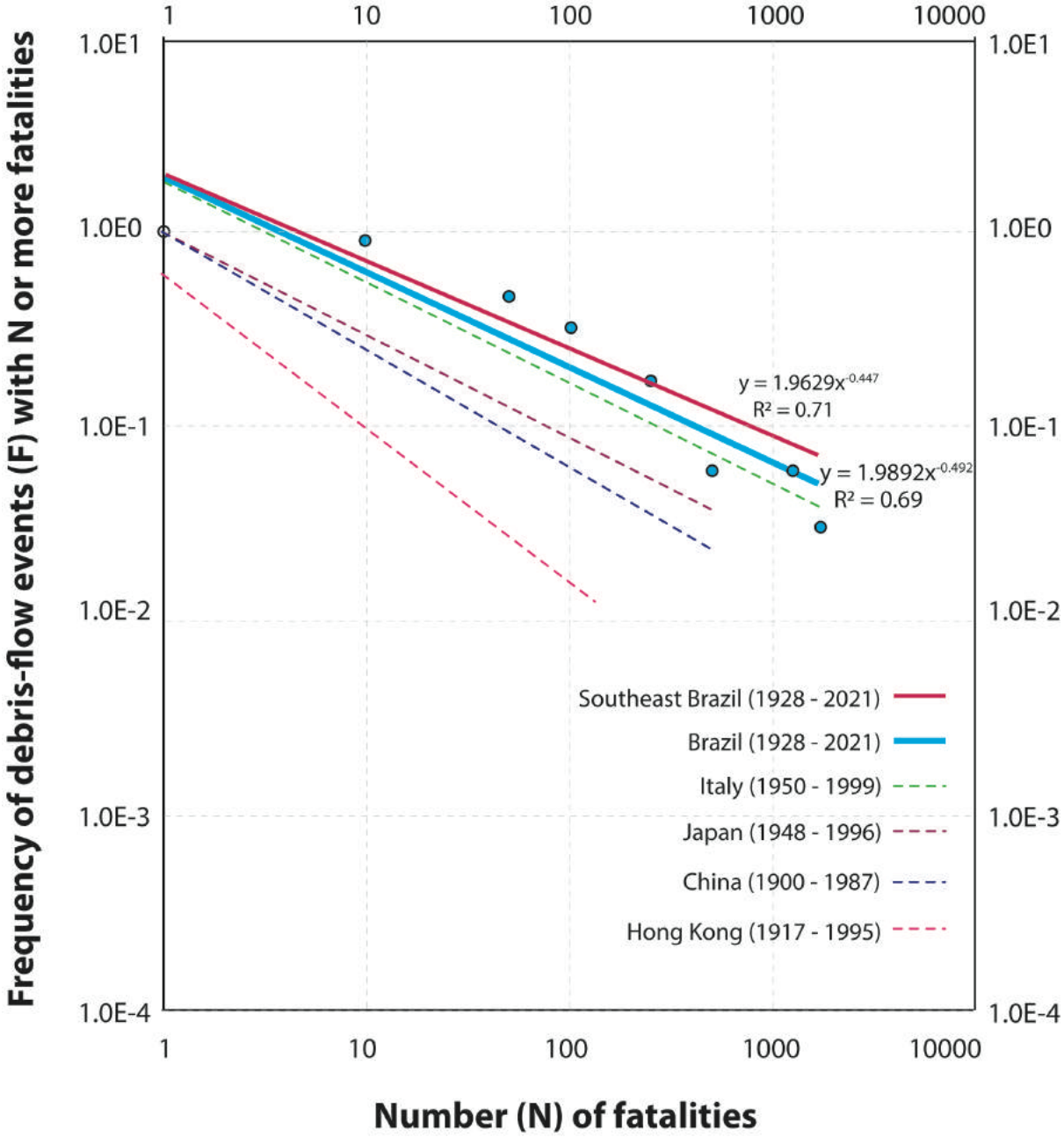

Figure 3-4. F-N curves of debris-flow events in Brazil compared to other countries. Debris flows represent a higher societal risk than landslide events (also comprising debris flows) in China (TIANCHI et al., 1989), Japan (CASCINI et al., 2008), Hong Kong (HO; KO, 2009), and Italy (GUZZETTI, 2000).

For instance, between 2016 and 2017, The Hong Kong Government budget for disaster prevention and preparedness was approximately 396 million USD, with 165 million USD for landslide preventive measures (SIM *et al*., 2018). In Brazil, the National Center of Monitoring and Early Warning of Natural Disasters (*Centro Nacional de Monitoramento e Alertas de Desastres Naturais* - CEMADEN), responsible for hazard management and monitoring for the whole country, had an annual budget upon its creation of 14 million USD in 2012-2013, which has been successively slashed through the years, reaching approximately 3.7 million USD in 2019-2020 (BRASIL, 2021b).

In addition to very different budgets implemented for natural disasters prevention, there are scale effects in the creation of risk thresholds over F-N plots that should be considered, as the x-axis (N) is affected by the size of the population affected, and the y-axis (F) by the return period of the phenomenon (STROUTH; MCDOUGALL, 2021). Comparing the probability of fatal debris-flow events in Brazil with other countries using F-N plots is also subjected to the scale effect, as already pointed out.

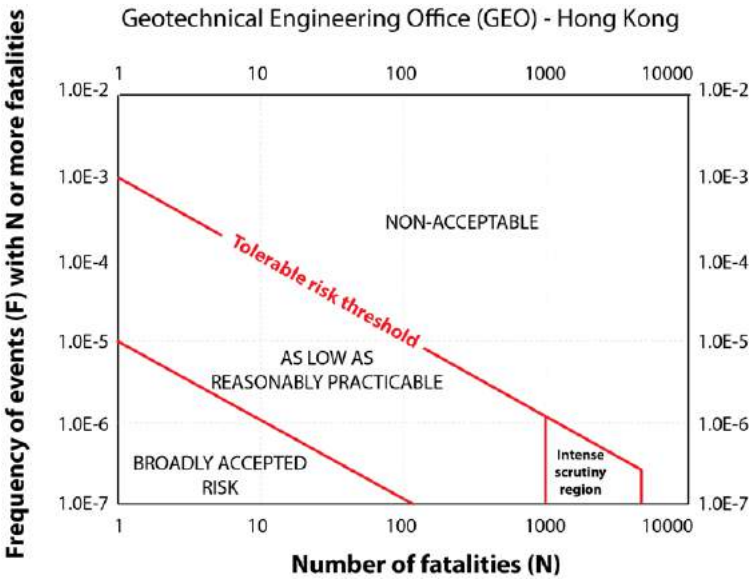

Figure 3-5. Societal risk thresholds adopted by Hong Kong, which commissioned the creation of the criterions specifically for landslides (ERM 1998).

Nonetheless, the use of the F-N plot provides a good indication of the impact that the phenomenon represents in Brazil and the steady debris-flow MR through the decades further shows that little has been made to reduce and prevent their negative impacts in the last 100 years. The temporal and spatial distribution of debris-flow events is a primordial step to understanding the impact of a phenomenon in a country and provides useful information for the definition of areas where mitigative measures must be implemented. Considering that

Brazil's population growth is most concentrated at coastal cities in the southeast (LONDE *et al*. ,2018), which are also the "hotspots" for debris-flow events, disaster prevention measures can and should be implemented in the region, such as local-scale risk analysis, development of early warning systems and installation of retention structures.

The outlook, however, is not promising. The results of the consistent underfunding of CEMADEN and the discontinuation of important disaster-prevention programs have been recently seen in the floods and landslides that struck Petrópolis in February 2022. No warning was issued prior to the catastrophe, causing hundreds of fatalities, despite extensive hazard and risk monitoring programs theoretically present in the municipality.

3.2. The main factors that initiate a debris flow in a catchment

Cubatão in the state of São Paulo is the city where the highest number of debris-flow events were recorded in the last 100 years, as pointed out in the analysis of the phenomenon's impact in Brazil. Cubatão is the largest petrochemical site in Latin America and, during the 1980s, it represented 2.5% of the Brazilian GDP (COSTA-RIBEIRO; MELLO-AWAZU, 1988) and was considered the most polluted city in the world, with very high rates of air and water pollution (COSTA-RIBEIRO; MELLO-AWAZU, 1988; HOGAN, 1988). Since the 1990s, however, the city and the state of São Paulo have implemented environmental monitoring and recuperation programs that have helped to restore acceptable levels of air and water quality in the region (VIEIRA-FILHO *et al*., 2015; LONDE *et al*., 2018).

Considering the high environmental and socioeconomic vulnerability of the city, the extensive history of debris-flow events, as well as the availability of high-resolution data, a more detailed analysis is conducted in Cubatão. The city is the test-site in our analysis of the factors that influence debris-flow initiation in a catchment, as well as in our proposal of a hazard assessment methodology presented in Paper III. Even though several landslide and debris-flow events have occurred in the region, the ones from 1985 and 1994 were the most notoriously widespread throughout the hillslopes and catchments of the city and are the events used in our analysis. Figure 3.6 shows the location of the catchments that are our study site.

The selection of the factors that influence debris-flow initiation is based on past studies worldwide and at Serra do Mar (e.g., WILFORD *et al*., 2004; DIAS *et al*., 2016; WU *et al*., 2018; NIKOLOVA *et al*., 2020), as well as on the factors that are assumed to be critical in the study area based on past events. Two assumptions were made in their selection: (1) new debris flows will occur in similar conditions as past ones and (2) the analyzed factors will not change

for a long period of time. The influencing factors are catchment slope, catchment relief, slope aspect, Stream Power Index (SPI), Topographic Wetness Index (TWI), lithology, soil cover, vegetation and 48-h accumulated rainfall (Table 3.3).

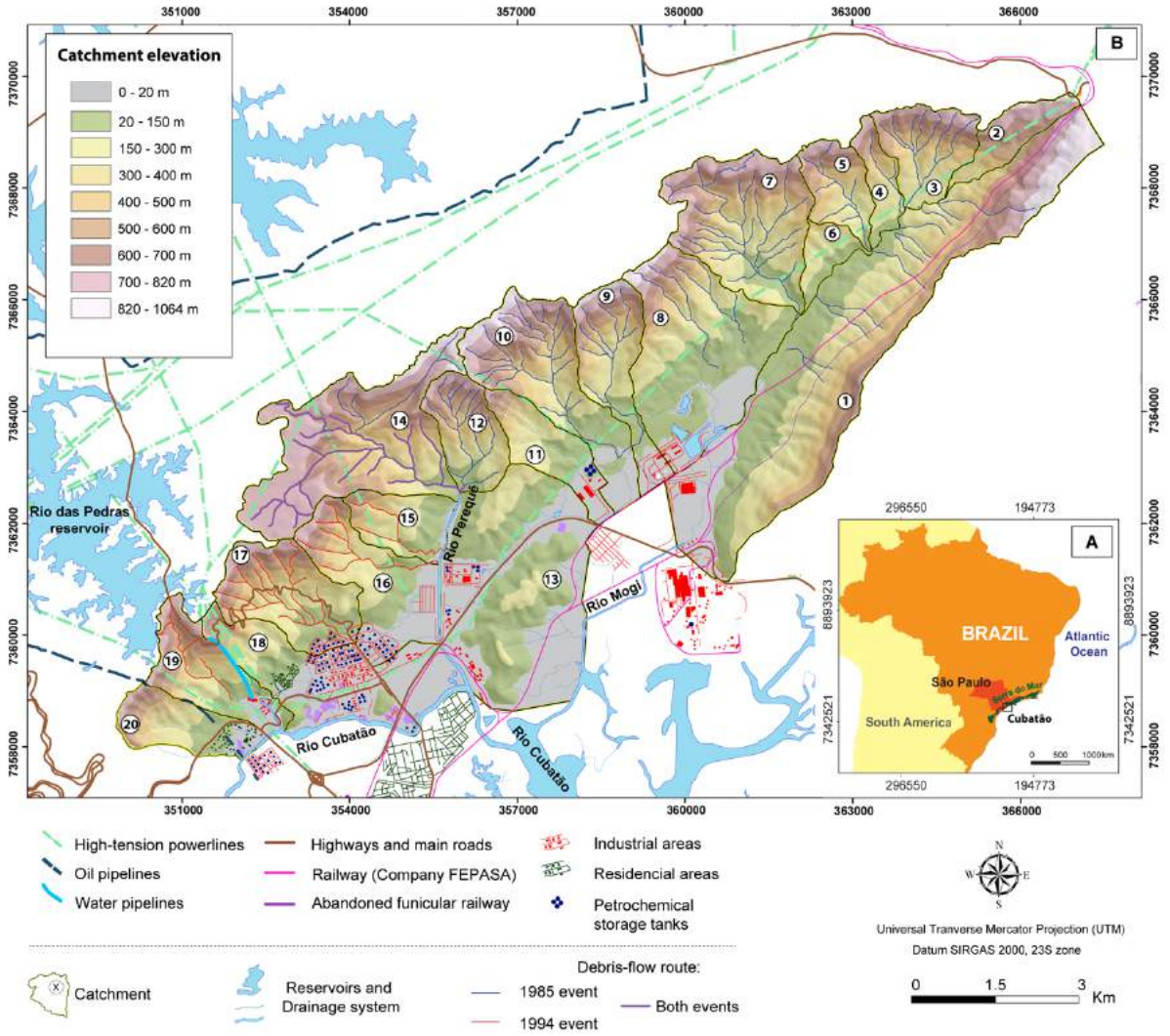

Figure 3-6. Location of the study area, where the hazard assessment is conducted, as well as the analysis of the factors that influence debris-flow initiation in a catchment. A) The study area (Cubatão, São Paulo State), located in the Serra do Mar Mountain Range, Brazil. B) Overview of the analyzed catchments (numbers in white circles), located at the central and northeastern hillslopes of Cubatão (2022).

A reclassification was conducted to standardize the scale of all the factors and facilitate the statistical evaluation. Frequency ratio was applied in the standardization and the statistical evaluation is conducted using Logistic Regression (LR) analysis, which predicts the probability of debris-flow initiation based on the dependent variable (occurrence or not of an event) and a number of independent variables (i.e., influencing factors) that are available in a spatially continuous manner across the region. The independent variables are assessed to establish the LR equation, which can be applied in susceptibility studies.

Table 3-3. Influencing factors analyzed in this study.

Factors	Symbol	Unit	Description
Catchment relief	H	km	The difference between the highest and the lowest elevation point
Catchment slope	Sl	%	Slope of the catchment
Slope aspect	Sa	-	The compass direction the slope surface faces
Strem Power Index (SPI)	SPI	-	The erosive power of flowing water
Topographic Wetness Index (TWI)	TWI	-	Terrain-driven variation in soil moisture
Lithology	Lit	-	Geology of the catchment's bedrock
Soil	So	-	The soil cover of the catchment
Vegetation	F	-	The type of vegetation cover of the catchment
48-h accumulated rainfall	P	mm	48-h accumulated rainfall prior to the debris flow

Since the influencing factors can potentially show a high to low correlation with each other, a factor combination was made to determine their degree of contribution to debris-flow initiation. In the first round of the LR, the influencing parameters were added one by one, independently, creating a one-factor model. The factor that showed a more positive effect in the model was retained and added in the following round of LR analysis – creating, then, a two-factor model. The process was repeated until all the influencing factors were combined. The performance validation of our LR analysis was based on a Receiver Operator Characteristics (ROC) analysis, following Fawcett (2006).

Based on the optimal model-fitting results obtained through the LR and on the priority of factors added to the model, the following sequence was established that indicates the order of the factors that most impact debris-flow initiation: (1) Rainfall, (2) Soil cover, (3) Basin slope, (4) SPI, (5) TWI, (6) Forest cover, (7) Lithology, (8) Slope aspect, and (9) Basin relief (Table 3.4).

Several studies at Serra do Mar highlight that rainfall is the main debris-flow initiation factor (LACERDA, 2007; KANJI *et al*., 2007; VIEIRA *et al*., 2010, VIEIRA; GRAMANI, 2015) and our analysis statistically corroborates the statement. In total, 10 rainfall index subclasses were identified across the study area, based on the rainfall distribution patterns. For the 1985 events, the subclass 200 – 220 mm is associated with a higher density of debris-flow triggering landslides, while for the 1994 event the subclass 270 – 290 mm is associated with a higher density of landslides. These results potentially indicate that a >200 mm rainfall accumulated in 48 hours can initiate high-magnitude debris flows.

Among the geomorphometric parameters, soil cover shows a stronger influence on debris-flow initiation. Cambisols (Ca2 and Ca3) are associated with a higher tendency to trigger debris flows, which can be related to the high boulder content that can more easily

enable rainfall infiltration (ROSSI; PFEIFER 1991). Ferralsols (LVa1 and LVa3) dominate in the study area, as it is typical of humid tropical and subtropical regions, and do not show a particularly strong tendency to triggering debris flows, which can be related to a more developed and stable soil profile.

Table 3-4. Results of the ROC analysis of the validation tests of the LR models, according to the Area Under the Curve (AUC) of the ROC Curve.

Factors	1 factor model	2 factor model	3 factor model	4 factor model	5 factor model	6 factor model	7 factor model	8 factor model	9 factor model
Rainfall	**0.853**	-	-	-	-	-	-	-	-
Lithology	0.755	0.768	0.863	0.859	0.876	0.882	**0.882**	-	-
Slope	0.595	0.853	**0.879**	-	-	-	-	-	-
Relief	0.641	0.752	0.837	0.84	0.882	0.879	0.869	0.879	**0.892**
Soil	0.709	**0.876**	-	-	-	-	-	-	-
Vegetation	0.598	0.859	0.863	0.866	0.873	**0.886**	-	-	-
TWI	0.605	0.853	0.878	0.876	**0.892**	-	-	-	-
SPI	0.503	0.846	0.876	**0.889**	-	-	-	-	-
Slope aspect	0.536	0.683	0.866	0.856	0.882	0.885	0.881	**0.886**	-

Slope angle is another significant morphometric factor that influences debris-flow initiation, due to the direct influence on surface run-off, vegetation and soil cover, loose material accumulation and groundwater infiltration (LACERDA, 2007). Slope varies from 0 to 172 % in the catchments, with the range of 70 to 90% (35º to 40º) the most prone to triggering debris flows at the study area, followed by the range of > 90% (> 40º). In general terms, the higher the slope the greater the tendency to slope failure, although in very steep slopes (>40º) the accumulation of mobilizable material (i.e., soil) might not be sufficient to initiate debris flows.

The SPI is another strong indicator of debris-flow triggering areas, as it influences the transport and erosion potential of the river/stream (DE ROSA *et al*., 2019). SPI can be used to characterize debris-flow initiation (Low SPI), transport (High SPI) and deposition areas (Low SPI) (CHEN *et al*., 2017), and our results show that areas with a low SPI are more prone to debris-flow initiation due very low stream flow in the hillslopes. Areas with a high SPI index (1.5 to 6) can also contribute to the debris-flow development, which can be associated with the erosion of lateral slopes as a result of a stronger flow power. Moreover, the catchments in the region have a moderate drainage density, which suggests a fairly impermeable substratum that results in overland flow that can acquire high erosive power – contributing, thus, to debris-flow entrainment.

The relationship of Topographic Wetness Index (TWI) with debris flows has also been demonstrated by other studies (e.g., NIKOLOVA *et al*., 2020), with high TWI areas having the ability to collect more surface water, i.e., associated to debris-flow deposition in flatter areas. In the study region, the lower the TWI the higher susceptibility to debris-flows initiation, since the main initiation areas are in steep portions at higher altitudes in the hillslopes.

Based on the LR model results, rainfall, soil, SPI and TWI are the most relevant parameters (Equation 1) that should be used in the prediction of debris-flow initiation in the region, due to a better performance in the output ROC analysis and high-significance of all the variables ($p < 0.05$) in the statistical evaluation of the model (Table 3.5). An LR model with all the influencing factors produced a similar performance in the ROC analysis (Table 3.4), although not all of the variables showed significance in the statistical evaluation (Table 3.5). For susceptibility studies in the region, therefore, we suggest the use of Equation 1.

$$Z = 1.98 + 1.54\,TWI + 4.6SPI + 6.47Slope - 4.39Soil - 15.4Precipitation \quad (1)$$

Although with a weaker statistical significance, vegetation is the sixth most influencing factor and is associated with a strong control over the strength of the superficial soil layer, representing a slope-stabilizing parameter, as it can affect surface runoff and create obstacles for flow propagation (LIU *et al*., 2021). Medium-height broadleaf vegetation (Am), Broadleaf and bush vegetation (AA) and Broadleaf vegetation (Ab2) are associated with a higher predisposition to initiate debris-flow and are weakly (Ab2) to strongly (Am, AA) degraded by the pollution of the region (especially acid rain) (MATTOS; MATSUKUMA, 1990). The effect of pollution on vegetation may contribute to weakening their support of the soil, leading more easily to slope failures.

Lithology is intrinsically associated with the soil type and vegetation of a region, especially in areas with well-developed regolith such as Serra do Mar. Even though a more explicit relationship between lithology and debris-flow initiation is not observed in our statistical analysis, Proterozoic stromatic migmatites (PSeMc), occurring at higher elevations in the catchments, are more prone to debris-flow initiation, accompanied by the other migmatite types (AcMn, AcMp, AcMg) and granitoid rocks (PSEOY). Schists (PSpX) and Phyllites (PSpF) show a lower tendency, which can be related to a more developed and stable regolith, as a result of a weaker strength to weathering.

Slope aspect and relief are the two least relevant factors to triggering debris flows, among the selected influencing parameters. In the study region, the slope direction most prone

to debris-flow initiation varied according to the event, with the eastern and northeastern slopes associated with a higher tendency to initiate debris flows in the 1985 event, and in the 1994 event the northern and northwestern slopes. This is directly related to the rainfall direction of these events: eastern-northeastern in 1985 and western-northwestern in 1994.

The relative relief can control the type of vegetation in the hillslopes, as well as influence both SPI and TWI. In study region, however, relief did not play a prominent role in debris-flow initiation, with the 600 – 700 m elevation range showing a higher tendency to trigger slope failures that can lead to debris flows. This elevation range is associated with stromatitic migmatites (PSeMc) and the 70 – 90% slope range, which show stronger influence on debris-flow initiation.

Table 3-5. Statistical validation of the LR models, showing the regression coefficients (B) and relevant statistical parameters.

	Factor	B	Standard Error	Wald test	Degrees of Freedom	P-value
9-Factor model	Rainfall	-27.758	10.622	6.829	1	0.009
	Soil	-1.117	4.652	0.058	1	0.081
	Basin slope	14.851	9.501	2.443	1	0.011
	SPI	0.214	6.068	0.001	1	0.097
	TWI	2.332	3.667	0.404	1	0.053
	Forest	-17.270	8.846	3.811	1	0.051
	Geology	-3.434	4.994	0.473	1	0.049
	Slope aspect	3.249	8.618	0.142	1	0.071
	Elevation	-6.832	10.188	0.450	1	0.050
	Constant (B_0)	7.282	3.630	4.025	1	0.045
5-factor model	Rainfall	-15.379	6.195	6.163	1	0.013
	Soil	-4.39	3.596	1.491	1	0.022
	Basin slope	6.468	6.962	0.863	1	0.035
	SPI	4.594	4.332	1.125	1	0.029
	TWI	1.537	2.783	0.305	1	0.048
	Constant (B_0)	1.978	1.679	1.388	1	0.024

3.3. Rainfall analysis and correlation with the consequences of a debris-flow event

As highlighted by the LR Analysis, rainfall is the main factor that triggers debris flows in catchments, corroborating several other studies (e.g., VIEIRA; GRAMANI, 2015; among many others). Debris-flow events are more common during the summer season (December – March), which is the wettest season in Southeast Brazil, where Serra do Mar and Serra da Mantiqueira are located. Figure 3.7 shows the seasonal distribution of events, with January exhibiting the largest number of debris-flow events, followed by March, February and

December. The phenomena can occasionally occur during winter season in the Southeast due to abnormally rainfall events (SELUCHI *et al*., 2011).

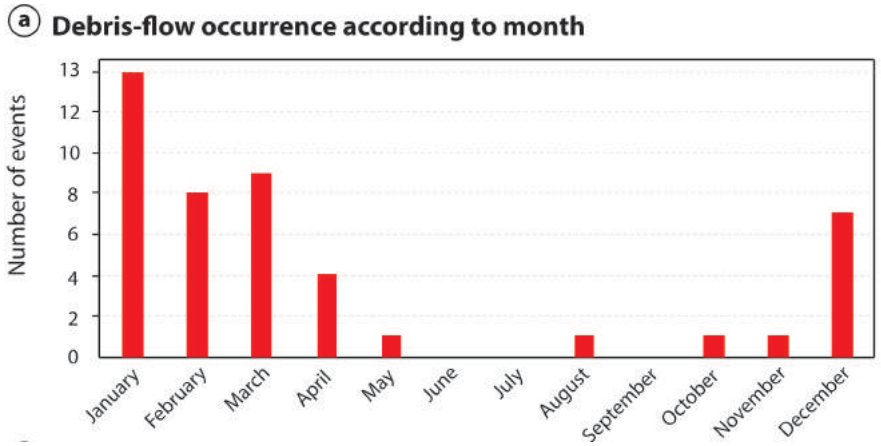

Figure 3-7: Occurrence of debris-flow according to month. Debris flows are more common in summer months (December – March).

Figure 3.8 shows the average annual rainfall indices for Brazil plotted against reported debris-flow events. Debris flows are concentrated in regions with high rainfall rates (> 1600 mm annually) that are also associated with mountain areas, highlighting the strong association between hilly areas and precipitation for their occurrence. In areas with very-high annual precipitation (> 2500 mm) and no debris-flow records, such as the North region of Brazil, the relatively flatter terrain or the remoteness of the mountain areas (e.g., Escudo das Guianas, at the border with Venezuela) can be associated to the lack of recorded events.

When looking specifically at the region of Cubatão, the rainfall patterns that have historically triggered debris flows show that the phenomena are mainly initiated by high-intensity, short-duration rainfall, as also highlighted by other studies in the region (e.g., TATIZANA *et al*., 1987; KANJI *et al*., 2007), with the rainfall accumulated 48 h prior to an event suggested as the most critical (Figure 3.9). Such pattern of short-duration/ high-intensity precipitation is also observed in other parts of the world (e.g, Taiwan, Chang et al. 2011; Japan, Fukuoka 1980; New Zealand, Selby 1976).

This pattern is highlighted in a more recent debris-flow event in Guaratuba (state of Paraná), also located in the Serra do Mar Mountain range. According to the testimonies of local farmers, the landslides that triggered the debris flow initiated between 2300 and 0000 UTC (20:00 and 21:00 Local Time – LT) by an accumulated rainfall of 188 mm in 3 hours, with maximum registered intensity of 128 mm h^{-1}, according to the nearest rain gauge data (Figure 3.10a). The recorded antecedent rainfall for the preceding 10 days is estimated at around 88 mm, 23 mm of which (26%) in the 48 hours before the event.

Precipitation recorded by the rain gauges integrated to the Brazilian pluviometer network are notably lower than what the nearest rain gauge documented, suggesting that the extreme rainfall rates were mainly concentrated near the hillslopes of Pedra Branca as a result of orographic effect. The rain gauge 'Garuva' recorded 72.8 mm in 12 h (10 km away), with a maximum intensity of 29.2 mm h^{-1}, while the rain gauge 'Estrada Geral Quiriri' (30 km away) barely recorded the event (Figure 3.10). While rainfall dynamics in the country can vary greatly according to region (SELUCHI *et al*., 2011; MARENGO *et al*., 2021), generally speaking a combination of antecedent, especially in the last 48 h, and high intensity peak precipitation (> 40 mm h^{-1}) is the main rainfall pattern that trigger debris-flow events (KOBIYAMA *et al*., 2010; DEBORTOLI *et al*., 2017).

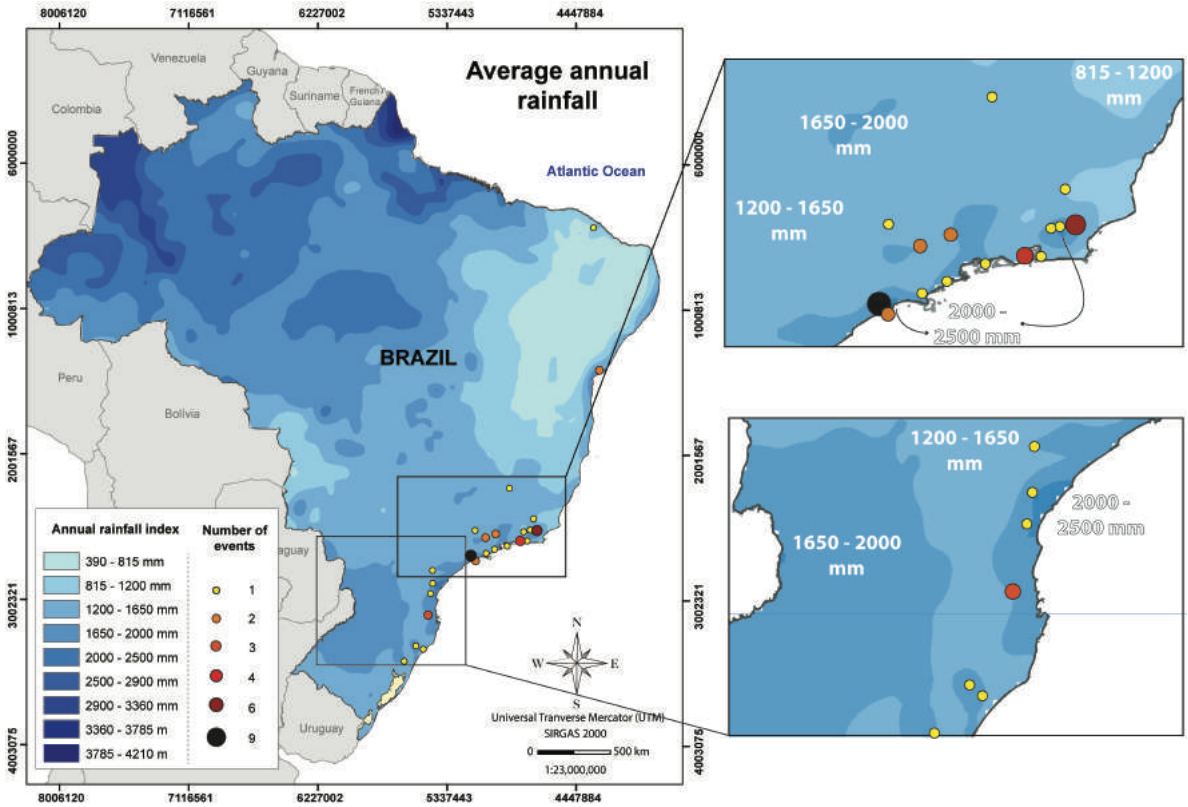

Figure 3-8. Average rainfall indices for Brazil, based on the climate data from Brazil's pluviometric atlas (CPRM, 2021). Debris flows generally occur in areas with average annual rainfall higher than 1,650 mm.

An important shortcoming in the historical analysis of debris-flow triggering rainfall is the lack of high-quality data with good resolution. Most of the pluviometers prior to 2013 in Brazil only show hourly data, when they are available. Their location can also represent an issue when determining rainfall indices, as most are located in the valley region and not at the top of the hillslopes, where landslides and debris flows initiate. Moreover, debris-flow triggering rainfall can be very localized, as demonstrated by the Guaratuba event, and the

distribution of pluviometers is usually close of urban areas and roads, challenging an accurate analysis as most are far away from the source areas.

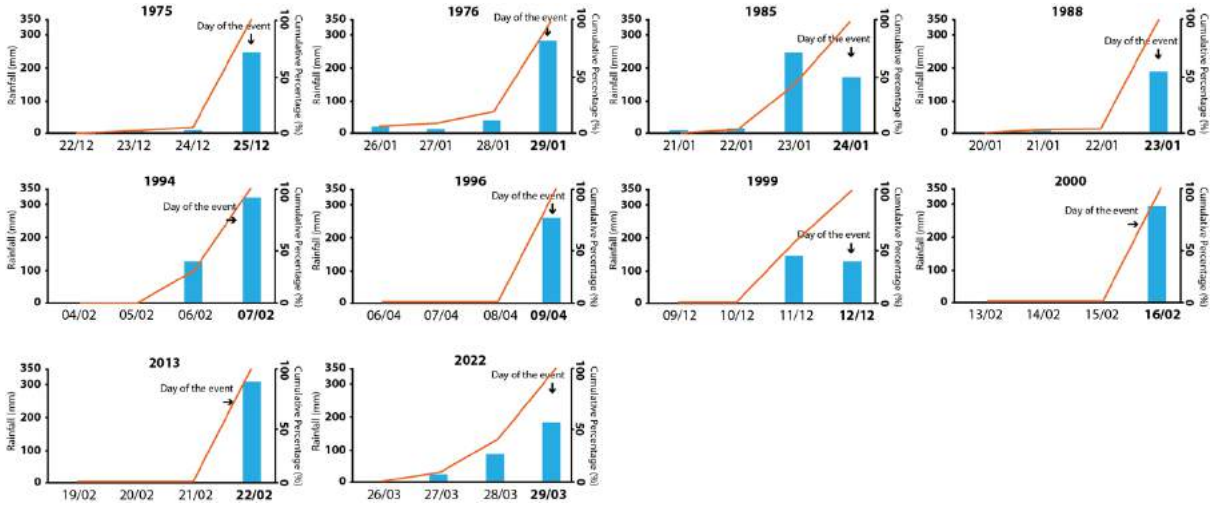

Figure 3-9. Daily rainfall indices up to 4 days (96 hours) prior to debris-flow events in the region of Cubatão (blue bars). The phenomenon's initiation is more strongly influenced by the rainfall accumulated 48 hours prior to an event, as highlighted by the cumulative percentage graph (orange lines).

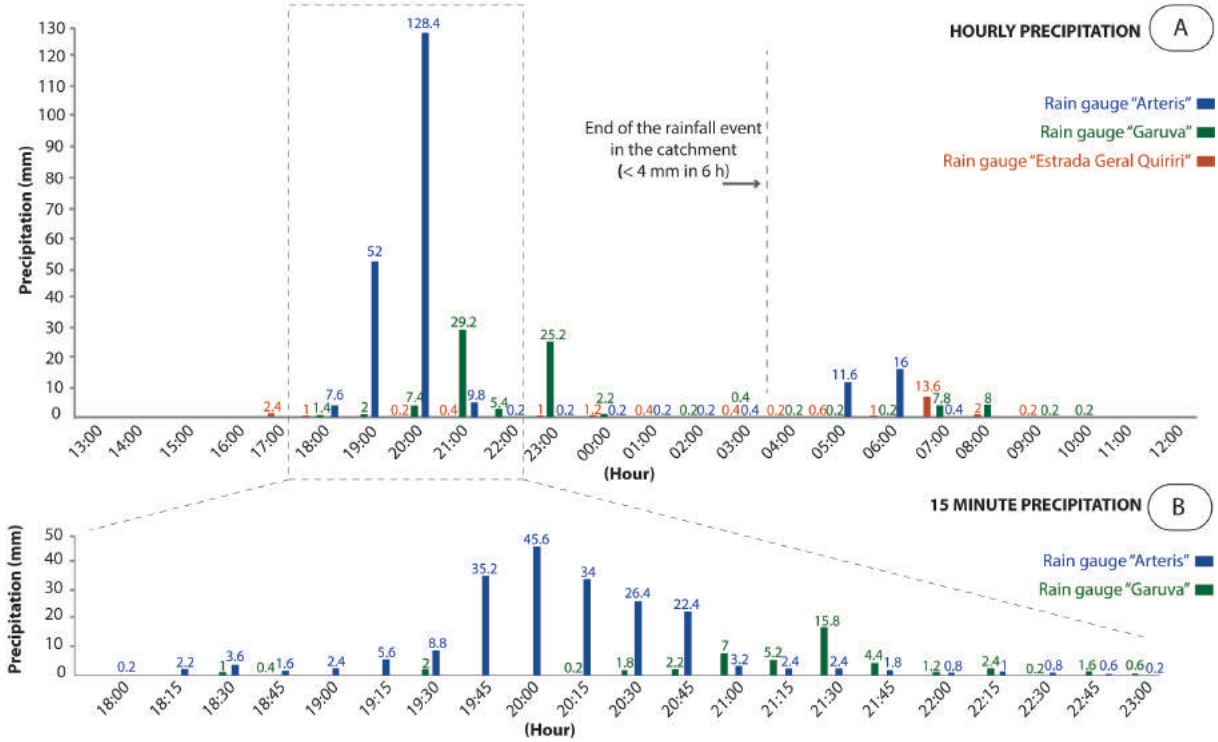

Figure 3-10. Rainfall event that triggered the February 2017 debris flow in Guaratuba (state of Paraná). A) Hourly precipitation for February 11 and 12, 2017, according to the three nearest rain gauges. Rain gauge 'Arteris' is located 1 km from Pedra Branca catchment, while 'Garuva' and 'Estrada Geral Quiriri' are located at approximately 10 km and 30 km away, respectively. B) Precipitation recorded every 15 minutes by the rain gauges 'Arteris' and 'Garuva' between 18:00 LT (2100 UTC) and 23:00 (0200 UTC).

Despite these challenges, we conducted correlations between rainfall and debris-flow impacts and magnitudes, both at a national (Paper I) and at a more local scale in the Cubatão

region (Paper III). At a national scale, comparing the 24-accumulated rainfall with reported data of magnitude, economic losses and fatalities, we can observe a very weak relationship between rainfall and these variables. The relationship between 24-h accumulated rainfall and magnitude, fatality number and economic losses show, respectively, a Spearman correlation coefficient of -0.01 (p-value of 0.52), 0.01 (p-value of 0.51) and -0.25 (p-value of 0.81) (Figure 3.11). In this analysis, the 24-h accumulated rainfall was chosen due to a more consistent historical report of the precipitation data than the 48 h.

When peak rainfall intensity (hourly precipitation) is considered, a stronger positive correlation with magnitude and number of fatalities is observed. The relationship between hourly rainfall and magnitude shows a positive Spearman correlation coefficient of 0.7 (p-value of 0.91), while the relationship between fatality cases and hourly rainfall shows a positive Spearman correlation coefficient of 0.36 (p-value of 0.81). The correlation between daily rainfall and economic losses, on the other hand, is weaker, with a negative Spearman correlation coefficient of -0.2 (p-value 0.63) (Figure 3.11).

Even though hourly rainfall (peak intensity) showed a stronger correlation with magnitude and the number of fatalities, the small sample space of events with complete data of all the considered variables challenges a concrete conclusion about their relationship. It is expected, however, that the more intense the rainfall, the larger the event and, consequently, the larger the associated damage. The available rainfall data, however, is not sufficient to indicate a clear relationship between rainfall indices and these variables. These results can potentially indicate that the damage related to debris-flow events is not only a function of rainfall, but also to social (e.g., urbanization levels, occupation of risk areas) and geomorphic (e.g., vegetation cover, catchment and channel slope, in-channel material) factors.

The effect of the geomorphic aspects on debris-flow development can also be observed when rainfall is correlated with the characteristics of the events that occurred in Cubatão. Considering the effect of the 48-h accumulated rainfall on the volume of material mobilized in the slopes, a positive Spearman correlation between rainfall and landslide magnitude is observed for both 1985 (0.62) and 1994 (0.81) events, highlighting the direct effect of rainfall over slope failure. However, when the effect of rainfall on debris-flow magnitude is considered, such relationship is weaker, showing a low positive Spearman correlation index both for the 1985 event (0.3) and for the 1994 event (0.51) (Figure 3.12). These results can potentially indicate the strong influence of entrainment on debris-flow magnitude in the region, which can potentially also be extrapolated for other mountain areas in Brazil.

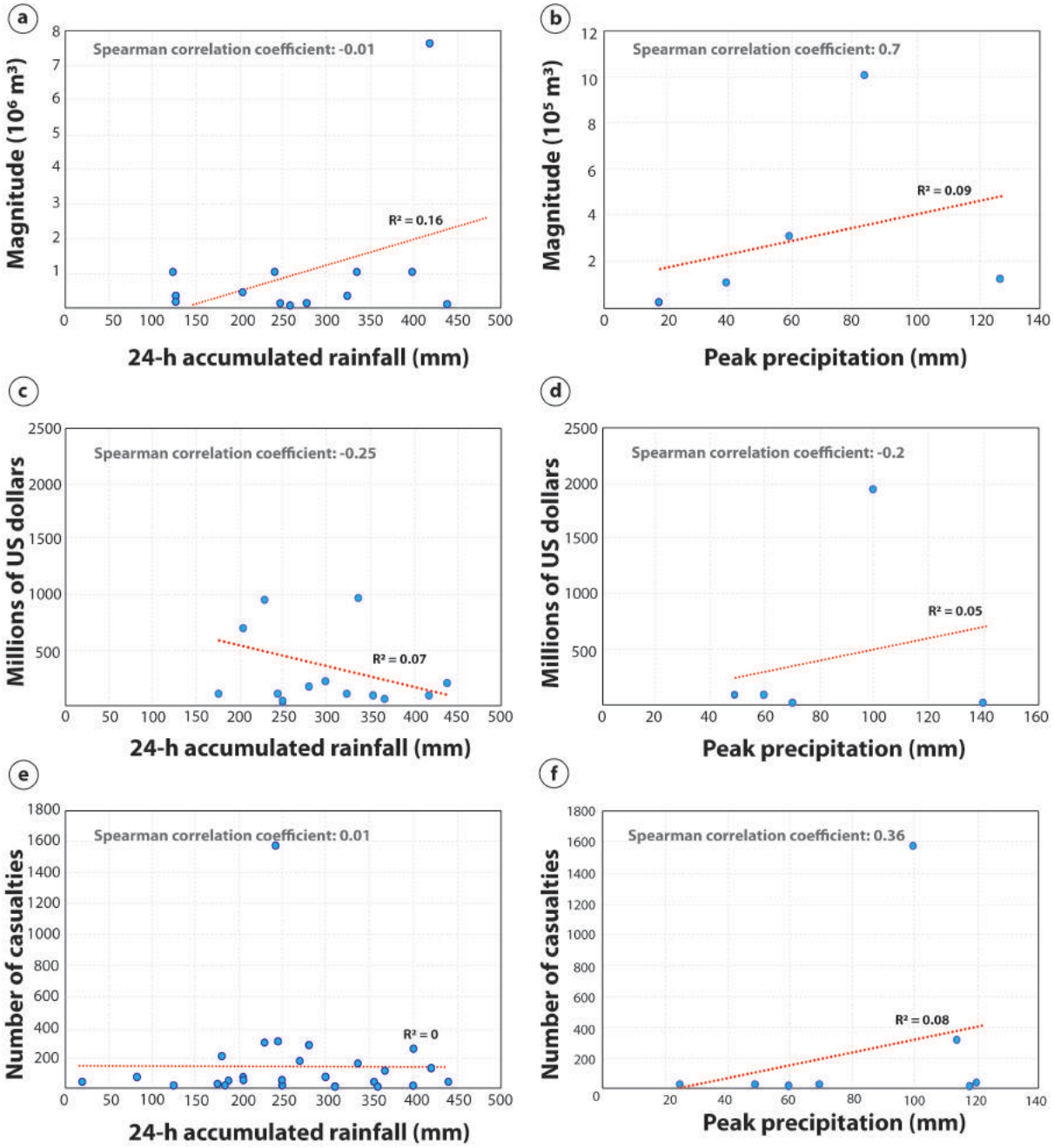

Figure 3-11. Rainfall analysis. a) Relationship between 24-h accumulated rainfall and magnitude. B) Relationship between hourly rainfall and magnitude. C) Relationship between daily rainfall and economic losses. D) Relationship between hourly rainfall and economic losses. E) Relationship between 24-h accumulated precipitation and number of fatalities. F) Relationship between hourly rainfall and number of fatalities.

Consequently, in a possible implementation of an Early Warning Systems in debris-flow prone areas, field information about the catchments should also be considered, due to the intense in-channel debris accumulation that can be remobilized in future events. Moreover, the hazard zonation must also be considered in Early Warning Systems implementation, as it identifies the most sensible areas that should be evacuated/attended first and where preventive measures, such as retention structures, should be installed.

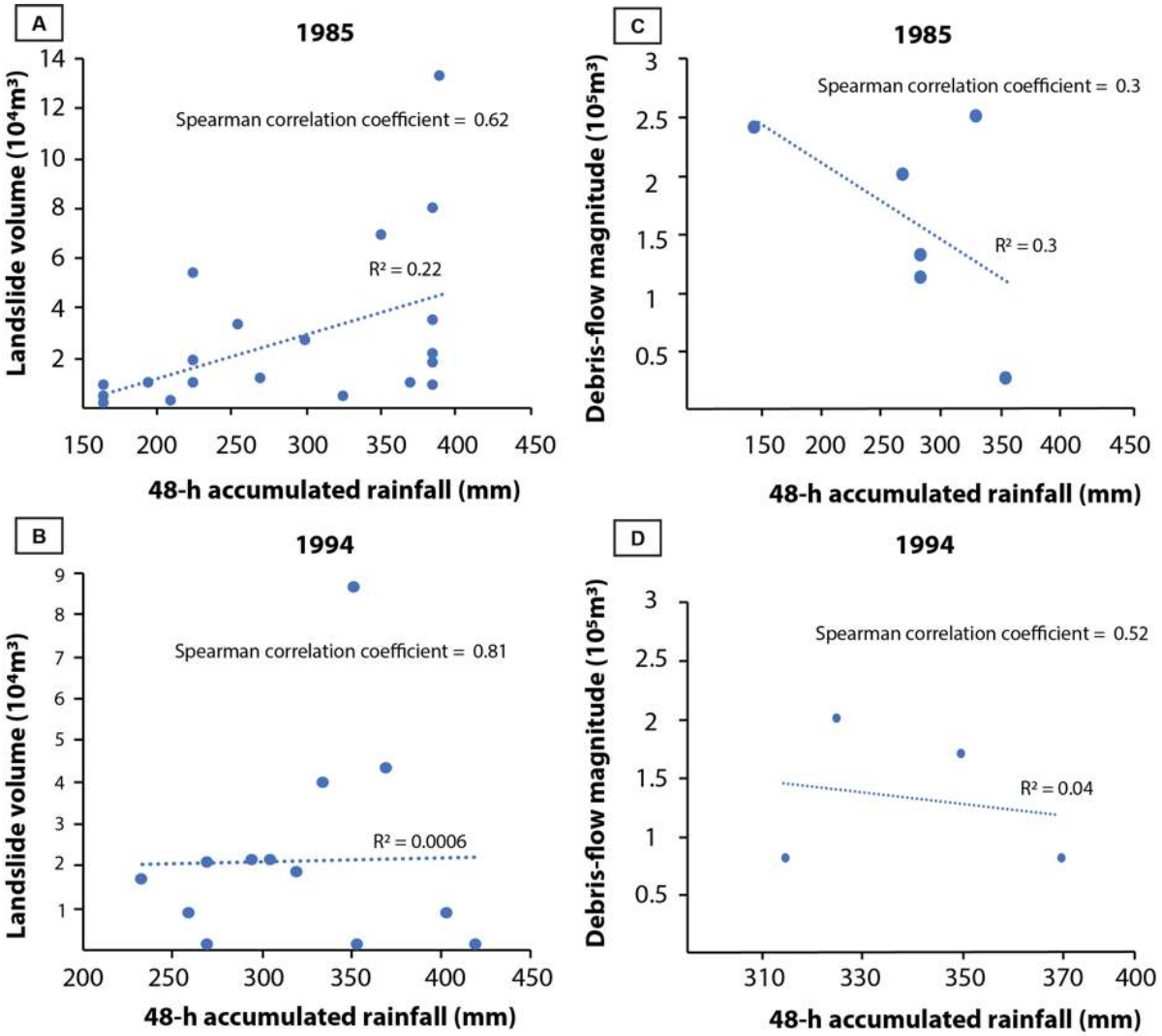

Figure 3-12. Correlation between rainfall and landslide volume (left) and rainfall and estimated debris-flow magnitudes (right), for the catchments located in Cubatão. The correlation is based on data from the 1985 and 1994 landslide and debris-flow events and the different rainfall indices are based on the spatial distribution of the rain event in the region. A) Correlation between 48-h accumulated rainfall and landslide volume – 1985. B) Correlation between 48-accumulated rainfall and landslide volume – 1994. C) Correlation between 48-h accumulated rainfall and estimated debris-flow magnitude – 1985. D) Correlation between 48-h accumulated rainfall and estimated debris-flow magnitude – 1994.

3.4. A detailed field characterization of a debris-flow event

We conducted a comprehensive characterization of the debris-flow event that occurred on February 2017 in the Pedra Branca catchment (Guaratuba, state of Paraná) (Figure 3.13), to characterize the main geomorphological features of a debris flow in Brazil, as well as to estimate important kinematic parameters, such as magnitude, peak discharge and velocity (we refer Paper II). The debris-flow event was triggered by three large landslides, which have their upgradient portions in moderate slopes (38% to 61%, or 21º to 31º). The mobilized material

were mainly residual soil and large wood, which suggest loss of suction as the initiation mechanism at the study area. The debris flow was initiated by first-time movements in the hillslopes, but also carried material (colluvium) from previous landslides, accumulated in upper portions of the channel.

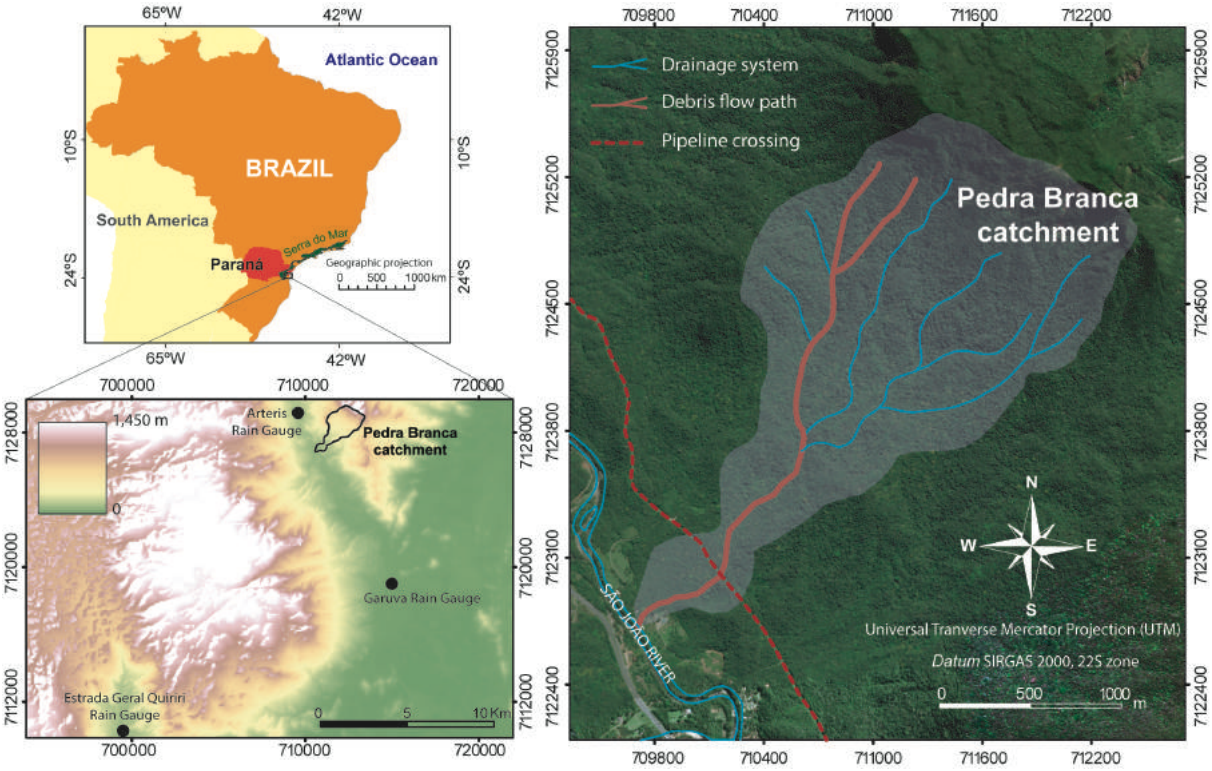

Figure 3-13. Pedra Branca catchment (right) in the municipality of Guaratuba, State of Paraná, Brazil. At the top left, the extension of the Serra do Mar mountain range. At the bottom left, the Digital Terrain Model (DTM) for the broader region of the catchment with the location of the three nearest rain gauges.

The channelization of the material mobilized by the landslides contributed to a magnification of the erosional process, with a pronounced entrainment and scour of debris in the upstream section of the channel. Erosion of the channel bed, lateral slopes and banks by the debris flow progressively decreased towards the outlet region, ranging from an average depth of 3 m at the upstream section to 0.3 m downstream. In bedrock exposed areas, erosion depth was assumed as 0 and these areas are mainly located in steep portions of the channel, near the initiation area and in knickpoints.

In-channel debris in the upstream section consists mainly of large monzogranite boulders (2 to 5 m in diameter), deposited at the perimeter of the flow route or exhumed from colluvial deposits of the lateral slopes (Figure 3.14a). In-channel debris accumulation becomes more frequent towards the catchment's outlet, with the largest volume of debris deposited in the middle portion of the channel (Figure 3.14b) where the average slope is 18.2% (10.3º), i.e.,

within the range of deposition angles for channelized debris flows (from 14% to 21%) (IVERSON *et al*., 2011). Debris deposition also occurs in the downstream portion of the catchment, although with smaller-sized boulders (<2 m in diameter) and less voluminous deposits than in the middle portion (Figure 3.15c). Recent in-channel debris deposits are easily identified from colluvial deposits due to the lack of pedogenetic evidences and the mixture of fresh wood and stony debris (Figure 3.14d).

Large wood (LW) deposition and accumulation, differently from stony debris, is more frequent in the downstream section of the channel. In this section, the influence of LW in the debris-flow evolution is prominent, with evidences of LW jams that were broken by the flow passage (Figure 3.15a). Debris dams (i.e., areas with intense debris deposition, blocking partially the flow) are observed along the channel and are in their majority clast supported with woody debris (Figure 3.15b), often exhibiting reversely graded patterns. The occurrence of these dams indicates that the debris flow had multiple surges, which is confirmed by the affected farmers that report at least four surges.

The imbricated boulders along the channel's length and the intense debris accumulation along in the middle section of the channel suggest that the event started as a debris flow, evolving into a debris flood as channel slope decreased. In the outlet region, according to testimonies, the flow consisted mainly of muddy water (with sand, silt, clay) mixed with woody debris (Figure 3.14e) and, minorly, by stony debris of up to 1 m. These characteristics indicate that in the final stages the event exhibited characteristics of a flash flood.

The average post-debris-flow width of the channel is ca. 20 m, ten times the previous average width (ca. 2 m) reported by testimonies. No prominent alluvial fan is formed, due to narrow valley and discharge to the larger São João river (Figure 3.14e). In the São João river, large deposits of coarse sand are cobbles are accumulated near the Pedra Branca outlet (Figure 3.14f), as well as small to medium-sized boulders (< 1.5 m in diameters) on the river channel.

Figure 3-14. A) Pronounced erosion and scour of channel bed is observed at the upstream section – 1.8 m human profile for scaling. B) Intense accumulation of debris at the middle section– in detail, a 1.75 m human profile for scaling. C) Accumulation of debris at the downstream section, with smaller sized-boulders than in the middle section - 1.75 m human profile for scaling. D) Reversely graded pattern observed in debris dams. E) Debouchment of the Pedra Branca river into the São João River, where flow height reached up to 2 m. F) São João river, which received sediments from the Pedra Branca debris flow (photo from August 2017).

The mapping of erosional and depositional areas along the Pedra Branca channel is shown in Figure 3.16, based on orthophotos acquired using Unmanned Aerial Vehicle (UAV). Even though debris deposition generally occurs in areas with gentler slope, a direct correlation between these two factors is not observed, with a very weak Spearman correlation coefficient (0.025) and regression line with very low R^2 (0.002) (Figure 3.17a and 3.17c). Debris deposition, therefore, might be influenced by other factors, such as valley width, presence of obstacles and availability of coarse material itself, which can further be related to a less

voluminous deposition in lower reaches of the channel, which show gentler slope angles than in intermediate reaches.

Erosion depth, on the other hand, shows a positive correlation with slope, being deeper near steeper portions of the channel (Figure 3.17b). Excluding areas where bedrock exposure is observed, a correlation between slope and erosion depth shows a weak/moderate positive spearman coefficient (0.39) and a regression line with a weak to moderate R^2 (0.3149) (Figure 3.17d). Hence, erosion is moderately influenced by slope, which can further be associated with a higher momentum of the flow's passage in steeper reaches of the channel. The exclusion of bedrock exposed reaches in the correlation is due to a different incision dynamic than at alluvial-colluvial reaches.

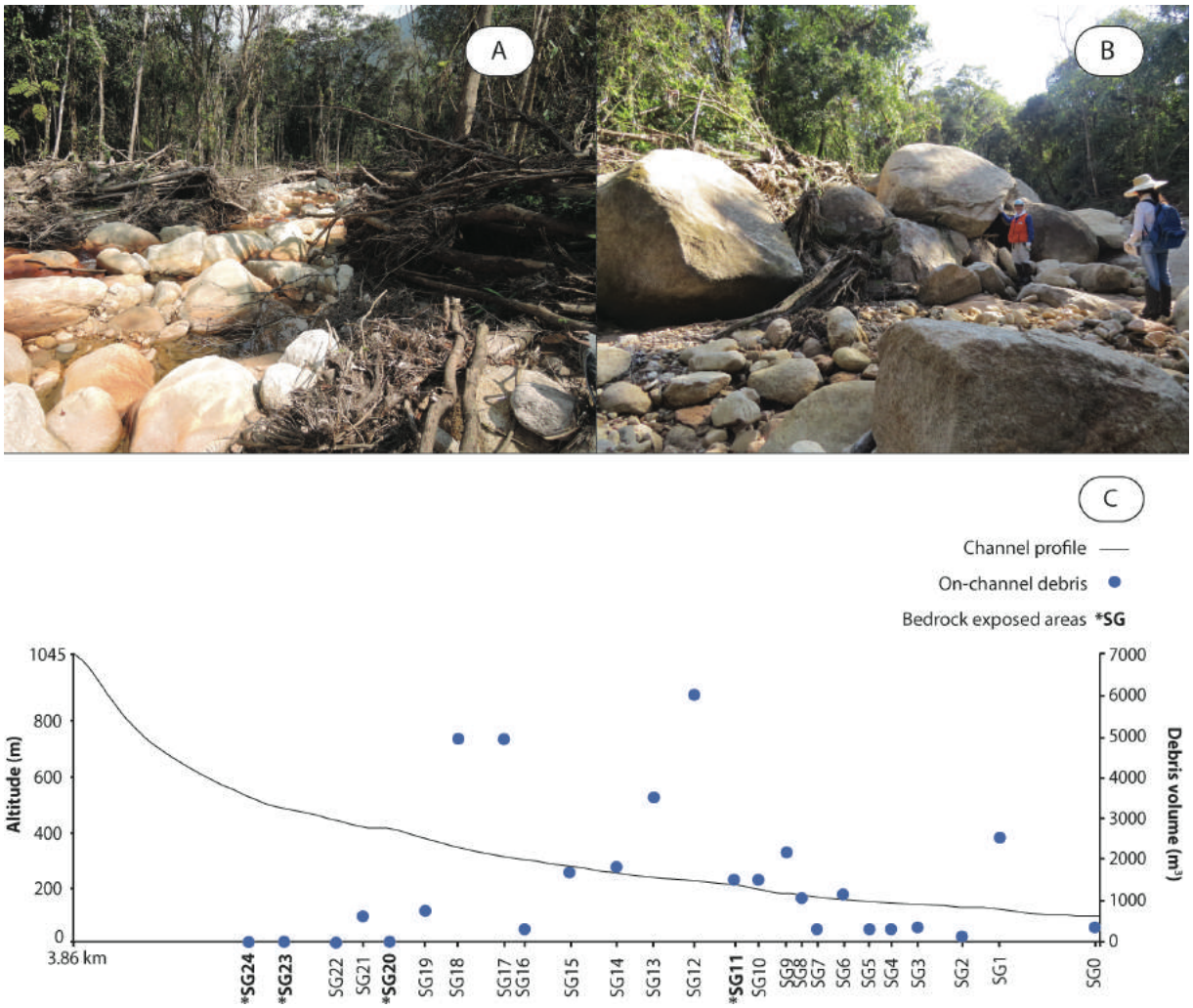

Figure 3-15. Debris deposition and jam formation. A) Large wood forming a jam that was later broken by the flow's passage (SG1). B) Mixture of woody and stony debris and formation of debris dams (SG12) – 1.75 m human profile for scaling. C) Plot showing the Pedra Branca channel profile and the volume of deposited debris along the debris flow route. Debris deposition is higher in the middle section of the channel (SG19 to SG11).

The distribution of maximum grain size (D_{90}) of debris along the debris-flow path shows that debris size decreased by approximately 80% along its trajectory (Figure 3.17e). Sharp reductions in D_{90} along the channel are related to regions where intense debris deposition is observed. Flow heights are generally higher in regions downstream to knickpoints in the channel, with the debris flow reaching a peak height of 7 m (Figure 3.17f). At the debouchment into the larger São João river, flow heights were up to 2 m (Figure 3.17f). Flow height can be affected by areas with intense debris accumulation, which can partially block the flow and raise the flow level. To minimize the uncertainties related to forensic discharge estimations, we documented flow heights in areas that were not directly affected by the intense accumulation of stony and woody debris.

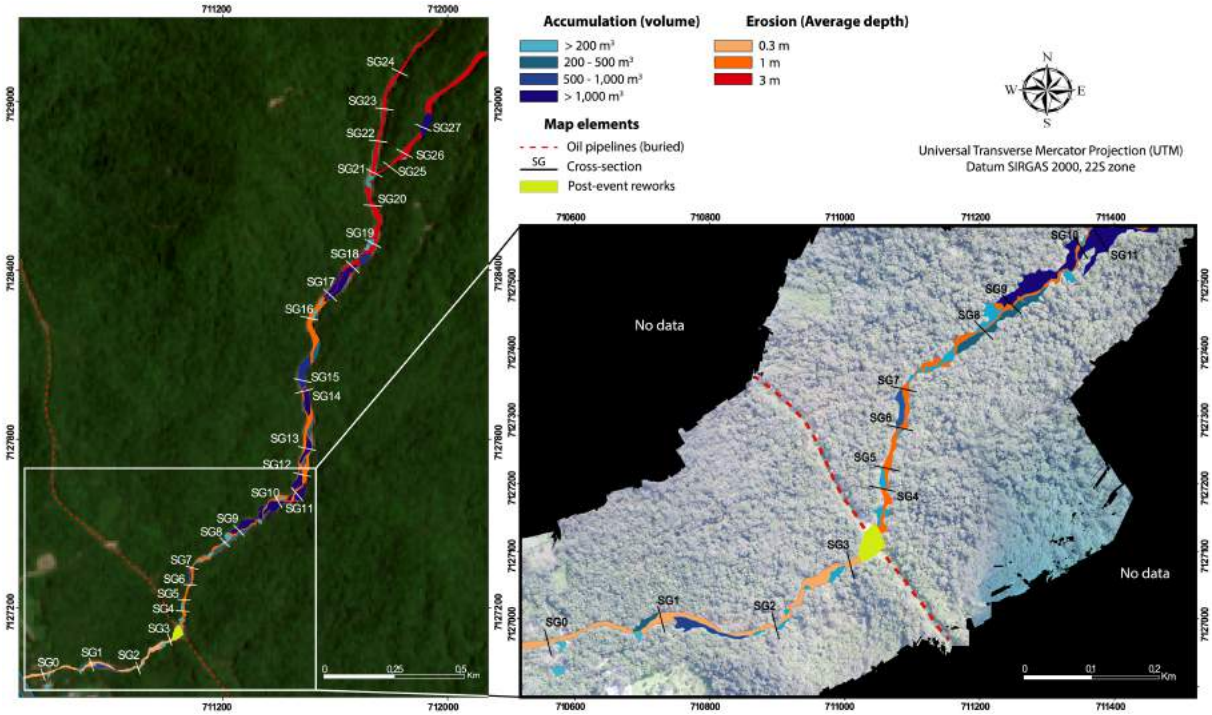

Figure 3-16. Mapping of entrainment and deposition areas based on the orthophotos acquired using UAV. Areas in shades of blue represent debris-accumulation areas and areas in shades of red represent entrainment areas.

The total volume of the debris flow (V_t) is estimated at approximately 120,195 m^3, based on the mapping of entrainment and deposition areas (Figure 3.16) and on the landslides that initiated the event (Figure 3.18). Volume entrained by the flow (V_e) is estimated at 121,037 m^3, while the volume of debris deposited along the debris flow path (V_d) accumulates to 36,688 m^3. The three landslides that initiated the event contributed with 35,846 m^3 of earth material. The largest landslide scar contributed with 22,497 m^3, while the other two contributed with 7,573 m^3 and 5,776 m^3, assuming an average depth of 1 m and that the totality of the material reached the channel. Despite the uncertainties associated with erosion depth at the study area,

due to the unknown channel morphology before the event, it is evident that entrainment significantly increased the total magnitude of the process, representing more than 75% of earth material input.

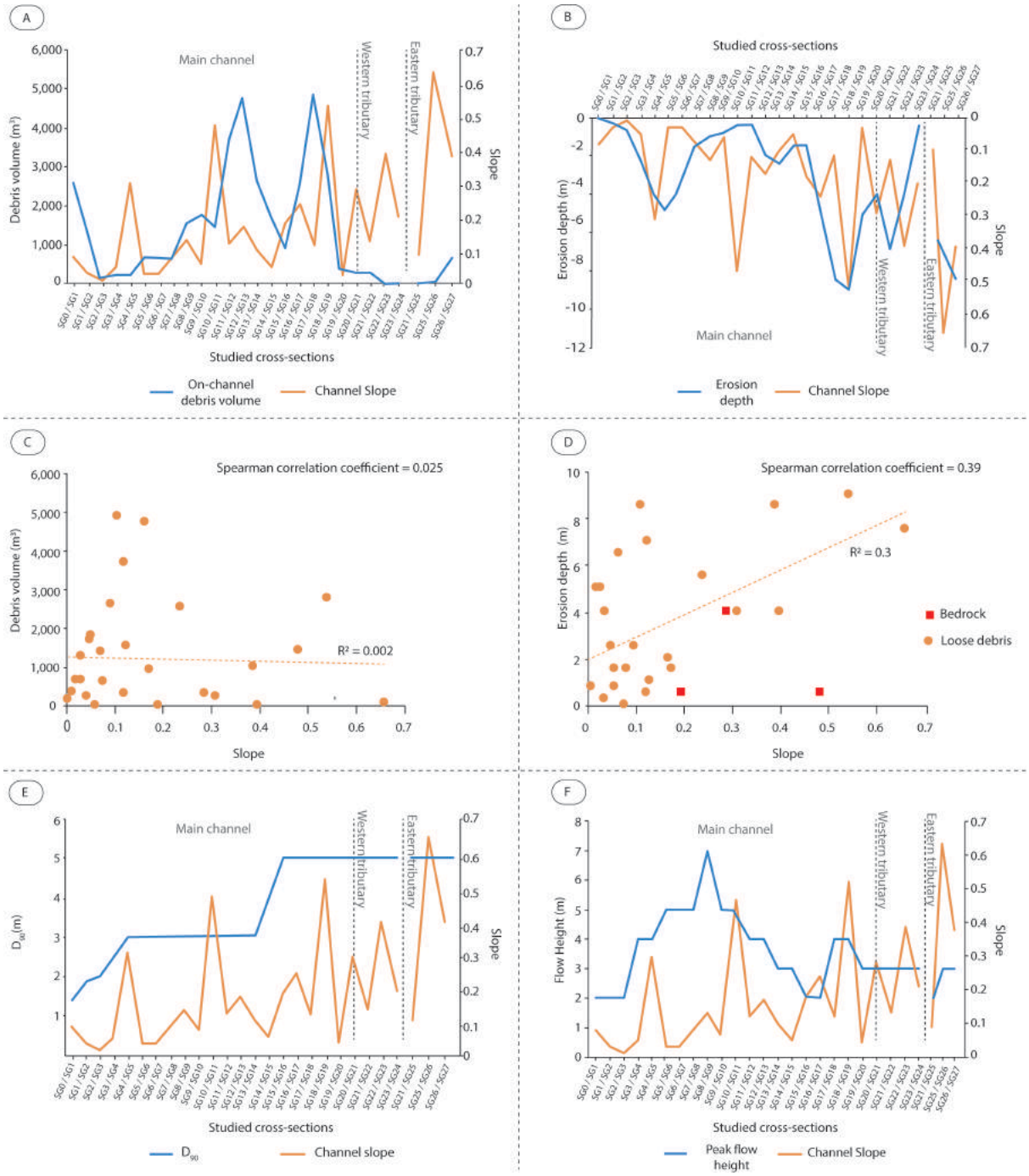

Figure 3-17. Characteristics of the 2017 debris flow. A) Distribution of on-channel debris volume along the debris flow path in relation to channel slope B) Erosion depth distribution along the debris flow path in relation to channel slope C) Scatterplot showing the relationship between on-channel debris volume and channel slope. D) Scatterplot showing the relationship between erosion depth and channel slope. Bedrock and loose debris refer to the on-channel material post-event. E) Maximum debris size (D_{90}) distribution along the debris flow path in relation to channel slope (measured between every two cross-sections). F) Peak flow height distribution in relation to channel slope.

Our estimations, therefore, suggest that the February 2017 debris flow had a large magnitude, within the range of the size-class 5 (10^5 – 10^6 m^3) proposed by Jakob (2005b). Size-class 5 debris flows can destroy parts of villages and infrastructures, destroy forest of up 2 km^2 and block creeks and rivers (JAKOB, 2005b).

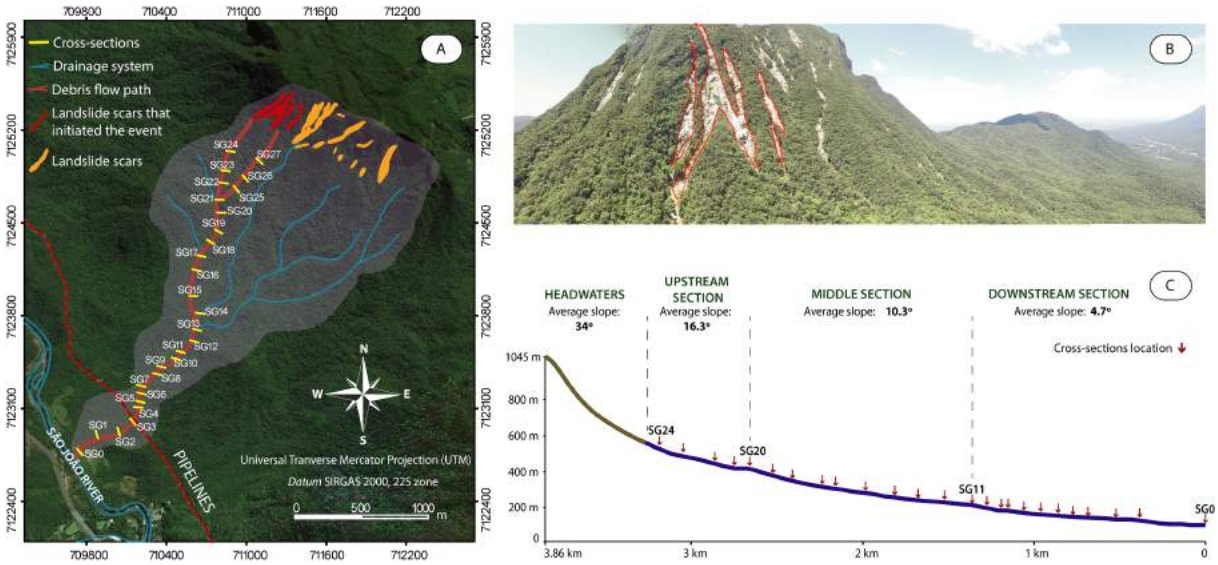

Figure 3-18. A) Location of the 28 cross-sections made along the debris-flow path that supported the magnitude estimation. B) Overview of the headwaters' region of the catchment, highlighting the three landslide scars that initiated the debris flow. C) Longitudinal profile of Pedra Branca catchment with the tentative location of the cross-sections. Channel in blue and slopes in brown.

Peak discharge (Q_{max}) is calculated based on the equation described in Jakob (2005a), as function of the product between the maximum cross-sectional area (A_{max}) of the channel and the mean cross-sectional velocity (v_f). The velocity is calculated following the Manning-Strickler equation, using the manning coefficient of 0.07 $m^{1/2}s^{-1}$ for bedrock rivers in mountain regions (ARCEMENT; SCHNEIDER, 1989; TAKAHASHI, 2006).

Highest discharge and velocity rates are, as expected, observed where channel slope is the steepest and cross-sectional area one of the largest. Discharge, in general, is higher in the immediate region downstream to the initiation area and in the confluency of the two tributaries (Between SG21 to SG17, Figure 3.19), progressively decreasing towards the outlet region (Figure 3.19). Velocity rate patterns are similar to the discharge (Figure 3.19).

It is important to point out, however, that the concurrence of debris flows and debris/flash floods might increase the uncertainty over peak discharge estimations, due to an alteration of the channel cross-section stability with the passage of large sediment volume (AMPONSAH *et al*., 2016; DESTRO *et al*. 2018).

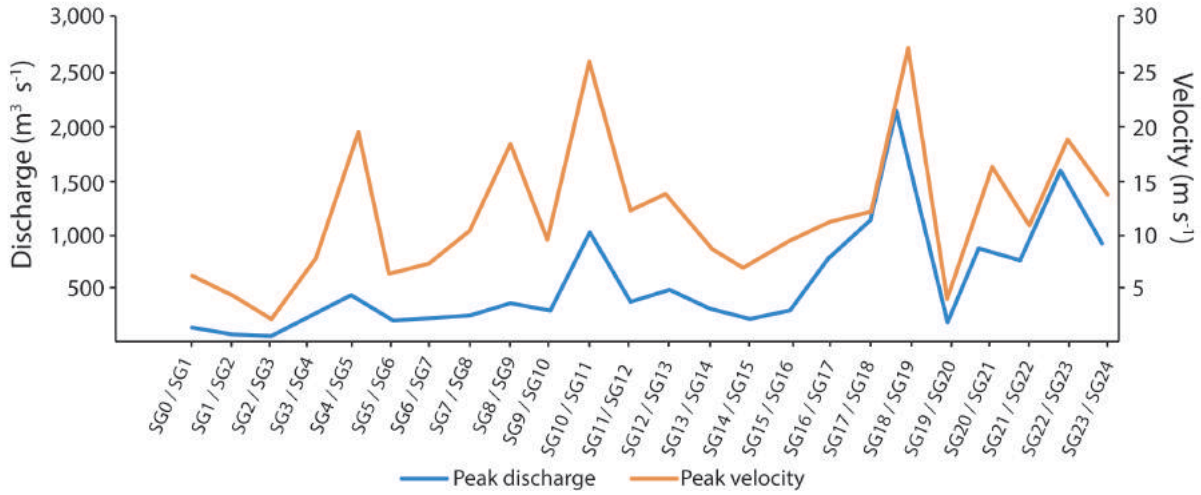

Figure 3-19. Discharge and flow velocity pattern along the debris flow path.

Debris-flow initiation is not controlled solely by rainfall, as it also depends on debris supply and recharge rate, which influences the magnitude and the frequency of new events in a catchment. The debris flow in the Pedra Branca catchment had a magnitude of approximately 120,000 m^3, thus a large debris flow. According to Jakob (2005b), such magnitude for a boulder-rich debris flows is atypical, although the statement could be biased due to the general lack of magnitude studies worldwide, especially in mountain areas where debris-flow studies are still incipient. In the Serra do Mar region, based on the few available magnitude estimates (e.g., KANJI *et al*., 2007; KOBIYAMA *et al*., 2015), a 10^5 m^3 debris flow is what is usually reported, probably also due to a bias towards reporting and characterizing only larger events and the lack of studies aiming at specifically estimating debris-flow magnitude.

3.5. Differences and similarities of debris-flow prone catchments at Serra do Mar

As pointed out by our historical analysis and other studies in the literature, Serra do Mar is the main site of debris-flow occurrence in Brazil. The initiation of rainfall-triggered debris flows in the region can generally be summarized in three stages, as Lacerda (2007) suggests: (1) rainfall infiltration in the soil that leads to (2) slope failure(s), which further (3) triggers a channelized debris flow. The main process associated with slope failure in the hillslopes of Serra do Mar is loss of suction due to rain infiltration (LACERDA, 2007).

High- to extreme-precipitation events often occur over Serra do Mar catchments (VIEIRA; GRAMANI, 2015), which can trigger large shallow landslides that initiate debris flows in isolated gullies (Figure 3.20a), often remaining unreported. An example is the

February 2017 debris-flow event in Guaratuba (South Brazil), discussed in the previous chapter. The debris flow was triggered by three large landslides (Figures 3.18), which initiating mechanism is interpreted as loss of suction (we refer Paper II). In the region of Cubatão (Southeast Brazil), an example of such an event is the 1975 debris flow in one of the streams of catchment 1 (Figure 3.6), triggered by shallow landslides in the headwater's region (Figure 3.20b).

"Shock wave", due to the impact of falling rock boulders, is another mechanism that can trigger debris flows in the Serra do Mar region (LACERDA, 2007), as well as dormant landslides, which material can accumulate in upstream reaches and be reactivated by primary landslides or rockfalls in the hillslopes. Debris flows initiated solely by the increase of the discharge in the channel, leading to the mobilization of in-channel material, is not yet reported in Brazil, which can be attribute to the lack of monitoring of catchments prone to the phenomenon.

Large-magnitude debris-flow events (> 10^5 m^3), such as those in 1985 and 1994 that occurred in Cubatão, are usually characterized by multiple source areas (landslides, rockfalls, in-channel material), both at upstream and middle reaches of the channel (Figure 3.21a). In-channel debris accumulation is an important characteristic that is common in both regions analyzed in this research, which can contribute to increasing the severity of debris flows as these debris' deposits can be remobilized by new events. In-channel debris accumulation can be observed in upstream (Figure 3.21c), middle (Figure 3.14b and Figure 3.20c) and downstream (Figure 3.14f) reaches of catchments, suggesting that these materials are leftovers from past-debris flows (such as the case for Guaratuba) or from recent, localized slope failures along the channel that were not mobilized.

The differences in the initiation mechanism of a debris flow in a catchment is directly related to the geological and morphometric characteristics of each region. For instance, Pedra Branca catchment has a very steep headwaters' region, with gentler side slopes in the intermediate and lower channel reaches. Catchments at the northern slope of the Mogi River in Cubatão (Figure 3.6), on the other hand, show steep side slopes in upper, intermediate and (often) lower reaches of the channel.

As pointed out earlier, both regions exhibit intense in-channel debris deposition, especially of large rock boulders (>1 m). The in-channel boulders in Cubatão are more sharp-edged when compared to the more round-edged in Guaratuba, which can be related to differences in lithology type (mainly Granite in Guaratuba; mainly Gneiss and Schists in Cubatão). This can also be related to the travel distance from the source areas, with boulders

traveling a longer distance from the headwaters' region (i.e., source area) in Guaratuba, while in Cubatão the boulders in middle and lower reaches can also come from side slopes.

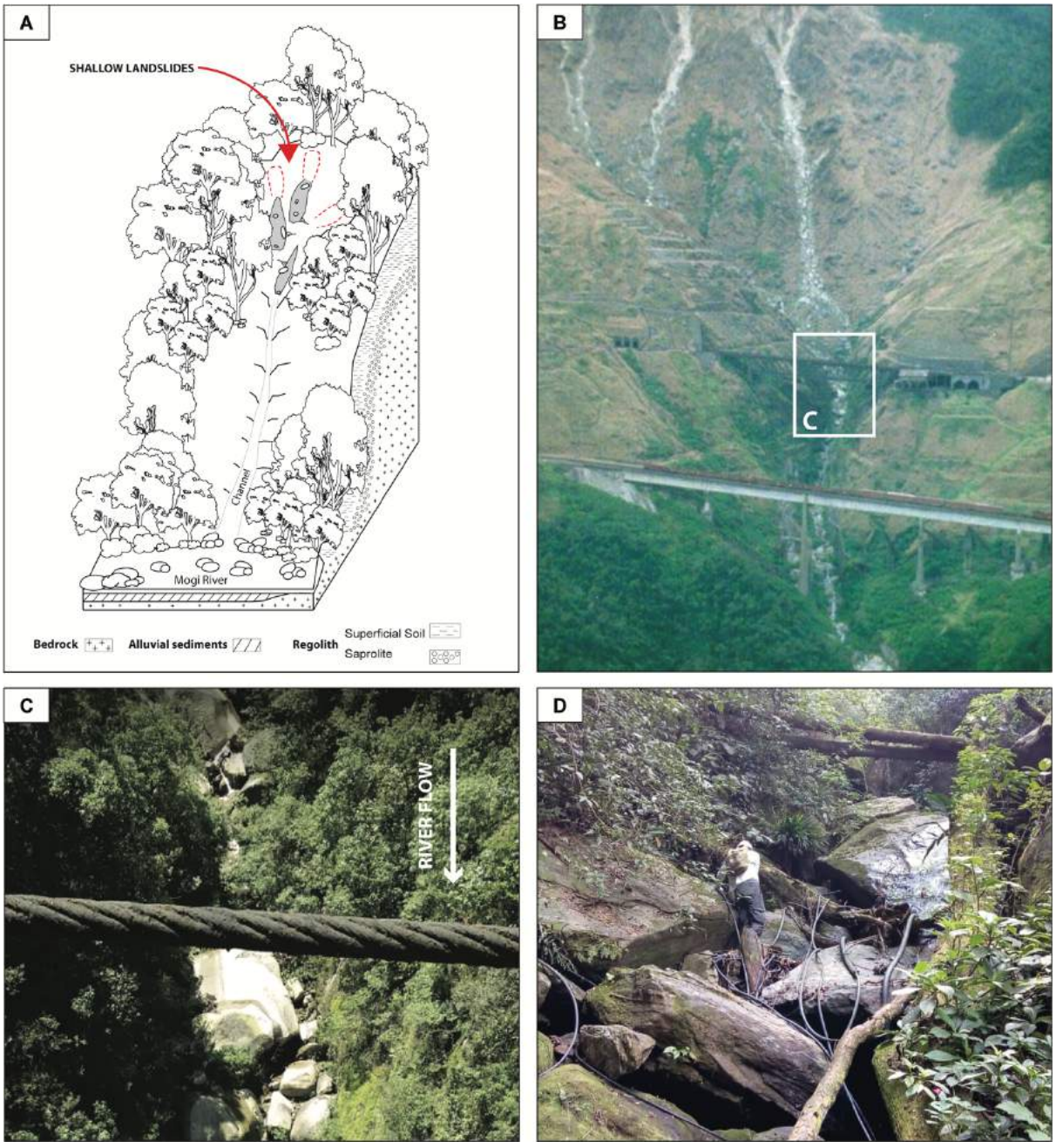

Figure 3-20. Debris-flow dynamics. A) Scheme of a debris flow in gullies/catchments, triggered by shallow landslides in the headwaters' region. B) the 1975 debris-flow event that occurred in one of the streams of catchment 1 in Cubatão. Photo from Prof. Dr. Milton Kanji, retrieved from Gramani (2001). C) Overview of the stream where the 1975 debris-flow event occurred, showing intense accumulation of rock boulders in the channel (Coordinates: 365926.79 m E, 7368058.54 m S). D) Upstream view of catchment 20 in Cubatão, showing intense stony debris accumulation in the channel, as well as Large Wood (Coordinates: 350665.03 m E, 7358314.49 m S).

The evaluation of the morphometric parameters of the catchments in these two different regions can further contribute to understanding their differences and similarities. Tables 3.6

and 3.7 show the main morphometric parameters of the catchments in Cubatão and Guaratuba, respectively, which are more commonly used in debris-flow studies worldwide (e.g., WILFORD *et al*., 2004, KOVANEN; SLAYMAKER, 2008, ILINCA, 2021; DIAS *et al*., 2022; among many others). These parameters are: Catchment Area, Relief Ratio, Catchment Relief, Drainage Density, Length and Melton Ration.

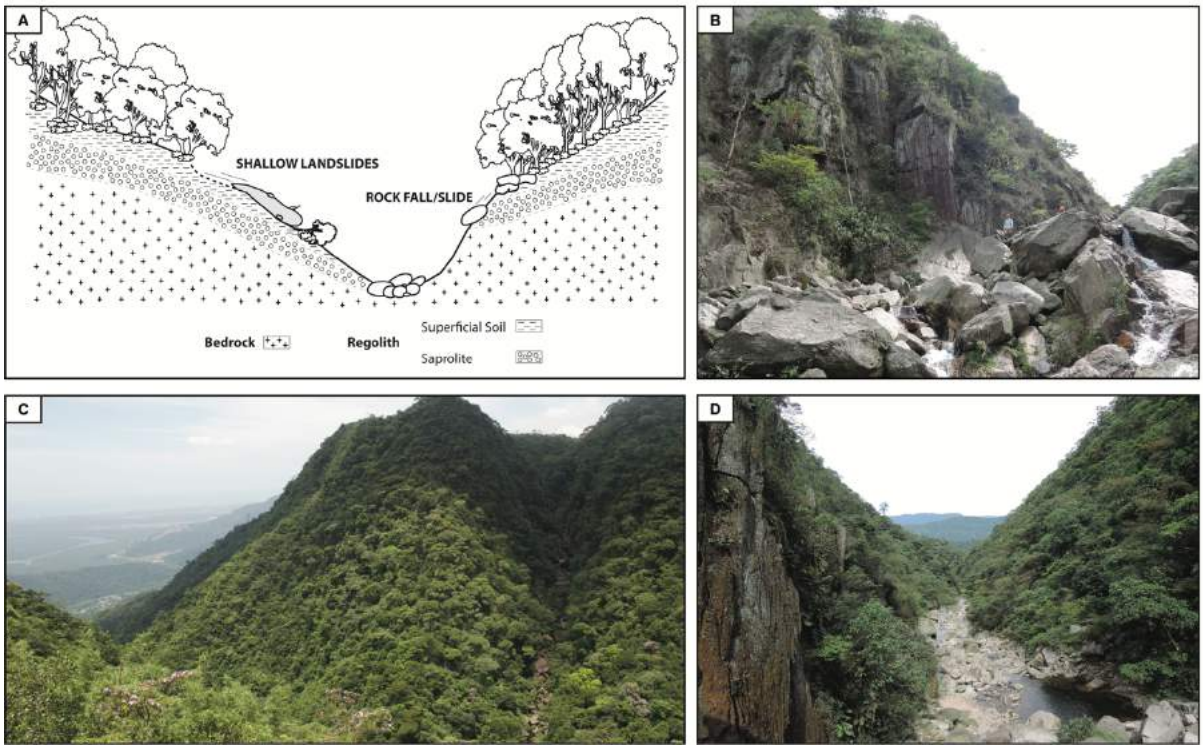

Figure 3-21. Debris-flow dynamics. A) Scheme of the initiation mechanism of the 1985 and 1994 debris-flow events in Cubatão, characterized by multiple source areas. B) Upstream view of catchment 7 in Cubatão, showing intense stony debris accumulation in the channel, as well as fractured bedrock outcrops in the margins (Coordinates: 360256.69 m E, 7367963.72 m S) C) Overview of the upstream section of catchment 19 in Cubatão, showing intense stony debris accumulation in a channel. A strong structural control is observed in the catchment (Coordinates: 350847.96 m E, 7360336.15 m S). D) Downstream view of the upstream section of catchment 7 in Cubatão, showing area with less accumulation of debris in the channel. Areas with intense stony and woody debris deposition are intercalated with areas with few accumulations along the catchment, suggesting that smaller debris-flow might have occurred more recently in small gullies or that slope failures occurred but did not trigger a debris-flow event, accumulating the material in the channel. (Coordinates: 360256.69 m E, 7367963.72 m S).

Generally speaking, debris-flow prone catchments have an area up to 10 km^2 (SLAYMAKER, 1990) and, on average, both Cubatão and Guaratuba show similar catchment area (ca. 3 km^2). A catchment area of 3 km^2 is what is also observed in other catchments in the Serra do Mar region where debris flows occurred (Table 3.8) and it is within the range of other debris-flow prone catchments worldwide (Table 3.8).

Table 3-6. Morphometric parameters of the catchments located in Cubatão (Southeastern portion of Serra do Mar). Catch. = Catchment.

Catchment	Area (km^2)	Relief ratio	Catch. Relief (km)	Drainage density (km/km^2)	Catch. Length (km)	Melton Ratio
1	1.4	0.51	0.98	1.09	1.91	0.25
7	5.39	0.23	0.75	2.04	3.33	0.32
9	2.94	0.33	0.94	1.42	2.86	0.55
10	4.9	0.28	0.96	2.34	3.42	0.43
12	2.1	0.37	0.8	2.73	2.19	0.53
14	7.19	0.19	0.75	0.88	3.85	0.13
15	2.75	0.24	0.73	1.93	3.06	0.32
16	5.3	0.23	0.74	1.22	3.193	0.44
17	3.53	0.28	0.8	3.74	2.87	0.43
19	1.86	0.35	0.7	4.72	2.01	0.51
20	2.12	0.43	0.76	2.31	1.76	0.52
Average	3.29	0.3	0.71	1.93	2.417	0.42

Table 3-7. Morphometric parameters of the catchment located in Guaratuba (Southern portion of Serra do Mar), where a debris flow occurred in February 2017. Catch. = Catchment.

Catchment	Area (km^2)	Relief ratio	Catch. Relief (km)	Drainage density (km/km^2)	Catch. Length (km)	Melton Ratio
Pedra Branca	3.43	0.35	1.01	3	2.9	0.6

Both regions also show a similar Relief ratio (ca. 0.3), which is related to the production and availability of the sediments (WILFORD *et al*., 2004). These values are slightly low when compared to other catchments worldwide (Table 3.8), which can potentially be associated to the lower recurrence rate of debris flows both in Cubatão and Guaratuba. These results, however, are similar to other catchments at Serra do Mar (Table 3.8), which also show a slightly lower Relief ratio (ca. 0.25). The Serra do Mar catchments presented in Table 3.8 are located in Itaóca (Guarda-mão catchment, São Paulo state) and in Morretes (Tingidor catchment, Paraná state) (DIAS *et al*., 2022).

Catchment relief is associated with the intensity and reach of debris flows (NIKOLOVA et al, 2020) and those in the Serra do Mar region are within the range of other catchments worldwide (Table 3.8). Guaratuba shows a higher catchment relief than the average in Cubatão, although catchment 1 in Cubatão shows a comparable relief to that of Guaratuba. Moreover, catchment 1 and Guaratuba also share the similarity of two debris-flow events initiated by large landslides in the headwaters' region, whereas the other catchments in Cubatão have their source areas more spread-out in the hillslopes.

Table 3-8. Morphometric Parameters of debris-flow prone catchments worldwide, adapted from Dias *et al*. (2022).

Location	Catchment Area (km^2)	Relief ratio	Catch. Relief (km)	Catch. Length (km)	Melton Ratio	Reference
Canada	0.2 - 4.1	0.3 - 0.49	0.6 - 1.4	1 - 4.68	0.66 - 1.21	Wilford *et al*. (2004)
New Zealand	0.18 - 9.66	0.25 - 0.88	0.55 - 1.93	1.05 - 4.5	0.45 - 1.59	Scally *et al*. (2010)
Bulgaria	0.015 - 39.27	0.05 - 0.68	0.16 - 0.82	0.33 - 15.50	0.13 - 1.59	Nikolova *et al*. (2020)
Romania	0.005 - 1.02	0.56	-	< 1.7	> 0.55	Ilinca (2021)
Taiwan	0.51 - 8.63	0.20 - 0.44	-	1.54 - 5.75	-	Chen and Yu (2011)
Brazil (Serra do Mar)	2.02 and 3.74	0.23 and 0.25	0.75 and 0.83	3.18 and 3.3	0.39 - 0.58	Dias *et al*. (2022)

Drainage density is associated to how rapidly a catchment drains the water that flows in their system, with those showing higher density indicating more intense/frequent hydrogeomorphic processes (e.g., floods, flash floods, debris floods, debris flow) (WILFORD *et al*., 2004). Cubatão (1.92 km/km^2), on average, shows a lower Drainage Density than Guaratuba (3 km/km^2), as well as the other two catchments at Serra do Mar (5.75 in Itaóca; 4.45 in Morretes), which could potentially indicate less frequent events or events with shorter runout distance. As pointed out by the historical record of debris-flows in Brazil, Cubatão (especially catchment 17) is the main site of debris-flow events, with 9 events between 1920 and 2021 and a more recent one in 2022 (Table 3.9).

Catchment Length is associate to the runout distance of debris flows, with those with a smaller length usually associated with a longer distance (IVERSON *et al*., 2001). Guaratuba and Cubatão show similar catchment length, which is also within the range of other catchments worldwide and in Serra do Mar (Table 3.9). As pointed out by Dias *et al*. (2022), some studies have suggested that debris-flow prone catchments usually show a length below 2.7 km, with those above this limit more prone to debris floods and other hydrogeomorphic processes (WELSH; DAVIES, 2011; ILINCA, 2021).

Furthermore, the Melton Ration of catchments also indicates a stronger tendency to initiate debris floods and not debris flows in the analyzed catchments. The Melton Ration (MELTON, 1958) has been widely applied in debris-flow studies, as it is suggested as a good indicator of the type of the hydrogeomorphic process that should dominate in a catchment (WILFORD *et al*., 2004). Debris-flow prone catchments usually show values above 0.6, while those more susceptible to debris floods show values between 0.3 to 0.6 (WILFORD *et al*., 2004). Guaratuba is on the limit between debris flood and debris flows (0.6), while all the catchments in Cubatão fall into the debris flood range.

Table 3-9. Debris flow events recorded in Cubatão since 1975, updated based on Gramani (2001).

Catchment	Date of the event	24-h accumulated rainfall	48-h accumulated rainfall	Peak rainfall intensity	Return period
1	25/12/1975	247.5 mm	255.5 mm	N/A	N/A
10	29/01/1976	279 mm	315 mm	40 mm h^{-1}	1.23 years
1, 2, 3, 4, 5, 6, 7, 8, 9, 10, 12, 14	24/01/1985	242 mm	411 mm	84 mm h^{-1}	10.4 years
9	24/01/1988	185 mm	186 mm	25 mm h^{-1}	1 year
14, 15, 16, 17, 18, 19	07/02/1994	325 mm	452 mm	60 mm h^{-1}	2.7 years
17	09/04/1996	260 mm	265 mm	18 mm h^{-1}	1 year
Rio Pilões (West of the study area)	12/12/1999	128 mm	274 mm	N/A	N/A
Rio Pilões (West of the study area)	16/02/2000	304 mm	304 mm	118 mm h^{-1}	90.5 years
Rio Marcolino, Rio Pilões, Ribeirão do cágado (West of the study area)	22/02/2013	312 mm	314 mm	118 mm h^{-1}	90.5 years
17	29/04/2022	169 mm	248 mm	35 mm h^{-1}	1 year

These results can potentially indicate that while debris flows can occur, they are not the main geomorphic process. As observed in the geomorphological investigation of the Guaratuba event, and suggested by field campaigns in Cubatão, in-channel accumulation of rock boulders in catchments at Serra do Mar are a common feature, with larger boulders (> 5 m) usually not reaching long distances from the source area, as they deposit along flatter portions of the channel. An evolution from a debris flow, to a debris flood, and, finally, to a flash flood in Guaratuba is suggested, due to the progressive deposition of material along the channel, a direct result of gentler channel slope from the middle section on, as well as to the length of the channel (2,900 m), which decreases the flow momentum.

In Cubatão, this evolution from a debris flows to a debris flood is also suggested by the geomorphological analysis conducted during field campaigns, and this evolution is also observed in other areas in Brazil at Serra do Mar (e.g., LACERDA, 2007; HUNGR *et al*., 2014; DIAS *et al*., 2022). The intense boulder accumulation in the channels of both Cubatão and Guaratuba can potentially be remobilized by future events, as erosion and entrainment are important elements of the sediment yield of debris flows in the Serra do Mar Mountain Range. In the estimation of the magnitude of the Guaratuba debris-flow event, approximately 75% of the total magnitude was due to entrainment and erosion. Even though the estimation of eroded material is affected by larger uncertainties than the volume of landslides and the in-channel debris deposits, other studies worldwide have also suggested the strong of influence of erosion

on debris-flow magnitude and related impacts (e.g., MARCHI *et al*., 2009; GABET; STERNBERG, 2008; BENNET *et al*., 2013; SHEN *et al*., 2020).

The maximum observed erosion depth in catchments of Cubatão, according to the RAMMS simulation, is of 3.67 m in catchment 7, while in the Pedra Branca catchment (Guaratuba) the maximum erosion depth observed was 10 m. The expressive difference can be mostly related to the resolution of the investigation/estimation. Other kinematic parameters, such as peak velocity, are similar for catchments in Cubatão and Guaratuba, averaging at about 23.1 m s^{-1} in Cubatão, according to the RAMMS simulation, and 29.04 m s^{-1} in Guaratuba, according to our field-based estimations.

It is important, however, to point out the bias towards large magnitude events, with smaller debris-flow events often going unnoticed or not investigated. The comparison presented in this study considers high-magnitude (> 10^5 m^3) events, which is triggered by very-high to extreme precipitation rates. Smaller magnitude events usually go unreported due to the remoteness of upstream reaches of catchments at Serra do Mar, where debris flows are expected to dominate as the main hydrogeomorphic process. The event of March 2022 (Table 3.9) in Cubatão is an exception (Figures 3.22a, 3.22b and 3.22c), because it affected a now tourist attraction, the century-old road that connected the coast to the city of São Paulo ("*Caminhos do Mar"*).

This event occurred in one of the tributaries of catchment 17, where the slopes are very steep (>30º, or >58%), but the material did not reach the outlet region near the oil refinery that is located at the downstream area of the catchment. The sediments mobilized by this event most likely deposited along the intermediary reaches of the channel, where the slopes become gentler. Another hypothesis would be that the sediments were trapped by the retention structures (Sabo dams) installed at the downstream portion of the catchment (Figures 3.22d and 3.22e). However, no evidence of a large accumulation of sediments upstream these dams were observed during our field campaigns, which indicates that the sediments deposited in upper portions of the channel.

The return period of the rainfall that triggered this recent debris-flow event in Cubatão is estimated at ca. 1 year, which can indicate that a similar event can potentially occur every year in a tributary of a catchment in Cubatão. However, when we consider the short return period of the rainfall that triggered the 1985 and 1994 debris-flow events (10 and 3.5 years, respectively), the complexity of the interactions between climate and geomorphology is highlighted, as no event of similar magnitude has occurred in the region since then.

Figure 3-22. Recent debris flow in Cubatão and retention structures installed in Catchment 17. A) The tributary of Catchment 17 before the March 2022 event. Photo from 2014. B) The tributary after the debris-flow event, showing the intense erosion of the channel and vegetation. The measured post-event channel width is of 7 m. Photo from July 2022. C) Photo of the debris-flow event on the day after its occurrence (March 30, 2022). Photo from Maicon, one of the monitors of the "Caminhos do Mar" Park. D) Retention structures installed in the downstream portion of catchment 17, to protect the oil refinery from debris-flow events. Photo from Marcelo Gramani. E) Detail of two Sabo dams located in catchment 17. Photo from Marcelo Gramani.

Nonetheless, considering the overall short return period of debris-flow triggering rainfall in Cubatão (Table 3.9) and in Guaratuba (15-20 years), combined with the intense in-channel material accumulation, future large-magnitude events are likely to occur in the next decade or so.

3.6. A multi-step hazard assessment methodology for debris-flow prone areas influenced by hydroclimatic events

Creating tools and methodologies that can be applied in the mitigation of disasters and in disaster-preparedness programs is a primordial and challenging task. Hazard assessment studies are a first step to understanding the potential negative effects that a phenomenon (i.e., debris flows) can cause in a specific region, which can later subsidize in-depth risk analysis. To contribute to the effort of debris-flow risk mitigation in Brazil, our study proposes a hazard assessment methodology to be applied in debris-flow prone areas influenced by high-intensity rain events. As our test-site, 20 catchments located in the region of Cubatão are chosen (Figure 3.6).

In the hazard assessment, we first conduct a data-driven Logistic Regression (LR) analysis to identify the main factors that influence debris-flow initiation in the region (shown in subchapter 3.2), as well as to identify the catchments that are more susceptible to the phenomenon. The most-susceptible catchments are, then, analyzed using the numerical model RAMMS, to simulate past debris-flow that can help to estimate important kinematic parameters about the debris-flow behavior. Based on the outcomes of the simulations and on the analysis of the rain events that led to debris flows in the study site (shown in subchapter 3.3), a hazard matrix is proposed for the creation of a hazard zonation map. The mapping of the infrastructures located in the region is also performed to support the hazard zonation.

Applying the equation based on the LR model (Equation 1) to assess the areas with high susceptibility to debris-flow initiation in the study site, catchments 20, 19, 17, 16, 15, 14, 12, 10, 9 and 7 are those most susceptible overall (Figure 3.23). The northeastern portion of catchment 1 also shows a high percentage of highly susceptible areas (Figure 3.23), which can be related to steeper slopes and the more widespread occurrence of Cambisols in the headwaters' region, which is a significant influencing factor in debris-flow initiation in the region according to the LR analysis.

Based on the susceptibility analysis, catchments 20, 19, 17, 16, 15, 14, 12, 10, 9, 7 and 1 are simulated using RAMMS. The simulations were calibrated based on the debris-flow event of 1985 in catchments 14, 12, 10, 9, 8, 7 and 1, while catchments 14, 15, 16, 17 and 19 were calibrated based on the 1994 debris-flow event. Catchment 20 was not modeled as no debris flow was recorded both in 1985 and 1994 and calibration could not be conducted. The initiation areas were determined according to the landslide inventories that we created using aerial

photographs prior and post event and a bulk density of 1,900 kg m^{-3} was assumed for the source areas and the entrainment zone.

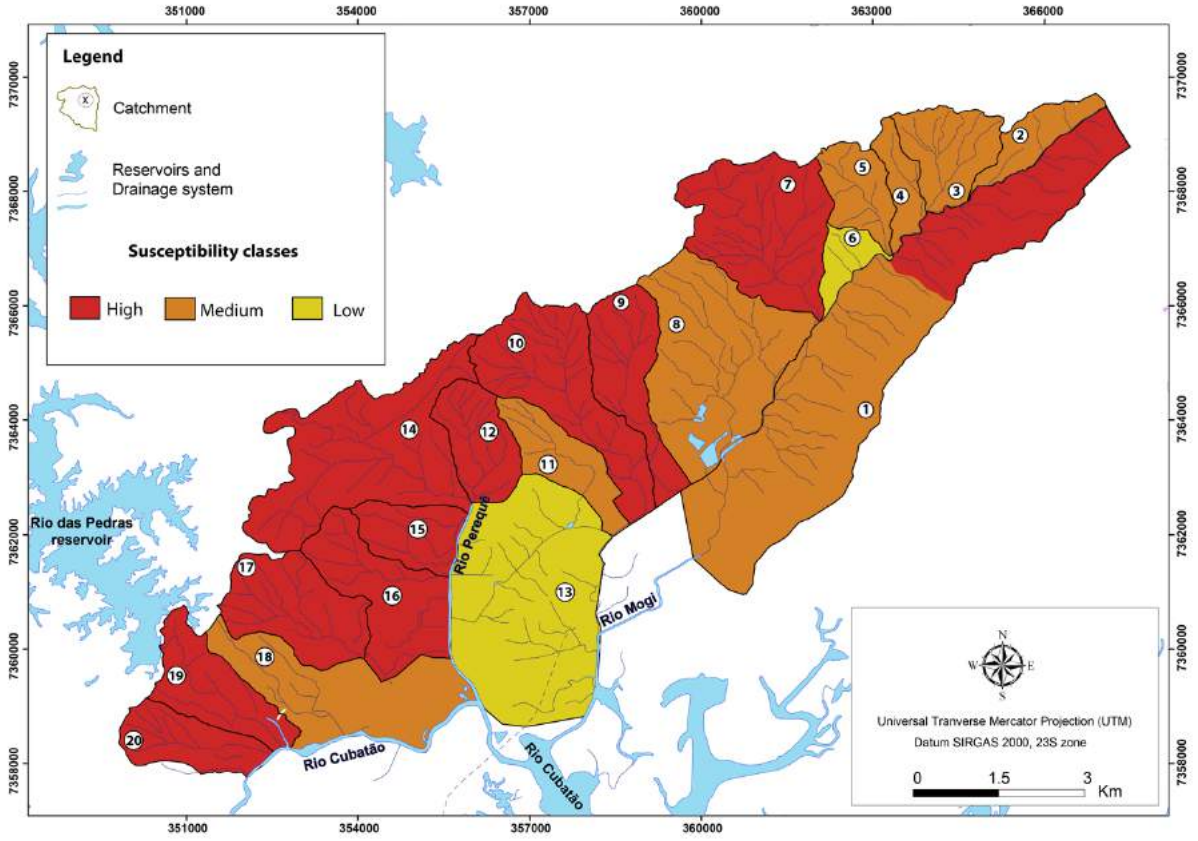

Figure 3-23. Map showing the overall susceptibility to debris-flow initiation of the 20 catchments at the study area, based on the LR model.

The volume of the landslides that initiated the debris flows in each catchment is shown in Table 3.10. Considering the whole study area, the magnitude of the 1985 landslide event is estimated at ca. 540,900 m^3, while the magnitude of the 1994 landslide event is estimated at ca. 227,000 m^3. The magnitude of the debris flows (i.e., volume of sediments mobilized) at each catchment is estimated based on magnitude equations from Marchi *et al*. (2019), as suggested by Cabral et al. (2021) for catchments at Serra do Mar (Table 3.10).

Figure 3.24 shows the calibration results based on the coverage index (Ω) (we refer paper III), which aided the identification of the best-matched simulations (Figure 3.25 and 3.26). The calibration is mainly based on the comparison of the observed runout distance with those modeled by RAMMS. One of the parameters subjected to most uncertainties during modeling is erosion depth, as no comprehensive information for any of the modeled catchments was available. In our simulations, we adopted for all the catchments two maximum erosional depths: 4 m at upper and intermediate reaches, and 0.5 at lower reaches of the catchments. A 4

m erosion depth was reported by Kanji *et al*. (2007) in catchment 17 (1994), which we extrapolated for all the other catchments in the study region.

Table 3-10. RAMMS-2D results and characteristics of the debris flows. Est. = estimated, Max. = maximum.

Catchment	Year of the event	Initiation volume (m^3)	Est. Magnitude (m^3)	Runout	Flow parameters					
					μ	ξ ($m\ s^{-2}$)	Max. Flow height	Max. erosion depth	Max. velocity	Max. Impact pressure
1	1985	68,422.3*	2.5×10^4	N/A*	0.1	300	3.2 m	0.88 m	30.96 $m\ s^{-1}$	1917.55 kPa
7	1985	131,737.6	2.5×10^5	N/A*	0.05	200	8.6 m	3.67 m	23.62 $m\ s^{-1}$	1115.38 kPa
8	1985	33,976.8	1.1×10^5	480 m	0.05	200	5.5 m	1.3 m	24.25 $m\ s^{-1}$	1175.73 kPa
9	1985	25,740.7	1.3×10^5	270 m	0.05	180	4 m	0.74 m	14.04 $m\ s^{-1}$	354.74 kPa
10	1985	78,865.6	2×10^5	700 m	0.05	180	4.7 m	1.74 m	14.25 $m\ s^{-1}$	406.1 kPa
12,14	1985	85,409.3	2.4×10^5	N/A*	0.05	200	5.4 m	1.59 m	30.87 $m\ s^{-1}$	346.35 kPa
14	1994	82,632.1	2×10^5	N/A*	0.05	200	5.6 m	1.8 m	32.93 $m\ s^{-1}$	550.87 kPa
15, 16	1994	10,150.7	0.8×10^5	510 m	0.03	200	4.7 m	2.11 m	16.75 $m\ s^{-1}$	561.26 kPa
17	1994	43,702.46	1.7×10^5	400 m	0.05	200	5.3 m	2.84 m	12.48 $m\ s^{-1}$	296.13 kPa
19	1994	17,673.8	0.8×10^5	N/A*	0.05	200	2.9 m	1.45 m	30.98 $m\ s^{-1}$	1919.97 k Pa

* Direct discharge in the drainage system of the region. Indirect effects of debris flows include floods and silting.

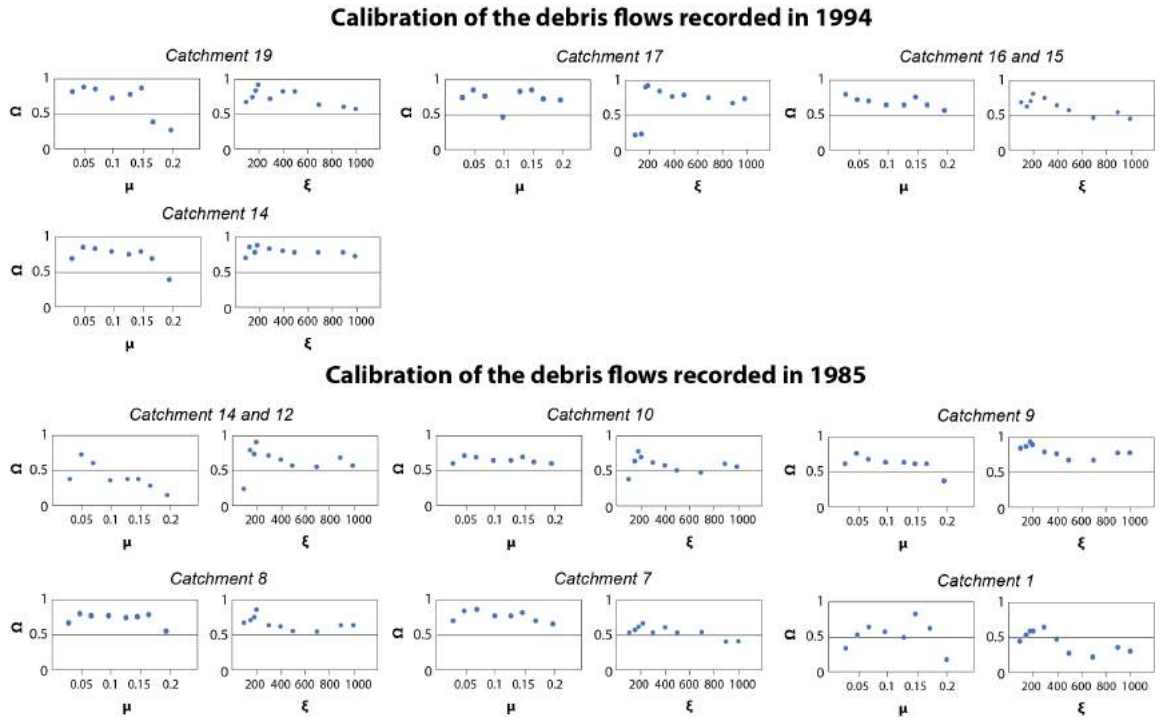

Figure 3-24. Calibration using the coverage index (Ω) of the debris-flow simulations for the selected catchments at the study area. The closer the coverage index is to 1, the more representative the simulation.

Another limitation was the lack of available information about catchments 19, 14, 12, 7 and 1, since no deposition pattern could be interpreted from aerial photographs. Even though

we performed calibrations in these catchments in the same manner as the others, the best matched parameters adopted were those of with μ equal to the channel slope of the downstream portion of the catchment and ξ was assumed to be similar to the general trend of the area (ξ = 200 m s^{-2}). The lack of depositional fan in these catchments, and in most of the catchments in the study region, is related to the direct debouchment into the rivers Mogi, Perequê and Cubatão, which receive most of the sediments of the 20 studied catchments.

Moreover, even though the debris flows in the study area exhibit a very high content of stony debris, most of the larger boulders (>1 m) are interpreted to deposit along the debris flow route and are not carried for long distances. Most of the damage in the downstream areas of the catchments is due to the smaller boulders (< 1 m), fine sediments and woody debris. These interpretations are supported by witnesses of the 1985 and 1994 events and the field campaigns that were conducted in the study area, where intense boulder accumulation in areas with gentler slopes at upper/intermediate reaches of channel were observed. Moreover, the geomorphic characteristics of the studied catchments are similar to others at Serra do Mar, such as Pedra Branca in Guaratuba (Paraná), as discussed in the previous chapter.

The average runout distance, according to the simulations, is ca. 470 m, with the largest distance observed in catchment 10 (700 m) and the shortest in catchment 9 (270 m). Highest flow heights (Figure 3.27 and 3.28) are observed in catchment 7 (8.6 m, 1985) and in catchment 14 (5.6 m, 1994), where the initiation volume is higher. Overall, flow height in the studied catchments averages 5 m. The average peak velocity of the debris flows is 23.1 m s^{-1}, with the highest velocities observed in catchment 14 (30.87 m s^{-1}) and catchment 1 (30.96 m s^{-1}). Maximum impact pressures are observed in catchments where steep knickpoints are observed (catchments 19, 1, 7 and 8).

As discussed in subchapter 3.2 and 3.3, rainfall is identified as the most influencing factor in debris-flow initiation in Cubatão and a hazard zonation matrix is, thus, proposed based on rainfall accumulated in 48 h, as well as the depositional areas and flow behavior patterns modeled by RAMMS. As pointed out in the rainfall analysis, the 48-h accumulated precipitation is more strongly associated to debris-flow initiation in our test-site area and is, as consequence, considered in the hazard matrix.

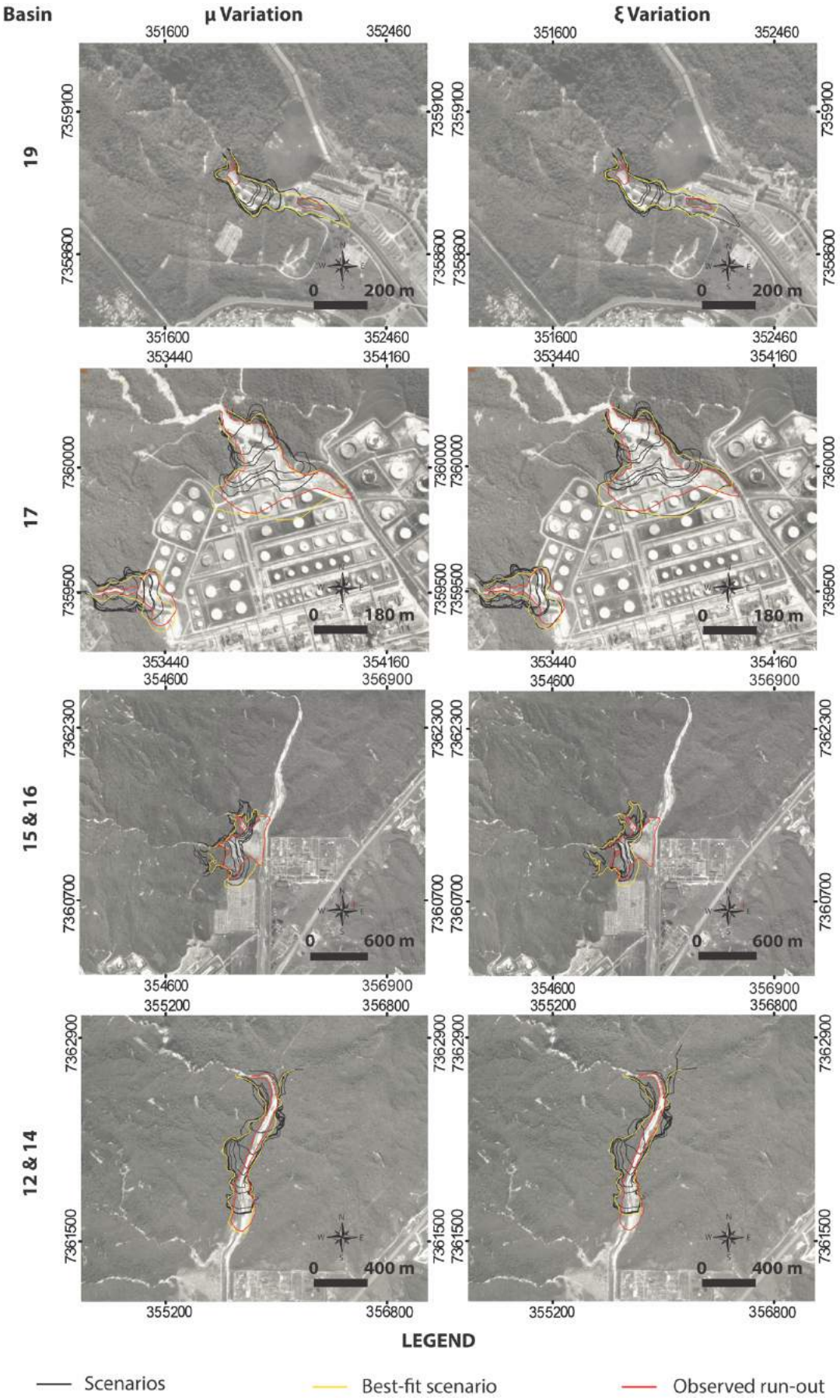

Figure 3-25. Comparison between modeled and observed run-out distance of the 1994 debris-flow event for the selected catchments.

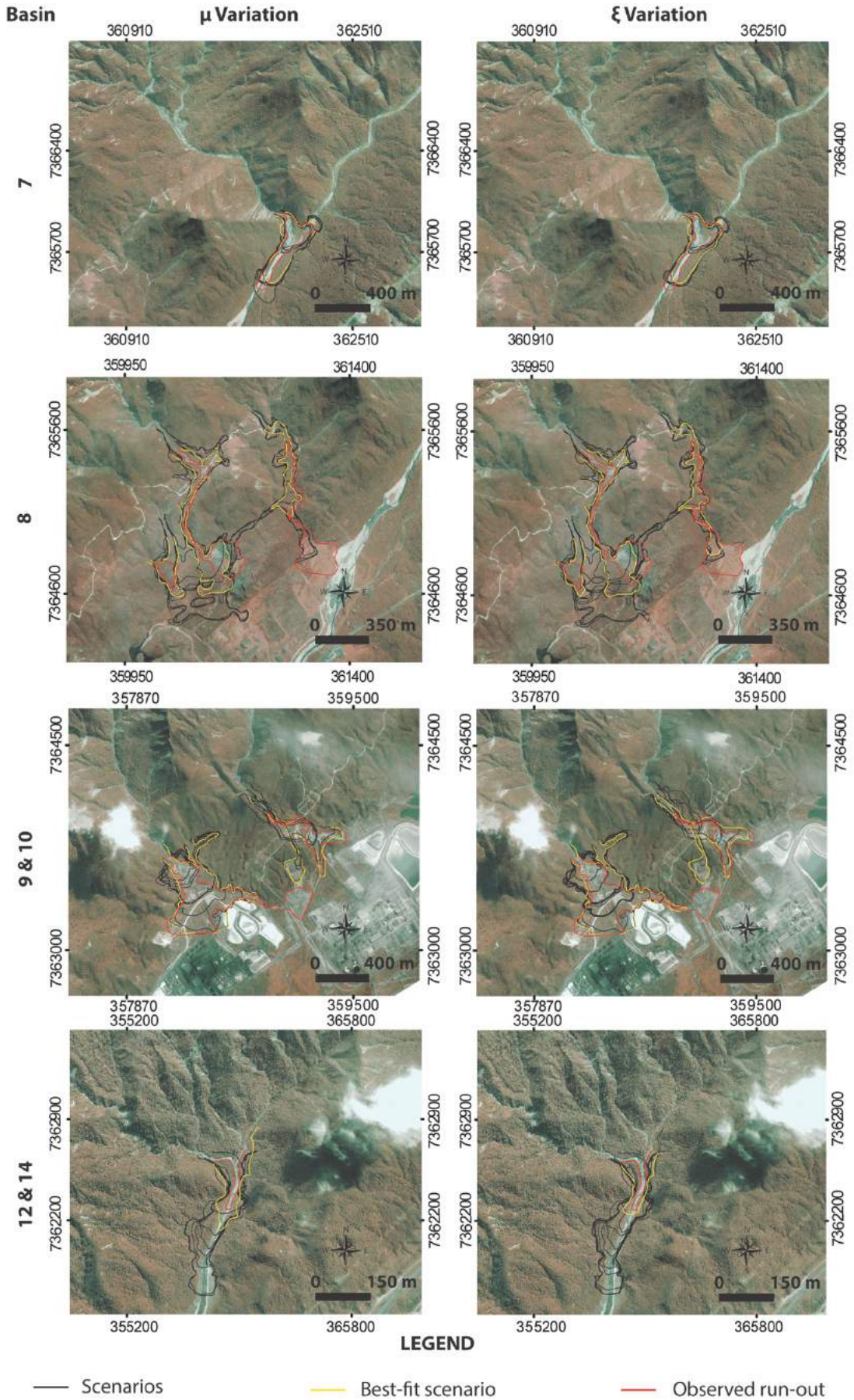

Figure 3-26. Comparison between modeled and observed run-out distances of the 1985 debris-flow event for the selected catchments.

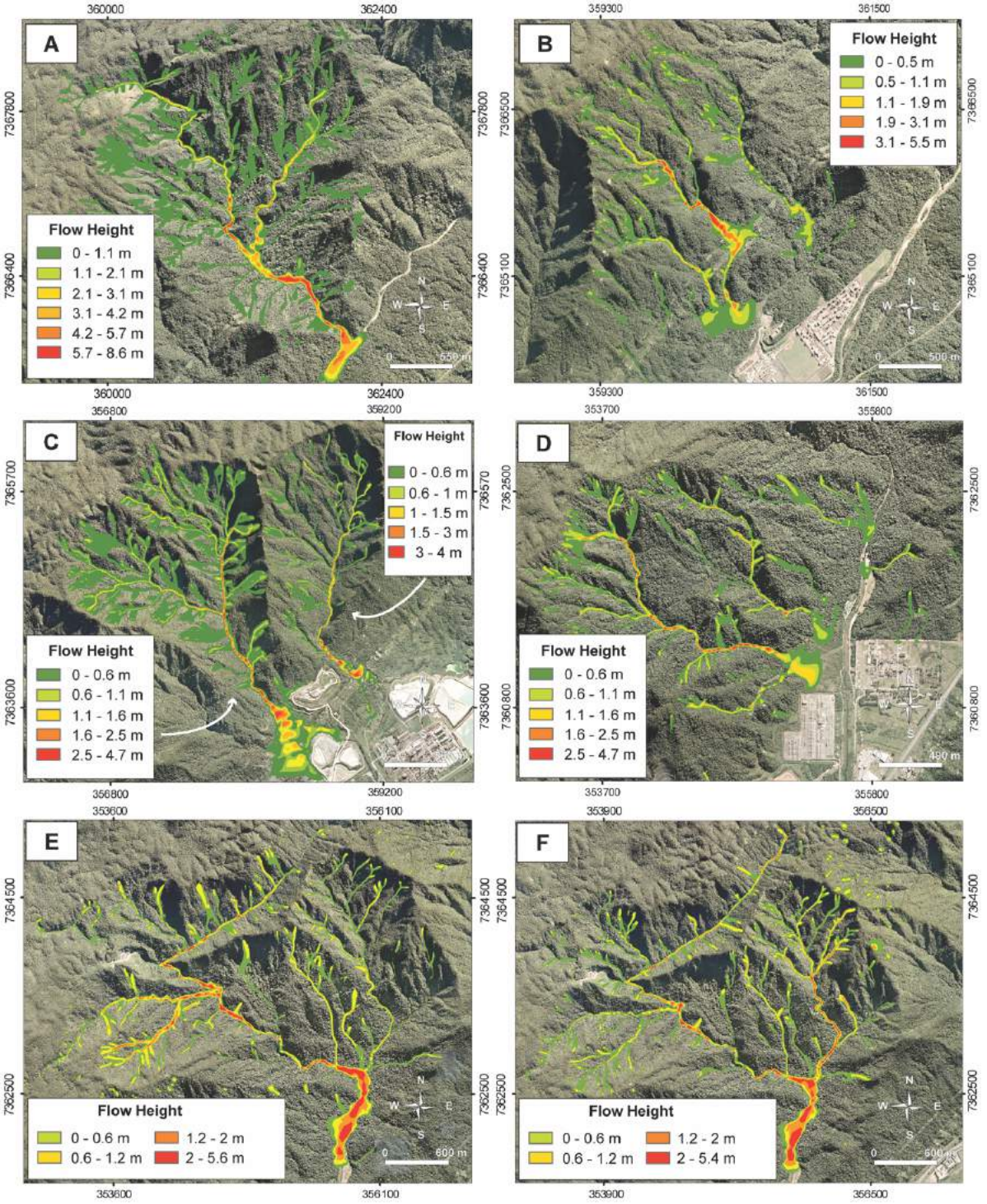

Figure 3-27.RAMMS modeling results showing maximum flow height. A) Catchment 7 (1985). B) Catchment 8 (1985). C) Catchments 9 and 10 (1985). D) Catchment 15 and 16 (1994). E) Catchment 14 (1994). F) Catchments 14 and 12 (1985).

Five levels of hazard are proposed: very high, high, medium, low, and very low (Table 3.11). Very high-hazard areas are those where RAMMS simulated a > 1 m flow height and velocity of > 1 m s^{-1}, as also proposed by Hürlimann *et al*. (2006), and humans and infrastructures are directly affected. High hazard areas are those where the debris flow runout

can reach up to 1 m in height and velocity of up to 1m s^{-1}, and infrastructures may be directly impacted. Medium hazard areas are those that are not directly impacted by the sediments transported by a debris flow, but can exhibit flooding or silting that may impact infrastructures. Areas with low hazards are those that can experience some kind of side impacts of the debris flows, such as floods, but are inhabited, or areas with retention structures installed, as it is the case of catchment 19. Areas with very low hazard are those where no impacts of any sort are expected.

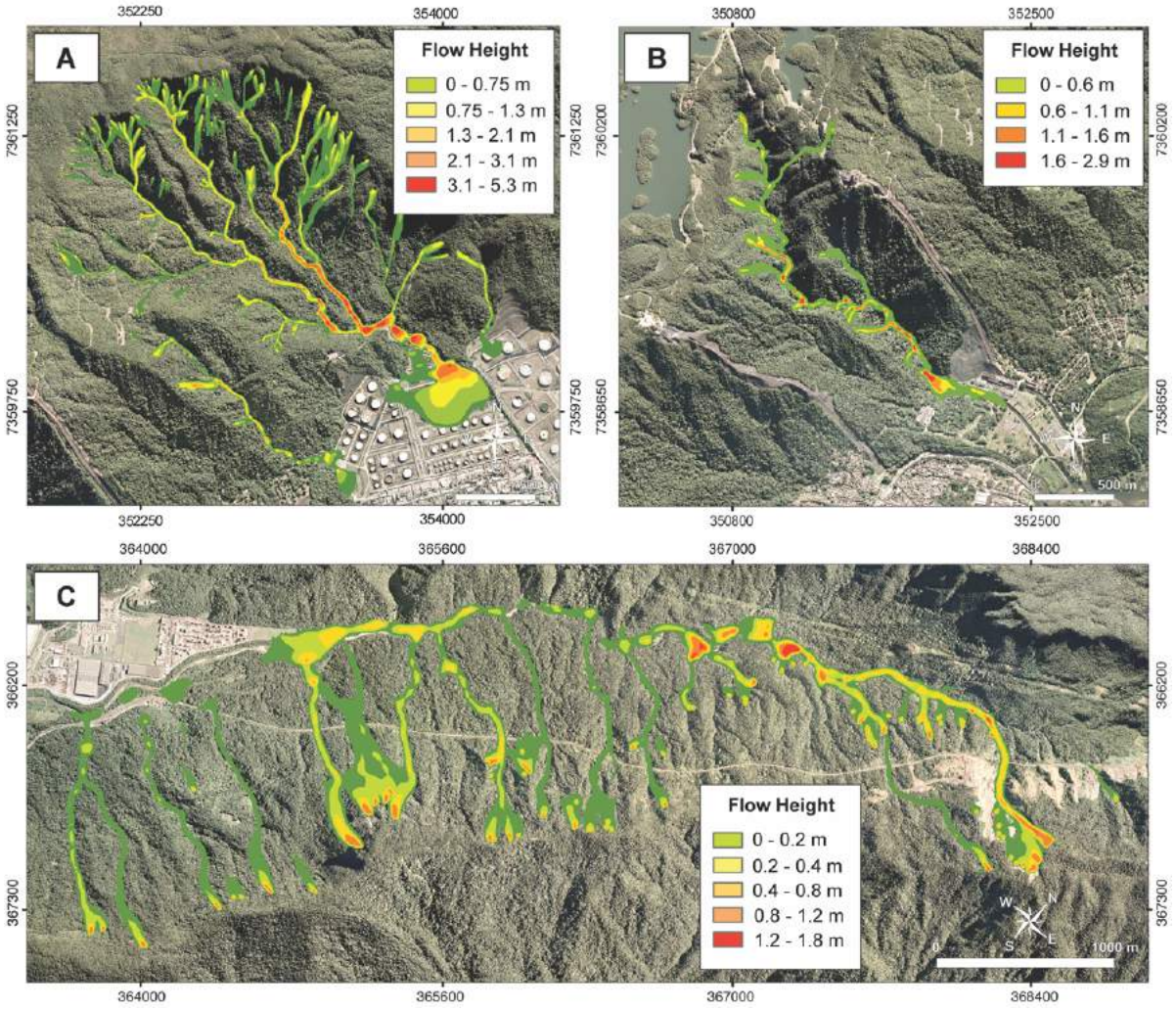

Figure 3-28. RAMMS modeling results showing maximum flow height. A) Catchment 17 (1994). B) Catchment 19 (1994). C) Catchment 1 (1985).

Based on the hazard level matrix and on the infrastructures at hazard in each catchment (Table 3.12), a hazard zonation map was created for the 20 catchments (Figure 3.29). The map of Figure 3.29 shows the zonation based on a rainfall of over > 200 mm in 48 h, which can be adapted to different hazard levels according to rainfall indices. Catchments 19, 16, 15, 11, 10 and 9 exhibit an overall higher hazard in the region (Table 3.12), due to a higher probability of

debris-flow related damages to humans and infrastructures. Retention structures in such catchments could potentially decrease their hazard level.

Areas that have not shown any history of debris-flow occurrence since 1975, such as catchment 20, were classified as high hazard areas in the context of >200 mm rainfall in 48 h, based on the LR susceptibility analysis. These catchments exhibit intense in-channel stony material accumulation, which contributes to increasing their potential hazard to residential areas and infrastructures that are located within their limits. The average runout distance with a 470 m radius was assumed as a very high hazard area, in catchments where no debris flows were recorded.

Catchment 17, which has an extensive history of debris flows (Table 3.9), is classified with a medium/low hazard level, due mainly to the retention structures installed (Figure 3.22d and 3.22e) and the removal of in-channel debris deposits, promoted after the 1996 debris-flow event.

Table 3-11. Hazard level matrix developed for the study area, based on different rainfall indices and the impacts on infrastructures and population.

			Rainfall index in 48 hours		
			> 200 mm	< 200 mm, > 150 mm	<150 mm, >100 mm
Severity	Direct impacts	flow height ≥ 1m; velocity ≥ 1 m s^{-1}	Very high	Very high	High
		flow height < 1m; velocity < 1 m s^{-1}	High	High	Medium
	Indirect impacts	floods or silting	Medium	Medium	Low
		Areas with retention structures installed; Remote areas	Medium	Low	Very low
	No impacts	-	Very low	Very low	Very low

An integrated analysis of the hazard assessment presented and studies about the economic/social vulnerability of the region is encouraged in future risk analyses. As DeBortoli *et al*. (2017) point out, the mapping of vulnerability of the community is crucial, as it is fundamental to preventing and reducing the risk to which the society is potentially exposed. Such mapping, however, demands a more in-depth and multidisciplinary approach. Moreover, the expansion of the city towards mountain areas, especially by socially vulnerable communities, can increase the risk of new events, even those with smaller magnitudes.

The multi-step hazard assessment here proposed and applied in the hazard zonation of Cubatão joins other studies that aimed at creating new methodologies that can help to mitigate future landslide-related damage, such as the works of Cardinali *et al*. (2022), Hürliman *et al*. (2006; 2008), Wu *et al*. (2018), Huangfu *et al*. (2021), among many others. When assessing debris-flow hazard, especially in areas where the initiation factor is landslides, it is necessary

to combine analysis of all the factors that can lead to the initiation of the phenomena (STEGER *et al*., 2021), as well as aspects of their dynamics, represented mainly by the runout distance (COROMINAS *et al*., 2013; FRANK *et al*., 2017). The transition from landslides to debris flows occurs especially during periods of heavy rainfall, although, as demonstrated in our analysis and other studies (e.g., TAKAHASHI, 2001; COROMINAS *et al*. 2013; HUNGR, 1997), rainfall intensity is not always directly related to the magnitude of an event.

Table 3-12. Infrastructures, both public and private, at hazard in each catchment and overall hazard level, for a 200 mm rainfall in 48 h.

Catchment	Elements at hazards	Overall Hazard level
1	Railways from the company MRS Logistica; Fertilizer company "Yara Cubatão", Container storage company "Rodopark"	Medium
2	-	Low
3	-	Low
4	-	Low
5	-	Low
6	-	Low
7	Container storage company "Depotce"	Medium
8	-	High
9	Fertilizer company "Mosaic Fertilizantes do Brasil"	High
10	Petrochemical company "Copebras"; industrial gas company "White Martins"	High
11	Chemical plant "Birla Carbon Brasil"	High
13	Petrochemical company "Braskem", Logistic company "Brado Logistica", Chemical industry "Hidromar", Carbocloro Oxypar Chemical Industries; Industrial gas company "Messer Gases", Three transportation companies	Low
12, 14, 15, 16	Electrical substation	High
17	Petrobras oil refinery	Medium/Low
18	Vila Light (Residential area with approximately 140 houses, 60 of which have residents), FAFEN (Oil refinery), Thermoelectric Plant "Euzébio Rocha"; Fertilizers company "Yara Brasil"	High
19	Hydropower plant "Henry Boden", with electrical subestations	High
20	Anchieta and Imigrantes Highway, Vila Fabril (residential area with more than 400 houses), oil pipelines	High

The combination, therefore, of different, data-driven methodologies is fundamental to ensuring the reliability of the hazard evaluation, focusing on the different aspects related to a phenomenon. As pointed out by Wu *et al*. (2018), LR is considered one of the most reliable methods in landslide susceptibility assessment, identifying the main characteristics that influence the phenomenon in a particular region. When combined with the state-of-the-art, numerical model RAMMS, which provides concrete, physically-based results (FRANK *et al*.

2017), the hazard evaluation can reliably represent the potential impact of future debris-flow events in a region. Moreover, the inclusion of the rainfall analysis provides a good indication of future events probability and the different associated hazard levels according to the intensity of the rain event.

This thesis, therefore, is a small contribution to the effort of better understanding the dynamics and impacts of debris flows in Brazil, as well as to the effort of preventing future disasters. As for future studies in Brazil, Large Wood (LW) mobilization in densely forested catchments should be focused, as LW can contribute to significantly increasing debris-flow hazard and risk (LUCÍA *et al*., 2015; RICKENMANN, 2016).

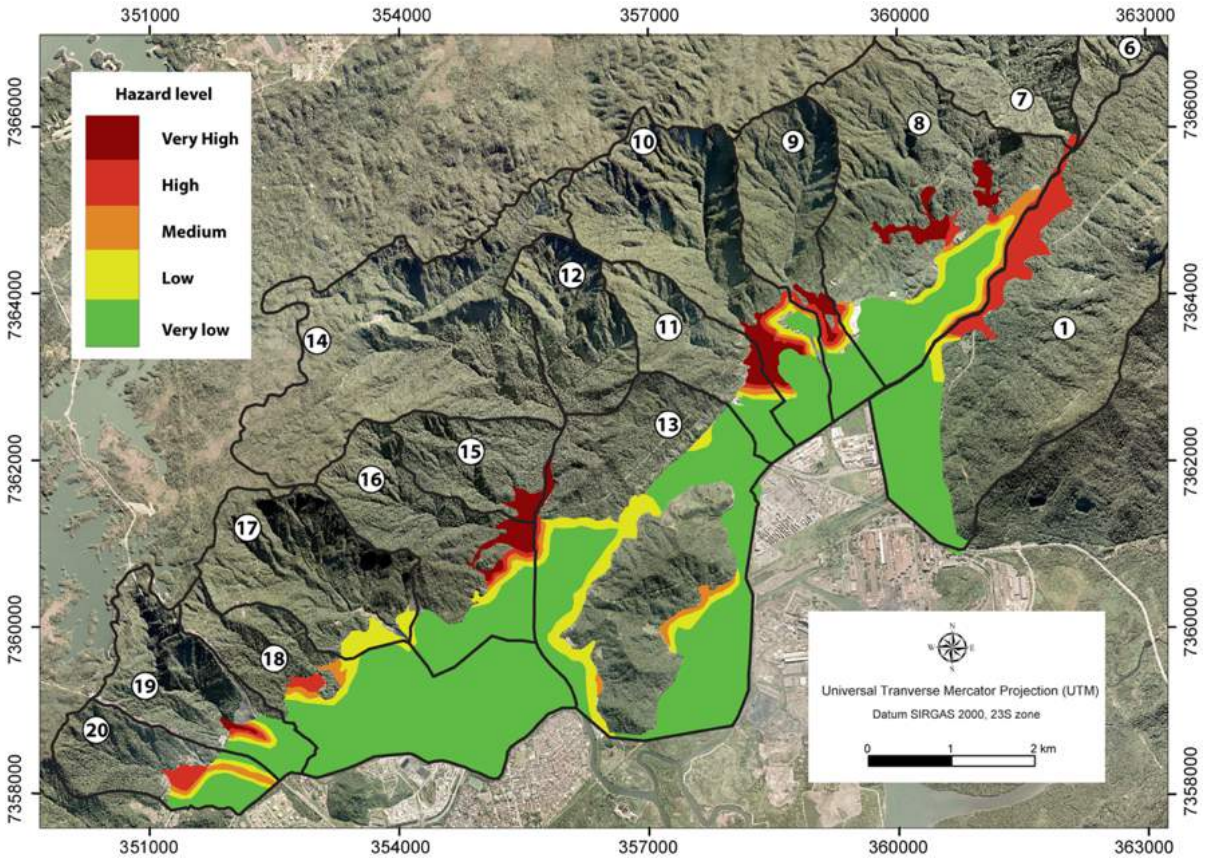

Figure 3-29. Debris-flow hazard zonation, based mainly on flow properties and on rainfall intensity (> 200 mm in 48 h), as well as on the analysis of the elements at hazard.

4. Final considerations

Cataloguing and estimating the consequences that a natural hazard represents based on past events is one of the most effective methods to provide reasonable damage assessments to the society. Our historical analysis shows that debris-flow events are concentrated mostly in the Serra do Mar and Serra da Mantiqueira regions in Southeast Brazil, where population density is higher and occupation of hilly areas is more common. Between 1920 and 2021, debris-flow events were responsible for over 5,771 fatalities and 5.5 billion USD in economic losses in Brazil, most of which in the Southeast region (91% of the fatalities, 67% of the economic losses).

The city of Cubatão, in the state of São Paulo, is one the most affected areas by debris flows in the country, with an extensive history of fatal and destructive events. The region is characterized by high rainfall indices and urban and industrial areas near or at the hilly areas. The city, therefore, was chosen as test-site for our proposed multi-step hazard assessment, based on Logistic Regression (LR) analysis, simulation of flow parameters using numerical model and rainfall back-analysis. The LR analysis highlighted that rainfall is the main influencing factor on the initiation of the phenomenon and the back-analysis of rain events suggests that the precipitation accumulated 48 h prior to the initiation of a debris flow plays a more significant role on their deflagration.

Furthermore, the LR analysis also highlighted the catchments most susceptible to debris-flow initiation, which were further analyzed using the numerical model RAMMS. The simulation using RAMMS aimed at characterizing the kinematic patterns of debris flows in these catchments, as it is a fundamental step when analyzing the hazard that the phenomenon represents. The kinematic parameters of debris flows in Cubatão are similar to those estimated based in the debris-flow event in Guaratuba (February 2017), highlighting an overall similarity between catchments in the Serra do Mar mountain range. Based on the kinematic parameters, the LR and the rainfall back-analysis, a hazard zonation matrix with five levels of hazard (very low to very high) was proposed to assess debris-flow hazard.

The methodology proposed is relevant, as hazard zonation, in conjunction with vulnerability studies, can subsidize the creation of risk management programs for debris-flow prone areas and establish guidelines that should be followed during emergency situations. Such guidelines do not currently exist for Cubatão, as well as for most debris-flow prone regions in Brazil. Moreover, a systematic geomorphological investigation of catchments that show history of debris-flow events, such as the one performed in the Pedra Branca catchment in Guaratuba,

is fundamental to quantifying the potential magnitude of future events, as well as to understanding the type of sediments (e.g., size, woody and/or stony, etc.) that will reach and affect the downstream portions.

Magnitude studies are also a pathway for the development of Frequency-Magnitude relationships that can support reliable monitoring programs and for prioritizing areas where Early Warning Systems should be installed. Considering the short return period of the debris-flow triggering rainfall (between 1 and 15 years) in the sites more profoundly analyzed in the thesis (Cubatão and Guaratuba), new events with large magnitudes ($>10^5$ m^3) are likely to occur in the next decade. It is crucial, therefore, that these regions are prepared for emergency situations, with a reliable rain gauge network, hazard zonation maps and an emergency plan for evacuation of the potentially affected areas.

The outlook, however, is not promising. The Brazilian National Center for Monitoring and Warning of Natural Disasters - CEMADEN (*Centro de Monitoramento e Alerta de Desastres Naturais*), responsible for hazard and disaster management in the whole country, has been continuously underfunded in the past 4 years, going from an annual budget of 14 million USD on its creation in 2012-2013 to just over 3 million USD in 2019-2020. The recent landslide and flash flood disaster of February 2022 in Petrópolis (state of Rio de Janeiro), which caused 231 fatalities, is a direct example of how the lack of continuity in public policies and political interest in disaster prevention can be catastrophic. A challenge for the scientific community in Brazil, therefore, is to decrease the distance between politics and science.

Bibliography

AARON, J.B.; MCDOUGALL, S.D. Rock avalanche mobility: the role of path material. **Engineering Geology**, v. 257, p. 105126, 2019.

AB'SÁBER, A.N. Política de Meio Ambiente. In: **Anais dos Seminários Temáticos: política de meio ambiente e aproveitamento do potencial hidrelétrico brasileiro,** Rio de Janeiro: Eletrobrás, p. 43-54, 1991.

AGÊNCIA NACIONAL DE ÁGUAS – ANA. Pluviômetros "Garuva - 420580301A", "Estrada Geral Quiriri - 420580302A". Disponíveis em: http://www.snirh.gov.br/hidroweb/serieshistoricas, Acesso em 20 de novembro de 2020.

ALCÁNTARA-AYALA, I. Geomorphology, natural hazards, vulnerability and prevention of natural disasters in developing countries. **Geomorphology**, v. 47, n. 2-4, p. 107-124, 2002.

ALCÁNTARA-AYALA, I. Time in a bottle: challenges to disaster studies in Latin America and the Caribbean. **Disasters**, v. 43, p. S1, 2019.

ALMEIDA, M.C.J., NAKAZAWA, V.A.; TATIZANA, C. Levantamento e cadastro dos escorregamentos no município de Petrópolis, RJ. In: **Simpósio de Geografia Física Aplicada**, 4., Porto Alegre. Anais... Porto Alegre: UFGRS. p. 292 – 299, 1991.

ALVALÁ, R.S.; ASSIS DIAS, M.; SAITO, S.; STENNER, C.; FRANCO, C.; AMADEU, P.; RIBEIRO, J.; SANTANA, R.S.M.; NOBRE, C. Mapping characteristics of at-risk population to disasters in the context of Brazilian early warning system. **International Journal of Disaster Risk Reduction**, v. 41, p. 101326, 2019.

AMARAL, S.; FUCK, G. Sobre o deslizamento de lama turfosa ocorrido em Campos do Jordão, SP, em agosto de 1972. **Boletim IG**, v. 4, n. 0, p. 21, 1973. doi: 10.11606/issn.2316-8978.v4i0p21-37

AMPONSAH, W.; MARCHI, L.; ZOCCATELLI, D.; BONI, G.; CAVALLI, M., COMITI, F.; CREMA, S.; LUCÍA, A.; MARRA, F.; BORGA, M. Hydrometeorological characterization of a flash flood associated with major geomorphic effects: assessment of peak discharge uncertainties and analysis of the runoff response. **Journal of Hydrometeorology**, v. 17, n. 12, p. 3063–3077, 2016.

ANDRES, N.; BADOUX, A. The Swiss flood and landslide damage database: Normalisation and trends. **Journal of Flood Risk Management**, v. 12, p. S1, 2018.

ARCEMENT, G.J.; SCHNEIDER, V.R. Guide for Selecting Manning's Roughness Coefficients for Natural Channels and Flood Plains. **U. S. Geological Survey Water-Supply Paper**, n. 2339, 1989.

ASSIS DIAS, M.C.; SAITO, S.M.; ÁLVALA, R.C.; STENNER, C.; PINHO, G.; NOBRE, C.A.; FONSECA, M.R.S.; SANTOS, C.; AMADEU, P.; SILVA, D.; LIMA, C.O.; RIBEIRO, J.; NASCIMENTO, F.; CORRÊA, C.O. Estimation of exposed population to landslides and floods risk areas in Brazil, on an intra-urban scale. **International Journal of Disaster Risk Reduction**, v. 31, p. 449–459, 2018. https://doi.org/10.1016/j.ijdrr.2018.06.002.

ATKINSON, P.M.; MASSARI, R. Generalized linear modelling of susceptibility to landsliding in the central Apennines, Italy. **Computers and Geosciences**, v. 24, n. 4, p. 373 – 385, 1998.

AUGUSTO FILHO, O. Caracterização geológico-geotécnica voltada à estabilização de encostas: uma proposta metodológica. In: **Conferência Brasileira sobre Estabilidade de Encostas-COBRAE...Anais**, p. 721-733, 1992.

AYALEW, L.; YAMAGISHI, H. The application of GIS-based logistic regression for landslide susceptibility mapping in the Kakuda-Yahiko Mountains, Central Japan. **Geomorphology**, v. 65, p. 15–31, 2005.

BACK, A.J.; HENN, J.A.; OLIVEIRA, J.L.R. Heavy rainfall equations for Santa Catarina, Brazil. **Revista Brasileira de Ciências do Solo**, v. 35, p. 2127-2134, 2011.

BALL, D.J. Risk management and the decommissioning of off-shore structures. In: **Society for Risk Analysis annual conference**, Paris, 1998.

BĂLTEANU, D.; CHENDEŞ, V.; SIMA, M.; ENCIU, P. A country-wide spatial assessment of landslide susceptibility in Romania. **Geomorphology**, v. 124, n. 3 – 4, 102 – 112, 2010. doi: 10.1016/j.geomorph.2010.03.005

BASTOS, M.; BANDEIRA, R.; CAMPOS, V. Operações de resposta a desastres: proposta de um modelo de gestão e de um protótipo de banco de dados. **Revista Produção Online**, v. 15, n. 2, p. 482, 2015.

BARROS, W.T.; AMARAL, C.P.; SOBREIRA, F.G.; D'ORSI, R.N.; MAIA, H.S.; CUNHA, R.P. Catastrophic avalanche at the St. Genoveva slope. **Solos e Rochas**, v. 11, n. 1, p. 17–25, 1989.

BAUM, R.L.; GODT, J.W. Early warning of rainfall-induced shallow landslides and debris flows in the USA. **Landslides**, v. 7, p. 259–272, 2010.

BEGUERÍA, S.; VAN ASCH, T.; MALET, J.; GRÖNDAHL, S. A GIS-based numerical model for simulating the kinematics of mud and debris flows over complex terrain. **Natural Hazards and Earth System Sciences**, v. 9, n. 6, p. 1897-1909, 2009.

BENISTON, M. Trends in joint quantiles of temperature and precipitation in Europe since 1901 and projected for 2100. **Geophysical Research Letters**, v. 36, p. L07707, 2009.

BENNETT, G.; MOLNAR, P.; MCARDELL, B.; SCHLUNEGGER, F.; BURLANDO, P. Patterns and controls of sediment production, transfer and yield in the Illgraben. **Geomorphology**, v. 188, p. 68-82, 2013.

BERGER, C.; MCARDELL, B.W.; SCHLUNEGGER, F. Direct measurement of channel erosion by debris flows, Illgraben, Switzerland. **Journal of Geophysical Research**, v. 116, p. F01002, 2011.

BERTRAND, M.; LIÉBAULT, F.; PIÉGAY, H. Debris-flow susceptibility of upland catchments. **Natural Hazards**, v. 67, p. 497–511, 2013.

BIANCO, G.; FRANZI, L. Estimation of debris-flow volumes from storm events. In: WIECZOREK, G.F.; NAESER, N.D. (Eds.) **Debris-flow Hazards Mitigation: Mechanics, Prediction and Assessment**. Balkema, Rotterdam, pp. 441-448, 2000.

BOLLSCHWEILER, M.; STOFFEL, M. Tree rings and debris flows: Recent developments, future directions. **Progress in Physical Geography: Earth and Environment**, v. 34, n. 5, p. 625-645, 2010.

BORDEN, K.; CUTTER, S. Spatial patterns of natural hazards mortality in the United States. **International Journal of Health Geographics**, v. 7, n. 1, p. 64, 2008.

BORGA, M.; STOFFEL, M.; MARCHI, L.; MARRA, F.; JAKOB M. Hydrogeomorphic response to extreme rainfall in headwater systems: Flash floods and debris flows. **Journal of Hydrology**, v. 518, p. 194–205, 2014.

BOVIS, M.J.; JAKOB, M. The role of debris supply conditions in predicting debris flow activity. **Earth Surface Processes and Landforms**, v. 24, p. 1039–1054, 1999.

BRASIL (2021a) Ministério da Integração Nacional. Secretaria Nacional de Defesa Civil. **Banco de dados e registros de desastres**: sistema integrado de informações sobre desastres - S2ID. 2013. Disponível em: <http://s2id. integracao.gov.br/>. Acesso em 01 de Maio de 2021.

BRASIL (2021b) Portal da transparência do Governo Federal – Controladoria Geral da União (CGU). Convênios por Estado/Município: banco de dados. Disponível em: https://falabr.cgu.gov.br/publico/Manifestacao/SelecionarTipoManifestacao.aspx?ReturnUrl=%2f Acesso em 07 de novembro de 2021.

BUDIMIR, M.E.A.; ATKINSON, P.M.; LEWIS, HG. A Systematic Review of Landslide Probability Mapping Using Logistic Regression. **Landslides**, v. 12, n. 3, 2015. 419-36. https://doi.org/10.1007/s10346-014-0550-5.

BÜHLER, Y.; CHRISTEN, M.; KOWALSKI, J.; BARTELT, P. Sensitivity of snow avalanche simulations to digital elevation model quality and resolution. **Annals of Glaciology**, v. 52, n. 58, p. 72–80, 2011.

BURTON, I.; KATES, R.W. The Perception of Natural Hazards in Resource Management. **Natural Resources Journal**, v. 3, p. 412, 1963.

CABRAL, V.; REIS, F.; VELOSO, V.; CORREA, C.; MENDOZA, C.; ALMEIDA, N.; GIORDANO, L. Assessment of the Influence of Rainfall and Landform on Landslide Initiation Using Physiographic Compartmentalisation. **Anuário Do Instituto De Geociências - UFRJ**, v. 42, n. 2, p. 407-420, 2019.

CABRAL, V.; REIS, F. Assessment of Shallow Landslides Susceptibility Using SHALSTAB and SINMAP at Serra Do Mar, Brazil. In: GUZZETTI, F.; MIHALIĆ ARBANAS, S.; REICHENBACH, P.; SASSA, K.; BOBROWSKY, P.T.; TAKARA, K. (Eds) **Understanding and Reducing Landslide Disaster Risk. WLF 2020. ICL Contribution to Landslide Disaster Risk Reduction**. Springer, Cham, 10 p, 2020. https://doi.org/10.1007/978-3-030-60227-7_28

CABRAL, V.C.; REIS, F.A.; D'AFFONSECA, F.M.; LUCÍA, A.; CORRÊA, C.V.; VELOSO, V.; GRAMANI, M.F. *et al* (2021) Characterization of a Landslide-Triggered Debris Flow at a Rainforest-Covered Mountain Region in Brazil. **Natural hazards**, v. 108, p. 3021–3043, 2021. https://doi.org/10.1007/s11069-021-04811-9.

CABRAL, V.C.; REIS, F.A., MARTINEZ, C.M., SANTOS, A. (2022). Model-based assessment of landslide susceptibility at a petrochemical site in Brazil. **Revista Brasileira de Geomorfologia**,

CAINE, N. The Rainfall Intensity: Duration Control of Shallow Landslides and Debris Flows. **Geografiska Annaler**, v. 62, p. 23 – 27, 1980. https://doi.org/10.2307/520449

CANNON, S.; GARTNER, J.; WILSON, R.; BOWERS, J.; LABER, J. Storm rainfall conditions for floods and debris flows from recently burned areas in southwestern Colorado and southern California. **Geomorphology**, v. 96, n. 3 – 4, 250 – 269, 2008. doi: 10.1016/j.geomorph.2007.03.019

CARDINALI, M.; REICHENBACH, P.; GUZZETTI, F.; ARDIZZONE, F.; ANTONINI, G.; GALLI, M.; CACCIANO, M.; CASTELLANI, M.; SALVATI, P. A geomorphological approach to the estimation of landslide hazards and risks in Umbria, Central Italy. **Natural Hazards and Earth System Sciences**, v. 2, p 57–72, 2002. https://doi.org/10.5194/nhess-2-57-2002

CASCINI, L.; FERLISI, S.; VITOLO, E. Individual and societal risk owing to landslides in the Campania region (southern Italy). **Georisk,** v. 2, n. 3, p. 125 – 140, 2008. Doi: 10.1080/17499510802291310

CASTELLI, F.; FRENI, G.; LENTINI, V.; FICHERA, A. Modelling of a Debris Flow Event in the Enna Area for Hazard Assessment. **Procedia Engineering**, v. 175, p. 287 – 292, 2017 doi: 10.1016/j.proeng.2017.01.026

CAVALCANTI, I.F.A. Large Scale and Synoptic Features Associated with Extreme Precipitation over South America: A Review and Case Studies for the First Decade of the 21st Century. **Atmospheric Research**, *v.* 118, p. 27 – 40, 2012. https://doi.org/10.1016/j.atmosres.2012.06.012.

CAVALCANTI, I.A.; NUNES, L.H.; MARENGO, J.A.; GOMES, J.L.; SILVEIRA, V.P.; CASTELLANO, M.S. Projections of Precipitation Changes in Two Vulnerable Regions of São Paulo State, Brazil. **American Journal of Climate Change**, v. 6, p. 268-293, 2017. https://doi.org/10.4236/ajcc.2017.62014

CENTRO NACIONAL DE MONITORAMENTO E ALERTA DE DESASTRES NATURAIS – CEMADEN. Rain gauges "Garuva - 420580301A" and "Estrada Geral Quiriri - 420580302A". Disponível em: http://www.cemaden.gov.br/mapainterativo/. Acesso em 20 de novembro de 2020.

CENTRO TECNOLÓGICO DE MINAS GERAIS - CETEC (1992) **Laudo geotécnico sobre o escorregamento de Vila Barraginha, Contagem (MG)**, Vol. 1. CETEC: Belo Horizonte, Brasil. 110p.

CENTRO UNIVERSITÁRIO DE ESTUDOS E PESQUISAS SOBRE DESASTRES – CEPED; UNIVERSIDADE FEDERAL DE SANTA CATARINA - UFSC. 2013. **Atlas Brasileiro de Desastres Naturais: 1991-2013**. Vol. Brasil. Centro Universitário de Estudos e Pesquisas sobre Desastres. Florianópolis

CERRI, R.I.; REIS, F.A.V.; GRAMANI, M.F.; ROSOLEN, V.; LUVIZOTTO, G.; GIORDANO, L.C; GABELINI, B.M. Assessment of Landslide Occurrences in Serra Do Mar Mountain Range Using Kinematic Analyses. **Environmental Earth Sciences**, v. 77, n. 9, 2018. https://doi.org/10.1007/s12665-018-7508-1.

CHANG, C.; LIN, P.; TSAI, C. Estimation of sediment volume of debris flow caused by extreme rainfall in Taiwan. **Engineering Geology**, v. 123, n. 1-2, p. 83-90, 2011.

CHANG, M.; DOU, X.; HALES, T.C.; YU, B. Patterns of Rainfall-Threshold for Debris-Flow Occurrence in the Wenchuan Seismic Region, Southwest China. **Bulletin of Engineering Geology and the Environment**, *v.* 80, n. 3, p. 2117-30, 2021 https://doi.org/10.1007/s10064-020-02080-7

CHEN, L.J.; SHIEH, C.L. A study on the danger ranks of potential debris flows. **Journal of Chinese Soil and Water Conservation**, v. 24, n. 1, p. 13–20, 1993.

CHEN, N.S.; YUE, Z.Q.; CUI, P. A rational method for estimating maximum discharge of a landslide- induced debris flow: a case study from south western China. **Geomorphology**, v. 84, p. 44–58, 2007.

CHEN, C.Y.;YU, F.C. Morphometric analysis of debris flows and their source areas using GIS. **Geomorphology**, v. 129, n. 3–4, p. 387–397, 2011

CHEN, J.; LI, Y.; ZHOU, W.; IQBAL, J.; CUI, Z.J. Debris-flow susceptibility assessment model and its application in semi-arid mountainous areas of the southeastern Tibetan plateau. **Natural Hazards Review**, v. 18, n. 2, 05016005, 2016

CHEN, W.; XIE, X.; WANG, J.; PRADHAN, B.; HONG, H.; BUI, D.T.; DUAN, Z.; MA, J.. A comparative study of logistic model tree, random forest, and classification and regression tree models for spatial prediction of landslide susceptibility. **Catena**, v. 151, p. 147–160, 2017

CHOI, G.; LEE, I.; YUNE, C. Risk Assessment of Debris Flow at Regional Scale Considering Catchment Area in Chuncheon, Korea. **KSCE Journal of Civil Engineering**, v. 25, n. 4, p. 1176 – 90, 2021. https://doi.org/10.1007/s12205-021-0136-4.

CHRISTEN, M.; BÜHLER, Y.; BARTELT, P.; LEINE, R.; GLOVER, J.; SCHWEIZER, A. *et al*. Integral hazard management using a unified software environment. Numerical simulation tool "RAMMS" for gravitational natural hazards. In: KOBOLTSCHNIG, G.; HÜBL, J.; BRAUN, J. (Eds.). **Protection of living space from natural hazards**. INTERPRAEVENT 2012, France, p. 77-86, 2012

CHURCH, M.; JAKOB, M. What Is a Debris Flood? **Water Resources Research**, v. 56, p. e2020WR027144, 2020.

COROMINAS, J.; VAN WESTEN, C.; FRATTINI, P.; CASCINI, L.; MALET, J.P.; FOTOPOULOU, S.; CATANI, F. *et al.* Recommendations for the Quantitative Analysis of Landslide Risk. **Bulletin of Engineering Geology and the Environment***, v.* 73, p. 209 – 263, 2014. https://doi.org/10.1007/s10064-013-0538-8.

CORRÊA, C.V.; REIS, F.A.; GIORDANO, L.C.; CABRAL, V.C.; TARGA, D.A.; BRITO, H.D. Possibilities and limitations for the back analysis of an event in mountain areas on the coast of São Paulo State, Brazil using RAMMS numerical simulation. Debris-Flow Hazards Mitigation: Mechanics, Monitoring, Modeling, and Assessment. In: **Proceedings of the 7th International Conference on Debris-Flow Hazards Mitigation**, p. 265-272, 2019.

COSTA, J.E. Rheologic, geomorphic, and sedimentologic differentiation of water floods, hyperconcentrated flows, and debris flows. In: BAKER, V.R.; KOCHEL, R.C.; PATTON, P.C. (eds) **Flood geomorphology**. Wiley, New York, 28 p., 1988.

COUSSOT, P.; MEUNIER, M. Recognition, classification and mechanical description of debris flows. **Earth-Science Reviews**, v. 40, n. 3 – 4, p. 209 – 227, 1996.

CROSTA, G.B.; IMPOSIMATO, S.; RODDEMAN, D.G. Numerical modelling of large landslides stability and runout. **Natural Hazards and Earth System Sciences**, v. 3, p. 523–538, 2003. doi:10.5194/nhess-3-523- 2003

CRUZ, O. A serra do mar e o litoral na área de Caraguatatuba - SP: contribuição à geomorfologia litorânea tropical - 2. **Revista Brasileira de Geografia***, v. 37*, n. 3, p. 73-138, 1975.

CRUZ, P.T.; MASSAD, F.; KANJI, M.A.; ARAUJO FILHO, H.A. Concepts on the design of dams for debris flow mitigation. In: **9th International Symposium on Landslides**, Rio de Janeiro. Balkema, 2: 1643–1650, 2004.

DAMM, B.; KLOSE.; M. The landslide database for Germany: Closing the gap at national level. **Geomorphology***, v.* 249, p. 82-93, 2015.

DAS, I.; SAHOO, S.; VAN WESTEN, C.; STEIN, A.; HACK, R. Landslide susceptibility assessment using logistic regression and its comparison with a rock mass classification system, along a road section in the northern Himalayas (India). **Geomorphology**, v. 114, p. 627–637, 2010.

de HAAS, T.; DENSMORE, A.L. Debris-flow volume quantile prediction from catchment morphometry. **Geology**, v. 47, p. 791–794, 2019.

de ROSA, P.; FREDDUZZI, A.; CENCETTI, C. Stream Power Determination in Gis: An Index to Evaluate the Most 'Sensitive'points of a River. **Water**, v. 11, n. 6, p. w11061145, 2019 https://doi.org/10.3390/w11061145.

DEBORTOLI, N.S.; CAMARINHA, P.I.M.; MARENGO, J.A. *et al.* An index of Brazil's vulnerability to expected increases in natural flash flooding and landslide disasters in the context of climate change. **Natural Hazards,** v. 86, p. 557 – 582, 2017. https://doi.org/10.1007/s11069-016-2705-2

DENG, Y.C.; HWANG, J.; LYU, Y.D. Developing Real-Time Nowcasting System for Regional Landslide Hazard Assessment under Extreme Rainfall Events. **Water***, v. 13*, p. 732, 2021. https://doi.org/10.3390/w13050732

DESTRO, E.; AMPONSAH, W., NIKOLOPOULOS, E.; MARCHI, L.; MARRA, F.; ZOCCATELLI, D.; BORGA, M. Coupled prediction of flash flood response and debris flow occurrence: Application on an alpine extreme flood event. **Journal of Hydrology**, v. 558, p. 225-237, 2018.

DEVOLI, G.; STRAUCH, W.; CHÁVEZ, G.; HØEG, K. A landslide database for Nicaragua: a tool for landslide-hazard management. **Landslides**, v. 4, n. 2, p. 163-176, 2007.

DIAS, V.C.; VIEIRA, B.C.; GRAMANI, M.F. Parâmetros morfológicos e morfométricos como indicadores da magnitude das corridas de detritos na Serra do Mar Paulista. **Confins**, n. 29, 2016.

DIAS, V.C.; MITCHELL, A.; VIEIRA, B.C.; MCDOUGALL, S. Differences in the occurrence of debris flows in tropical and temperate environments: field observations and geomorphologic characteristics in Serra do Mar (Brazil) and British Columbia (Canada). **Brazilian Journal of Geology**, v. 52, n. 3, p. e20210064, 2022. Doi: 10.1590/2317-4889202220210064.

DIETRICH, W.; DUNNE, T. Sediment budget for a small catchment in mountainous terrain. **Zeitschrift für Geomorphologie**, v. 29, p. 191 – 206, 1978.

DOURADO, F.; ARRAES, T.; SILVA, M. O Megadesastre da Região Serrana do Rio de Janeiro – as Causas do Evento, os Mecanismos dos Movimentos de Massa e a Distribuição Espacial dos Investimentos de Reconstrução no Pós-Desastre. **Anuário do Instituto Geológico da Universidade Federal do Rio de Janeiro**, v. 35, n. 2, p. 43 – 54, 2012.

DOWLING, C.A.; SANTI, P.M. Debris flows and their toll on human life: a global analysis of debris-flow fatalities from 1950 to 2011. **Natural Hazards**, *v.* 71, p. 203–227, 2014. https://doi.org/10.1007/s11069-013-0907-4

EM-DAT- **The International Disaster Database**. Disponível em: <http://www.emmat.be/classification>. Accesso em 7 de setembro 2021.

ERCANOGLU, M.; TEMIZ, F.A. Application of Logistic Regression and Fuzzy Operators to Landslide Susceptibility Assessment in Azdavay (Kastamonu, Turkey). **Environmental Earth Sciences**, v. 64, n. 4, p. 949 – 64, 2011. https://doi.org/10.1007/s12665-011-0912-4.

ESTADÃO (2010). Drama no Rio. Disponível em: https://internacional.estadao.com.br/blogs/olhar-sobre-o-mundo/drama-no-rio/. Acesso em 07 de setembro de 2021.

EVANS, S.G. Fatal landslides and landslide risk in Canada. In: CRUDEN, D.; FELL, R. (Eds.) **Landslide Risk Assessment**. Balkema, Rotterdam, pp. 185–196, 1997.

EVANS, A.; VERLANDER, N. What Is Wrong with Criterion FN-Lines for Judging the Tolerability of Risk? **Risk Analysis**, v. 17, n. 2, p. 157 – 168, 1997.

FACURI, G.; PICANÇO, J.L. Evaluations and proposals for the debris flow hazard mapping. **Landslides**, v. 18, n. 1, p. 339 – 352, 2020.

FAWCETT, T. An introduction to ROC analysis. **Pattern Recognition Letters**, v. 27, n. 8, p. 861–874, 2016. Doi: 10.1016/j.patrec.2005.10.010

FELL, R.; HARTFORD, D. Landslide risk management. In: CRUDEN, D.; FELL, R. (Eds.) **Landslide Risk Assessment**. Balkema, Rotterdam, pp. 51 – 109, 1997.

FERREIRA, K.; ABIKO, A. Urban Resilience and Landslide Risk Management: The Case of Santos (Brazil). In: BRUNETTA, G.; CALDARICE, O.; TOLLIN, N.; ROSAS-CASALS, M.; MORATÓ, J. (Eds) **Urban**

Resilience for Risk and Adaptation Governance. Resilient Cities (Re-thinking Urban Transformation). Springer, p. 229 – 270, 2019. https://doi.org/10.1007/978-3-319-76944-8_12

FISCHER, J.; KOWALSKI, J.; PUDASAINI, S. Topographic curvature effects in applied avalanche modeling. **Cold Regions Science And Technology**, v. 74, p. 21-30, 2012. doi: 10.1016/j.coldregions.2012.01.005

FOWLER, A.M.; HENNESSY, K.J. Potential impacts of global warming on the frequency and magnitude of heavy precipitation. **Natural Hazards,** v. 11, p. 283–303, 1995. https://doi.org/10.1007/BF00613411

FRANK, F.; MCARDELL, B.W.; HUGGEL, C.; VIELI, A. The Importance of Entrainment and Bulking on Debris Flow Runout Modeling: Examples from the Swiss Alps. **Natural Hazards and Earth System Sciences**, v. 15, n. 11, p. 2569 – 83, 2015. https://doi.org/10.5194/nhess-15-2569-2015.

FRANK, F., MCARDELL, B.W.; OGGIER, N.; BAER, P.; CHRISTEN, M.; VIELI, ANDREAS. Debris-Flow Modeling at Meretschibach and Bondasca Catchments, Switzerland: Sensitivity Testing of Field-Data-Based Entrainment Model. **Natural Hazards and Earth System Sciences**, v. 17, n. 5, p. 801 – 15, 2017. https://doi.org/10.5194/nhess-17-801-2017.

FUCHS, S.; HEISS, K.; HÜBL, J. Towards an empirical vulnerability function for use in debris flow risk assessment. **Natural Hazards and Earth System Sciences**, v. 7, p. 495 – 506, 2007. https://doi.org/10.5194/nhess-7-495-2007.

FUKUOKA, M. Landslides associated with rainfall. **Geotechnical Engineering**, v. 11, p. 1 – 29, 1980

FÚLFARO, V.; PONÇANO, W.L.; BISTRICHI, C.A.; STEIN, D.P. Escorregamentos de Caraguatatuba: expressão atual, e registro na coluna sedimentar da planície costeira adjacente. In: **Congresso Brasileiro de Geologia de Engenharia. Anais...** Rio de Janeiro: ABGE, pp. 341 – 350, 1976.

GABELINI, B.M.; CORRÊA, C.V.; CERRI, R.I.; REIS, F.A.; ZAINE, J.E.; GIORDANO, L.C. Avaliação da suscetibilidade a escorregamento na Serra do Mar pela aplicação da compartimentação fisiográfica. **Geologia USP. Série Científica**, v. 19, n. 1, 193 – 211, 2019. https://doi.org/10.11606/issn.2316-9095.v19-138528

GABET, E.; STERNBERG, P. The effects of vegetative ash on infiltration capacity, sediment transport, and the generation of progressively bulked debris flows. **Geomorphology**, v. 101, n. 4, p. 666-673, 2008.

GALDERISI, A.; CEUDECH, A.; PISTUCCI, M. A method for na-tech risk assessment as supporting tool for land use planning mitigation strategies. **Natural Hazards**, v. 46, p. 221e241, 2008.

GAUME, E.; BORGA, M. Post-flood field investigations in upland catchments after major flash floods: proposal of a methodology and illustrations. **Journal of Flood Risk Management**, v. 1, n. 4, p. 175–189, 2008.

GEORIO. Estudos Geológicos-Geotécnicos a Montante dos Condomínios Capim Melado e Vilarejo, Jacarepaguá. **Relatório Técnico**, 96 p., 1996.

GEOTECHNICAL ENGINEERING OFFICE - GEO (1998). Landslides and Boulder Falls from Natural Terrain: Interim Risk Guidelines. **GEO Report 75**, Geotechnical Engineering Office, Civil Engineering Department. Government of the Hong Kong SAR.

GIORGI, F.; IM, E.S.; COPPOLA, E.; DIFFENBAUGH, N.S.; GAO, X.J.; MARIOTTI, L.; SHI, Y. Higher hydroclimatic intensity with global warming. **Journal of Climate**, v. 24, p. 5309–5324, 2011.

GONÇALVES, N.M.S. **Impactos Pluviais e Desorganização do Espaço Urbano em Salvador/Ba**. PhD Thesis, Universidade de São Paulo, 300 p., 1992.

GONÇALVES, L.F.H. Avaliação e diagnóstico da distribuição espacial e temporal dos movimentos de massa com a expansão da área urbana em Petrópolis – R.J. Masters' dissertation. Programa de Pós-Graduação em Geografia Universidade Federal do Rio de Janeiro - UFRJ, Rio de Janeiro, 232 p., 1998.

GORSEVSKI, P.V.; GESSLER, P.E.; FOLTZ, R.B.; ELLIOT, W.J. Spatial prediction of landslide hazard using logistic regression and ROC analysis. **Trans GIS**, v. 10, n. 3, p. 395 – 415, 2006.

GRAMANI, M.F. **Caracterização geológica-geotécnica das corridas de detritos ("Debris Flows") no Brasil e comparação com alguns casos internacionais**. Masters' dissertation, Universidade de São Paulo, São Paulo, 372 p., 2001.

GRAMANI, M.F. A corrida de massa em Itaoca: transporte e deposição de sedimentos. In*:* **Simpósio de Geologia do Sudeste, 14.; Simpósio do Cretáco do Brasil***,* Campos do Jordão, 5 p., 2015.

GRAMANI, M.F.; MARTINS, V.T.S. Debris flows occurrence by intense rains on January 13, 2014 at Itaoca City, São Paulo, Brazil: impacts and field observations. In: **International Symposium of Landslides, Napoli**, Italy, 8 p, 2016.

GRAMANI, M.F. Corridas de massa na Serra da Mantiqueira: descrição e avaliação da ocorrência no Córrego do Braço, SP. In: **Conferência brasileira sobre estabilidade de encostas - COBRAE**, Florianópolis, 8 p, 2017.

GREGORETTI, C.; DEGETTO, M.; BERNARD, M.; BOREGGIO, M. The Debris Flow Occurred at Ru Secco Creek, Venetian Dolomites, on 4 August 2015: Analysis of the Phenomenon, Its Characteristics and Reproduction by Models. **Frontiers on Earth Sciences**, v. 6, n. 80, 2018.

GUERRA, A. Catastrophic Events in Petrópolis City (Rio De Janeiro State), between 1940 and 1990. **GeoJournal***, v.* 37, n. 3, p. 349 – 354, 1995.

GUERRA, A.; LOPES, P.; SANTOS FILHO, R. Características Geográficas e Geomorfológicas da APA, Petrópolis, RJ. **Revista Brasileira de Geomorfologia***,* v. 8, n. 1, p. 77 – 86, 2007

GUZZETTI, F.; CARRARA, A.; CARDINALI, M.; REICHENBACH, P. Landslide hazard evaluation: a review of current techniques and their application in a multi-scale study, Central Italy. **Geomorphology**, v. 31, n. 1 – 4, p. 181 – 216, 1999.

GUZZETTI, F. Landslide fatalities and evaluation of landslide risk in Italy. **Engineering Geology**, v. 58, p. 89 – 107, 2000.

GUZZETTI, F.; TONELLI, G. SICI: an information system on historical landslides and floods in Italy. **Natural Hazards and Earth System Sciences**, v. 4, p. 213–232, 2004.

GUZZETTI, F.; MONDINI, A.C.; CARDINALI, M.; FIORUCCI, F.; SANTANGELO, M.; CHANG, K.T. Landslide Inventory Maps: New Tools for an Old Problem. **Earth-Science Reviews***,* v. 112, n. 1-2, p. 42 – 66, 2012. https://doi.org/10.1016/j.earscirev.2012.02.001.

GUZZETTI, F.; PERUCCACCI, S.; ROSSI, M.; STARK, C.P. The Rainfall Intensity–Duration Control of Shallow Landslides and Debris Flows: An Update. **Landslides**, v. 5, n. 1, p. 3-17, 2017. https://doi.org/10.1007/s10346-007-0112-1.

HEALTH AND SAFETY EXECUTIVE – HSE (2009). Societal Risk: Initial briefing to the Societal Risk Technical Advisory Group. **HSE Research Report RR703** – available at: www.hse.gov.uk/research/rrhtm/rr703.htm, accesso em 23 de novembro de 2021.

HEISER, M.; SCHEIDL, C.; EISL, J.; SPANGL, B.; HÜBL, J. Process type identification in torrential catchments in the eastern Alps. **Geomorphology**, v. 232, p. 239–247, 2015.

HO, K.; KO, F. Application of quantified risk analysis in landslide risk management practice: Hong Kong experience. **Georisk: Assessment and Management of Risk for Engineered Systems and Geohazards**, v. 3, n. 3, p. 134 – 146, 2009.

HOGAN, D.J. Condições de vida e morte em Cubatão. In: **VI Encontro Nacional de Estudos Populacionais. Anais...** Olinda: Abep, 1988.

HUANGFU, W.; WU, W.; ZHOU, X.; LIN, Z.; ZHANG, G.; CHEN, R.; SONG, Y.; LANG, T.; QIN, Y.; OU, P. *et al*. Landslide Geo-Hazard Risk Mapping Using Logistic Regression Modeling in Guixi, Jiangxi, China. **Sustainability***, v. 13*, p. 4830, 2021. https://doi.org/ 10.3390/su13094830

HUANG, J.; JU, N.P.; LIAO, Y.J.; LIU, D.D. Determination of rainfall thresholds for shallow landslides by a probabilistic and empirical method. **Natural Hazards and Earth System Sciences**, v. 15, p. 2715–2723, 2015. https://doi.org/10.5194/nhess-15-2715-2015, 2015.

HUEBL, J.; FIEBIGER, G. Debris-flow mitigation measures. In: **Debris-flow Hazards and Related Phenomena**. Springer Praxis Books. Springer, Berlin, Heidelberg, 30 p., 2005. https://doi.org/10.1007/3-540-27129-5_18

HUGGEL, C.; CLAGUE, J.J.; KORUP, O. Is climate change responsible for changing landslide activity in high mountains? **Earth Surface Processes and Landforms**, v. 37, p. 77-91, 2012.

HUNGR, O.; LEROUEIL, S.; PICARELLI, L. The Varnes classification of landslide types, an update. **Landslides**, v. 11, n. 2, p. 167–194, 2014.

HUNGR, O.; MCDOUGALL, S. Two numerical models for landslide dynamic analysis. **Computers & Geosciences**, v. 35, n. 5, p. 978 – 992, 2009. DOI: 10.1016/j.cageo.2007.12.003

HUNGR, O.; MORGAN, G.C.; KELLERHALS, R. Quantitative analysis of debris torrent hazards for design of remedial measures. **Canadian Geotechnical Journal**, v. 21, p. 663–677, 1984.

HÜRLIMANN, M.; COPONS, R.; ALTIMIR, J. Detailed debris flow hazard assessment in Andorra: A multidisciplinary approach. **Geomorphology**, v. 78, n. 3 – 4, p. 359 – 372, 2006.. doi: 10.1016/j.geomorph.2006.02.003

HUSSIN, H.Y.; QUAN LUNA, B.; VAN WESTEN, C.J.; CHRISTEN, M.; MALET, J.P.; VAN ASCH, T.W.J. Parameterization of a Numerical 2-D Debris Flow Model with Entrainment: A Case Study of the Faucon Catchment, Southern French Alps. **Natural Hazards and Earth System Sciences***,* v. 12, n. 10, p. 3075-90, 2012. https://doi.org/10.5194/nhess-12-3075-2012.

ILINCA, V. Using Morphometrics to Distinguish between Debris Flow, Debris Flood and Flood (Southern Carpathians, Romania). **Catena**, v. 197, p. 104982, 2021. https://doi.org/10.1016/j.catena.2020.104982.

INSTITUTO BRASILEIRO DE GEOGRAFIA E ESTATÍSTICA – IBGE. 2019. Tábuas completa de mortalidade para o Brasil. Disponível em < https://biblioteca.ibge.gov.br/index.php/biblioteca-catalogo?view=detalhes&id=73097>, Acesso em 01 de novembro de 2021.

INSTITUTO BRASILEIRO DE GEOGRAFIA E ESTATÍSTICA – IBGE. 2021. Projeção da população do Brasil e das Unidades da Federação. Disponível em: < https://www.ibge.gov.br/apps/populacao/projecao/index.html>, Acesso em 01 de novembro de 2021.

INSTITUTO DE PESQUISA TECNOLÓGICAS – IPT (1975) Estudo preventivo e corretivo dos movimentos coletivos de solo e rochas na serra de Maranguape. **Relatório Técnico - Fase de Diagnóstico**. São Paulo. v. 1, n.1, 1975.

INSTITUTO DE PESQUISAS TECNOLÓGICAS - IPT (1986) **Programa Serra do Mar – levantamentos básicos nas folhas de Santos e Riacho Grande, Estado de São Paulo**. Publicação IPT nº 23.394(2), 120p.

INSTITUTO DE PESQUISA TECNOLÓGICAS – IPT (1988) Estudo das instabilizações das encostas da Serra do Mar na região de Cubatão, objetivando a caracterização do fenômeno "corrida de lama" e a prevenção dos seus efeitos. **Relatório técnico nº 25.402**. São Paulo, pp. 125

IVERSON, R. Landslide triggering by rain infiltration. **Water Resources Research**, v. 36, n. 7, p. 1897-1910, 2000.

IVERSON, R.M.; REID, M.E.; LOGAN, M.; LAHUSEN, R.G.; GODT, J.W.; GRISWOLD, J.P. Positive feedback and momentum growth during debris-flow entrainment of wet bed sediment. **Nature geosciences**, v. 4, p. 116-121, 2011.

JAKOB, M. Debris-flow hazard analysis. In: JAKOB, M.; HUNGR, O. (Ed) **Debris-Flow Hazards and Related Phenomena**. Springer-Verlag, Berlin, pp. 411–443, 2005a

JAKOB, M. A size classification for debris flows. **Engineering Geology**, v. 79, p. 151–161, 2005b.

JAKOB, M.; STEIN, D.; ULMI, M. Vulnerability of buildings to debris flow impact. **Natural Hazards***, v.* 60, p. 241–261, 2012. https://doi.org/10.1007/s11069-011-0007-2

JAPAN INTERNATIONAL COOPERATION AGENCY - JICA (1991) **The Study on the Disaster Prevention and Restoration Project in Serra do Mar, Cubatão Region**, São Paulo. January, vol. 2

JONES, F.O. Landslides of Rio de Janeiro and the Serra das Araras Escarpment, Brazil. **Geological Survey Professional Paper**, vol. 697. Department of the Interior, US Printing Office, Washington, 1973.

KAHN, M.E. The Death Toll from Natural Disasters: The Role of Income, Geography, and Institutions. **The Review of Economics and Statistics**, v. 87, n. 2, p. 271 – 284, 2005.

KANJI, M.A.; CRUZ, P.T.; MASSAD, F.; ARAUJO, F.H.A. Basic and Common Characteristics of Debris Flows. In: **Proceedings of the 2nd Panamerican Symposium**, Rio de Janeiro, v. 10, p. 223-231, 1997.

KANJI, M.A.; CRUZ, P.T.; MASSAD, F.; ARAUJO FILHO, H.A. Basic and common characteristics of debris flows. In: **2nd Panamerican Symposium on Landslides and 2 Congr. Bras. Estabilidade Enconstas COBAE**, R. Janeiro, v. 1, p. 223–231, 1997.

KANJI, M.A.; GRAMANI, M.F.; MASSAD, F.; CRUZ, P.T.; ARAUJO FILHO, H.A. Main factors intervening in the risk sssessment of debris flows. In: **International Workshop on the Debris Flow Disaster of Dec. 1999 in Venezuela, Caracas** (CD ROM), 10 p., 2000.

KANJI, M.A., CRUZ, P.T., MASSAD, F. Debris flow affecting the Cubatão oil refinery, Brazil. **Landslides**, v. 5, n. 1, p. 71-82, 2007.

KEAN, J.W.; MCCOY, S.W.; TUCKER, G.E.; STALEY, D.M.; COE, J.A. Runoff-generated debris flows: Observations and modeling of surge initiation, magnitude, and frequency. **Journal of Geophysical Research: Earth Surface**, v. 118, p. 2190–2207, 2013.

KELLER, B. Massive rock slope failure in Central Switzerland: history, geologic–geomorphological predisposition, types and triggers, and resulting risks. **Landslides***, v.* 14, p. 1633 – 1653, 2017. https://doi.org/10.1007/s10346-017-0803-1

KLEINEN, T.; PETSCHEL-HELD, G. Integrated assessment of changes in flooding probabilities due to climate change. **Climatic Change**, v. 81, p. 283–312, 2007. https://doi.org/10.1007/s10584-006-9159-6

KOBIYAMA, M.; CHAFFE, P.L.B.; GOERL, R.F.; GIGLIO, J.N.; REGINATTO, G.M.P. Hydrological disasters reduction: lessons from hydrology. In: SENS, M.L.; MONDARDO, R.I. (Orgs.) **Science and Technology for Environmental Studies: Experiences from Brazil, Portugal and Germany**. Florianópolis: Universidade Federal de Santa Catarina, p. 49 – 72, 2010.

KOBIYAMA M, MICHEL GP. Bibliografia dos trabalhos de fluxos de detritos ocorridos no Brasil no período de 1949-2014: Atualização. Porto Alegre: Trabalho Técnico GPDEN/IPH/UFRGS, n. 2, 16 p. 2015a.

KOBIYAMA, M.; MICHEL, G.; ENGSTER, E.; PAIXÃO, M. Historical analyses of debris flow disaster occurrences and of their scientific investigation in Brazil. **Labor e Engenho**, v. 9, n. 4, p. 76, 2015b.

KOBIYAMA, M.; MICHEL, G.; GOERL, R.F. Proposal of debris flow disasters management in Brazil based on historical and legal aspects. **International Journal of Erosion Control Engineering***, v.* 11, n. 3, p. 85 – 93, 2019.

KOPECKÝ, M.; MACEK, M.; WILD, J. Topographic Wetness Index calculation guidelines based on measured soil moisture and plant species composition. **Science Of The Total Environment**, v. *757*, p. 143785, 2021. doi: 10.1016/j.scitotenv.2020.143785

KOVANEN, D.J.; SLAYMAKER, O. The Morphometric and Stratigraphic Framework for Estimates of Debris Flow Incidence in the North Cascades Foothills, Washington State, USA. **Geomorphology***, v.* 99, n. 1-4, p. 224 – 45, 2008. https://doi.org/10.1016/j.geomorph.2007.11.003.

KRONFELLNER-KRAUS, G. Quantitative estimation of torrent erosion. In: **International Symposium of Erosion, Debris Flow Disasters Prevention**, Tsukuba, Japan, p. 107–110, 1985.

LACERDA, W. Landslide initiation in saprolite and colluvium in southern Brazil: Field and laboratory observations. **Geomorphology**, v. 87, n. 3, p. 104-119, 2007.

LANG, A.; MOYA, J.; COROMINAS, J.; SCHROTT, L.; DIKAU, R. Classic and new dating methods for assessing the temporal occurrence of mass movements. **Geomorphology**, v. 30, n. 1-2, p. 33-52, 1999.

LAY, U.S.; PRADHAN, B.; YUSOFF, Z.B.M.; ABDALLAH, A.F.B.; ARYAL, J.; PARK, H.J. Data Mining and Statistical Approaches in Debris-Flow Susceptibility Modelling Using Airborne LiDAR Data. **Sensors**, *v.* 19*,* p. 3451, 2019 https://doi.org/10.3390/s19163451

LIMA, K.; SATYAMURTI, P.; FERNANDEZ, J.P.R. Large-scale atmospheric conditions associated with heavy rainfall episodes in Southeast Brazil. **Theoretical and Applied Climatology**, v. 101, p. 121 – 135, 2009. http://dx.doi.org/10.1007/s00704-009-0207-9.

LIN, P.S.; FENG, T.Y.; LEE, C.M. A study on the initiation characteristics of debris flow in gravelly deposits. **Journal of Chinese Soil and Water Conservation**, v. 24, n. 1, p. 55 – 64, 1993.

LIN, P.S.; LIN, J.Y.; HUNG, J.C.; YANG, M.D. Assessing debris-flow hazard in a watershed in Taiwan. **Engineering Geology**, v. 66, p. 295–313, 2002.

LIU, K.F.; LI, H.C.; HSU, Y.C. Debris flow hazard assessment with numerical simulation. **Natural Hazards**, v. 49, p. 137-161, 2009

LIU, Q.; JIAN, W.; NIE, W. Rainstorm-Induced Landslides Early Warning System in Mountainous Cities Based on Groundwater Level Change Fast Prediction. **Sustainable Cities and Society***,* v. 69, p. 102817, 2021. https://doi.org/10.1016/j.scs.2021.102817.

LISTO, F.; GOMES, M.; VIEIRA, B. Avaliação da variação do fator de segurança com o modelo TRIGRS. **Revista Brasileira de Geomorfologia**, v. 19, n. 1, p. 207 – 220, 2018.

LONDE, L.; MOURA, L.; COUTINHO, M.; MARCHEZINI, V.; SORIANO, E. Vulnerability, health and disasters in São Paulo coast (Brazil): challenges for a sustainable development. **Ambiente & Sociedade, v.** 21, n. 0, p e01022, 2018.

LOPES, E.S.S.; RIEDEL, P.S.; BENTS, C.M.; FERREIRA, M.V.; NALETO, J.L.C. Inventário de escorregamentos naturais em banco de dados geográfico – análise dos fatores condicionantes na região da Serra de Cubatão – SP. In: XIII Simpósio Brasileiro de Sensoriamento Remoto, 13., 2007, Florianópolis. **Anais…** São José dos Campos: INPE, 2007. p. 2785-2796.

LOPES, ESS.; RIEDEL, P.S. Simulação da corrida de massa do Km42 ocorrido na Rodovia Anchieta. In: **Simpósio Brasileiro de Desastres Naturais e Tecnológicos**, 2, Santos, 6 p., 2007.

LUCÀ, F.; ROBUSTELLI, G. Comparison of Logistic Regression and Neural Network Models in Assessing Geomorphic Control on Alluvial Fan Depositional Processes (Calabria, Southern Italy). **Environmental Earth Sciences***, v.* 79, n. 1, 2020. https://doi.org/10.1007/s12665-019-8775-1.

LUCÍA, A.; COMITI, F.; BORGA, M.; CAVALLI, M.; MARCHI, L. Dynamics of large wood during a flash flood in two mountain catchments. **Natural Hazards and Earth System Sciences**, v. 15, p. 1741–1755, 2015.

LUCÍA, A.; SCHWIENTEK, M.; EBERLE, J.; ZARFL, C. Planform changes and large wood dynamics in two torrents during a severe flash flood in Braunsbach, Germany 2016. **Science of the Total Environmental**, v. 640-641, p. 315-326, 2018.

LUNA, B.; REMAÎTRE, A.; VAN ASCH, T.; MALET, J.; VAN WESTEN. C. Analysis of debris flow behavior with a one-dimensional run-out model incorporating entrainment. **Engineering Geology**, v. 128, p. 63-75, 2012.

MAACK, R. 2002. **Geografia física do Estado do Paraná**. Curitiba, Imprensa Oficial, 440p.

MACCIOTTA, R.; MARTIN, C.D.; MORGENSTERN, N.R. *et al.* Quantitative risk assessment of slope hazards along a section of railway in the Canadian Cordillera—a methodology considering the uncertainty in the results. **Landslides***, v.* 13, p. 115 – 127, 2016.

MAIA, A.C.N.; SEDREZ, L. Enchentes que destroem, enchentes que constroem: Natureza e memória da Cidade de Deus nas chuvas de 1966 e 1967. **Revista do Arquivo Geral do Rio de Janeiro**, v. 8, p. 183 – 199, 2014.

MARCHI, L.; D'AGOSTINO, V. Estimation of debris-flow magnitude in the Eastern Italian Alps. **Earth Surface Processes and Landforms**, v. 29, n. 2, p. 207-220, 2004.

MARCHI, L.; CAVALLI, M.; SANGATI, M.; BORGA, M. Hydrometeorological controls and erosive response of an extreme alpine debris flow. **Hydrological Processes**, v. 23, n. 19, p. 2714-2727, 2009.

MARCHI, L,; BRUNETTI, M.; CAVALLI, M.; CREMA, S. Debris-flow volumes in northeastern Italy: Relationship with drainage area and size probability. **Earth Surface Processes and Landforms**, v. 44, n. 4, p. 933-943, 2019.

MARENGO, J.; CAMARINHA, P.; ALVES, L.; DINIZ, F.; BETTS, R. Extreme Rainfall and Hydro-Geo-Meteorological Disaster Risk in 1.5, 2.0, and 4.0°C Global Warming Scenarios: An Analysis for Brazil. **Frontiers in Climate**, v. 3, 2021.

MASSAD, F.; KANJI, M.A.; CRUZ, P.T.; UEHARA, K.; ISHITANI, H.; ARAUJO FILHO, H.A. Debris flows" em Cubatão, São Paulo: obras de controle e impactos ambientais. In: ***XI Congresso Brasileiro de Mecânica dos Solos e Engenharia Geotécnica***. Brasília: ABMS, 8 p., 1998.

MASSAD, F. Corridas de massas geradas por escorregamentos de terra: relação entre a área deslizada e a intensidade de chuva. In: ***XII Congresso Brasileiro de Mecânica dos Solos e Engenharia Geotécnica***. São Paulo, São Paulo, 7 p., 2002.

MATTOS, I. F. A. ; MATSUKUMA, C. K. . Mapeamento evolutivo da vegetação da Serra do Mar-Cubatão-SP. In: **6º Congresso Florestal Brasileiro, 1990**, Campos do Jordão. Florestas e meio ambiente: conservação e produção, patrimônio social. Campos do Jordão: Sociedade Brasileira de Sivicultura, 1990. v. 3. p. 330-342.

MCDOUGALL, S. 2014 Canadian Geotechnical Colloquium: landslide runout analysis – current practice and challenges. **Canadian Geotechnical Journal**, v. 54, n. 5, p. 605–620, 2017.

MEDINA, V.; HÜRLIMANN, M.; BATEMAN, A. Application of FLAT- Model a 2-D finite volume code, to debris flows in the northeast- ern part of the Iberian Peninsula. **Landslides**, v. 5, p. 127–142, 2008.

MEIS, M.R.M.; SILVA, J.X. (1968) Considerações Geomorfológicas a Propósito dos Movimentos de Massa Ocorridos no Rio de Janeiro. **Revista Brasileira de Geografia**, v. 30, n. 1, p. 55 – 73, 1968.

MELTON, M.A. Correlation Structures of Morphometric Properties of Drainage Systems and Their Controlling Agents. **Journal of Geology**, v. 66, p. 442 – 460, 1958. http://dx.doi.org/10.1086/626527

MENDONCA, M.; SILVA, D. Integration of census data based vulnerability in landslide risk mapping - The case of Angra dos Reis, Rio de Janeiro, Brazil. **International Journal Of Disaster Risk Reduction**, v. 50, p. 101884, 2020. doi: 10.1016/j.ijdrr.2020.101884

MEYER, N.K.; SCHWANGHART, W.; KORUP, O.; ROMSTAD, B.; ETZELMÜLLER, B. Estimating the topographic predictability of debris flows. **Geomorphology**, v. 207, p. 114 – 125, 2014.

MILNE, F. 2008. Topographic and material controls on the Scottish debris flow geohazard. PhD Thesis, University of Dundee, Scotland.

MIRUS, B.; JONES, E.; BAUM, R.; GODT, J.; SLAUGHTER, S.; CRAWFORD, M.; LANCASTER, J.; STANLEY, T.; KIRSCHBAUM, D.; BURNS, W.; SCHMITT, R.; LINDSEY, K.; MCCOY, K. Landslides across the USA: occurrence, susceptibility, and data limitations. **Landslides***, v.* 17, n. 10, p. 2271 – 2285, 2020.

MOCOCHINSKI, A.Y.; SCHEER, M.B. Campos De Altitude Na Serra Do Mar Paranaense: Aspectos Florísticos. **Floresta**, v. 38, n. 4, p. 625–640, 2014.

MOINE, M.; PUISSANT, A.; MALET, J.P. Detection of landslides from aerial and satellite images with a semi-automatic method-Application to the Barcelonnette basin (Alpes-de-Haute-Provence, France). In: MALET, J.P.; REMAITRE, A.; BOGAARD, T. (Eds.), **Landslide Processes: from geomorphological mapping to dynamic modelling**. CERG, Strasbourg, France, p. 63-68, 2009.

MUIR, I.; HO, K.S.S.; SUN, H.W.; HUI, T.H.H.; KOO, Y C. Quantitative risk assessment as applied to natural terrain land- slide hazard management in a mid-levels catchment, Hong Kong. In: NADIM, F.; PO¨TTLER, R.; EINSTEIN, H.; KLAPPERICH, H.; KRAMER, S. (Eds.) **Geohazards**. ECI Symposium Series, P07, 8 pp., 2006.

NAKAZAWA, V.A.; CERRI, L.E.S. Os escorregamentos ocorridos em Petrópolis – RJ em fevereiro de 1988: ações emergenciais. In: **Simpósio Latino-Americano sobre Risco Geológico Urbano**, Atas.../ABGE, p.325 – 333, 1990.

NIKOLOVA, V.; KAMBUROV, A.; RIZOVA, R. Morphometric Analysis of Debris Flows Basins in the Eastern Rhodopes (Bulgaria) Using Geospatial Technologies. **Natural Hazards**, v. 105, n. 1, p. 159 – 75, 2020. https://doi.org/10.1007/s11069-020-04301-4.

NOBRE, C.A.; MARENGO, J.A.; SELUCHI, M.E.; CUARTAS, L.A.; ALVES, L.M. Some Characteristics and Impacts of the Drought and Water Crisis in Southeastern Brazil during 2014 and 2015. **Journal of Water Resource and Protection**, v. 8, p. 252 – 262, 2016. http://dx.doi.org/10.4236/jwarp.2016.82022

O'GORMAN, P.; SCHNEIDER, T. The physical basis for increases in precipitation extremes in simulations of 21st-century climate change. **Proceedings of the National Academy of Sciences**, v. 106, n. 35, p. 14773 – 14777, 2009.

OHLMACHER, G.C.; DAVIS, J.C. Using multiple logistic regression and GIS technology to predict landslide hazard in northeast Kansas, USA. **Engineering Geology**, v. 69, n. 3 – 4, p. 331 – 343, 2003.

OLIVEIRA FILHO, O. Os movimentos de massa na região serranda do estado do Rio de Janeiro em 2011: diagnóstico e proposição de medidas para enfrentamento de desastres ambientais. **CES Revista**, v. 26, n. 1, p. 149 – 164, 2012.

PÁNEK, T. Recent progress in landslide dating. **Progress in Physical Geography: Earth and Environment**, v. 39, n. 2, p. 168-198, 2014.

PAK, J., LEE, J. A Statistical sediment yield prediction model incorporating the effect of fires and subsequent storm events. **Journal of the American Water Resources Association**, v. 44, n. 3, p. 689-699, 2008.

PATEL, R.; BURKE, T. Urbanization — An Emerging Humanitarian Disaster. **New England Journal of Medicine**, v. 361, n. 8, p. 741-743, 2009.

PELLERIN, J., DUARTE, G.M.; SCHEIBE, L.F.; MENDONÇA, M.; BUSS, M.D.; MONTEIRO, M.A. Timbé do Sul - Jacinto Machado: avaliação preliminar da extensão da catástrofe de 23-24/12/95. **Geosul***, v.* 12, n. 23, p. 71 – 86, 1997.

PEREIRA FILHO, A.J.; VEMADO, F.; REIS, F.A.G.V.; GIORDANO, L.C.; CERRI, R.I.; SANTOS, C.S., LOPES, E.S.S.; GRAMANI, M.F.; OGURA, A.T.; ZAINE, J.E.; CERRI, L.E.S.; AUGUSTO FILHO, O.; D'AFFONSECA, F.M.; AMARAL, C.S. A Step towards Integrating CMORPH Precipitation Estimation with Rain Gauge Measurements. **Advances in Meteorology**, v. 2018, p. 1-24, 2018.

PETLEY, D. Global Patterns of Loss of Life from Landslides. **Geology**, v. 40, n. 10, p. 927 – 30, 2012. https://doi.org/10.1130/g33217.1.

PEULVAST, J.P.; BÉTARD, F.; MAGALHÃES, A.O. Scarp morphology and identification of large-scale mass movements in tropical tablelands: the eastern Araripe basin (Ceará, Brazil). **Géomorphologie: relief, processus, environnement**, v. 17, n. 1, p. 33 – 52, 2011. DOI : https://doi.org/10.4000/geomorphologie.8800

PINTO, R.C.; PASSOS, E.; CANEPARO, S.C. Movimentos de Massa como Processos Naturais de Evolução das Encostas, Estudo de Caso: Bacia do Rio Jacareí, Municípios de Morretes e Paranaguá–PR. **Geoingá: Revista do Programa de Pós-Graduação em Geografia***, v.* 6, n. 1, p. 23 – 45, 2014.

QUAN LUNA, B.; BLAHUT, J.; VAN WESTEN, C.J.; STERLACCHINI, S.; VAN ASCH, T.W.J.; AND AKBAS, S.O. The application of numerical debris flow modelling for the generation of physical vulnerability curves. **Natural Hazards and Earth System Sciences**, v. 11, p. 2047 – 2060, 2011. https://doi.org/10.5194/nhess-11-2047-2011

REID, M.E.; COE, J.A.; DIANNE, L.B. Forecasting inundation from debris flows that grows volumetrically during travel, with application to the Oregon Coast Range, USA. **Geomorphology**, v. 273, p. 396–411, 2016.

RICKENMANN, D.; ZIMMERMANN, M. The 1987 debris flows in Switzerland: documentation and analysis. **Geomorphology**, v. 8, p. 175 – 189, 1993.

RICKENMANN, D. Empirical relationships for debris flows. **Natural Hazards**, v. 19, n. 1, p. 47-77, 1999.

RICKENMANN, D.; KOSCHNI, A. Sediment loads due to fluvial transport and debris flows during the 2005 flood events in Switzerland. **Hydrological Processes**, v. 24, n. 8, p. 993–1007, 2010.

RICKENMANN, D. 2016. **Methods for the quantitative assessment of channel processes in torrents (steep streams)**. CRC Press, Taylor and Francis Group, Leiden, Netherlands.

RILEY, K.L.; BENDICK, R.; HYDE, K.D.; GABET, E.J. Frequency–Magnitude Distribution of Debris Flows Compiled from Global Data, and Comparison with Post-Fire Debris Flows in the Western U.S. **Geomorphology**, v. 191, p. 118 – 28, 2013. https://doi.org/10.1016/j.geomorph.2013.03.008.

ROSA FILHO, A.; CORTEZ, A.T.C. A problemática socioambiental da ocupação urbana em áreas de risco de deslizamento da "Suíça brasileira". **Revista Brasileira de Geografia Física**, v. *3*, n. 1, p. 33 – 40, 2010. doi: 10.26848/rbgf.v3i1.232610

ROSI, A.; CANAVESI, V.; SEGONI, S.; DIAS NERY, T.; CATANI, F.; CASAGLI, N. Landslides in the Mountain Region of Rio de Janeiro: A Proposal for the Semi-Automated Definition of Multiple Rainfall Thresholds. **Geosciences**, v. 9, p. 203, 2019.

ROSSI, M.; PFEIFER, R.M. Pedologia do Parque Estadual da Serra do Mar. I. Levantamento de reconhecimento de solos. **Revista do Instituto Florestal**, v. 3.1, p. 1 – 44, 1991.

ROSSI, M. Mapa pedológico do Estado de São Paulo: revisado e ampliado. **São Paulo: Instituto Florestal**, v. 1, p. 118, 2017.

SALVATICI, T.; MORELLI, S.; PAZZI, V.; FRODELLA, W.; FANTI, R. Debris Flow Hazard Assessment by Means of Numerical Simulations: Implications for the Rotolon Creek Valley (Northern Italy). **Journal of Mountain Science***, v.* 14, n. 4, p. 636 – 48, 2017 https://doi.org/10.1007/s11629-016-4197-7.

SANTANGELO, M.; MARCHESINI, I.; BUCCI, F.; CARDINALI, M.; CAVALLI, M.; CREMA, S.; MARCHI, L.; ALVIOLI, M.; GUZZETTI, F. Exposure to landslides in rural areas in Central Italy. **Journal of Maps**, *v.* 17, n. 4, p. 124 -132, 2020. Doi: 10.1080/17445647.2020.1746699

SANTI, P.M.; DEWOLFE, V.G.; HIGGINS, J.D.; CANNON, S.H.; GARTNER, J.E. Sources of debris flow material in burned areas. **Geomorphology**, v. 96, n. 3–4, p. 310–321, 2008.

SANTI, P. Precision and accuracy in debris-flow volume measurement. **Environmental and Engineering Geosciences**, v. 20, n. 4, p. 349-359, 2014.

SASSA, K. The mechanism of debris flow. In: **Proc 11th Intern. Conf. on Soil Mechanics and Foundation Engineering, San Francisco**, U.S.A., v. 3, p. 1173–1176, 1985.

SCALLY, F.; SLAYMAKER, O.; OWENS, L. Morphometric controls and basin response in the Cascade mountains. **Geografiska Annaler: Series A, Physical Geography**, v. 83, n. 3, p. 117-130, 2001. Doi: 10.1111/j.0435-3676.2001.00148.x

SCALLY, F.A.; OWENS, I.F.; LOUIS J. Controls on fan depositional processes in the schist ranges of the Southern Alps, New Zealand, and implications for debris-flow hazard assessment. **Geomorphology**, v. 122, n. 1-2, p. 99-116, 2010. Doi: 10.1016/j.geomorph.2010.06.002

SCHRAML, K.; THOMSCHITZ, B.; MCARDELL, B.W.; GRAF, C.; KAITNA, R. Modeling Debris-Flow Runout Patterns on Two Alpine Fans with Different Dynamic Simulation Models. **Natural Hazards and Earth System Sciences***, v.* 15, n. 7, p. 1483 – 92, 2015. https://doi.org/10.5194/nhess-15-1483-2015.

SEDREZ, L.F.; MAIA, A.C.N. Enchentes que destroem, enchentes que constroem: natureza e memória da Cidade de Deus. **Revista do Arquivo Geral da Cidade do Rio de Janeiro**, v. 8, p. 183 – 200, 2014.

SEGONI, S.; LAGOMARSINO, D.; FANTI, R. *et al.* Integration of rainfall thresholds and susceptibility maps in the Emilia Romagna (Italy) regional-scale landslide warning system. **Landslides**, v. 12, p. 773–785, 2015. https://doi.org/10.1007/s10346-014-0502-0

SEGONI, S.; PICIULLO, L.; GARIANO, S. A review of the recent literature on rainfall thresholds for landslide occurrence. **Landslides,** v. *15*, n. 8, p. 1483 – 1501, 2018. doi: 10.1007/s10346-018-0966-4

SELBY, M.J. Slope erosion due to extreme rainfall: a case study from New Zealand. **Geografiska Annaler**, v. 58A, p. 131 – 138, 1976.

SELUCHI, M.; CHAN CHOU, S.; GRAMANI, M. A case study of a winter heavy rainfall event over the Serra do Mar in Brazil. **Geofísica Internacional**, v. 50, n. 1, p. 41 – 56, 2011.

SERVIÇO GEOLÓGICO DO BRASIL – CPRM (2021). Atlas Pluviométrico do Brasil. Disponível em: http://www.cprm.gov.br/publique///Mapas-e-Publicacoes/Atlas-Pluviometrico-do-Brasil-1351.html, Acesso em 07 de novembro de 2021.

SHAN, Y.; CHEN, S.; ZHONG, Q. Rapid Prediction of Landslide Dam Stability Using the Logistic Regression Method. **Landslides***,* v. 17, n. 12, p. 2931 – 56, 2020 https://doi.org/10.1007/s10346-020-01414-6.

SHEN, P.; ZHANG, L.; WONG, H.; PENG, D.; ZHOU, S.; ZHANG, S.; CHEN, C. Debris flow enlargement from entrainment: A case study for comparison of three entrainment models. **Engineering Geology**, v. 270, p. 105581, 2020.

SLAYMAKER, O. Debris torrent hazard in Eastern Fraser and Coquihalla Valleys. **Western Geography**, v. 1, n. 1, p. 34-48, 1990.

SOETERS, R., VAN WESTEN, C.J. Slope Instability Recognition Analysis and Zonation. In: TURNER, A.K.; SCHUSTER, R.L. (Eds.) **Landslides: Investigation and Mitigation**. National Academy Press, Washington D.C.: 1996, p. 129-177.

STALEY, D.M.; KEAN, J.W.; CANNON, S.H.; SCHMIDT, K.M.; LABER, J.L. Objective definition of rainfall intensity–duration thresholds for the initiation of post-fire debris flows in southern California. **Landslides**, v. 10, n. 5, 547 – 562, 2013. https://doi.org/10.1007/s10346- 012-0341-9.

STEEB, N.; RICKENMANN, D.; BADOUX, A.; RICKLI, C.; SCHEWALDNER, P. Large wood recruitment processes and transported volumes in Swiss mountain streams during the extreme flood of August 2005. **Geomorphology**, v. 279, p. 112–127, 2017.

STEGER, S.; MAIR, V.; KOFLER, C.; PITTORE, M.; ZEBISCH, M.; SCHNEIDERBAUER, S. Correlation Does Not Imply Geomorphic Causation in Data-Driven Landslide Susceptibility Modelling - Benefits of Exploring Landslide Data Collection Effects. **Science of the Total Environment**, v. 776, p. 145935, 2021. https://doi.org/10.1016/j.scitotenv.2021.145935.

STERNBERG, H.O. Enchentes e movimentos coletivos do solo no vale do Paraíba em dezembro de 1948. Influência da exploração destrutiva das terras. **Revista Brasileira de Geografia**, v. 11, n. 2, p. 223-261, 1949.

STILLWELL, H.D. Natural hazards and disasters in Latin America. **Natural Hazards**, v. 6, p. 131–159, 1992. https://doi.org/10.1007/BF00124620

STOFFEL, M. Magnitude–frequency relationships of debris flows - A case study based on field surveys and tree-ring records. **Geomorphology**, v. 116, p. 67-76, 2010.

STOFFEL, M.; HUGGEL, C. Effects of climate change on mass movements in mountain environments. **Progress in Physical Geography**, v. 36, p. 421–439, 2012.

STOFFEL, M., D. TIRANTI, AND C. HUGGEL. Climate Change Impacts on Mass Movements--Case Studies from the European Alps. **Science of the Total Environment***, v.* 493, p. 1255 – 66, 2014. https://doi.org/10.1016/j.scitotenv.2014.02.102.

STROUTH, A.; MCDOUGALL, S. Societal risk evaluation for landslides: historical synthesis and proposed tools. **Landslides***, v. 18*, n. 3, p. 1071-1085, 2020. doi: 10.1007/s10346-020-01547-8

STROUTH, A.; MCDOUGALL, S. Historical Landslide Fatalities in British Columbia, Canada: Trends and Implications for Risk Management. **Frontiers in Earth Science***, v.* 9, p. 606854, 2021.

SURIAN, N.; RIGHINI, M.; LUCÍA, A.; NARDI, L.; AMPONSAH, W.; BENVENUTI, M.; BORGA, M.; CAVALLI, M.; COMITI, F.; MARCHI, L.; RINALDI, M.; VIERO, A. Channel response to extreme floods: insights on controlling factors from six mountain rivers in northern Apennines, Italy. **Geomorphology**, v. 272, p. 78-91, 2016.

SÜZEN, M.L.; KAYA, B.Ş. Evaluation of environmental parameters in logistic regression models for landslide susceptibility mapping. **International Journal of Digital Earth**, v. 5, n. 4, p. 338 – 355, 2012. DOI: 10.1080/17538947.2011.586443

TABARELLI, M.; PINTO, L.; SILVA, J.; HIROTA, M.; BEDÊ, L. Challenges and opportunities for biodiversity conservation in the Brazilian Atlantic forest. **Conservation Biology**, v. 19, n. 3, p. 695–700, 2005.

TAKAHASHI, T. 1991. **Debris Flow**. A.A. Balkema, Rotterdam.

TAKAHASHI, T.; NAKAGAWA, H.; HARADA, T.; YAMASHIKI, Y. Routing Debris flows with particle segregation. **Journal of Hydraulic Engineering**, v. 118, p. 1490-1507, 1992.

TAKAHASHI, T. 2006. **Debris Flows: Mechanics, Prediction and Countermeasures**. Taylor and Francis, Balkema, Leiden.

TAKEI, A. Interdependence of sediment budget between individual torrents and a river-system. In: **Proceeding of the Internation Symposium INTERPRAEVENT**, Villach, Austria, 2:35–48, 1984.

TAN, D.Y.; YIN, J.H.; QIN, J.Q.; ZHU, Z.H.; FENG, W.Q. Experimental study on impact and deposition behaviours of multiple surges of channelized debris flow on a flexible barrier. **Landslides**, v. 17, p. 1577 – 1589, 2020

TANG, C.; RENGERS, N.; VAN ASCH, T.; YANG, Y.; WANG, G. Triggering conditions and depositional characteristics of a disastrous debris flow event in Zhouqu city, Gansu Province, northwestern China. **Natural Hazards and Earth System Sciences**, v. 11, n. 11, p. 2903-2912, 2011.

TAVARES, R.; MENDONÇA, F. Ritmo climático e risco socioambiental urbano: chuvas e deslizamentos de terra em Ubatuba-SP (BR) entre 1991 e 2009. In: **Seminário latino-americano de geografia física**, VI, Coimbra, Actas, 13 p., 2010.

TATIZANA, C.; OGURA, A.T.; CERRI, L.E.; ROCHA, M.C.M. (1987) Análise de Correlação entre Chuvas e Escorregamentos - S. do Mar, Mun. Cubatão. .. Proc Braz Congr Eng Geol 2:225–236 Terzaghi K (1947) Memorandum concerning the slide area at the power plant. In from theory to practice in soil mechanics, 1967, 2nd edn. Wiley, New York, pp 410– 415

TEIXEIRA, M.S.; SATYAMURTY, P. Trends in the Frequency of Intense Precipitation Events in Southern and Southeastern Brazil during 1960–2004. **Journal of Climate**, v. 24, p. 1913-1921, 2011.

TIANCHI, L. Landslides: extent and economic significance in China. In: Brabb EE, Harrod BL (Eds.) Landslides: Extent and Economic Significance. In: **28th International Geological Congress: Symposium on Landslides**. Washington D.C., United States. Rotterdam: Balkema, pp. 271 – 287, 1989.

TRENBERTH, K.E. Changes in precipitation with climate change. **Climate Research**, v. 47, p. 123–138, 2011.

UNITED NATIONS OFFICE FOR DISASTER RISK REDUCTION – UNDRR (2015) Sendai Framework for Disaster Risk Reduction 2015-2030. Disponível em: http://www.unisdr.org/we/inform/publications/43291, Acesso em 23 de novembro de 2021.

UNITED STATES GEOLOGICAL SURVEY – USGS (2021). EarthExplorer. Disponível em: https://earthexplorer.usgs.gov, Acesso em 23 de novembro de 2021.

VAN DEN EECKHAUT, M.; HERVÁS, J. State of the art of national landslide databases in Europe and their potential for assessing landslide susceptibility, hazard and risk. **Geomorphology**, v. 139-140, p. 545 – 558, 2012.

VAN WESTEN, C.J.; CASTELLANOS, E.; KURIAKOSE, S.L. Spatial Data for Landslide Susceptibility, Hazard, and Vulnerability Assessment: An Overview. **Engineering Geology**, v. 102, n. 3 – 4, p. 112 – 31, 2012. https://doi.org/10.1016/j.enggeo.2008.03.010.

VANELLI, F.; ROMERO MONTEIRO, L.; FAN, F.; GOLDENFUM, J. The 1974 Tubarão River flood, Brazil: reconstruction of the catastrophic flood. **Journal Of Applied Water Engineering And Research**, v. *8*, n. 3, p. 231 – 245, 2020. doi: 10.1080/23249676.2020.1787251

VARNES, D.J. Slope movement types and processes. In: SCHUSTER, R.L.; KRIZEK, R.J. (Eds.) **Special report 176: landslides: analysis and control**. Transportation and Road Research Board, National Academy of Science, Washington DC, pp 11–33, 1978.

VASCONCELLOS, F.C.; CAVALCANTI, I.F.A. Uma avaliação das previsões do modelo regional Eta em alta resolução para dois casos de chuva intensa ocorridos na região da Serra do Mar. **Revista Brasileira de Meteorologia**, v. 25, p. 287–294, 2010

VIEIRA, B.C.; FERNANDES, N.F.; AUGUSTO FILHO, O.A. Shallow landslide prediction in the Serra do Mar, São Paulo, Brazil. **Natural Hazards and Earth System Sciences**, v. 10, p. 1829–1837, 2010. https://doi.org/10.5194/nhess-10-1829-2010

VIEIRA, B.; GRAMANI, M. Serra do Mar: The Most "Tormented" Relief in Brazil. In: MIGON, P (Ed) **World Geomorphological Landscapes**. Springer, Berlin, pp. 285-297, 2015.

VIJITH, H.; DODGE-WAN, D. Modelling Terrain Erosion Susceptibility of Logged and Regenerated Forested Region in Northern Borneo through the Analytical Hierarchy Process (Ahp) and Gis Techniques. **Geoenvironmental Disasters**, v. 6, n. 1, 2019. https://doi.org/10.1186/s40677-019-0124-x.

VOELLMY, A. Über die Zerstörungskraft von Lawinen. **Schweizerische Bauzeitung**, v. 73, n. 12, p. 159 – 162, 1955.

VOS, T.; LIM, S.; ABBAFATI, C.; ABBAS, K.; ABBASI, M.; ABBASIFARD, M. *et al*. Global burden of 369 diseases and injuries in 204 countries and territories, 1990–2019: a systematic analysis for the Global Burden of Disease Study 2019. **The Lancet**, v. 396, n. 10258, p. 1204-1222, 2020. Doi: 10.1016/s0140-6736(20)30925-9

WELSH, A.; DAVIES, T. Identification of alluvial fans susceptible to debris-flow hazards. **Landslides**, v. 8, p. 183-194, 2011. Doi: 10.1007/ s10346-010-0238-4

WESTRA, S.; FOWLER, H.; EVANS, J.; ALEXANDER, L.; BERG, P.; JOHNSON, F.; KENDON, E.; LENDERINK, G.; ROBERTS. N. Future changes to the intensity and frequency of short-duration extreme rainfall. **Reviews of Geophysics**, v. 52, p. 522-555, 2014.

WILFORD, D.J.; SAKALS, M.E.; INNES, J.L.; SIDLE, R.C.; BERGERUD, W.A. Recognition of Debris Flow, Debris Flood and Flood Hazard through Watershed Morphometrics. **Landslides**, v. 1, n. 1, p. 61-66, 2004. https://doi.org/10.1007/s10346-003-0002-0.

WILSON, J.P.; GALLANT, J.C. Digital terrain analysis. **Terrain Analysis: Principles and Applications**, v. 6, n. 12, p. 1–27, 2000.

WINTER, M.G.; SHEARER, B. Landslide hazard and risk in a changing climate. In: SASSA, K.; CANUTI, P.; YIN, Y (Eds.). **Landslide Science for a Safer Geoenvironment**, Volume 1: The International Programme on Landslides (IPL). Springer, New York, pp. 281-286, 2014.

WIRTZ, A.; KRON, W.; LÖW, P. *et al* The need for data: natural disasters and the challenges of database management. **Natural Hazards**, v. 70, p. 135–157, 2014. https://doi.org/10.1007/s11069-012-0312-4

WOLLE, C.M.; HACHICH, W. Rain-induced landslides in Southeastern Brazil. In: **Proceeding of 12th International Conference on Soil Mechanics and Foundation Engineering**, Rio de Janeiro, Brazil, vol. 3, pp. 1639–1642, 1989.

WOLLE, C.M.; CARVALHO, C.S. Taludes Naturais. In: FALCONI, F.F.; JUNIOR, A.N. (Org.) **Solos do Litoral de São Paulo**. ABMS, São Paulo: 1994, p. 180-203.

WU, S.; CHEN, J.; ZHOU, W.; IQBAL, J.; YAO, L. A Modified Logit Model for Assessment and Validation of Debris-Flow Susceptibility. **Bulletin of Engineering Geology and the Environment**, v. 78, n. 6 p. 4421 – 38, 2018. https://doi.org/10.1007/s10064-018-1412-5.

YANG, Z.; WANG, L.; QIAO, J.; UCHIMURA, T.; WANG, L. Application and Verification of a Multivariate Real-Time Early Warning Method for Rainfall-Induced Landslides: Implication for Evolution of Landslide-Generated Debris Flows. **Landslides**, v. 17, n. 10, p 2409-19, 2020. https://doi.org/10.1007/s10346-020-01402-w.

YILMAZ, I. GIS based susceptibility mapping of karst depression in gypsum: a case study from Sivas basin (Turkey). **Engineering Geology**, v. 90, p. 89– 103, 2007.

ZANANDREA, F.; MICHEL, G.; KOBIYAMA, M.; CARDOZO, G. Evaluation of different DTMs in sediment connectivity determination in the Mascarada River Watershed, southern Brazil. **Geomorphology**, v. 333, p. 80 – 87, 2019. doi: 10.1016/j.geomorph.2019.02.005

ZHANG, S.; LI, C.; LIU Y. Quantitative Assessment of Human Risk from Landfill Failure in Shenzhen, China. In: ZHAN, L.; CHEN, Y.; BOUAZZA, A. (Eds) **Proceedings of the 8th International Congress on Environmental Geotechnics** Volume 3. ICEG 2019, Environmental Science and Engineering. Springer, Singapore. https://doi.org/10.1007/978-981-13-2227-3_69

ZHOU, W.; TANG, C.; VAN ASCH, T.W.J.; CHANG, M. A Rapid Method to Identify the Potential of Debris Flow Development Induced by Rainfall in the Catchments of the Wenchuan Earthquake Area. **Landslides**, v. 13, n. 5, p. 1243 – 59, 2015. https://doi.org/10.1007/s10346-015-0631-0.

ZHUANG, J.Q.; CUI, P.; WANG, G.H.; CHEN, X.Q.; IQBAL, J.; GUO, X.J. Rainfall thresholds for the occurrence of debris flows in Jiangjia Gully, Yunnan Province, China. **Engineering Geology**, v. 195, p. 335-346, 2015.

APPENDIX A - Accepted manuscripts

A.1 The consequences of debris flows in Brazil: a historical analysis based on recorded events in the last 100 years

A.2 Characterization of a landslide-triggered debris flow at a rainforest-covered mountain region in Brazil

A.3 A multi-step hazard assessment for debris-flow prone areas influenced by hydroclimatic events

APPENDIX A.1

The consequences of debris flows in Brazil: a historical analysis based on recorded events in the last 100 years

[1,2]Victor Cabral, [1,3]Fábio Reis, [1]Vinicius Veloso, [1]Claudia Correa, [1,2]Caiubi Kuhn, [2]Christiane Zarfl

[1] Applied Geology Department, Institute of Geosciences and Exact Sciences - IGCE, São Paulo State University – UNESP. Address: Av. 24A, 1555 – Rio Claro, São Paulo, Brazil. Email: victor.carvalho@unesp.br

[2] Geo- und Umweltforschungszentrum (GUZ), University of Tübingen. Address: Schnarrenbergstraße 94 – 96, Tübingen, Germany

[3]Center for Geosciences Applied to Petroleum (UNESPetro), São Paulo State University – UNESP. Address: Av. 24A, 1555 – Rio Claro, São Paulo, Brazil.

Abstract

This study aims at providing an overview of the socioeconomic consequences that debris-flow events have caused in Brazil, positioning the country in the international scenario and identifying areas where targeted actions are necessary. The analysis is conducted by calculating the debris-flow Mortality Rate (MR) and by using the so-called F-N plots (Frequency of events that have caused N or more fatalities vs. the Number of fatalities), based on a compilation of debris-flow related disasters from 1920 to 2021. In total, 45 debris-flow events were documented in the considered period, responsible for 5771 fatalities and more than 5.5 billion USD in economic losses. The Serra do Mar Mountain Range is the main site of reported debris-flow occurrences (64.5%), followed by Serra da Mantiqueira (13.3%), and Serra Geral (13.3%). Southeast Brazil (SEB) is the region most affected by debris-flow events, due to the highest population density and the development of several cities in mountainous and hilly areas, such as Petrópolis (Rio de Janeiro state) and Cubatão (São Paulo state). The debris-flow MR of SEB is higher than any other region in Brazil, pushing the national debris-flow MR upwards, and the F-N curve of SEB consolidates the region as the one with the highest risk, indicating a higher probability of fatal debris-flow events. The F-N plots further show that the phenomena in Brazil represent a higher societal risk than in countries such as China, Japan and Italy. While there are differences in country size and the scale effect should be considered, these results highlight the urgent need for investments in disaster prevention and preparedness programs.

Keywords: Landslide database, F-N curve, Mortality rate, Debris flows, Natural disasters.

1 Introduction

A natural hazard occurs when processes of the geophysical environment have the potential to cause damage or loss to a vulnerable human community (Stillwell 1992; Alcántara-Ayala 2019); when their consequences have major negative impacts on society, they become natural disasters (Burton and Kates 1963; Alcántara-Ayala 2002). Economic, political, and social factors of countries of the Global South[2] can contribute to increasing their vulnerability to natural hazards, which results in higher number of fatalities and loss of infrastructures when compared to developed countries (Devoli et al. 2007; Patel and Burke 2009).

Exogenous processes (e.g., floods, landslides, snow avalanches) are some of the most commonly occurring phenomena that negatively affect humans and infrastructures worldwide (Kahn 2005; Álvala et al. 2019). In Brazil, hydrogeomorphic processes, triggered by high-intensity precipitation, are the most recurrent and deadly among the natural disasters (Kahn 2005; CEPED/UFSC 2013; Assis Dias et al. 2018; Kobiyama et al. 2019). The increasing frequency of extreme and high-intensity rainfall events due to global warming have been associated with an increase in the frequency and magnitude of floods and landslides in Brazil (Cavalcanti et al. 2017; Marengo et al. 2021), as well as worldwide (Fowler and Hennessy 1995; O'Gorman and Schneider 2009; Westra et al. 2014; Deng et al. 2021), which highlights the importance of risk and vulnerability studies.

Approximately 9 out of 100 people in Brazil live in disasters-prone areas, with landslides and debris flows associated to a higher number of fatalities per event (Kahn 2005; Álvala et al. 2019). Between 2000 and 2010, landslide and debris-flow events have caused approximately 1,700 deaths in the country, affected almost 8 million people and caused economic losses of U$1.5 billion (Bastos et al. 2015). In 2011, high-magnitude landslides and debris flows in the state of Rio de Janeiro officially caused more than 942 deaths and U$1.4 billion in losses, being considered the 8th worst landslide event in world history (Assis Dias et al. 2018; Rosi et al. 2019). The 2011 catastrophe led to the creation of the National Center of Monitoring and Early Warning of Natural Disasters (*Centro Nacional de Monitoramento e Alertas de Desastres Naturais* – CEMADEN), an important advance towards natural disasters prevention and monitoring in Brazil (CEMADEN, 2022).

With the creation of CEMADEN in 2011, the national disasters database (*Sistema Integrado de Informações sobre Desastres* – S2ID*)*, managed by the Ministry of Regional Development (*Ministério do Desenvolvimento Regional* – MDR), was also established to document natural disasters. Prior to S2ID, no centralized record of natural disasters at a federal level existed, with states having autonomy over disasters cataloguing. A national disasters

[2] According to the definition of the United Nations Finance Center for South-South Cooperation (UN FCSSC, 2022)

database is crucial in risk assessment studies and in the understanding of the underlying dynamics of a phenomenon, helping to reduce and mitigate associated damage (Bollschweiler and Stoffel 2010; Wirtz et al. 2012).

The comprehension of the impact that a specific natural hazard represents in a country is a basic step in their management and monitoring, as highlighted by the targets of the Sendai Framework for Disaster Risk Reduction (2015-2030, UNDRR 2015). The continental dimension of Brazil and the heterogenous management of natural disasters is a great challenge for the implementation of a thorough database, as different states implement different budgets for disaster monitoring and prevention (CEPED/UFSC 2013). An effective database should cover a long period of time with reliable information about the socioeconomic losses (Borden and Cutter 2008), and a consistent documentation of natural disasters in Brazil is recent (from 1991) compared to European and North American countries (e.g., Italy: Guzzetti 2000; Germany: Damm and Klose 2015; United States: Mirus et al. 2020).

Among the landslide types, debris flows are associated to a specifically high damage per event due to their high impact force, velocity and high sediment content per unit volume (Coussot and Meunier 1996; Takahashi 2006). Debris flows are characterized by bulk densities that vary from 1,800 to 2,300 kg m^{-3}, velocities that range from 3 to 25 m s^{-1} and sediments contents of 40% to 80%, which can range from organic matter to large (> 5 m) rock boulders (Costa 1988; Takahashi 2006; Iverson et al. 2011; Zhuang et al. 2015; Santangelo et al. 2020). In Brazil, debris flows are mainly initiated by rainfall-triggered landslides (Wolle and Hachich 1989; Lacerda 2007) and their rheological characteristics vary according to the geology and geomorphology of the catchments (Lacerda 2007). Moreover, debris floods, flash floods and floods are some of the phenomena that often occur in association to debris flows, especially during large magnitude events (Wilford et al. 2004; Dowling and Santi 2014; Hungr et al. 2014; Church and Jakob 2020).

Increasing urbanization in mountain regions, especially in south and southeast Brazil, has been highlighted by recent studies (Guerra et al. 2007; Patel and Burke 2009; Londe et al. 2018), which increases the exposure to potential debris-flow related damages, as changes in society and economic development are the main driving forces that can magnify associated losses to a natural phenomenon (Andres and Badoux 2018). In this context, the aim of this study is to quantitatively estimate the socioeconomic consequences that debris flows have caused in Brazil, by calculating the phenomenon's Mortality Rate and by applying F-N plots (Frequency of events that have caused N or more fatalities vs. the Number of fatalities), based on a compilation of historical events that have caused fatalities and/or economic losses between 1920 and 2021. The debris-flow event cataloguing is conducted

based on different disasters databases, both worldwide and national, on scientific publications and on governmental and journalistic reports. This catalogue is seen as a contribution to the collaborative effort among the scientific community to provide basic debris-flow data for a long-term hazard and risk analysis.

2 Methods

2.1 Debris-flow data collection

Two main data-source types are used for data compilation: disasters databases, both national and international, and technical and scientific documents that describe debris flows in Brazil, including journalistic reports. The data gathered from these sources are combined to create a new catalogue, which considers the following attributes: date of the event, trigger time, mountain range, catchment, city, state, triggering-event intensity (i.e., rainfall in mm), magnitude (i.e., volume of sediments mobilized by the debris flow, in m^3), human losses (fatalities, injuries, missing, homeless, displaced), material losses (houses, public and private building, public infrastructures) and economic losses (in United States Dollar - USD). Economic losses are estimated by using the conversion rate of the date of the event from Brazilian currency to USD, according to the reports of exchange rates of the United States Treasury. The values were then adjusted to inflation (**www.usinflationcalculator.com**).

Varnes' (1978) landslide classification, updated by Hungr et al. (2014), is adopted in our analyses to identify debris-flow events. The Brazilian Code of Disasters (COBRADE 2022) also adopts Varnes' (1978) classification, adapted by Augusto Filho (1992). Although, officially, Brazilian databases follow international standards (CEPED/UFSC 2013), COBRADE differs from the international peril terminology and classification proposed by the Center for Research on the Epidemiology and Disasters (CRED 2022), used in international databases. Landslides are classified as hydrological disasters by CRED (when triggered by rainfall and snow melt) and as a geological disaster by COBRADE. Moreover, in CRED, debris flows are classified as landslide events, which is not the case for COBRADE. See online resources for the comparison of definitions.

2.1.1 Databases

The databases used in this work are the Brazilian disasters database (S2ID), the International Disasters Database (EM-DAT 2021), and the databases maintained by some research institutes of the federate states. It is important to note that S2ID exclusively documents a disaster when a city or state declares state of emergency (CEPED/UFSC 2013). Similarly, in the EM-DAT, a natural disaster is only documented when a state of emergency is declared and more than 10 fatalities are reported or 100 people are affected (Van den Eeckhaut and Hervás 2012; CEPED/UFSC 2013).

The S2ID is the official database for natural disasters in Brazil since January 2013 (https://s2id.mi.gov.br). It systematically documents disasters that occurred in the country from 1991 onwards, although more expressive disasters prior to 1991 are also documented inconsistently. The identification of a disaster in the platform is conducted since 2013 via the "Identification of Disasters Form" (FIDE) and, prior to 2013, through either the "Preliminary Notification of Disasters Form" (NOPRED), the "Damage Evaluation Form" (AVADAN) or journalistic reports. These forms and reports are available for events from 1940 to 2016 in the S2ID platform, with those after 2016 having to be requested privately via the Fala.Br platform, which is the official channel to request public information from government institutions. The distinction between landform processes was made based on photographs and the description provided in the database, as well as with the aid of publications and news reports.

The International Disasters Database (EM-DAT 2021) is developed and operated by CRED, within the Université Catholique de Louvain (Belgium) (https://public.emdat.be). The database is based on information retrieved from United Nations (UN) agencies, official governmental offices, the International Federation of Red Cross and Red Crescent Societies (IRFC), research organizations, insurance periodicals and reinsurance publications (Wirtz et al. 2012). EM-DAT provides a more complete documentation of Brazilian disasters when compared to other freely-available international databases.

São Paulo state also catalogues disasters in the state via the Geological Institute (IG). IG systematically documents disasters since 1991, even those for which no casualties are reported, based on journalistic articles and the on-site activities of the authorities during disasters response, granting a more thorough depiction of the landslide and debris-flow consequences in the state. Similar database for the other 26 states was not available according to their Civil Defense departments, with their disasters data accessible only through S2ID.

2.1.2 Publications

Since no official documentation of landslides and debris-flow events prior to 1991 is available in a consistent and systematic manner, technical reports and scientific documents that describe and compile debris-flow events in Brazil since 1920 were also analyzed. Data from debris-flow publications were mainly retrieved using bibliographic search tools: SCOPUS, from Elsevier (2022); Web of Science, from Clarivate Analytics (2022); and "Periódicos CAPES", from the Brazilian Research Agency "*Coordenação de Aperfeiçoamento de Pessoal de Nível Superior*", (CAPES 2022). The keywords used, both in English and Portuguese, were "landslides" (*escorregamentos*), "debris flows" (*fluxos de detritos*), "mudslides" (*fluxo de lama*), "flash floods" (*enxurrada*), "floods" (*inundação*).

A total of 7,638 publications were accessed and analyzed for data compilation on debris flows. Among those, 4% of the publications were identified by the keywords "debris flows" and "*fluxo de detritos*", respectively (see online resources for the table with the bibliographic search results). Studies about floods, flash floods and landslides were also analyzed due to the close relationship between these processes and debris flows in mountain areas of Brazil, as well in other parts of the world (Hungr et al. 2014).

A good review of Brazilian debris-flow events was made by Kobiyama and Michel (2015a) and is also used as a reference. The Kobiyama and Michel (2015a) study based the creation of an incipient debris-flow database by Kobiyama et al. (2015b) and Kobiyama et al. (2019), which included the year and location (municipality) of the event and the number of casualties. Dowling and Santi (2014) also conducted a comprehensive compilation of debris-flow events worldwide, encompassing events from 1950 to 2011 and describing the magnitude, triggering event intensity, as well as the number of fatalities and economic losses. In Dowling and Santi's (2014) database, however, only large Brazilian debris-flow events are documented.

Furthermore, for each event identified in the bibliographic search and in the disasters databases, different sources of information for the same debris-flow event were compared to more accurately depict the extent of the associated damages, including information from journalistic reports. A great challenge during cataloguing was mismatched information between sources, which challenged an accurate estimation of the real damage. When uncertainties occurred, information from peer-reviewed articles were favored, followed by governmental reports, S2ID, EM-DAT and journalistic reports. When mismatched information from the same type of source was found, the worst-case scenario was adopted, i.e., the highest number of fatalities or largest economic losses. Data scarcity in disasters documentation, especially of economic losses, is observed across all different sources of information, even for more recent events.

2.2 Analysis of the consequences

Based on the compiled catalogue of debris-flow events, the consequences that the phenomena represent was estimated based on the calculation of the Mortality Rate (MR), as well as by the relationship between the frequency of events and their consequences using the so-called F-N plots.

Calculating the MR is a direct method of estimating the debris-flow risk in a country and is expressed as the number of deaths by debris flows per a specified population size in a defined period of time, e.g., a specific year (Guzzetti 2000). Here, the MR is calculated per 100,000 people (Evans 1997).

Another method to estimate the impact of debris flow to the society is the application of F-N plots. F-N plots provide the likelihood of multiple fatalities due to a debris-flow event, by plotting the cumulative frequency of

events that have cause N or more fatalities (F) with the number of fatalities (N), in a log-log scale (Fell and Hartford 1997). Following Ball (1998), the equation for the F-N criterion can be represented as:

$$F = k * N^{-a} \quad (1)$$

With F as the cumulative frequency of events with N or more fatalities, N is the number of fatalities, a is the aversion factor and k is a constant. The slope of F-N curves is an indicative of the risk of a country or location is under, with steeper slopes indicating a lower frequency of high magnitude events when compared to curves with gentler slopes (Ball 1998).

3 Results

According to our catalogue, 45 debris-flow events have occurred in Brazil between 1920 and 2021, which have caused fatalities and/or economic losses. Table 1 shows the characterization of each event and Fig. 1 shows pictures of some of the country's most expressive ones. The full editable and updatable version of the database is available as a Supplementary Information in the online resources, with the inclusion of the references that contain a more complete description of the events for the purpose of this study.

3.1 Database compilation: challenges and constraints

The direct relationship of debris-flow events with high-intensity rainfall, which is also associated to flash floods and floods (Hungr et al. 2014), can undermine their recognition (Dowling and Santi 2014) and result in their misclassification and consequent underreporting (Guzzetti et al. 2004), especially in the disasters databases. The misclassification is observed more often in high-magnitude events, such as the 2011 event in Rio de Janeiro, which is classified as a flood event in the S2ID and EM-DAT.

Another shortcoming found during cataloguing is related to the correct technical classification of debris flows in the databases, where most documented debris-flow events are, in fact, localized landslides. In S2ID, from 2012 to 2020, 61 debris-flow events are catalogued, although only three are indeed debris flows when analyzing their description and photos. In the IG database, from 1991 to 2018, 70 debris-flows events are recorded in the state of São Paulo, though only four can be considered debris flows. As pointed out by Dowling and Santi (2014), while technical literature usually correctly classifies the type of slope movement, such carefulness with terminology by journalistic reports, government and international aid documents (i.e., non-technical literature) is usually not observed.

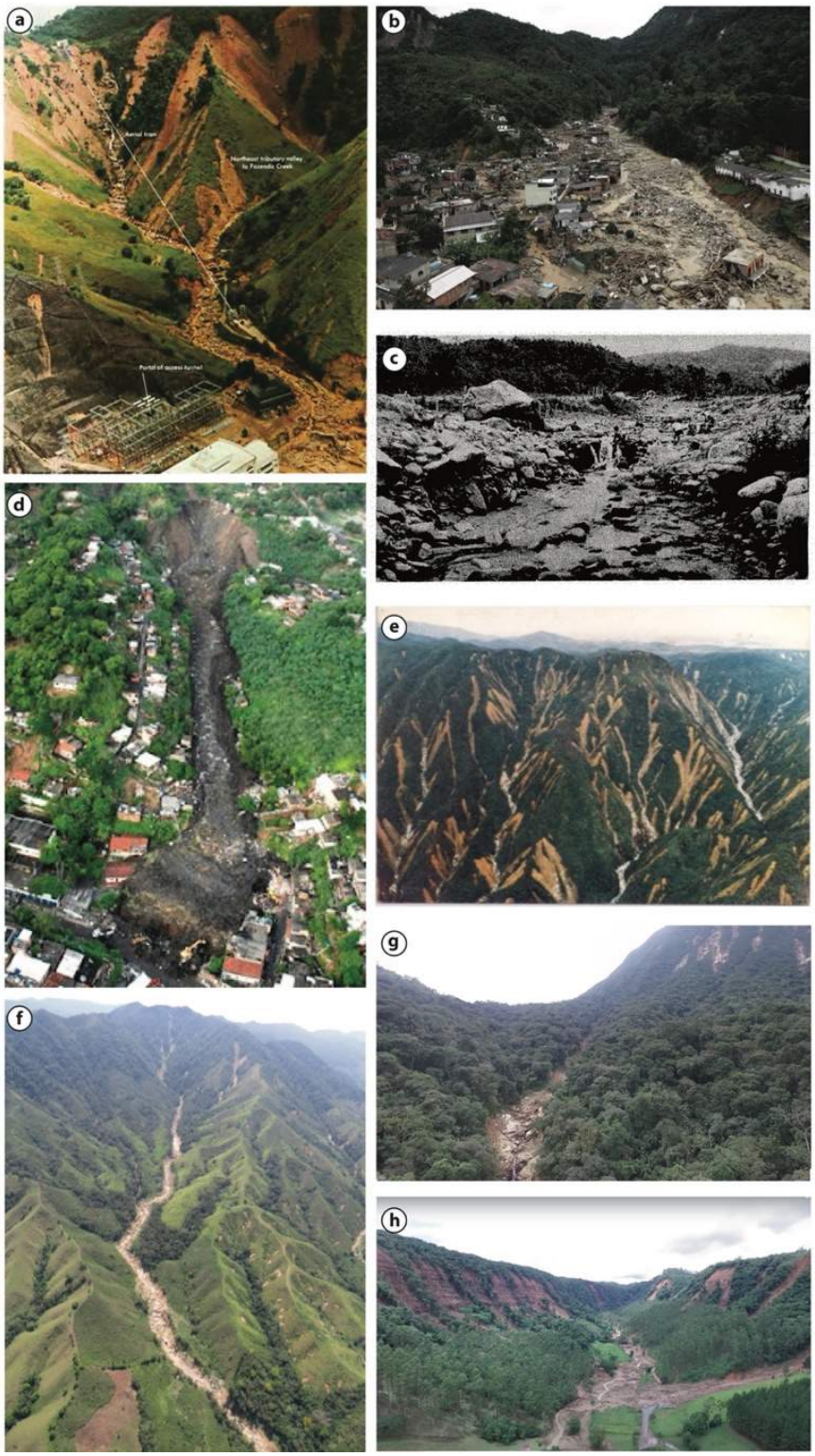

Fig. 1 Debris-flow events in Brazil. a) Serra das Araras (Piraí, Rio de Janeiro state) in 1967. Mudslide in the Fazenda catchment, one of many that destroyed the city. Picture from Jones (1973). a) Teresópolis 2011. Generalized landslides triggered debris flows in several catchments. Picture from Oliveira Filho (2012). c) Caraguatatuba 1967. In the picture, large rock boulders are deposited at the Santo Antonio catchment outlet. Picture from Cruz (1975). d) Niterói 2010. Debris avalanche at a deactivated landfill area, which caused the death of 48 people and 221 missing. Picture from Estadão (2010). e) Cubatão 1985. Generalized landslides at the Serra do Mar hillslopes that triggered high-magnitude debris flows at the region's catchments. Picture from IPT (1988). f) Itaoca 2014. Landslides at the headwaters' region triggered a high magnitude debris flow. Picture from Gramani and Arduin (2015). g) Guaratuba 2017. Landslides at the headwaters' region triggered a high magnitude debris flow (120,000 m^3). Picture from the authors. h) Vale do Itajaí (Ibirama city) 2020. Generalized landslides triggered high-magnitude debris flows, debris floods and flash floods. Picture from youtube video: "Um vale de destruição!" uploaded by Vale Agrícola, 19 Dec. 2020, https://www.youtube.com/watch?v=xH900IPzgow.

220 **Table 1** Debris flow database, catalogued based on different sources. Inj = injured; Mis = Missing people; Hom = homeless; Dis = Displaced; Infra = Infrastructures. N/A =
221 Not available.

Date	Time (GMT - 3)	Mountain range	Catchment	Location	State	Rainfall intensity	Magnitude (m^3)	Human losses					Material losses			Economic losses (USD)
								Death	Inj	Mis	Hom	Dis	House	Building	Infra	
10.03.1928	05:00	Serra do Mar	Monte Serrat Hills	Santos	São Paulo (SP)	N/A	130,000	81	7	N/A	N/A	N/A	15	01	N/A	24,112,000
15.12.1948	N/A	Serra da Mantiqueira	Angu, Aventureiro, Pirapetinga, Pomba	Region of Volta Grande	Minas Gerais (MG)	400 mm / 24 h	> 10^6	250	N/A	N/A	N/A	N/A	60	N/A	3	N/A
01.03.1956	18:00	Serra do Mar	Monte Serrat Hills	Santos	São Paulo (SP)	954 mm / month	N/A	21	102	N/A	N/A	N/A	50	N/A	1	N/A
11.01.1966	N/A	Serra do Mar	Guanabara bay Hydrographic basin	Rio de Janeiro	Rio de Janeiro (RJ)	245 mm / 24 h	N/A	250	1000	N/A	18910	39203	1000	N/A	> 100	75,547,344
11.01.1966	N/A	Serra do Mar	Quitandinha	Petrópolis	Rio de Janeiro (RJ)	327 mm / 72 h	N/A	45	35	N/A	N/A	N/A	N/A	N/A	N/A	
26.03.1966	N/A	Serra do Mar	N/A	Petrópolis	Rio de Janeiro (RJ)	188 mm / 24 h	N/A	40	N/A	N/A	N/A	N/A	N/A	N/A	N/A	N/A
20.01.1967	N/A	Serra do Mar	Guanabara bay Hydrographic basin	Rio de Janeiro	Rio de Janeiro (RJ)	181 mm / 24 h	N/A	200	300	N/A	N/A	N/A	1	2	N/A	N/A
22.01.1967	23:00	Serra do Mar	Ribeirão da Floresta, Ribeirão das Lajes	Serra das Araras (Piraí)	Rio de Janeiro (RJ)	114 mm / hour	> 10^6	300	N/A	1400	N/A	> 10000	> 100	1	1	N/A
18.03.1967	15:00	Serra do Mar	Santo Antônio, Guaxinduba, Pau d'alho, Canivetal, Camburu	Caraguatatuba	São Paulo (SP)	420 mm / 24 h	7,600,000	436	N/A	N/A	3000	N/A	400	N/A	N/A	63,449,964
27.04.1971	N/A	Salvador Fault Hills	Miolo	Salvador	Bahia (BA)	368 mm / 24 h	N/A	104	2000	N/A	N/A	7,000	1400	N/A	N/A	34,884,425
27.02.1971	N/A	Serra do Mar	Ultrafértil	Cubatão	São Paulo (SP)	N/A	N/A	N/A	N/A	N/A	N/A	N/A	0	1	N/A	N/A
18.08.1972	08:15	Serra da Mantiqueira	Piracuama	Campos do Jordão	São Paulo (SP)	N/A	70,000	17	NA	N/A	N/A	1000	80	1	N/A	N/A
23.03.1974	N/A	Serra Geral	Tubarão river basin	Tubarão	Santa Catarina (SC)	205 mm / 24 h	N/A	40	N/A	N/A	N/A	32500	N/A	N/A	N/A	666,840,081
29.04.1974	N/A	Serra de Maranguape	Pirapora	Maranguape	Ceará (CE)	N/A	N/A	91	N/A	NA	N/A	N/A	N/A	N/A	N/A	N/A
25.12.1975	N/A	Serra do Mar	Grota funda	Cubatão	São Paulo (SP)	248 mm / 24 h	> 10^5	0	N/A	N/A	N/A	N/A	N/A	N/A	1	N/A
28.01.1976	N/A	Serra do Mar	Braço norte	Cubatão	São Paulo (SP)	40 mm / hour	100,000	0	N/A	N/A	N/A	N/A	N/A	1	N/A	N/A

23.01.1985	N/A	Serra do Mar	Perequê, Mogi	Cubatão	São Paulo (SP)	84 mm / hour	> 10^6	0	N/A	N/A	N/A	N/A	N/A	1	1	N/A
12.1986	N/A	Serra da Mantiqueira	Braço	Lavrinhas	São Paulo (SP)	70 mm / hour	160,000	11	N/A	N/A	N/A	N/A	N/A	N/A	N/A	2,329,412
22.01.1988	N/A	Serra do Mar	Rio das Pedras	Cubatão	São Paulo (SP)	25 mm / hour	N/A	10	N/A	N/A	N/A	N/A	10	N/A	N/A	N/A
05.02.1988	N/A	Serra do Mar	Cuiabá, Quitandinha	Petrópolis	Rio de Janeiro (RJ)	384 mm / 48 hours	N/A	171	600	N/A	N/A	5000	1100	N/A	N/A	N/A
19.02.1988	N/A	Serra do Mar	N/A	Rio de Janeiro	Rio de Janeiro (RJ)	230 mm / 24 hours	N/A	289	734	N/A	N/A	18560	N/A	N/A	N/A	935,000,000
19.05.1989	N/A	Salvador Fault Hills	Central area of the city (Miolo)	Salvador	Bahia (BA)	83 mm / 24 hours	N/A	69	30	N/A	N/A	N/A	N/A	1	N/A	N/A
14.10.1990	03:00	Serra do Mar	Itajaí river basin	Blumenau region	Santa Catarina (SC)	89 mm / hour	N/A	17	764	N/A	N/A	754	66	N/A	N/A	N/A
18.03.1992	13:40	-	Vila Barraginho (old landfill)	Contagem	Minas Gerais (MG)	19.3 mm / 24 hour	30,000	36	70	N/A	N/A	3000	300	N/A	N/A	N/A
13.02.1996	N/A	Serra do Mar	Quitite, Papagio, Pau da Fome, Vale Encantado, Travessa do alemão, Rio das Pedras	Rio de Janeiro	Rio de Janeiro (RJ)	202.5 mm / 24 h	> 400,000	65	65	N/A	N/A	N/A	500	1	N/A	N/A
06.02.1994	N/A	Serra do Mar	RPBC	Cubatão	São Paulo (SP)	60 mm / hour	300,000	0	N/A	N/A	N/A	N/A	N/A	1	N/A	73,332,253
23.12.1995	16:30	Serra Geral	Rio Figueira	Timbé do Sul	Santa Catarina (SC)	176 mm / 24 hour	N/A	10	N/A	6	250	580	N/A	N/A	N/A	71,311,286
14.02.1996	N/A	Serra do Mar	N/A	Ubatuba	São Paulo (SP)	359.4 mm / 24 hour	N/A	11	N/A	N/A	300	N/A	30	N/A	N/A	N/A
09.04.1996	N/A	Serra do Mar	RPBC	Cubatão	São Paulo (SP)	18 mm / hour	16,000	0	N/A	N/A	N/A	500	0	1	N/A	0
12.12.1999	N/A	Serra do Mar	km 42, Anchieta Highway	Cubatão	São Paulo (SP)	128 mm / 24 hour	300,000	0	N/A	N/A	N/A	N/A	N/A	N/A	1	N/A
01.01.2000	N/A	Serra da Mantiqueira	Seco stream	Lavrinhas	São Paulo (SP)	55 mm h-1	N/A	N/A	N/A	N/A	N/A	N/A	N/A	N/A	N/A	N/A
01.01.2000	N/A	Serra da Mantiqueira	Morro do Britador	Campos do Jordão	São Paulo (SP)	400 mm / 96 h	N/A	10	N/A	N/A	N/A	N/A	300	N/A	N/A	N/A
24.12.2001	16:18	Serra do Mar	Cuiabá, Araras	Petrópolis	Rio de Janeiro (RJ)	300 mm / 24 hour	N/A	45	29	22	777	4000	N/A	113	N/A	190,757,690
23.11.2008	10:00	Serra do Mar	Itajaí river Basin	Ilhota, Brusque, Blumenau region	Santa Catarina (SC)	337 mm / 24 hour	> 10^6	151	4201	N/A	5617	9390	4355	583	N/A	946,442,920

07.04.2010	21:00	Serra do Mar	Morro do Bumba (old landfill)	Niterói	Rio de Janeiro (RJ)	280 mm / 24 hour	N/A	48	56	221	N/A	3,200	60	2	N/A	146,587,277
01.01.2010	03:30	Serra do Mar	Enseada do Bananal	Ilha Grande (Angra dos Reis)	Rio de Janeiro (RJ)	440 mm / 36 hour	55,600	31	2	N/A	N/A	N/A	7	1	N/A	180,668,819
11.01.2011	N/A	Serra do Mar	Cuiabá	Petrópolis	Rio de Janeiro (RJ)	273.8 mm / 24 hour	$> 10^6$	71	N/A	300	187	6956	N/A	N/A	N/A	1,932,584,390
			Vieira, Príncipe	Teresópolis		161.6 mm / 24 hour		429	N/A		6727	9110				
			Rio Grande	Nova Friburgo		249 mm / 24 hour		392	N/A		789	4528				
11.03.2011	05:00	Serra do Mar	Jacareí, Tingidor	Antonina, Morretes	Paraná (PR)	49 mm / hour	N/A	4	21	N/A	2500	10000	211	12	N/A	76,095,510
22.02.2013	17:00	Serra do Mar	Ribeirão do Cágado, Rio Marcolino, Rio Pilões	Cubatão	São Paulo (SP)	118 mm / hour	N/A	1	N/A	N/A	500	107	15	6	1	N/A
17.03.2013	20:30	Serra do Mar	Quitandinha	Petrópolis	Rio de Janeiro (RJ)	355 mm / 24 hour	N/A	34	49	0	1074	1120	662	N/A	54	56,111,211
12.01.2014	23:00	Serra do Mar	Guarda mão, Palmital	Itaóca	São Paulo (SP)	150 mm / 6 hour	N/A	23	4	0	20	332	110	10	3	5,578,975
29.03.2016	18:00	Serra da Mantiqueira	Córrego dos Araújos	Bom repouso	Minas Gerais (MG)	N/A	N/A	0	0	0	71	126	2	0	9	718,275
05.01.2017	N/A	Serra Geral	Mascarada river	Rolante	Rio Grande do Sul (RS)	270 mm / 3 hours	N/A	0	0	0	0	1600	400	N/A	N/A	24,683,356
11.02.2017	20:00	Serra do Mar	Pedra Branca	Guaratuba	Paraná (PR)	128 mm / hour	120,000	0	0	0	4	0	1	0	2	N/A
16.12.2020	N/A	Serra do Mar	Itajaí river basin	Presidente Getúlio, Ibirama	Santa Catarina (SC)	85 mm / 4 hour	$> 10^6$	13	35	6	175	1686	90	64	N/A	9,155,290

222

223 Moreover, even though there can be several hydrogeomorphic processes associated to a debris flow, the
224 phenomena are responsible for greater direct damage and fatalities (Costa 1988; Coussot and Meunier 1996;
225 Corominas et al. 2014). Economic losses involved with debris flows are, however, more uncertain, since the
226 associated processes, especially flash floods and floods, are responsible for a larger radius of structural damages
227 (Jakob et al. 2012; Álvala et al. 2019). In our debris-flow event dataset, due to the difficulties in separating the
228 economic losses related to the main debris-flow event and the associated processes, the losses for the whole event
229 are considered.
230 Furthermore, scientific publications and governmental reports tend to focus on larger events, which can potentially
231 create a bias on the magnitude and frequency of debris-flow events in the country. This is also the case for the
232 databases, which report only events with fatalities/economic losses, with those in remote areas or with smaller
233 magnitudes often going unreported. Therefore, it must be highlighted that the compiled database is based on the
234 available reported data, representing a baseline estimation of the damage that debris flows cause in Brazil.

235 ### *3.2 Impact of debris flows*

236 Debris-flow events have caused at least U$ 5.5 billion in direct economic losses during the considered period, and
237 were responsible for over 5,771 fatalities (including missing people) (Table 2). Debris-flow events have also
238 caused the destruction of more than 11,325 residences, 803 public and private buildings, and 177 infrastructures.
239 The combined number of homeless and displaced people is 211,153, with 10,104 people injured due to the
240 phenomenon. According to our estimates, the average fatality rate per event is around 128 (total number of
241 deaths/total number of debris-flow events) and the average economic loss per event is of ca. U$ 122 million (total
242 sum of economic losses/total number of debris-flow events).
243 The largest event in terms of reported fatalities is the 1967 debris flow in Serra das Araras (Piraí, Rio de Janeiro
244 state) (Fig. 1a), followed by the 2011 event in the mountain region of Rio de Janeiro (Tersópolis, Petrópolis) (Fig.
245 1b). These events have caused, respectively, 300 and 893 and deaths and, at least, 1,400 and 300 reported missing
246 people. In terms of magnitude, the 1967 debris-flow event in Caraguatatuba (São Paulo state) has the largest
247 reported magnitude (7,600,000 m^3) (Fúlfaro et al. 1976).
248 The number of reported fatalities in the Caraguatatuba event is low (436) when compared to the magnitude and
249 the destructive power of the event (Fig. 1c), and some studies suggest that the real figures are much higher (Listo
250 et al. 2018). Both the Serra das Araras and Caraguatatuba events exhibit stark incompleteness of data despite their
251 very extensive losses, which could be attributed to the lack of transparency from governmental data during the

Brazilian military dictatorship (1964 – 1988), as some studies suggest (e.g., Ab'Saber 1991; Sedrez and Maia 2014).

Considering that there are great uncertainties related to the 1967 events of Caraguatatuba and Serra das Araras, the 2011 event is the largest and most-destructive debris-flow event in Brazil's history, based on the more reliable reported figures. The 2011 catastrophe is also the largest when direct economic losses are considered, with reported losses estimated at ca. U$ 1.9 billion in 2022 (Table 3).

3.3 Geographic distribution

Fig. 2 shows the spatial distribution of debris-flow events in the Brazilian territory. In total, 64.5% of the recorded debris flows occur in the Serra do Mar Mountain range, followed by Serra da Mantiqueira (13.3%) and Serra Geral (13.3%). The southeast region of Brazil is the most affected by debris flows, both in terms of number of events and socioeconomic losses (Table 4). This can be related to the highest population density in the southeast (especially in the states of Rio de Janeiro and São Paulo), the intense urbanization of the coast and the presence of two mountain areas: Serra do Mar and Serra da Mantiqueira.

Table 2 Analysis of debris-flow related damages according to state. Fatalities include missing people. Avg. = average, N/A = not available.

State	Number of events	Economic losses (USD)	Fatalities	Avg. Fatality/event	Avg. Economic loss/event (USD)
Bahia (BA)	2	34,884,425	173	87	17,442,212
Ceará (CE)	1	N/A	91	91	N/A
Minas Gerais (MG)	3	718,275	286	95	359,138
Paraná (PR)	2	76,095,510	4	2	38,047,755
Rio de Janeiro (RJ)	13	3,517,256,731	4,353	335	270,558,210
São Paulo (SP)	18	168,802,604	621	35	9,377,922
Santa Catarina (SC)	5	1,693,749,577	243	49	338,749,915
Rio Grande do Sul (RS)	1	24,683,356	0	0	24,683,356
Total:	45	5,516,190,478	5,771	128	122,582,011

São Paulo is the state with the highest number of reported debris-flow events, followed by Rio de Janeiro and Santa Catarina (Table 2). The state of Rio de Janeiro is, by far, the most impacted by debris flows, with 4,353 fatalities in the last 100 years and ca. U$ 3.5 billion in economic losses, which corresponds to approximately 75% of all fatalities and 64% of the economic losses reported in the whole country. Rio de Janeiro also shows the highest fatality rate per event than any other state, averaging 335 deaths per event, while Santa Catarina shows highest economic losses per event, averaging at ca. U$ 339 million per event (Table 2). These numbers are based on reported numbers and the available data.

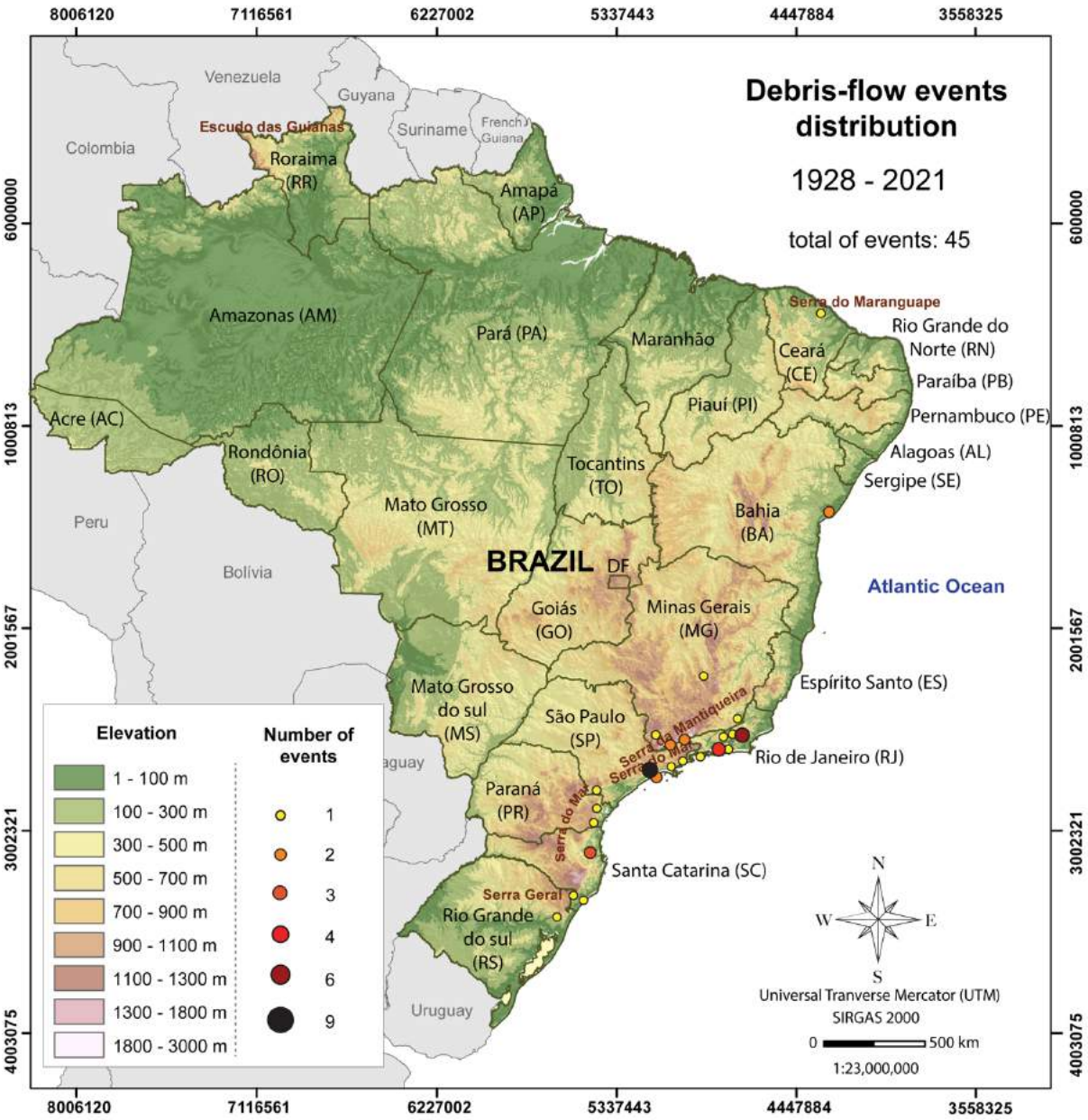

Fig. 2 Geographic distribution of reported debris-flow events in Brazil. The reported events are more often associated to the mountain ranges of Serra do Mar, Serra da Mantiqueira and Serra Geral. The underlying Digital Elevation Model (DEM) is created using GTOPO30 data retrieved from Earth Explorer (USGS 2021).

Among the cities most affected by debris flows, Cubatão (São Paulo) and Petrópolis (Rio de Janeiro) stand out with the highest numbers of events in the last 100 years (9 and 6 events, respectively), whereas the city of Rio de Janeiro, Petrópolis and Tubarão (Santa Catarina) show the highest economic losses (Table 3). Serra das Araras (Piraí), the city of Rio de Janeiro, Petrópolis and Caraguatatuba show the largest number of fatalities (Table 3).

288 **Table 3** Analysis of debris-flow related damages according to municipality. Fatalities include reported cases of dead and
289 missing people. N/A = not available.

Municipality/Region	Number of events	Economic losses (USD)	Fatalities	Material losses (unit)
Além Paraiba (MG) and Volta Grande (MG) region	1	N/A	250	63
Antonina, Morretes (PR)	1	76,095,510	25	223
Bom repouso (MG)	1	718,275	0	11
Campos do Jordão (SP)	2	N/A	27	381
Caraguatatuba (SP)	1	63,449,964	436	400
Contagem (MG)	1	N/A	36	300
Cubatão (SP)	9	73,332,253	11	40
Guaratuba (PR)	1	N/A	0	1
Ilha Grande (RJ)	1	180,668,819	31	8
Itaóca (SP)	1	5,578,975	23	123
Lavrinhas (SP)	2	2,329,412	11	N/A
Maranguape (CE)	1	N/A	91	N/A
Niterói (RJ)	1	146,587,2770	269	62
Nova Friburgo (RJ)	1	1,932,584,390*	392**	N/A
Petrópolis (RJ)	6	322,416,245 + 1,932,584,390*	428**	1,929
Rio de Janeiro (RJ)	4	1,010,547,344	804	> 1,500
Rolante (RS)	1	24,683,356	0	400
Salvador (BA)	2	34,884,425	173	1,401
Santos (SP)	2	24,112,000	102	67
Serra das Araras – Piraí (RJ)	1	N/A	1700	> 100
Teresópolis (RJ)	1	1,932,584,390*	429**	N/A
Timbé do Sul (SC)	1	71,311,286	16	N/A
Tubarão (SC)	1	666,840,081	40	N/A
Ubatuba (SP)	1	N/A	11	30
Vale do Itajaí region (SC)	3	946,442,920	187	5158

290 * Economic losses associated to the 2011 debris flow event, undistinguished between cities
291 ** +300 missing people, undistinguished between cities
292

293 ## *3.4 Temporal and seasonal analysis*

294 Debris-flow events are more common during the summer season (December – March), which is the wettest season
295 in Southeast Brazil, where Serra do Mar and Serra da Mantiqueira are located. Fig. 3a shows the seasonal
296 distribution of events, with January having the largest number of reported debris-flow events, followed by March,
297 February and December. The phenomena can occasionally occur during winter season in the Southeast due to
298 abnormally rainfall events (Seluchi et al. 2011), as the one in Campos do Jordão (São Paulo state) in August 1972
299 at Serra da Mantiqueira (Table 3).

Table 4 Analysis of reported debris-flow related damages according to region. Fatalities include missing people. For state abbreviations, please refer to Fig. 2. Avg. = average.

Regions	Number of events	Economic damages (US$)	Fatalities	Avg. Fatality per event	Avg. Economic loss per event (USD)
North (AC, AM, AP, PA, RO, RR, TO)	0	0	0	0	0
Northeast (AL, BA, CE, MA, PB, PE, PI, RN, SE)	3	34,884,425	264	88	11,628,142
Center-West (DF, GO, MS, MT)	0	0	0	0	0
Southeast (ES, MG, RJ, SP)	34	3,686,777,610	5,260	155	102,410,489
South (PR, RS, SC)	8	1,794,528,444	249	31	224,316,056

The economic losses associated to debris-flow events have been increasing since 1920, although no reports are available for the decades of 1930s, 1940s and 1950s (Fig. 3b). In the 1990s, a sharp decrease in reported economic losses is observed, which is also followed by a decrease in the number of fatalities (Fig. 4b), although not by the number of events (Fig 4a). The general trend, however, is a growth in the associated economic losses over the two more recent decades, which can be related to a better reporting of disasters, as well as to an urbanization increase.

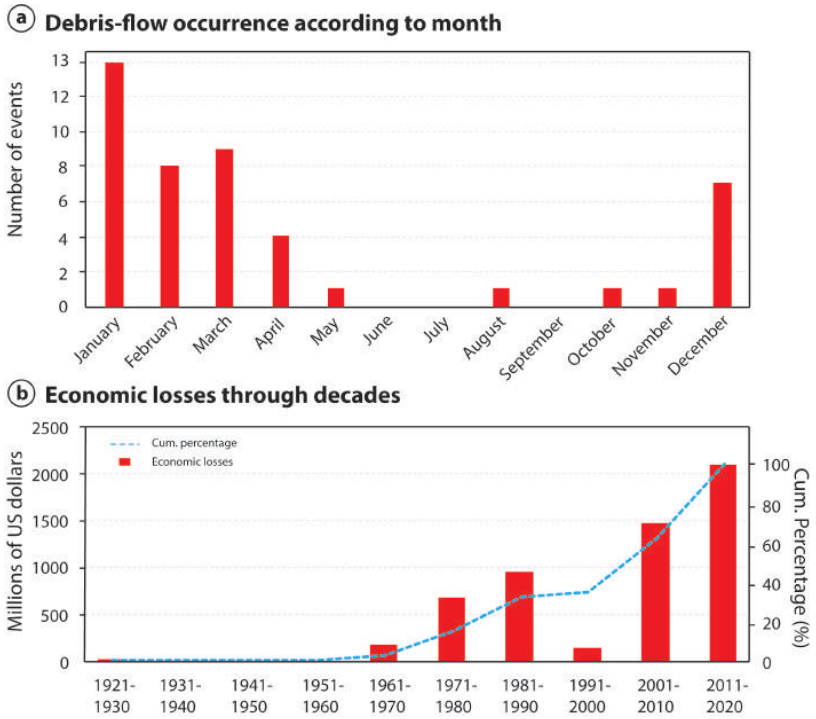

Fig. 3 Seasonal and temporal occurrence of debris-flow events and associated economic losses. a) Monthly distribution of debris-flow events in Brazil. Debris flows are more common in summer months (December – March), which show highest rainfall indices. b) Temporal distribution of economic losses related to debris-flow events. There is an increase in debris-flow related economic losses in the last two decades (2000 – 2020), which could be related to a better reporting and monitoring, as well as to an urbanization increase.

As for the number of reported events, there has not been a significant increase in recent decades, with the frequency averaging at about seven per decade since the 1960s. Prior to 1960s, the documentation of debris-flow events is scarcer, which can be associated to lower levels of urbanization and, consequently, a lower societal impact. The number of fatalities along the years have also been steady since the 1960s, with the decades of 1960s

and 2010s standing out as those with the highest number of fatalities, particularly in the years of 1967 and 2011 (Fig. 4b). These two years are characterized by the high-magnitude debris-flow events in Caraguatatuba and Serra das Araras (1967), and Teresópolis, Petrópolis and Nova Friburgo (2011).

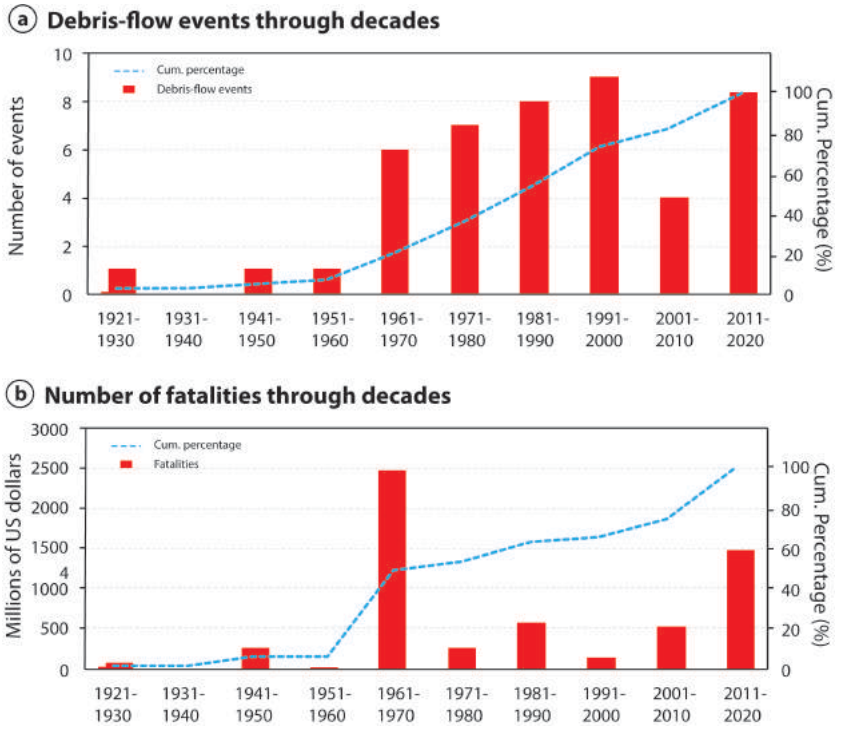

Fig. 4 Temporal analysis of debris-flow events and human-related damages. A) Number of debris-flow events, which have been steady since the 1960s, averaging at 6 events per decade. B) Casualties related to debris flows in Brazil. The years of 1967 and 2011 stand out, due to the high-magnitude events of Serra das Araras (1967) and Teresópolis, Petrópolis and Nova Friburgo (2011).

3.5 Rainfall analysis

Fig. 5 shows the average annual rainfall indices for Brazil plotted against debris-flow events. Debris flows are concentrated in regions with high rainfall rates (> 1600 mm annually) that are also associated with mountain areas, highlighting the strong association between hilly areas and precipitation for their incidence. In areas with very-high annual precipitation (> 2500 mm) and no debris-flow records, such as the North region of Brazil, the relatively flatter terrain or the remoteness of the mountain areas (e.g., "Escudo das Guianas", at the border with Venezuela – Fig. 2) can be associated to the lack of recorded events.

In our catalogue, high-resolution rainfall information was often deficient and, for the most cases, only daily rainfall was available (Table 1). Comparing the 24-h accumulated rainfall with reported data of magnitude, economic losses and fatalities, we can observe a very weak relationship between rainfall and these variables. The relationship between 24-h accumulated rainfall and magnitude, fatality number and economic losses show, respectively, a Spearman correlation coefficient of -0.01 (p-value of 0.52), 0.01 (p-value of 0.51) and -0.25 (p-value of 0.81).

When peak rainfall intensity is considered, a slightly stronger positive correlation between magnitude and number of fatalities is observed. The relationship between hourly rainfall and economic losses shows a positive Spearman correlation coefficient of 0.7 (p-value of 0.91), while the relationship between fatality cases and hourly rainfall shows a positive Spearman correlation coefficient of 0.36 (p-value of 0.81). The correlation between daily rainfall and economic losses, on the other hand, is weaker, with a negative Spearman correlation coefficient of -0.2 (p-value 0.63). See online resources for supplementary information on the correlation of rainfall data and debris-flow magnitude, fatality toll and economic losses.

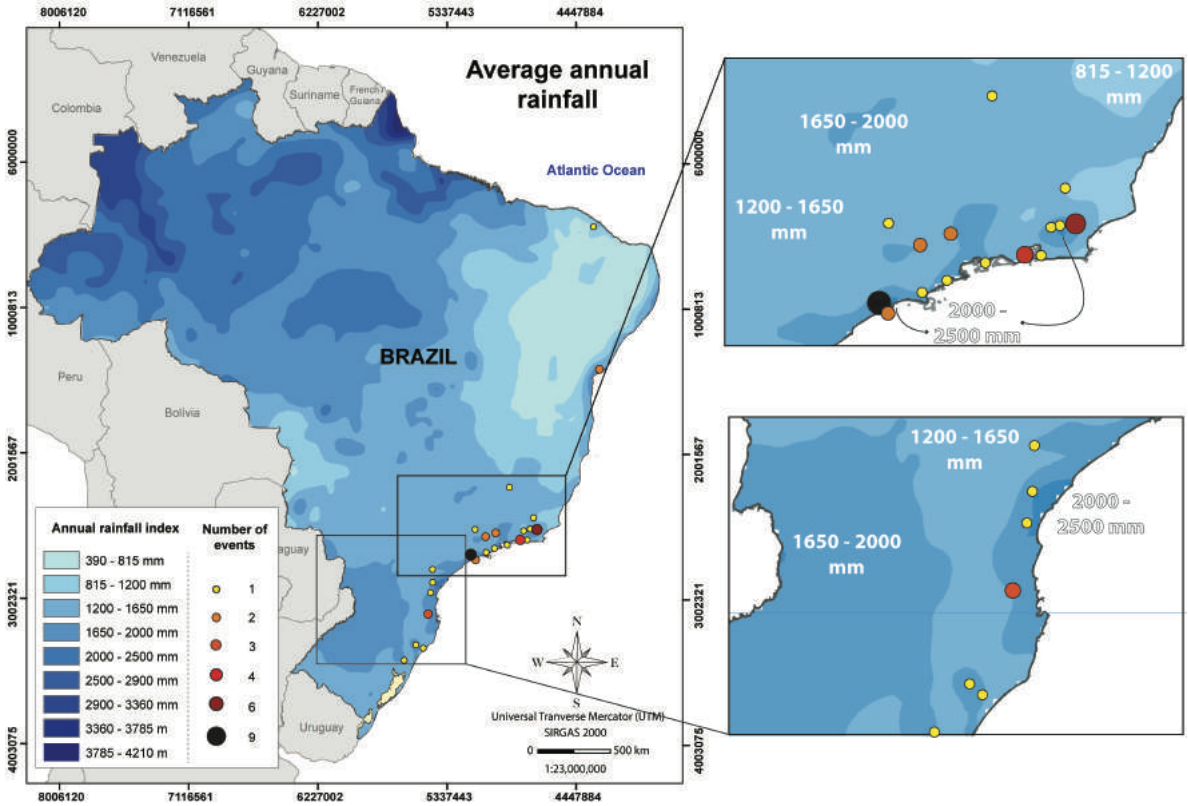

Fig. 5 Average rainfall indices for Brazil, based on the climate data from Brazil's pluviometric atlas (CPRM 2021). Debris flows generally occur in areas with average annual rainfall higher than 1,650 mm.

The available rainfall data, therefore, is not sufficient to indicate a clear relationship between rainfall indices and economic losses, fatality number and magnitude. These results can indicate that the damage related to debris-flow events is not only a function of rainfall, but also to social (e.g., urbanization levels, occupation of risk areas) and geomorphic (e.g., vegetation cover, catchment and channel slope, on-channel material) factors.

Even though hourly rainfall (peak intensity) showed a stronger correlation with magnitude and the number of fatalities, the small sample space of events with complete data of all the considered variables challenges a concrete conclusion about their relationship. It is expected, however, that the more intense the rainfall, the larger the event and, consequently, the larger the associated damage.

3.6 Debris-flow risk evaluation

Fig. 6a shows the average MR of debris flows per 100,000 habitants in Brazil for every decade since 1920 to 2020, whereas the average national MR (combining all death causes) is shown in Fig. 6b, plotted against the population growth of Brazil. The results indicate that while the average national MR has been going down since 1920, the national MR of debris flows has been somewhat steady through the decades. The comparison between the declining average national MR with the steady debris-flow MR can suggest that while there have been several advances in public health and public security policies in Brazil since 1920, the same is not observed for debris-flow prevention and mitigation measures.

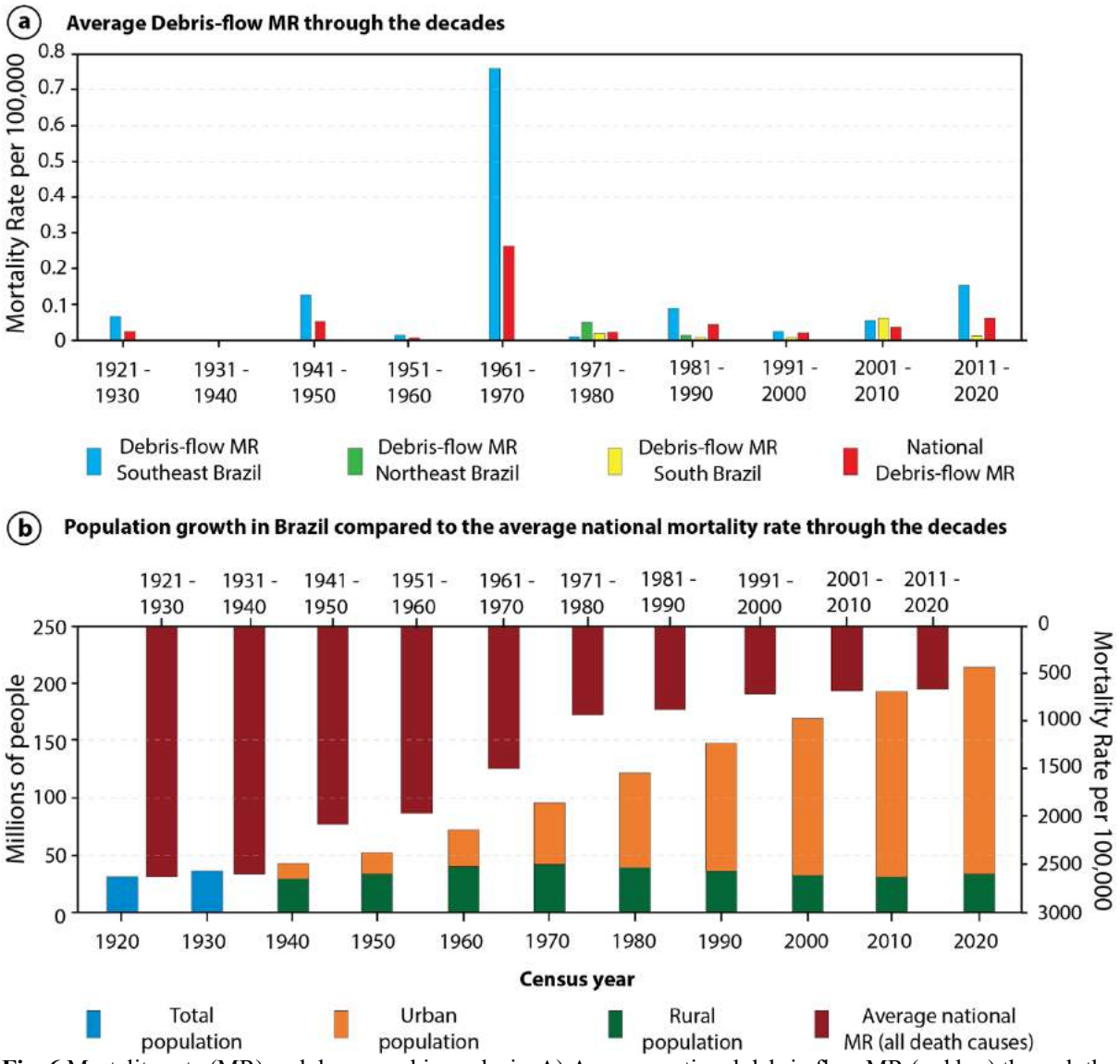

Fig. 6 Mortality rate (MR) and demographic analysis. A) Average national debris-flow MR (red bar) through the decades, compared to the debris-flow MR of the Southeastern (blue), Northeastern (green), and Southern (yellow) region. B) Populational growth of Brazil according to census year, compared to the average mortality rate through the decades comprising all death causes (dark red bar). The number of people living in urban areas has been steadly increasing since 1960. The Demographic and average MR data for Brazil is retrieved from IBGE (2019; 2021).

Southeast Brazil (SEB) exhibits the highest debris-flow MR, with debris-flow related fatalities reported in all decades since 1920, except for the 1930s (Fig. 6a). The average MR in SEB ranged from 0.06 in 1920s to 0.76 in the 1960s, decreasing in the 1970s (0.004) and increasing again in the last decade (0.15). In South Brazil (SB), debris-flow related fatalities are recorded every decade since the 1970s, with the highest average debris-flow MR in the 2000s (0.06), due to the debris-flow event in the Itajaí river basin in 2008 (Table 3). In northeast Brazil (NEB), only in the 1970s and 1980s the region reported debris-flow related deaths, with the highest debris-flow MR in the 1970s (0.05).

The debris-flow MR in the country compared to the MR of other diseases and human-induced causes is shown in Fig. 7, considering the average MR values for the last decade (2011-2020) according to the Global Burden of Diseases (Vos et al. 2020). Fatalities related to debris flows in Brazil are rather rare when compared to other death causes, with approximately 127 deaths per year during the last decade, while homicides and drowning cause each year approximately 61,000 and 6,380 deaths per year, respectively (Fig. 7). The primary cause of death in Brazil are diseases, followed by public violence, with COVID-19 related deaths representing the leading cause of deaths between 2020-2021.

Furthermore, according to the F-N curves for debris flows in the country (Fig. 8), an event with the fatality number of 1,200 or more, such as the one in 2011 in Rio de Janeiro, has a probability of occurring every 50 years if no mitigative measures are adopted, and a debris flow with 10 or more fatalities has a probability of occurring every 3 years.

When debris-flow risk in Brazil is compared to landslide risk in other countries, which also includes debris-flow events, Brazil stands out showing a higher societal risk than China (Tianchi et al. 1989), Japan (Cascini et al. 2008), and Hong Kong (Ho and Ko 2009), and a similar risk to Italy (Guzzetti 2000) (Fig. 9). As already observed using the debris-flow MR to analyze the risk in Brazil, SEB exhibits a higher risk to debris flow events than the national average (Fig. 9), showing a gentler slope (-0.447) when compared to the whole nation (-0.492), consolidating its status as the most susceptible region to fatal debris-flow events.

In our analysis, however, we only focus on debris-flow events, which tend to cause higher number of fatalities and are less frequent than localized fatal landslides (Corominas et al. 2014), which could potentially impact the slope of the F-N curve. Moreover, Japan, Italy and Hong Kong are much smaller in territorial area than Brazil and SEB, which can also potentially impact the probability of fatal events due to the scale effect.

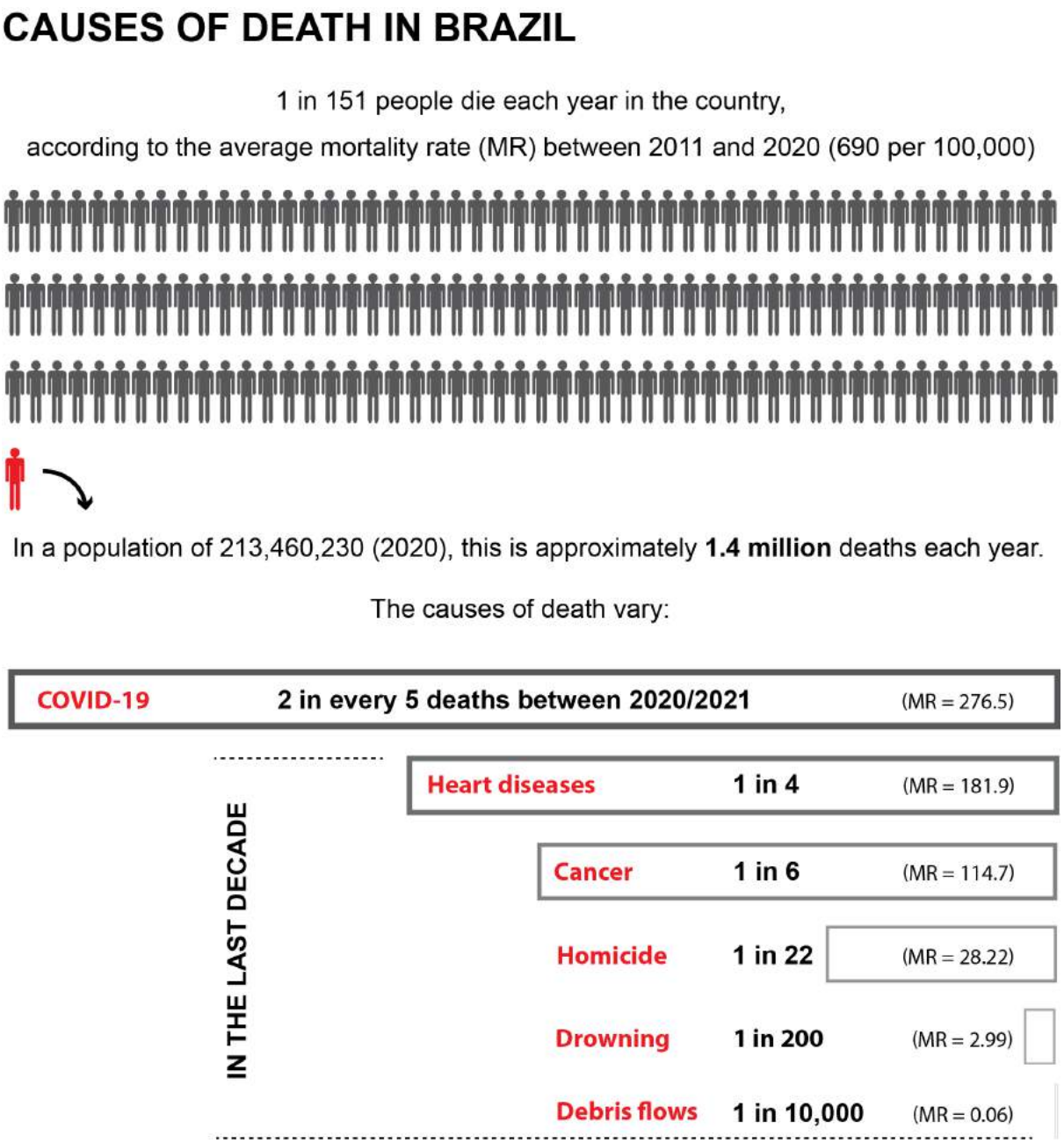

Fig. 7 Mortality Rate (MR) per 100,000 people per year of different death causes in Brazil. The average mortality rates for the last decade (2011-2020) are based on data from the Global Burden of Diseases (Vos et al. 2020). The MR of coronavirus in Brazil is based on data from data from the Brazilian Health Ministry (Brasil 2021c). The figure is based on Strouth and McDougall (2021).

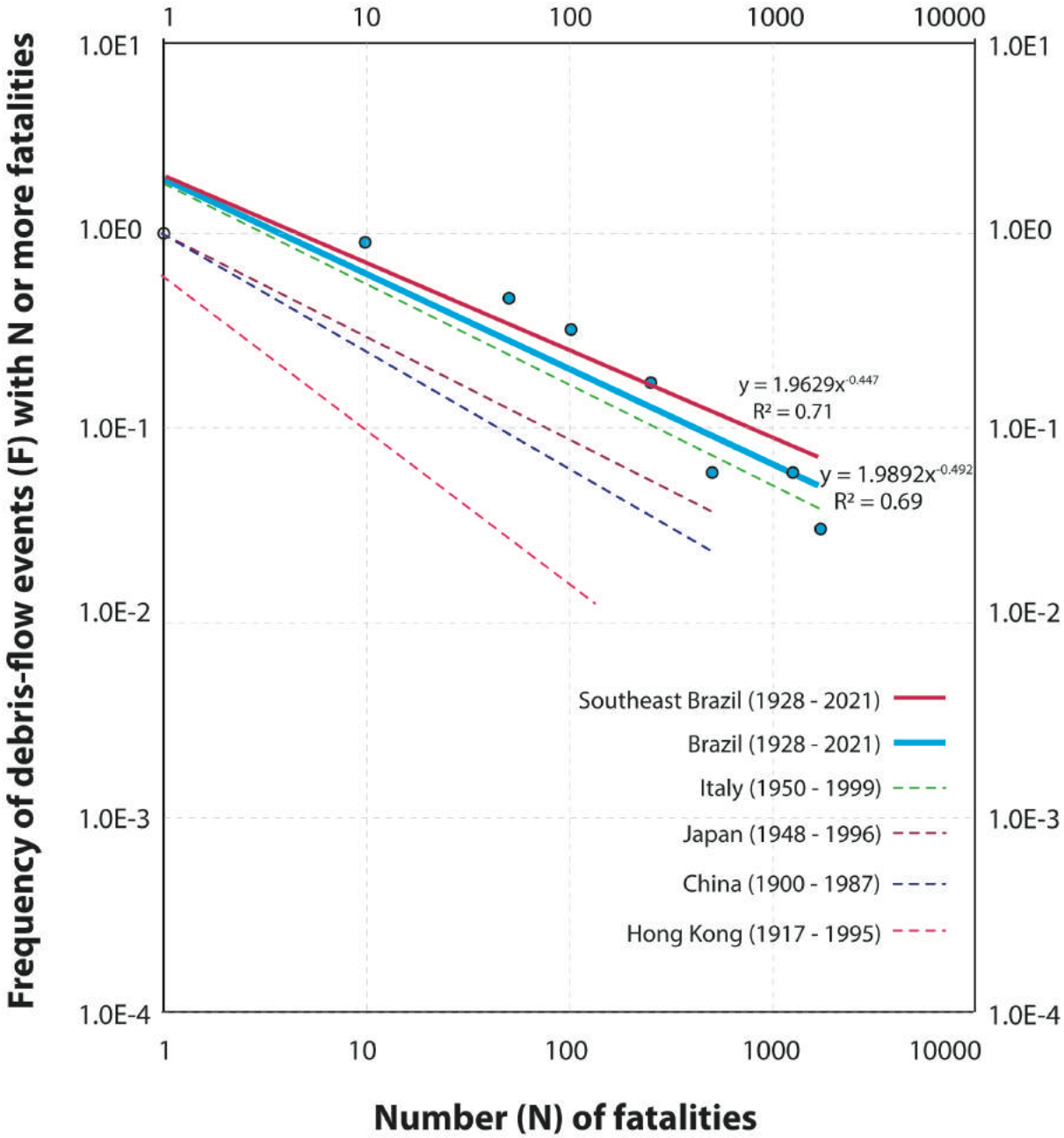

Fig. 8 F-N curves of debris-flow events in Brazil compared to other countries. Debris flows represent a higher societal risk than landslide events (also comprising debris flows) in China (Tianchi et al. 1989), Japan (Cascini et al. 2008), Hong Kong (Ho and Ko 2009), and Italy (Guzzetti 2000).

4 Discussions

F-N plots are commonly applied in landslide studies worldwide (e.g., Macciotta et al. 2015; Keller 2017; Zhang et al. 2019; Strouth and McDougall 2021; among others), even though they are not universally acknowledged as a good indicator of risk (Evans and Verlander 1997; Strouth and McDougall 2021). F-N plots have also been applied in the establishment of thresholds of what is deemed as an acceptable risk by society for different types of natural hazards, including specifically for landslides (Malone 2005; Strouth and McDougall 2021).

Hong Kong, through the country's Geotechnical Engineering Office (GEO), established landslide risk thresholds (ERM 1998) (Fig. 9), which have been adopted by some countries (e.g., Australia, AGS 2007; Western Canada, Porter and Morgenstern 2013), though, as pointed out by Strouth and McDougall (2021), to no great success taking Canada as an example.

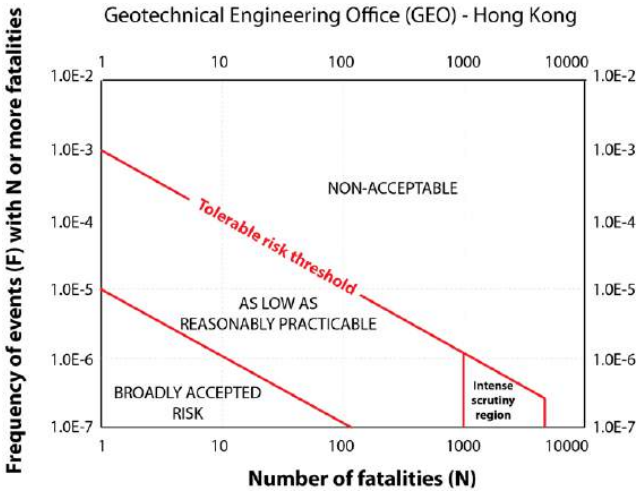

Fig. 9 Societal risk thresholds adopted by Hong Kong, which commissioned the creation of the criterions specifically for landslides (ERM 1998).

F-N curves can potentially be applied in risk analysis studies in cities with extensive historical incidence of debris-flow events in Brazil, such as Petrópolis and Cubatão, providing a good estimation of the probability of fatal events occurrence, which can later subsidize decisions about preventive measures and potentially be incorporated in municipal laws to guide urban occupation in areas prone to these phenomena. While F-N curves can be useful, the adoption of risk thresholds, such as the one from GEO (ERM 1998), can be more challenging. Despite similar climate and hydrogeomorphic process dynamics (Ho and Ko 2009; Lacerda 2007), especially at SEB (sub-tropical climate), economic and cultural differences on the perception of landslides and debris flows risk are some of the factors that are not easily transferable (Strouth and McDougall 2021).

For instance, between 2016 and 2017, The Hong Kong Government budget for disaster prevention and preparedness was approximately 396 million USD, with 165 million USD for landslide preventive measures (Sim et al. 2018). CEMADEN in Brazil had an annual budget upon its creation of 14 million USD in 2012-2013, which has been successively slashed through the years, reaching approximately 3.7 million USD in 2019-2020 (Brasil 2021b). In addition to very different budgets implemented for natural disasters prevention, there are scale effects in the creation of risk thresholds over F-N plots that should be considered, as the x-axis (N) is affected by the size of the population affected, and the y-axis (F) by the return period of the phenomenon (Strouth and McDougall

2021). Comparing the probability of fatal debris-flow events in Brazil with other countries using F-N plots is also subjected to the scale effect, especially when we compare it to Italy and Hong Kong.

Nonetheless, the use of the F-N plot provides a good indication of the risk that the phenomenon represents in Brazil, especially at SEB, and the steady debris-flow MR through the decades further shows that little has been made to reduce and prevent their negative impacts in the last 100 years. The temporal and spatial distribution of debris-flow events is a primordial step to understand the impact of the phenomenon and provides useful information for the definition of areas where mitigative measures must be implemented. Considering that Brazil's population growth is most concentrated at coastal cities in southeast (Londe et al. 2018), which are also the "hotspots" for debris-flow events, disaster prevention measures can and should be implemented, such as local-scale risk analysis, early warning systems and installation of retention structures.

The outlook, however, is not promising. The results of the consistent underfunding of CEMADEN and discontinuation of important disasters prevention programs have been recently seen in the floods and landslides that struck Petrópolis in February 2022, where no warning was issued, causing hundreds of fatalities despite extensive hazard and risk mapping of the municipality. As our study shows, the city is one the most historically affected by debris-flow events and is characterized by high rainfall indices and the occupation of hilly/mountain areas by residences and industries.

While rainfall dynamics in the country can vary greatly according to region (Seluchi et al. 2011; Marengo et al. 2021), generally speaking a combination of antecedent and high intensity peak precipitation is the main rainfall pattern that trigger debris-flow events (Kobiyama et al. 2010; Debortoli et al. 2017). However, as pointed out by Borga et al. (2014), the past is not necessarily the key to the future, especially when land use and/or global warming changes precipitation patterns, altering the dynamics of hydrogeomorphic process in a region or country (Westra et al. 2014; DeBortoli et al. 2017; Marengo et al. 2021).

Furthermore, studies in regions that can also be susceptible to debris-flow initiation, but no fatal events have been recorded so far, are valuable, both considering the population increase trend and the comprehension of the debris-flow dynamics in different geological-geomorphological settings, such as at the Serra do Araripe in Pernambuco state (Peulvast et al. 2011), Escudo das Guianas in Amapá state, and the hilly areas at the central region of Brazil (Mato Grosso and Mato Grosso do Sul states), among others. The lack of recorded debris-flow events in these areas can be linked to less frequent heavy-rainfall events and to lower levels of occupation of mountain areas when compared to Southeast and South Brazil.

5 Conclusions

Cataloguing and estimating the consequences that a natural hazard represents based on past events is one of the most effective methods to provide reasonable damage assessments to the society, even though incompleteness of data and lack of minor events are common challenges that have to be minded. Our historical analysis shows that debris-flow events are concentrated mostly in the Serra do Mar and Serra da Mantiqueira mountains in the Southeast region of Brazil, where population density is higher and occupation of hilly areas is more common. Between 1920 and 2021, 45 debris-flow events were responsible for over 5,771 fatalities and 5.5 billion USD in economic losses. Petrópolis (Rio de Janeiro State), the city of Rio de Janeiro, Cubatão (São Paulo State) and the Vale do Itajaí region (Santa Catarina State) are the most affected areas by debris flows in Brazil, with an extensive history of fatal and destructive events. These regions are characterized by high rainfall indices, especially during summer, and urban and industrial areas near or at mountain areas.

The application of F-N plots shows that the phenomenon represents great risk to the Brazilian society, with a probability of a debris-flow event with a fatality rate of over 1,200 people occurring every 50 years. Based on the average debris-flow MR for the last decade (2011-2020), 1 in every 10,000 deaths were due to the phenomenon, which is low when compared to other deaths causes, such as drowning (1 in 200) and homicide (1 in 22). However, contrasting with the evolution of the national MR (all death causes), which has been decreasing in the last 100 years, the steady MR for debris-flow through the decades indicates that little has been made to reduce the negative impacts of the phenomena in the considered period.

Finally, as landslides are the main triggering mechanism of debris flows in Brazil, the creation of a national landslide inventory can help to identify patterns that lead to the phenomena in the catchments, further aiding the characterization of debris-flow dynamics. The use and widespread availability of GIS technology can facilitate the creation of collaborative database, with researchers and technicians from different institutions responsible for the update as new data is available and mapped. Efforts in this regard have been recently made by Brazilian research groups and researchers (e.g., Uehara et al., 2020; Dias et al. 2021; Osako 2021; among others).

Declarations

Funding

This study was financed in part by the Coordenação de Aperfeiçoamento de Pessoal de Nível Superior—Brasil (CAPES —Finance Code 001) and the National Council for Scientific and Technological Development (CNPq Brasil, 311962/2018-1)

Acknowledgments

The authors would like to thank Prof. Dr. Masato Kobiyama, from The Federal University of Rio Grande do Sul (UFRGS), and Prof. Dr. Tiago Martins, from The Federal University of São Paulo (UNIFESP), for their comments during the development of this study. The authors would also to thank the two anonymous reviewers, who contributed to significantly improving the manuscript.

Conflict of interest

The authors declare that they do not have any competing interests.

References

Ab'Sáber AN (1991) Política de Meio Ambiente. In: Anais dos Seminários Temáticos: política de meio ambiente e aproveitamento do potencial hidrelétrico brasileiro. Rio de Janeiro: Eletrobrás, p. 43 – 54.

Alcántara-Ayala I (2019) Time in a bottle: challenges to disaster studies in Latin America and the Caribbean. Disasters 43(S1) Doi: 10.1111/disa.12325

Alcántara-Ayala I (2002) Geomorphology, natural hazards, vulnerability and prevention of natural disasters in developing countries. Geomorphology 47(2-4): 107 – 124. Doi: https://doi.org/10.1016/S0169-555X(02)00083-1

Almeida MCJ, Nakazawa VA, Tatizana C (1991) Levantamento e cadastro dos escorregamentos no município de Petrópolis, RJ. In: Simpósio de Geografia Física Aplicada, Porto Alegre. Anais... Porto Alegre: UFGRS. p. 292 - 299.

Alvalá RS, Assis Dias M, Saito S, Stenner C, Franco C, Amadeu P, Ribeiro J, Santana RSM, Nobre C (2019) Mapping characteristics of at-risk population to disasters in the context of Brazilian early warning system. Int J Disaster Risk Reduc 41: 101326. Doi: https://doi.org/10.1016/j.ijdrr.2019.101326

Amaral S, Fuck G (1973) Sobre o deslizamento de lama turfosa ocorrido em Campos do Jordão, SP, em agosto de 1972. Boletim IG 4(0): 21. Doi: 10.11606/issn.2316-8978.v4i0p21-37

Andres N, Badoux A (2018) The Swiss flood and landslide damage database: Normalisation and trends. J Flood Risk Manag 12(S1). Doi: 10.1111/jfr3.12510

Augusto Filho O (1992) Caracterização geológico-geotécnica voltada à estabilização de encostas: uma proposta metodológica. In: Conferência Brasileira sobre Estabilidade de Encostas-COBRAE...Anais, p. 721 – 733.

Australian Geomechanics Society (AGS) (2007) Guideline for Landslide Susceptibility, Hazard and Risk Zoning for Land Use Planning. Vol 42

Assis Dias MC, Saito SM, Álvala RC, Stenner C, Pinho G, Nobre CA, Fonseca MRS, Santos C, Amadeu P, Silva D, Lima CO, Ribeiro J, Nascimento F, Corrêa CO (2018) Estimation of exposed population to landslides and floods risk areas in Brazil, on an intra-urban scale. Int J Disaster Risk Reduc 31: 449–459 https://doi.org/10.1016/j.ijdrr.2018.06.002.

Ball DJ (1998) Risk management and the decommissioning of off-shore structures. Society for Risk Analysis annual conference, Paris.

Bastos M, Bandeira R, Campos V (2015) Operações de resposta a desastres: proposta de um modelo de gestão e de um protótipo de banco de dados. Revista Produção Online 15(2): 482. Doi: 10.14488/1676-1901.v15i2.1813

Brasil (2021a) Ministério da Integração Nacional. Secretaria Nacional de Defesa Civil. Banco de dados e registros de desastres: sistema integrado de informações sobre desastres - S2ID. 2013. Available at: <http://s2id.integracao.gov.br/>. Accessed in 01 May 2021

Brasil (2021b) Portal da transparência do Governo Federal – Controladoria Geral da União (CGU). Convênios por Estado/Município: banco de dados. Available at: https://falabr.cgu.gov.br/publico/Manifestacao/SelecionarTipoManifestacao.aspx?ReturnUrl=%2f Accessed in 07 November 2021.

Brasil (2021c) Painel Coronavirus– Ministério da Saúde. Available at: https://covid.saude.gov.br. Accessed in 07 December 2021.

Bollschweiler M, Stoffel M (2010) Tree rings and debris flows: Recent developments, future directions. Prog in Phys Geogr: Earth and Environment 34(5): 625 – 645. Doi: 10.1177/0309133310370283

Borden K, Cutter S (2008) Spatial patterns of natural hazards mortality in the United States. Int J Health Geogr 7(1): 64. Doi: 10.1186/1476-072X-7-64

Borga M, Stoffel M, Marchi L, Marra F, Jakob M (2014) Hydrogeomorphic response to extreme rainfall in headwater systems: Flash floods and debris flows. J Hydrol 518: 194 – 205. Doi: 10.1016/j.jhydrol.2014.05.022

Burton I, Kates RW (1963) The Perception of Natural Hazards in Resource Management. Nat Resources J 3: 412.

Cabral VC, Reis FA, D'Affonseca FM, Lucía A, Corrêa CV, Veloso V, Gramani MF et al (2021) Characterization of a Landslide-Triggered Debris Flow at a Rainforest-Covered Mountain Region in Brazil. Nat Hazards 108: 3021 – 3043. Doi: 10.1007/s11069-021-04811-9.

Cascini L, Ferlisi S, Vitolo E (2008) Individual and societal risk owing to landslides in the Campania region (southern Italy). Georisk 2(3): 125 – 140. Doi: 10.1080/17499510802291310

Cavalcanti IFA, Nunes LH, Marengo JA, Gomes JL, Silveira VP, Castellano MS (2017) Projections of Precipitation Changes in Two Vulnerable Regions of São Paulo State, Brazil. Am J Clim Change 6: 268 – 293. Doi: 10.4236/ajcc.2017.62014

Centro Universitário de Estudos e Pesquisas sobre Desastres (CEPED), Universidade Federal de Santa Catarina (UFSC) (2013) Atlas Brasileiro de Desastres Naturais: 1991-2013. Volume Brasil. Centro Universitário de Estudos e Pesquisas sobre Desastres. Florianópolis

Centro Tecnológico de Minas Gerais - CETEC (1992) Laudo geotécnico sobre o escorregamento de Vila Barraginha, Contagem (MG), Vol. 1. CETEC: Belo Horizonte, Brasil. 110p.

Church M, Jakob M (2020) What Is a Debris Flood? Water Resour Res 56(8). Doi: 10.1029/2020WR027144

Corominas J, van Westen C, Frattini P, Cascini L, Malet JP, Fotopoulou S, Catani F *et al.* (2014) Recommendations for the Quantitative Analysis of Landslide Risk. Bull Eng Geol Environ 73: 209 – 263. Doi: 10.1007/s10064-013-0538-8.

Costa JE (1988) Rheologic, geomorphic, and sedimentologic differentiation of water floods, hyperconcentrated flows, and debris flows. In: Baker VR, Kochel RC, Patton PC (Eds) Flood geomorphology. Wiley, New York.

Cruz O (1975) A Serra do Mar e o litoral na área de Caraguatatuba - SP: contribuição à geomorfologia litorânea tropical - 2. Revista Brasileira de Geografia 37(3): 73 – 138.

Coussot P, Meunier M (1996) Recognition, classification and mechanical description of debris flows. Earth-Science Reviews 40(3-4): 209 – 227. Doi: 10.1016/0012-8252(95)00065-8

Damm B, Klose M (2015) The landslide database for Germany: Closing the gap at national level. Geomorphology 249: 82 – 93. Doi: 10.1016/j.geomorph.2015.03.021

Debortoli NS, Camarinha PIM, Marengo JA *et al.* (2017) An index of Brazil's vulnerability to expected increases in natural flash flooding and landslide disasters in the context of climate change. Nat Hazards 86: 557–582. Doi: 10.1007/s11069-016-2705-2.

Deng YC, Hwang JH, Lyu YD (2021) Developing Real-Time Nowcasting System for Regional Landslide Hazard Assessment under Extreme Rainfall Events. Water 13: 732. Doi: 10.3390/ w13050732

Devoli G, Strauch W, Chávez G, Høeg K (2007) A landslide database for Nicaragua: a tool for landslide-hazard management. Landslides 4(2): 163 – 176. Doi: 10.1007/s10346-006-0074-8

Dias HC, Hölbling D, Grohmann CH. (2021) Landslide inventory mapping in Brazil: Status and challenges. In XIII International Symposium on Landslides.

Dourado F, Arraes T, Silva M (2012) O Megadesastre da Região Serrana do Rio de Janeiro – as Causas do Evento, os Mecanismos dos Movimentos de Massa e a Distribuição Espacial dos Investimentos de Reconstrução no Pós-Desastre. Anuário do Instituto Geológico da Universidade Federal do Rio de Janeiro 35(2): 43 – 54. Doi: 10.11137/2012_2_43_54

Dowling CA, Santi PM (2014) Debris flows and their toll on human life: a global analysis of debris-flow fatalities from 1950 to 2011. Nat Hazards 71: 203 – 227. Doi: 10.1007/s11069-013-0907-4

EM-DAT (2021) The Internacional Disaster Database. General Classification. Disponível em: <http://www.emmat.be/classification>. Accessed in 7 set. 2021.

Estadão (2010) Drama no Rio. Retrieved 24 November 2021, from https://internacional.estadao.com.br/blogs/olhar-sobre-o-mundo/drama-no-rio/

ERM - Hong Kong Ltd. (ERM) (1998) Landslides and Boulder Falls from Natural Terrain: Interim Risk Guidelines. GEO Report No. 75. Geotechnical Engineering Office, Hong Kong

Evans A, Verlander N (1997) What Is Wrong with Criterion FN-Lines for Judging the Tolerability of Risk? Risk Analysis 17(2): 157-168. Doi: 10.1111/j.1539-6924.1997.tb00855.x

Evans SG (1997) Fatal landslides and landslide risk in Canada. In: Cruden D, Fell R (Eds.) Landslide Risk Assessment. Balkema, Rotterdam, pp. 185 – 196.

Facuri G, Picanço JL (2020). Evaluations and proposals for the debris flow hazard mapping. *Landslides* 18(1): 339 – 352

Fell R, Hartford D (1997) Landslide risk management. In: Cruden D, Fell R. (Eds.) Landslide Risk Assessment. Balkema, Rotterdam, pp. 51 – 109.

Fowler AM, Hennessy KJ (1995) Potential impacts of global warming on the frequency and magnitude of heavy precipitation. Nat Hazards 11: 283 – 303. Doi: 10.1007/BF00613411

Ferreira K, Abiko A (2019) Urban Resilience and Landslide Risk Management: The Case of Santos (Brazil). In: Brunetta G, Caldarice O, Tollin N, Rosas-Casals M, Morató J (Eds) Urban Resilience for Risk and Adaptation Governance. Resilient Cities (Re-thinking Urban Transformation). Springer, Cham. Doi: 10.1007/978-3-319-76944-8_12

Fúlfaro V, Ponçano WL, Bistrichi CA, Stein DP (1976) Escorregamentos de Caraguatatuba: expressão atual, e registro na coluna sedimentar da planície costeira adjacente. In: Congresso Brasileiro de Geologia de Engenharia. Anais... Rio de Janeiro: ABGE, pp. 341 – 350.

Geotechnical Engineering Office - GEO (1998) Landslides and Boulder Falls from Natural Terrain: Interim Risk Guidelines. GEO Report 75, Geotechnical Engineering Office, Civil Engineering Department. Government of the Hong Kong SAR.

GEORIO (1996) Estudos Geológicos-Geotécnicos a Montante dos Condomínios Capim Melado e Vilarejo, Jacarepaguá. Relatório Técnico, 96 pp.

Gramani MF (2001) Caracterização geológica-geotécnica das corridas de detritos ("Debris Flows") no Brasil e comparação com alguns casos internacionais. Dissertation, Universidade de São Paulo.

Gramani MF (2015) A corrida de massa em Itaoca: transporte e deposição de sedimentos. In*: Simpósio de Geologia do Sudeste, 14.; Simpósio do Cretáco do Brasil,* Campos do Jordão. Anais..., 5 p.

Gramani MF, Arduin DH (2015) Morfologia da drenagem dos depósitos de *debris flow* em Itaóca, São Paulo. In: Anais 15° Congresso Brasileiro de Geologia de Engenharia e Ambiental (CBGE), Bento Gonçalves, Rio Grande do Sul.

Gramani MF (2017) Corridas de massa na Serra da Mantiqueira: descrição e avaliação da ocorrência no Córrego do Braço, SP. In: Conferência brasileira sobre estabilidade de encostas - COBRAE, Florianópolis

Gonçalves NMS (1992) Impactos Pluviais e Desorganização do Espaço Urbano em Salvador/Ba. PhD Thesis, Universidade de São Paulo

Gonçalves LFH (1998) Avaliação e diagnóstico da distribuição espacial e temporal dos movimentos de massa com a expansão da área urbana em Petrópolis – R.J. Dissertation, Universidade Federal do Rio de Janeiro Rio de Janeiro.

Guerra A (1995) Catastrophic Events in Petrópolis City (Rio De Janeiro State), between 1940 and 1990. GeoJournal 37(3): 349 – 354. Doi: 10.1007/BF00814015

Guerra A, Lopes P, Santos Filho R (2007) Características Geográficas e Geomorfológicas da APA, Petrópolis, RJ. Revista Brasileira de Geomorfologia 8(1): 77 – 86. Doi: 10.20502/rbg.v8i1.87

Guzzetti F (2000) Landslide fatalities and evaluation of landslide risk in Italy. Eng Geology 58: 89 – 107. Doi: 10.1016/S0013-7952(00)00047-8

Guzzetti F, Tonelli G (2004) SICI: an information system on historical landslides and floods in Italy. Nat Hazards Earth Syst Sci 4: 213 – 232.

Ho K, Ko F (2009) Application of quantified risk analysis in landslide risk management practice: Hong Kong experience. Georisk 3(3): 134 – 146. Doi: 10.1080/17499510902873074

Health and Safety Executive – HSE (2009). Societal Risk: Initial briefing to the Societal Risk Technical Advisory Group. HSE Research Report RR703 – available at: www.hse.gov.uk/research/rrhtm/rr703.htm, accessed on 23 November 2021.

Hungr O, Leroueil S, Picarelli L (2014) The Varnes classification of landslide types, an update. Landslides 11(2): 167 – 194. Doi: 10.1007/s10346-013-0436-y

Instituto Brasileiro de Geografia e Estatística – IBGE (2019) Tábuas completa de mortalidade para o Brasil. Available at < https://biblioteca.ibge.gov.br/index.php/biblioteca-catalogo?view=detalhes&id=73097>, Accessed on 01 November 2021.

Instituto Brasileiro de Geografia e Estatística – IBGE (2021) Projeção da população do Brasil e das Unidades da Federação. Available at: < https://www.ibge.gov.br/apps/populacao/projecao/index.html>, Accessed on 01 November 2021.

Instituto de Pesquisa Tecnológicas – IPT (1975) Estudo preventivo e corretivo dos movimentos coletivos de solo e rochas na serra de Maranguape. Relatório Técnico - Fase de Diagnóstico. São Paulo. v. 1, n.1, 1975.

Instituto de Pesquisa Tecnológicas – IPT (1988) Estudo das instabilizações das encostas da Serra do Mar na região de Cubatão, objetivando a caracterização do fenômeno "corrida de lama" e a prevenção dos seus efeitos. Relatório Técnico nº 25.402. São Paulo, pp. 125

Iverson RM, Reid ME, Logan M, LaHusen RG, Godt JW, Griswold JP (2011) Positive feedback and momentum growth during debris-flow entrainment of wet bed sediment. Nat Geosci 4: 116 – 121. Doi: 10.1038/ngeo1040

Jakob M, Stein D, Ulmi M (2012) Vulnerability of buildings to debris flow impact. Nat Hazards 60: 241 – 261 Doi: 10.1007/s11069-011-0007-2

Japan International Cooperation Agency - JICA (1991) The Study on the Disaster Prevention and Restoration Project in Serra do Mar, Cubatão Region, São Paulo. January, vol. 2

Jones FO (1973) Landslides of Rio de Janeiro and the Serra das Araras Escarpment, Brazil. Geological Survey Professional Paper, vol. 697. Department of the Interior, US Printing Office, Washington.

Kahn ME (2005) The Death Toll from Natural Disasters: The Role of Income, Geography, and Institutions. Rev Econ Stat 87(2): 271 – 284.

Kanji MA, Cruz PT, Massad F (2007) Debris flow affecting the Cubatão oil refinery. Brazil. Landslides 5(1):71–82. Doi: 10.1007/s10346-007-0110-3

Keller B (2017) Massive rock slope failure in Central Switzerland: history, geologic–geomorphological predisposition, types and triggers, and resulting risks. Landslides 14: 1633 – 1653. Doi: 10.1007/s10346-017-0803-1

Kobiyama M, Chaffe PLB, Goerl RF, Giglio JN, Reginatto GMP (2010) Hydrological disasters reduction: lessons from hydrology. In: Sens ML, Mondardo RI (Orgs.) Science and Technology for Environmental Studies: Experiences from Brazil, Portugal and Germany. Florianópolis: Universidade Federal de Santa Catarina, p.49-72.

Kobiyama M, Michel GP (2015a) Bibliografia dos trabalhos de fluxos de detritos ocorridos no Brasil no período de 1949-2014: Atualização. Porto Alegre: GPDEN/IPH/UFRGS, 2015. 16p. (Trabalho Técnico GPDEN. No. 02).

Kobiyama M, Michel G, Engster E, Paixão M (2015b) Historical analyses of debris flow disaster occurrences and of their scientific investigation in Brazil. Labor e Engenho 9(4): 76 – 89. Doi: 10.20396/lobore.v9i4.8639477

Kobiyama M, Michel G, Goerl RF (2019) Proposal of debris flow disasters management in Brazil based on historical and legal aspects. Int J Erosion Control Engineering 11(3): 85 – 93. Doi: 10.13101/ijece.11.85

Lacerda WA (2007) Landslide Initiation in Saprolite and Colluvium in Southern Brazil: Field and Laboratory Observations. Geomorphology 87(3): 104 – 19. Doi: 10.1016/j.geomorph.2006.03.037.

Listo F, Gomes M, Vieira B (2018) Avaliação da variação do fator de segurança com o modelo TRIGRS. Revista Brasileira de Geomorfologia 19(1): 207 – 220. Doi: 10.20502/rbg.v19i1.1256

Londe L, Moura L, Coutinho M, Marchezini V, Soriano E (2018) Vulnerability, health and disasters in São Paulo coast (Brazil): challenges for a sustainable development. Ambiente & Sociedade 21(0): e01022. Doi: 10.1590/1809-4422asoc0102r2vu18L1AO

Lopes ESS, Riedel PS (2007) Simulação da corrida de massa do Km42 ocorrido na Rodovia Anchieta. In: Anais do II Simpósio Brasileiro de Desastres Naturais e Tecnológicos, Santos, São Paulo.

Macciotta R, Martin CD, Morgenstern NR *et al.* (2016) Quantitative risk assessment of slope hazards along a section of railway in the Canadian Cordillera—a methodology considering the uncertainty in the results. Landslides 13: 115 – 127. Doi: 10.1007/s10346-014-0551-4

Maia ACN, Sedrez L (2014) Enchentes que destroem, enchentes que constroem: Natureza e memória da Cidade de Deus nas chuvas de 1966 e 1967. Revista do Arquivo Geral do Rio de Janeiro 8: 183 – 199.

Malone AW (2005) The story of quantified risk and its place in slope safety policy in Hong Kong. In: Landslide hazard and risk: 643 – 674.

Marengo JA, Camarinha PI, Alves LM, Diniz F, Betts RA (2021) Extreme Rainfall and Hydro-Geo-Meteorological Disaster Risk in 1.5, 2.0, and 4.0°C Global Warming Scenarios: An Analysis for Brazil. Frontiers in Climate 3(13): 610433. Doi: 10.3389/fclim.2021.610433

Massad F, Kanji MA, Cruz PT, Uehara K, Ishitani H, Araujo Filho HA (1998). Debris flows em Cubatão, São Paulo: obras de controle e impactos ambientais. In: XI Congresso Brasileiro de Mecânica dos Solos e Engenharia de Geologia, Brasília.

Massad F (2002) Corridas de massas geradas por escorregamentos de terra: relação entre a área deslizada e a intensidade de chuva. In: XII Congresso Brasileiro de Mecânica dos Solos e Engenharia Geotécnica. São Paulo, São Paulo

Meis MRM, Silva JX (1968) Considerações Geomorfológicas a Propósito dos Movimentos de Massa Ocorridos no Rio de Janeiro. Revista Brasileira de Geografia 30(1): 55 – 73.

Mendonca M, Silva D (2020) Integration of census data based vulnerability in landslide risk mapping - The case of Angra dos Reis, Rio de Janeiro, Brazil. Int J Disaster Risk Reduc 50: 101884. Doi: 10.1016/j.ijdrr.2020.101884

Mirus B, Jones E, Baum R, Godt J, Slaughter S, Crawford M, Lancaster J, Stanley T, Kirschbaum D, Burns W, Schmitt R, Lindsey K, McCoy K (2020) Landslides across the USA: occurrence, susceptibility, and data limitations. Landslides 17(10): 2271 – 2285. Doi: 10.1007/s10346-020-01424-4

Nakazawa VA, Cerri LES (1990) Os escorregamentos ocorridos em Petrópolis – RJ em fevereiro de 1988: ações emergenciais. In: Simpósio Latino-Americano sobre Risco Geológico Urbano, Atas.../ABGE, p.325 – 333.

O'Gorman P, Schneider T (2009) The physical basis for increases in precipitation extremes in simulations of 21st-century climate change. Proc Natl Acad Sci 106(35): 14773 – 14777. Doi: 10.1073/pnas.0907610106

Oliveira Filho O (2012) Os movimentos de massa na região serrana do estado do Rio de Janeiro em 2011: diagnóstico e proposição de medidas para enfrentamento de desastres ambientais. CES Revista 26(1): 149 – 164.

Osako LS (2021) Updating landslide inventory maps using high resolution digital orthophotos and digital surface and elevation modeling: the case study of Brusque city, Santa Catarina State, Brazil. ISPRS Annals of Photogrammetry, Remote Sensing & Spatial Information Sciences, vol. 3. Doi: 10.5194/isprs-annals-V-3-2021-251-2021

Patel R, Burke T (2009) Urbanization — An Emerging Humanitarian Disaster. N Eng J Med 361(8): 741 – 743. Doi: 10.1056/NEJMp0810878

Pellerin J, Duarte GM, Scheibe LF, Mendonça M, Buss MD, Monteiro MA (1997) Timbé do Sul - Jacinto Machado: avaliação preliminar da extensão da catástrofe de 23-24/12/95. Geosul 12(23): 71 – 86.

Peulvast JP, Bétard F, Magalhães AO (2011) Scarp morphology and identification of large-scale mass movements in tropical tablelands: the eastern Araripe basin (Ceará, Brazil). Géomorphologie: relief, processus, environnement 17(1): 33 – 52. Doi: 10.4000/geomorphologie.8800

Pinto RC, Passos E, Caneparo SC (2014) Movimentos de Massa como Processos Naturais de Evolução das Encostas, Estudo de Caso: Bacia do Rio Jacareí, Municípios de Morretes e Paranaguá–PR. Geoingá: Revista do Programa de Pós-Graduação em Geografia 6(1): 23 – 45

Porter M, Morgenstern N (2013) Landslide risk evaluation: Canadian technical guidelines and best practices related to landslides: A national initiative for loss reduction. Natural Resources Canada

Public Safety Canada (PSC) (2020) The Canadian Disaster Database. Retrieved from https://www.publicsafety.gc.ca/cnt/rsrcs/cndn-dsstr-dtbs/index-en.aspx. Accessed on August 1, 2022.

Rosa Filho A, Cortez ATC (2010) A problemática socioambiental da ocupação urbana em áreas de risco de deslizamento da "Suíça brasileira". Revista Brasileira de Geografia Física *3*(1): 33 – 40. Doi: 10.26848/rbgf.v3i1.232610

Rosi A, Canavesi V, Segoni S, Nery TD, Catani F, Casagli N (2019) Landslides in the Mountain Region of Rio De Janeiro: A Proposal for the Semi-Automated Definition of Multiple Rainfall Thresholds. Geosciences 9(5): 203 Doi: 10.3390/geosciences9050203.

Santangelo M, Marchesini I, Bucci F, Cardinali M, Cavalli M, Crema S, Marchi L, Alvioli M, Guzzetti F (2020) Exposure to landslides in rural areas in Central Italy. Journal of Maps 17(4): 124 – 132. Doi: 10.1080/17445647.2020.1746699

Sedrez LF, Maia ACN (2014) Enchentes que destroem, enchentes que constroem: natureza e memória da Cidade de Deus. Revista do Arquivo Geral da Cidade do Rio de Janeiro 8: 183 – 200.

Seluchi M, Chan Chou S, Gramani M (2011) A case study of a winter heavy rainfall event over the Serra do Mar in Brazil. Geofísica Internacional 50(1): 41 – 56. Doi: 10.22201/igeof.00167169p.2011.50.1.121

Serviço Geológico do Brasil – CPRM (2021) Atlas Pluviométrico do Brasil. Retrieved 07 November 2021, from http://www.cprm.gov.br/publique///Mapas-e-Publicacoes/Atlas-Pluviometrico-do-Brasil-1351.html

Sim T, Wang D, Han Z (2018) Assessing the Disaster Resilience of Megacities: The Case of Hong Kong. Sustainability 10(4): 1137. Doi: 10.3390/su10041137

Sternberg HO (1949) Enchentes e movimentos coletivos do solo no vale do Paraíba em dezembro de 1948. Influência da exploração destrutiva das terras. Revista Brasileira de Geografia 11(2): 223-261.

Strouth A, McDougall S (2020) Societal risk evaluation for landslides: historical synthesis and proposed tools. Landslides 18(3): 1071 – 1085. Doi: 10.1007/s10346-020-01547-8

Strouth A, McDougall S (2021) Historical Landslide Fatalities in British Columbia, Canada: Trends and Implications for Risk Management. Frontiers in Earth Science 9: 606854. Doi: 10.3389/feart.2021.606854

Stillwell HD (1992) Natural hazards and disasters in Latin America. Nat Hazards 6: 131–159. Doi: 10.1007/BF00124620

Takahashi T (2006) Debris Flows: Mechanics, Prediction and Countermeasures. Taylor and Francis, Balkema, Leiden.

Tavares R, Mendonça F (2010) Ritmo climático e risco socioambiental urbano: chuvas e deslizamentos de terra em Ubatuba-SP (BR) entre 1991 e 2009. In: Seminário latino-americano de geografia física, VI, Coimbra, Portugal.

Tianchi L (1989) Landslides: extent and economic significance in China. In: Brabb EE, Harrod BL (Eds.) Landslides: Extent and Economic Significance. 28th International Geological Congress: Symposium on Landslides. Washington D.C., United States. Rotterdam: Balkema, pp. 271 – 287.

Uehara TDA, Corrêa SPLP, Quevedo RP, Körting TS, Dutra LV, Rennó C (2020) Landslide Scars Detection using Remote Sensing and Pattern Recognition Techniques: Comparison Among Artificial Neural Networks, Gaussian Maximum Likelihood, Random Forest, and Support Vector Machine Classifiers. Revista Brasileira de Cartografia 72(4): 665-680.

United Nations Office for Disaster Risk Reduction – UNDRR (2015) Sendai Framework for Disaster Risk Reduction 2015-2030. Available at: http://www.unisdr.org/we/inform/publications/43291, accessed on 23 November 2021.

United States Geological Survey – USGS (2021). EarthExplorer. Retrieved 07 November 2021, from https://earthexplorer.usgs.gov

Vanelli F, Romero Monteiro L, Fan F, Goldenfum J (2020) The 1974 Tubarão River flood, Brazil: reconstruction of the catastrophic flood. J Appl Water Eng Res 8(3): 231 – 245. Doi: 10.1080/23249676.2020.1787251

Van Den Eeckhaut M, Hervás J (2012) State of the art of national landslide databases in Europe and their potential for assessing landslide susceptibility, hazard and risk. Geomorphology 139 – 140: 545 – 558. Doi: 10.1016/j.geomorph.2011.12.006

Varnes DJ (1978) Slope movement types and processes. In: Schuster RL, Krizek RJ (Eds) Special report 176: landslides: analysis and control. Transportation and Road Research Board, National Academy of Science, Washington DC, p. 11 – 33

Vos T, Lim S, Abbafati C, Abbas K, Abbasi M, Abbasifard M. et al. (2020) Global burden of 369 diseases and injuries in 204 countries and territories, 1990–2019: a systematic analysis for the Global Burden of Disease Study 2019. The Lancet 396(10258): 1204 – 1222. Doi: 10.1016/s0140-6736(20)30925-9

Westra S, Fowler HJ, Evans JP, Alexander LV, Berg P, Johnson F, Kendon EJ, Lenderink G, Roberts NM (2014) Future Changes to the Intensity and Frequency of Short-Duration Extreme Rainfall. Rev Geophys 52(3): 522 – 555. Doi: 10.1002/2014rg000464.

Wilford DJ, Sakals ME, Innes JL, Sidle RC, Bergerud WA (2004) Recognition of Debris Flow, Debris Flood and Flood Hazard through Watershed Morphometrics. Landslides 1(1): 61 – 66. Doi: 10.1007/s10346-003-0002-0.

Wirtz A, Kron W, Löw P *et al* (2014) The need for data: natural disasters and the challenges of database management. Nat Hazards 70: 135 – 157. Doi: 10.1007/s11069-012-0312-4

Wolle CM, Hachich W (1989) Rain-Induced Land-Slides in Southern Brazil. In: Proceedings of the 12th International Conference on Soil Mechanics and Foundation Engineering, Rio de Janeiro.

Zanandrea F, Michel G, Kobiyama M, Cardozo G (2019). Evaluation of different DTMs in sediment connectivity determination in the Mascarada River Watershed, southern Brazil. Geomorphology 333*:* 80 – 87. Doi: 10.1016/j.geomorph.2019.02.005

Zhang S, Li C, Liu Y (2019) Quantitative Assessment of Human Risk from Landfill Failure in Shenzhen, China. In: Zhan L, Chen Y, Bouazza A (Eds) Proceedings of the 8th International Congress on Environmental Geotechnics Volume 3. ICEG 2018. Environmental Science and Engineering. Springer, Singapore. Doi: 10.1007/978-981-13-2227-3_69

Zhuang JQ, Cui P, Wang GH, Chen XQ, Iqbal J, Guo XJ (2015) Rainfall thresholds for the occurrence of debris flows in Jiangjia Gully, Yunnan Province, China. Eng Geol 195: 335 – 346. Doi: 10.1016/j.enggeo.2015.06.006

APPENDIX A.2

Characterization of a landslide-triggered debris flow at a rainforest-covered mountain region in Brazil

[1,2]Victor Carvalho Cabral*, [1]Fábio Augusto Gomes Vieira Reis, [2]Fernando Mazo D'Affonseca, [2]Ana Lucía, [1]Claudia Vanessa dos Santos Corrêa, [1]Vinicius Veloso, [3]Marcelo Fischer Gramani, [3]Agostinho Tadashi Ogura, [4]Andrea Fregolente Lazaretti, [5]Felipe Vemado, [5]Augusto José Pereira Filho, [6]Claudia Cristina dos Santos, [6]Eymar Silva Sampaio Lopes, [7]Lis Maria Reoni Rabaco, [1]Lucilia do Carmo Giordano, [2]Christiane Zarfl

[1] Applied Geology Department, Earth and Exact Sciences Institute, São Paulo State University – UNESP. Address: Av. 24A, 1555 – Rio Claro, São Paulo, Brazil.

[2] Center for Applied Geosciences, University of Tübingen, Germany. Address: Hölderlinstraße, 12 – Tübingen, Germany.

[3] Institute for Technological Research – IPT. Address: Av. Prof. Almeida Prado, 532 – São Paulo, São Paulo, Brazil.

[4] Brazilian Geological Service – CPRM. Address: Rua Costa, 55 – São Paulo, São Paulo, Brazil.

[5] Institute of Astronomy, Geophysics and Atmospheric Sciences, University of São Paulo – USP. Address: Rua do Matão, 1226 – São Paulo, São Paulo, Brazil.

[6] National Institute for Space Research – INPE. Address: Av. Dos Astronautas, 1758 – São José dos Campos, São Paulo, Brazil.

[7] Centro de Pesquisas e Desenvolvimento - CENPES. Address: Av. Horácio de Macedo, 950 - Rio de Janeiro, Rio de Janeiro, Brazil.

*Corresponding author: victor.carvalho@unesp.br, ORCID: 0000-0002-9910-0508

Abstract

• Debris flows represent great hazard to humans due to their high destructive power. Understanding their hydrogeomorphic dynamics is fundamental in hazard assessment studies, especially in subtropical and tropical regions where debris flows have scarcely been studied when compared to other mass-wasting processes. Thus, this study aims at systematically analyzing the meteorological and geomorphological factors that characterize a landslide-triggered debris flow at the Pedra Branca catchment (Serra do Mar, Brazil), to quantify the debris flow's magnitude, peak discharge and velocity. A magnitude comparison with empirical equations (Italian Alps, Taiwan, Serra do Mar) is also conducted. The meteorological analysis is based on satellite data and rain gauge measurements, while the geomorphological characterization is based on terrestrial and aerial investigations, with high-spatial resolution. The results indicate that it was a large-sized stony debris flow, with a total magnitude of 120,195 m^3, a peak discharge of 2,146.7 $m^3 s^{-1}$ and a peak velocity of 26.5 m s^{-1}. The debris flow was triggered by a 188 mm rainfall in 3 h (maximum intensity of 128 mm h^{-1}), with an estimated return period of 20 years, which, combined with the intense accumulation of on-channel debris (ca. 37,000 m^3), indicates that new high-magnitude debris flows in the catchment and the region are likely to occur within the next two decades. The knowledge of the potential frequency and magnitude (F-M) can support the creation of F-M relationships for Serra do Mar, a prerequisite for reliable hazard management and monitoring programs.

KEYWORDS: Shallow landslides, Magnitude, Serra do Mar, forensic geomorphological analysis, Mass movements, Bedrock rivers.

Declarations

Acknowledgments

The authors would like to thank Prof. Dr. Peter Grathwohl and Prof. Dr. Todd Ehlers, from the University of Tübingen, for the help during the development of this research. We would also like to thank Dr. Lorenzo Marchi and an anonymous reviewer for their comments, which contributed to significantly improve the manuscript.

Funding

This study was financed in part by the Coordenação de Aperfeiçoamento de Pessoal de Nível Superior – Brasil (CAPES) – Finance Code 001. Dr. Pereira Filho was sponsored by Conselho Nacional de Desenvolvimento Científico e Tecnológico - Brasil (CNPq) under grant 302349/2017-6.

Data availability

The datasets generated during our study are available from the corresponding author upon request.

Competing interests

The authors declare that they do not have any competing interests.

Compliance with Ethical Standards

The authors declare that they have no conflict of interest.

Author contributions

Mr. Cabral worked on the development and writing of the manuscript, organized and collected fieldwork data. Dr. Reis organized the fieldwork campaign, contributed with the development and organization of the manuscript. Dr. D'Affonseca aided the development and writing of the manuscript. Dr. Lucía contributed to the writing and organization of the manuscript. Dr. Correa aided the collection of fieldwork data and data processing. Mr. Veloso helped in the collection of fieldwork data and data processing. Mr. Gramani contributed to the organization of the fieldwork and data collection. Mr. Ogura contributed to fieldwork data collection and organization of the manuscript. Ms. Lazaretti aided the development of the manuscript and the acquisition of rain gauge data. Dr. Vemado contributed with satellite meteorological data. Dr. Pereira Filho contributed with the meteorological data and development of the manuscript. Dr. Santos organized and aided the acquisition of high-resolution aerial photographs. Dr. Lopes aided the acquisition of high-resolution aerial photographs and in the organization of the fieldwork campaign. Ms. Rabaco aided the organization of the fieldwork campaign. Dr. Giordano aided the organization of the fieldwork campaign. Dr. Zarfl worked on the writing and organization of the manuscript.

Introduction

Debris flows pose great threat to human life and infrastructure, especially in mountain regions, due to their sudden occurrence, high mobility, volume, impact energy and large run-out distance (Iverson 2000; Begueria et al. 2009; Luna et al. 2012). These phenomena occur when a mixture of earth material, water and air very rapidly surge down steep drainage paths (Varnes 1978; Takahashi 2006; Hungr et al. 2014) and their primary triggering factor is high-intensity rainfall (Milne et al. 2009). The increasing frequency of extreme rainfall events on a global scale (Beniston 2009; Giorgi et al. 2011; Borga et al. 2014; Westra et al. 2014) has been associated to an observed increase in the frequency and magnitude of debris-flow events (Stoffel and Huggel 2012; Winter and Shearer 2014; Borga et al. 2014), which, combined with landslides, were responsible for more than 32,000 casualties between 2004 – 2010 (Petley 2012; Borga et al. 2014).

An increase in the frequency of extreme precipitation events has also been observed for southern and southeastern Brazil (Teixeira and Satyamurti 2011), which could alter mass movement dynamics in the country. Over 4,000 debris-flow related fatalities were recorded in the last 100 years from 22 fatal events in Brazil (Kobiyama et al. 2015), 95% of which concentrated at the Serra do Mar, a mountain range that extends for about 1,500 km in the Brazilian southern and southeastern coast (Vieira and Gramani, 2015). Despite their highly destructive potential, debris flows are still poorly studied when compared to other mass-wasting processes in Brazil, mainly due to insufficient monitoring (Borga et al. 2014; Kobiyama et al. 2015; Gregoretti et al. 2018).

Direct field investigations are essential for understanding the hydrogeomorphic dynamics of a catchment during debris flows (Gaume and Borga 2008; Borga et al. 2014; Lucía et al. 2018). They also provide a sound knowledge of the magnitude of a debris-flow event (i.e., the total volume of transported debris), which is a prerequisite for understanding and quantifying associated hazards (Jakob 2005a). The irregular occurrence of debris flows, however, and their development in terrains of difficult, often dangerous, accessibility pose a challenge to detailed pre- and post-event field studies (Kean et al. 2013; Gregoretti et al. 2018; Destro et al. 2018).

Magnitude estimations are more commonly carried out by statistical and empirical methods (e.g., Takahashi 1992; Bianco and Franzi 2000; Massad 2002; Takahashi 2006; Kanji et al. 2007; Chang et al. 2011) or by post-event (forensic) geomorphological investigation of the debris-flow route in a catchment (e.g., Marchi and D'Agostino 2004; Liu et al. 2009; Gregoretti et al. 2018). Geomorphology-based estimations are considered one of the most accurate since they are based on direct field evidences (Liu et al. 2009; Gregoretti et al. 2018) and do not necessarily require information about previous events (Marchi and D'Agostino, 2004), which can be rare in some mountain regions.

Due to the high costs and difficulties involved using direct field investigations, empirical equations have been developed to estimate magnitude, as a result of extensive debris-flow documentation in highly prone regions, such as the European Alps, west coast of North America, Japan and Taiwan (e.g., Kronfellner-Krauss 1984; Takei 1984; Takahashi 1991; Rickenmann and Zimmermann 1993; Marchi and D'Agostino 2004; Chang et al. 2011). Empirical equations and semi-empirical equations, however, are mainly site-specific (Rickenmann 1999; Gregoretti et al. 2018) and can potentially be inadequate in areas with different geological-geomorphological settings.

By estimating the magnitude, important kinematic parameters such as peak discharge and flow velocity can also be obtained (Rickenmann 1999; Pak and Lee 2008; Santi et al. 2008; Reid et al. 2016), which are crucial in the proper design of retention structures (Kanji et al 2007; Santi 2014; Gregoretti et al. 2018). Peak discharge and velocity are directly related to the entrainment potential of debris flows, which can significantly increase the magnitude, in some cases by an order of magnitude, and the overall hazard of the process (Milne 2008; Santi et al. 2008; Berger et al. 2011; de Hass and Densmore 2019).

Debris-flow magnitude estimations based on forensic geomorphological characterizations are scarce in mountain regions (Stoffel 2010), being often focused on flash-flood events (e.g., Gaume and Borga 2008; Borga et al. 2014; Surian et al. 2016; Steeb et al. 2017; Lucía et al. 2018) or are mostly concentrated on alpine catchments with extensive documented history of debris-flow events (e.g., Marchi and D'Agostino 2004; Tang et al. 2011; Gregoretti et al. 2018). For Serra do Mar in Brazil, which is a region typical for rainstorms that often trigger mass movements (Vieira and Gramani 2015), such studies are non-existent.

In this study, we characterize a landslide-triggered debris flow that occurred on February 11, 2017, at the Pedra Branca catchment in the Serra do Mar mountain range. A forensic geomorphological analysis with an unprecedented spatial resolution is conducted to characterize the source area, transport path and deposits of the debris flow and to estimate the debris flow's magnitude, peak discharge and flow velocity. A forensic meteorological characterization is also performed to analyze the precipitation pattern of the debris-flow event, based on satellite data and rain gauge measurements.

Furthermore, a comparison between the geomorphology-based estimation with magnitudes calculated using empirical equations from the literature is conducted to assess their applicability to the study area, which can support further debris-flow susceptibility studies for Serra Mar. The equations are chosen due to their simplicity in input parameters (Italian alps - Marchi and D'Agostino 2004; Marchi et al. 2019), their consideration of rainfall and

landslides volume in calculations (Taiwan - Chang et al. 2011) and the similar geological-geomorphological context (Serra do Mar – Kanji et al. 2007).

Study area

The Pedra Branca catchment (Fig. 1) is characterized by a great difference in altitude when compared to the surrounding region, with elevations that range from 90 to 1,100 m a.s.l (above sea level). The 3.43 km^2 catchment exhibits moderate drainage density (3 km km^{-2}) and a relief ratio (0.35) and Melton number (0.6) that indicate the tendency to initiate debris flows and debris floods (Wilford et al. 2004) (Table 1).

In the region, rainfall is well distributed year-round, averaging 2,500 mm annually and reaching up to 3,500 mm in some years (Maack 2002; Mocochinski and Scheer 2014). The Proterozoic monzogranite that comprises the bedrock of Pedra Branca's headwaters is one of the most weathering-resistant rock types in Serra do Mar (Vieira and Gramani 2015), generating shallow residual soil (up to 2 m deep) and steep slopes that stand out in the landform (Fig. 2b). The catchment is covered by the Atlantic Forest biome, a tall, broad-leaf rainforest, considered the second largest tropical forest of the American continent (Tabarelli et al. 2005).

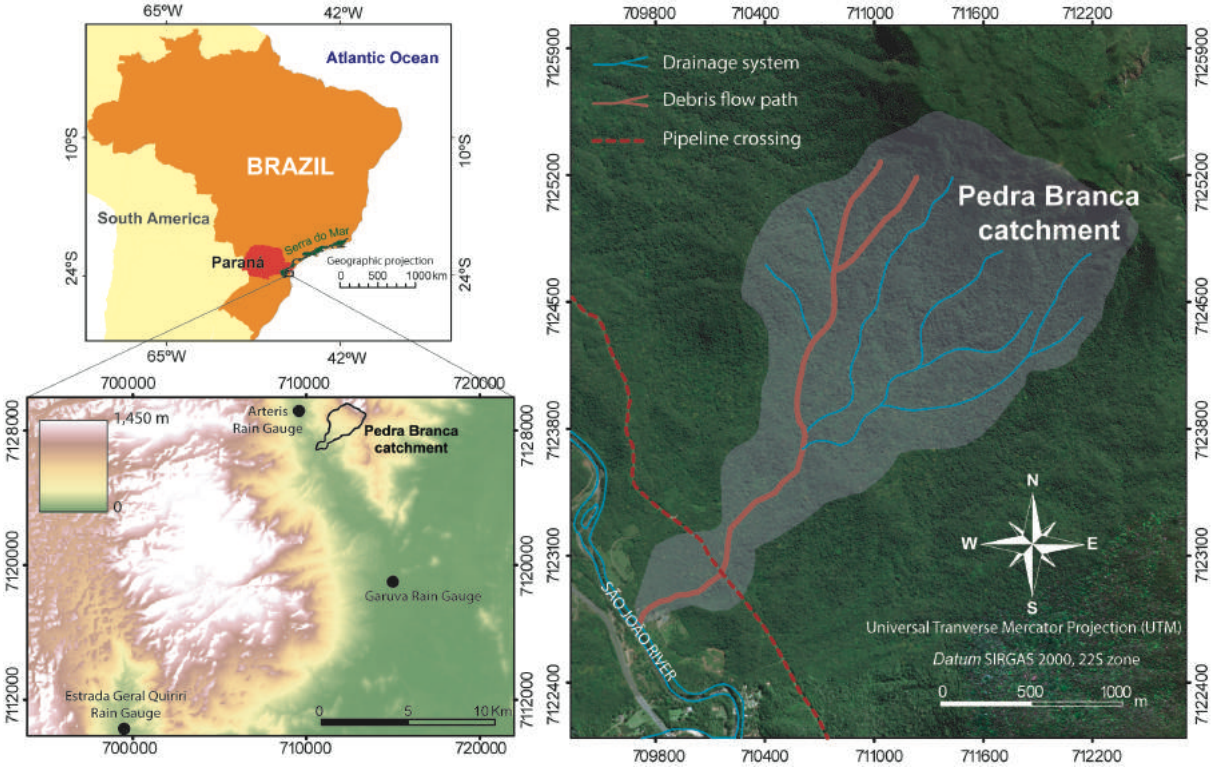

Figure 1: Pedra Branca catchment (right) in the municipality of Guaratuba, State of Paraná, Brazil. At the top left, the extension of the Serra do Mar mountain range. At the bottom left, the Digital Terrain Model (DTM) for the broader region of the catchment with the location of the three nearest rain gauges.

The February 2017 debris flow was initiated by shallow landslides in the headwaters' region. Three landslides were identified as the triggers of the event (highlighted in red in Fig. 2), from a total of 17 landslide scars mapped. For the sake of simplicity, merged scars were counted as one single scar. The debris flow affected oil pipelines

that cross the catchment (buried at a 1 m depth) and destroyed a small bridge and a farm located at the outlet region. An interview with one of the affected farmers describing the event is available as supplementary data. No casualties were reported.

Table 1: Pedra Branca's physiographic features. H_t is maximum amplitude, L_t is length of channels, A is watershed area, L_h is watershed length.

Parameter	Formulae	Value	Unit
Watershed area	-	3.43	km^2
Maximum elevation	-	1,100	m a.s.l.
Elevation at the outlet region	-	90	m a.s.l.
Average watershed slope	-	16.8	Degrees
Channel length	-	2,900	m
Slope at the initiation area	-	67 / 34	Percent / Degrees
Slope at the outlet region	-	7 / 4	Percent / Degrees
Average channel slope	-	18 / 10	Percent / Degrees
Drainage density	L_t / A	3	km km^{-2}
Relief Ratio	H_t / L_h	0.35	km km^{-1}
Melton Ratio (1)	H_t / $A^{-1/2}$	0.6	-

(1) Melton ratio is a morphometric parameter used to differentiate flood and debris-flow prone catchments. Debris-flow prone catchments generally have > 0.6 (Wilford et al. 2004).

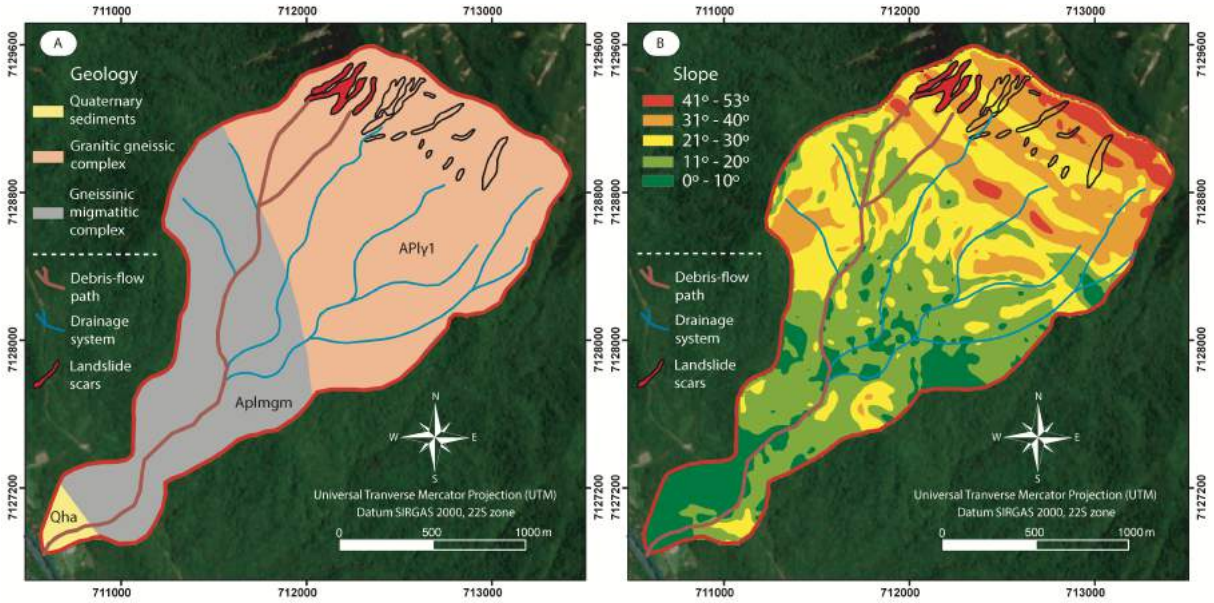

Figure 2: A) Geological map of the Pedra Branca catchment based on the 1:250,000 map (Folha Curitiba) made by the Geological Service of the State of Paraná (Mineropar). Qha – Quaternary fluvial sediments and alluvium. APlγ1 – Archean/Lower Proterozoic monzogranites, porphyritic and equigranular. APlmgm – Archean/Lower Proterozoic ophthalmic migmatites, with biotite gneiss paleossome. B) Slope map of the catchment based on a topographic map at a scale of 1:25,000. Landslide scars that triggered the debris flow are highlighted in red.

Material and methods

Forensic meteorological analysis

The rainfall analysis combined satellite and rain gauge data. The Geostationary Operational Environmental Satellite (GOES13) was used to characterize the start time and duration of the precipitation event, while intensity was retrieved from rain gauge measurements. The nearest rain gauge, located 1 km away from Pedra branca, is controlled by the private company Arteris - Litoral Sul, which provided hourly rainfall measurements for the month of February 2017 (Arteris Rain Gauge, Fig. 1). The other two rain gauges are part of the Brazilian rain gauge network and their measurements are freely available, provided by CEMADEN (Centro Nacional de Monitoramento e Alerta de Desastres Naturais 2020) and ANA (Agência Nacional de Águas 2020). The 'Garuva' rain gauge is located approximately 10 km southeastward of Pedra Branca catchment, while 'Estrada Geral Quiriri' is located 30 km southward (Fig. 1).

Forensic geomorphological analysis

Terrestrial and aerial investigation were carried out to characterize the physiography of the catchment after the debris flow. Field campaigns were conducted one and six months after the event (March and August, 2017) to characterize post-event geomorphological features and to acquire high-resolution aerial photographs of the debris-flow path using an Unmanned Aerial Vehicle (UAV).

Field observations were determinant in the identification of the sediment budget of the channel, aiding the assessment of the event's characteristics (a channelized, stony debris flow) and the movement dynamics in the catchment. On-channel deposits were assessed using cross-sections made along the Pedra Branca riverbed (available as supplementary material), which also depicted post-event channel width. Peak flow marks were documented, as well as estimated erosion depths, based on erosion marks and bedrock exposures. The measurements were made with the help of range finders, measuring tapes, rods and levels. A total of 28 cross-sections were surveyed at approximately every 120 m along the debris-flow route (Fig. 3).

The orthorectified aerial photographs further allowed the identification and delimitation of debris-accumulation areas along the channel, as well as the delimitation of entrainment areas along the riverbed and lateral slopes and banks. Sediment sources located at the headwaters (i.e., landslides) were identified and delimitated using non-orthorectified aerial photographs retrieved from the UAV survey. The drone DJI Phantom 3 was employed in the UAV survey, equipped with a camera with focal length of 3.61 mm and ground sampling distance (GSD) of 8.654 cm/pixel. Twenty-three (23) targets were used for georeferencing the orthophotos, which were processed with the

software PIX4D. The UAV overflight was done between August 28 and 30, 2017, in constant height of 200 m. The targets' coordinates were measured using a differential GPS (generating point presenting accuracy of 10 cm).

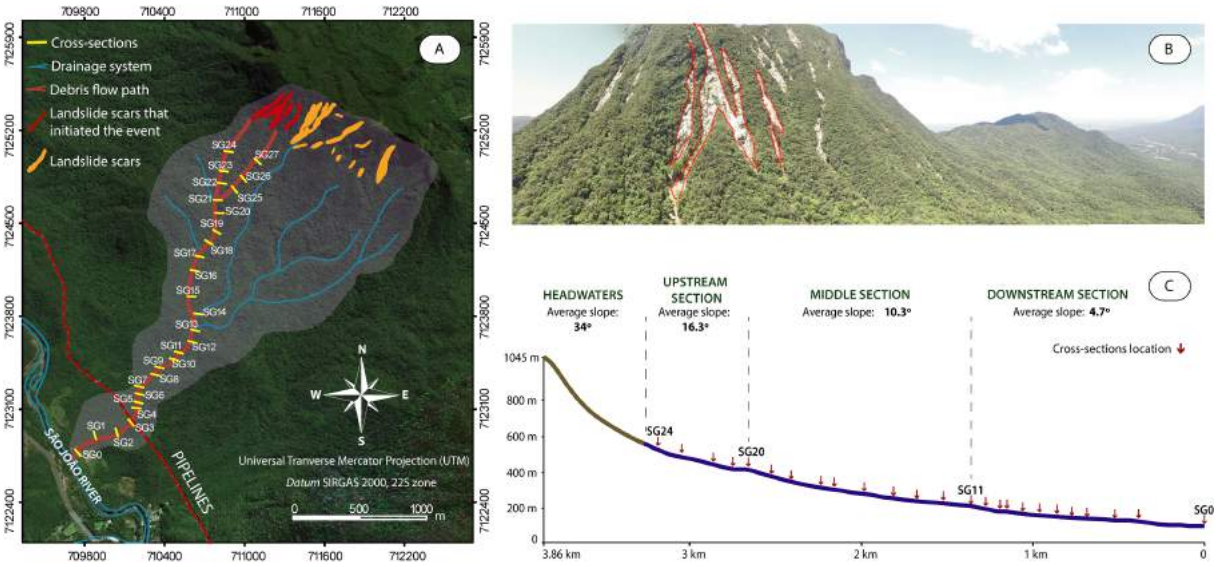

Figure 3: A) Location of the 28 cross-sections made along the debris-flow path. B) Overview of the headwaters' region of the catchment, highlighting the three landslide scars that initiated the debris flow. C) Longitudinal profile of Pedra Branca catchment with the tentative location of the cross-sections. Channel in blue and slopes in brown.

Magnitude estimation

The debris-flow magnitude was estimated based on the parameters obtained from the forensic analysis. The total volume (V_t) of the debris flow was calculated according to Jakob (2005a), being a mass balance of the landslides volume (V_i) that initiated the event, the volume of material entrained (V_e) by the flow and the volume deposited (V_d) along its path:

$$V_t = V_i + V_e - V_d \quad (1)$$

V_i was estimated using the equation:

$$V_i = A_i * e \quad (2)$$

Where A_i is the landslides area (m^2) and e the average depth of the landslides (1 m, estimated using the aerial photographs from the UAV survey), assuming that the totality of the material reached the channel.

The calculation of on-channel debris volume (V_d) is based on the areas of accumulation (A_d), delimitated with orthophotos, and on the average depth of the deposits (e_d) observed and depicted at the 28 cross-sections. In this study, Large Wood (logs with ≥10 cm in diameter and ≥1 m in length) is not individualized from other debris-types when estimating magnitude.

$$V_d = \sum (A_d * e_d) \quad (3)$$

The entrained volume (V_e) is based on the identification of erosional areas (A_e) and on the erosion depth (e_e) documented during field campaigns:

$V_{ero} = \sum (A_{ero} * e_{ero})$ (4)

At the intervals between cross-sections, average depth values of erosion and deposition were applied.

Peak discharge (Q_{max}) is calculated based on the equation described in Jakob (2005a) and Chen et al. (2007):

$Q_{max} = A_{max} * v_f$ (5)

Where A_{max} is the maximum cross-sectional area of the channel and v_f is the mean cross-sectional velocity during the time that the peak flow occurs. A_{max} is obtained from the 28 cross-sections and v_f is estimated according to the Manning-Strickler equation (6), traditional fluid-mechanics equation for Newtonian turbulent flows that considers the physiography of the river channel and can be suited to debris flows (Rickenmann 1999):

$v_f = \frac{1}{n} * H^{\frac{2}{3}} * S^{\frac{1}{2}}$ (6)

With H being the maximum flow height (m) measured in the field, S is the channel bed slope, and n is the Manning coefficient (0.07 $m^{1/2}s^{-1}$) for bedrock rivers in mountain regions (Arcement and Schneider 1989; Takahashi 2006). Furthermore, empirical equations from the literature are also employed in magnitude estimation. Based on sediment volume data collected in the Eastern Italian Alps, Marchi and D'Agostino (2004) suggest that the magnitude of a debris-flow event can be estimated according to the geomorphometric characteristics of a catchment, as per the equation:

$V = 65{,}000 * A^{1.35} * S^{1.7}$ (7)

Where A is the catchment area (km^2) and S the average channel slope (%). More recently, Marchi et al. (2019) updated equation 7 using a larger dataset and considering the severity of an event when estimating magnitude:

$V = K * A^{\gamma}$ (8)

With K (intercept) and γ (slope) representing the scaling parameters. Considering a moderate to large magnitude to the February 2017 event, the scaling parameters chosen to be assessed in this study are related, respectively, to the 50th, 98th and 99th percentile of the dataset presented in Marchi et al. (2019):

$V = (2620 \pm 60) * A^{0.67 \pm 0.02}$ (9)

$V = (52000 \pm 4000) * A^{0.94 \pm 0.04}$ (10)

$V = (77000 \pm 7000) * A^{1.01 \pm 0.06}$ (11)

Chang et al. (2011), based on 59 debris-flow prone catchments in Taiwan, found that the magnitude can be estimated by the equation:

$V = 0.023\ A_w + 0.064\ A_l + 13264.6\ GI - 1399.2\ D + 38.47\ CR$ (12)

With A_w being the watershed area (m^2), A_l the landslide area (m^2), GI is the geological index (dimensionless) based on Marchi and D'Agostino (2004), D the rainfall duration (h) and CR the rainfall intensity (mm). Due to the

uniform geology of Pedra Branca, comprised of crystalline rocks, the GI adopted is 0.5 (Marchi and D'Agostino 2004; Chang et al. 2011).

The equation presented in Kanji et al. (2007) considers that the magnitude (V) of a debris flow, assuming that these phenomena have a concentration of solids that vary from 40% to 80% (George and Iverson 2001), is a function of the concentration of solids per unit volume (c, equation 14) from Takahashi (1991), the catchment area (A, km^2) and the rainfall intensity one hour preceding the debris flow (I_1, mm):

$$V = 1000 \cdot c(1 - c) \cdot A \cdot I(1) \quad (13)$$

$$c = \rho(0) * tg\theta(\delta - \rho(0)) \cdot tg\phi - tg\theta(\quad) \quad (14)$$

Where θ is the average slope of the channel, ρ_0 is the specific weight of the slurry, δ is the granular material specific weight, and ϕ is the internal friction angle of the sediments. For simplicity, and since the physical parameters of the studied debris flow were not determined, c = 60% is adopted, as suggested by Takahashi (1991; 2006) for stony debris flows.

For further magnitude studies and empirical equations, we refer to Hungr et al. (1984), Rickenmann (1999), Takahashi (1991; 1992; 2006), Rickenmann and Koschini (2010), and Reid et al. (2016), among others.

Results

Forensic meteorological characterization

According to the testimonies of local farmers, the landslides that triggered the debris flow initiated between 2300 and 0000 UTC (20:00 and 21:00 Local Time – LT) on February 11. The landslides were triggered by an accumulated rainfall of 188 mm in 3 hours, with maximum registered intensity of 128 mm h^{-1}, according to the nearest rain gauge data (Arteris - Fig. 4). The rainfall ended at approximately 0700 UTC (4:00 LT) on February 12, assuming that a precipitation event ends when in six consecutive hours the accumulated rainfall is less than 4 mm (Chang et al. 2011). As the recorded antecedent rainfall for the preceding 10 days is estimated at around 88 mm, 23 mm of which (26%) in the last 48 hours before the event, soil water content was already significant.

Precipitation recorded by the rain gauges integrated to the Brazilian pluviometer network (Fig. 4) are notably lower than what the nearest rain gauge documented, suggesting that the extreme rainfall rates were mainly concentrated near the hillslopes of Pedra Branca as a result of orographic effect. The rain gauge 'Garuva' recorded 72.8 mm in 12 h, with a maximum intensity of 29.2 mm h^{-1}, while the rain gauge 'Estrada Geral Quiriri' barely recorded the event. Considering the difference in precipitation rates and the lag-time of 1 h between the rain gauges 'Arteris' and 'Garuva', it is suggested that the event developed from north to south and lost intensity during its trajectory.

The data from the GOES13 satellite indicates that the rainfall in the broader region of Pedra Branca initiated at

around 1800UTC (15:00 LT) on February 11 and ended at around 0700UTC (04:00 LT), as also shown by rain gauge data. Cloud tops reached 13-km altitude over the catchment, with high rainfall rates for about 4 hours, continuously. The return period for a rainfall with such intensity is estimated between 15 - 20 years, based on heavy-rainfall equations for the region (Back et al. 2011; Pereira Filho et al. 2018).

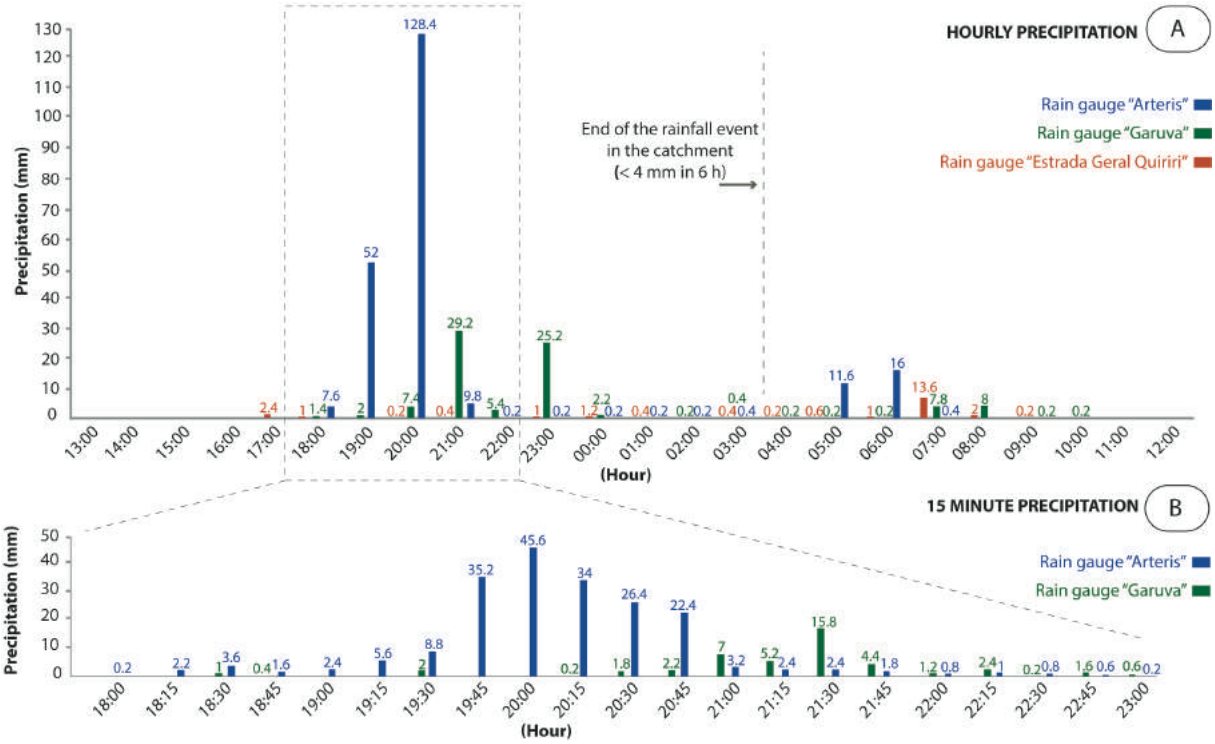

Figure 4: A) Hourly precipitation for February 11 and 12, 2017, according to the three nearest rain gauges. Rain gauge 'Arteris' is located 1 km from Pedra Branca catchment, while 'Garuva' and 'Estrada Geral Quiriri' are located at approximately 10 km and 30 km away, respectively. B) Precipitation recorded every 15 minutes by the rain gauges 'Arteris' and 'Garuva' between 18:00 LT (2100 UTC) and 23:00 (0200 UTC).

Forensic geomorphological analysis

The three shallow landslides that triggered the debris flow have their upgradient portions in moderate slopes (38% to 61%, or 21º to 31º), while those originated in steeper slopes (> 61%, or >31º) did not initiate an event in the other tributaries, probably due to thinner residual soils and colluvium (i.e., less material to generate a debris flow). The mobilized material by the three landslides are mainly residual soil and large wood, which suggest loss of suction as the initiation mechanism at the study area. The debris flow was initiated by first-time movements in the hillslopes (mapped in Fig. 3), but also carried material (colluvium) from previous landslides, accumulated at the upper portion of the channel.

The channelization of the material mobilized by the landslides contributed to a magnification of the erosional process, with a pronounced entrainment and scour of debris at the upstream section of the channel. Erosion of the channel bed, lateral slopes and banks by the debris flow progressively decreased towards the outlet region, ranging

from an average depth of 3 m at the upstream section to 0.3 m downstream. In bedrock exposed areas, erosion depth was assumed as 0 and the average depth between two sections was used in entrainment calculation, since no information about previous on-channel deposits or channel morphology are available. Bedrock exposed areas are mainly located in steep portions of the channel near the initiation area and in knickpoints.

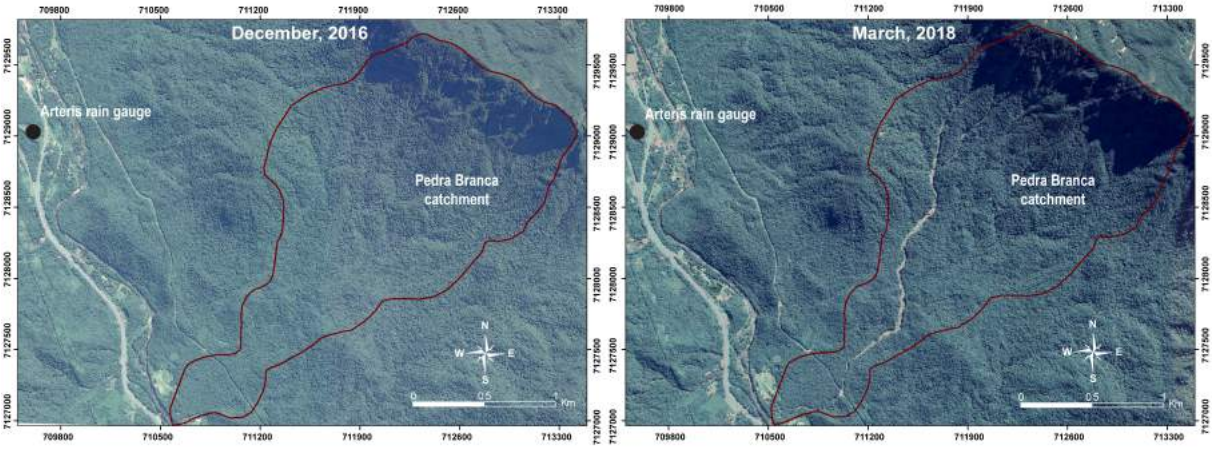

Figure 5: Before (left) and after (right) the debris-flow event at the Pedra Branca catchment. Aerial photographs from December 2016 and March 2018, from Google time-lapse. The location of the nearest rain gauge (Arteris) is indicated (Highway BR-376, km 676 +800 m).

On-channel debris at the upstream section (between SG20 and SG24 / SG27) consist mainly of large monzogranite boulders (2 to 5 m in diameter), deposited at the perimeter of the flow route or exhumed from colluvial deposits of the lateral slopes (Fig. 6A). On-channel debris accumulation becomes more frequent towards the catchment's outlet (Fig. 7C), with the largest volume of debris deposited at the middle portion of the channel (between SG11 and SG19, Fig. 6B) where the average slope is 18.2% (10.3º), i.e., within the range of deposition angles for channelized debris flows (from 14% to 21%) (Iverson et al. 2011). Debris deposition also occurs at the downstream portion of the catchment (SG0 to SG10), although with smaller-sized boulders (<2 m in diameter) and less voluminous deposits than at the middle portion (Fig. 6C). Recent on-channel debris deposits are easily identified from colluvial deposits due to the lack of pedogenetic evidences and the mixture of fresh wood and stony debris (Figure 6D).

Large wood (LW) deposition and accumulation, differently from stony debris, is more frequent at the downstream section of the channel (SG11 to SG0). At this section, the influence of LW in the debris-flow evolution is prominent, with evidences of LW jams that were broken by the flow passage (Fig. 7A). Debris dams (i.e., areas with intense debris deposition, blocking partially the flow) are observed along the channel and are in their majority clast supported with woody debris (Fig. 7B), often exhibiting reversely graded patterns. The occurrence of these dams indicates that the debris flow had multiple surges, which is confirmed by the affected farmers that report at least four surges.

Figure 6: A) Pronounced erosion and scour of channel bed is observed at the upstream section (SG23) – 1.8 m human profile for scaling. B) Intense accumulation of debris at the middle section (SG13) – in detail, a 1.75 m human profile for scaling. C) Accumulation of debris at the downstream section (SG6), with smaller sized-boulders than in the middle section - 1.75 m human profile for scaling. D) Reversely graded pattern observed in debris dams (SG5). E) Debouchment of the Pedra Branca river into the São João River, where flow height reached up to 2 m. F) São João river, which received sediments from the Pedra Branca debris flow (photo from August 2017).

The imbricated boulders along the channel's length and the intense debris accumulation along at the middle section of the channel suggest that the event started as a debris flow, evolving into a debris flood as channel slope decreased. At the outlet region, according to testimonies, the flow consisted mainly of muddy water (with sand, silt, clay) mixed with woody debris (Fig. 6E) and, minorly, by stony debris of up to 1 m. These characteristics indicate that in the final stages the event exhibited characteristics of a flash flood.

The average post-debris-flow width of the channel is ca. 20 m, ten times the previous average width (ca. 2 m) reported by testimonies (Fig. 5). No prominent alluvial fan is formed, due to narrow valley and discharge to the

larger São João river (Fig. 6E). At the São João river, large deposits of coarse sand are cobbles are accumulated near Pedra Branca outlet (Fig. 6F), as well as small to medium-sized boulders (< 1.5 m in diameters) on the river channel.

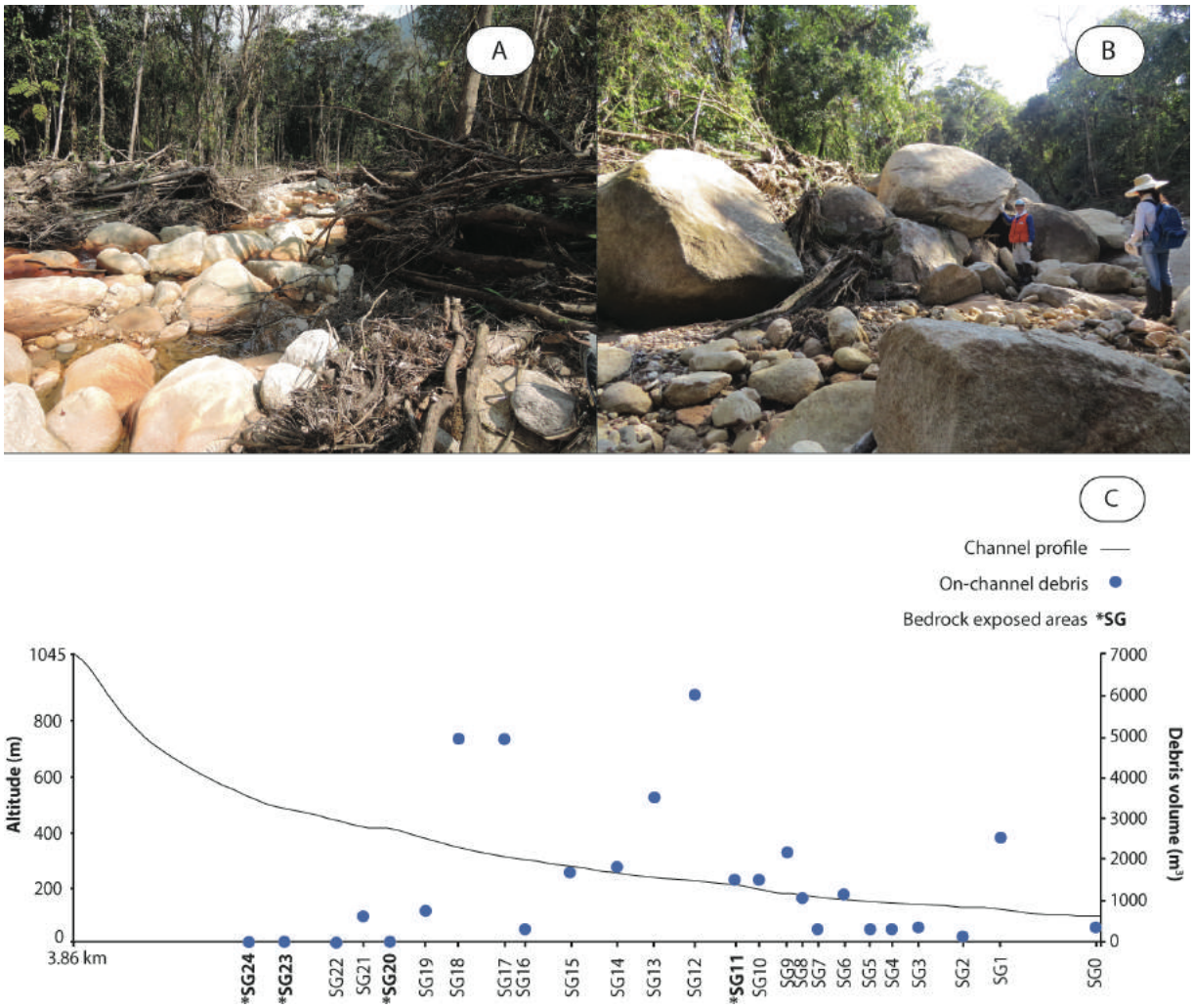

Figure 7: A) Large wood forming a jam that was later broken by the flow's passage (SG1). B) Mixture of woody and stony debris and formation of debris dams (SG12) – 1.75 m human profile for scaling. C) Plot showing the Pedra Branca channel profile and the volume of deposited debris along the debris flow route. Debris deposition is higher at the middle section of the channel (SG19 to SG11).

The mapping of erosional and depositional areas along the Pedra Branca channel is shown in Figure 8, based on the orthophotos. Even though debris deposition generally occurs in areas with gentler slope (Fig. 9A), a direct correlation between these two factors is not observed, with a very weak Spearman correlation coefficient (0.025) and regression line with very low R^2 (0.002) when their relationship is analyzed (Fig. 9C). Debris deposition, therefore, might be influenced by other factors, such as valley width, presence of obstacles and availability of coarse material itself, which can further be related to a less voluminous deposition in lower reaches of the channel with low slope than at intermediate reaches.

Erosion depth, on the other hand, shows a positive correlation with slope, being deeper near steeper portions of the channel (Fig. 9B). Excluding areas where bedrock exposure is observed, a correlation between slope and erosion depth shows a weak/moderate positive spearman coefficient (0.39) and a regression line with a weak to moderate R^2 (0.3149) (Fig. 9D). Hence, erosion is moderately influenced by slope, which can further be associated with a higher momentum of the flow's passage in steeper reaches of the channel. The exclusion of bedrock exposed reaches in the correlation is due to a different incision dynamic than at alluvial-colluvial reaches.

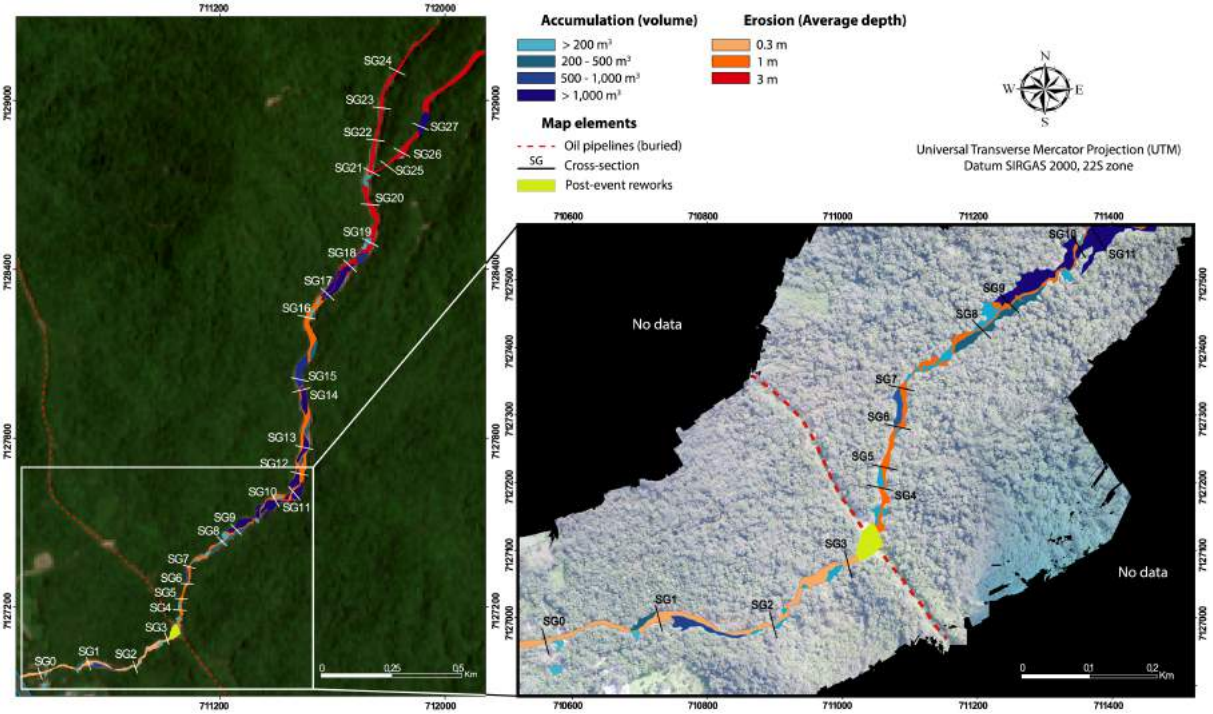

Figure 8: Mapping of entrainment and deposition areas based on the orthophotos acquired using UAV. Areas in shades of blue represent debris-accumulation areas and areas in shades of red represent entrainment areas.

The distribution of maximum grain size (D_{90}) of debris along the debris-flow path shows that debris size decreased by approximately 80% along its trajectory (Fig. 9E). Sharp reductions in D_{90} along the channel are related to regions where intense debris deposition is observed. Flow heights are generally higher in regions downstream to knickpoints in the channel (between SG4 and SG5, SG10 and SG11, SG18 and 19), with the debris flow reaching a peak height of 7 m at the region of the cross-section SG9 (Fig. 9F). At the debouchment into the larger São João river, flow heights were up to 2 m (Fig. 9F). Flow height can be affected by areas with intense debris accumulation, which can partially block the flow and raise the flow level. To minimize the uncertainties related to forensic discharge estimations, we documented flow heights in areas that were not directly affected by the intense accumulation of stony and woody debris.

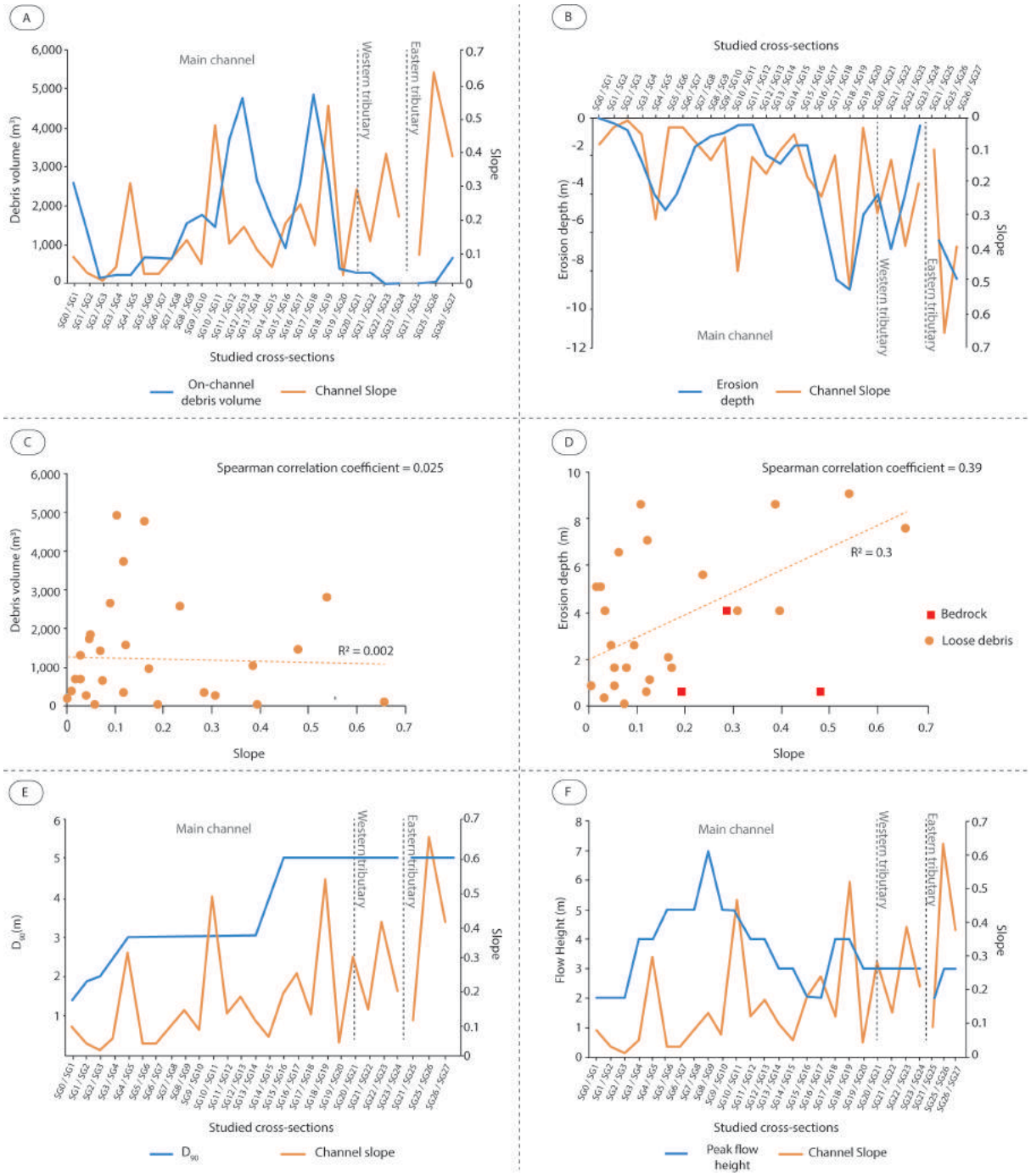

Figure 9: A) Distribution of on-channel debris volume along the debris flow path in relation to channel slope B) Erosion depth distribution along the debris flow path in relation to channel slope C) Scatterplot showing the relationship between on-channel debris volume and channel slope. D) Scatterplot showing the relationship between erosion depth and channel slope. Bedrock and loose debris refer to the on-channel material post-event. E) Maximum debris size (D_{90}) distribution along the debris flow path in relation to channel slope (measured between every two cross-sections). F) Peak flow height distribution in relation to channel slope.

Magnitude estimation

The total volume of the debris flow (V_t) is estimated at approximately 120,195 m^3, based on the mapping of entrainment and deposition areas (Fig. 7) and on the landslides that initiated the event. Volume entrained by the flow (V_e) is estimated at 121,037 m^3, while the volume of debris deposited along the debris flow path (V_d)

accumulates to 36,688 m^3. The table with the measurements used in the calculation of entrained and deposited volumes is available as a supplementary material.

The three landslides that initiated the event contributed with 35,846 m^3 of earth material. The largest landslide scar contributed with 22,497 m^3, while the other two contributed with 7,573 m^3 and 5,776 m^3, assuming an average depth of 1 m and that the totality of the material reached the channel. Despite the uncertainties associated with erosion depth at the study area, due to the unknown channel morphology before the event, it is evident that entrainment significantly increased the total magnitude of the process, representing more than 75% of earth material input.

Moreover, subjectivity and human error might decrease accuracy and is challenging to be considered during calculations. Nonetheless, our estimations suggest that the February 2017 debris flow had a large magnitude, within the range of the size-class 5 ($10^5 – 10^6$ m^3) proposed by Jakob (2005b). Size-class 5 debris flows can destroy parts of villages and infrastructures, destroy forest of up 2 km^2 and block creeks and rivers (Jakob, 2005b).

Comparing our field-based magnitude estimates with the results using empirical equations (Table 2), the equation from Marchi et al. (2019) is the best-fit for the study area. While using the scaling parameters of the 50^{th} and 99^{th} percentile considerably underestimated (ca. 5,983 m^3, 95% less than our estimates) and overestimated (ca. 267,385, 121% more) the magnitude, the 98^{th} percentile resulted in an approximate magnitude (ca. 143,645 m^3, 18% more) when considering the lower error threshold.

The equation based on Taiwanese debris-flow cases, from Chang et al. (2001), also provided fairly good results, estimating the magnitude at ca. 91,000 m^3, which is 24% less than the value calculated based on *in-situ* data. Marchi and D'Agostino (2004) equation performed similarly to the 50^{th} percentile of the updated version of the equation presented in Marchi et al. (2019), also underestimating the magnitude (18,600 m^3, 84% less than our estimations). the equations shown in Kanji et al. (2007) highly overestimated the magnitude (439,040 m^3, 265% more than our estimations).

Highest discharge and velocity rates are observed between cross-sections SG18 and SG19 (2,146.7 m^3 s^{-1} and 29.04 m s^{-1}, respectively), where channel slope is the steepest and cross-sectional area one of the largest. Discharge, in general, is higher at the immediate region downstream to the initiation area (SG24 to SG22 and SG27 to SG25) and at the confluency of the two tributaries (Between SG21 to SG17), progressively decreasing towards the outlet region (Fig. 10). Velocity rate patterns are similar to the discharge (Fig. 10). The table with the measurements used in the discharge and velocity calculation is also available as a supplementary material.

Table 2: Magnitude of the February 2017 debris flow, estimated according to empirical equations and the forensic geomorphological characterization.

Author	Magnitude
Marchi and D'Agostino (2004)	18,600 m^3
Marchi et al. (2019) – 50th percentile	5,983 ± 290 m^3
Marchi et al. (2019) – 98th percentile	165,645 ± 22,000 m^3
Marchi et al. (2019) – 99th percentile	267,385 ± 46,000 m^3
Kanji et al. (2007)	439,040 m^3
Chang et al. (2011)	90,851 m^3
This study	120,195 m^3

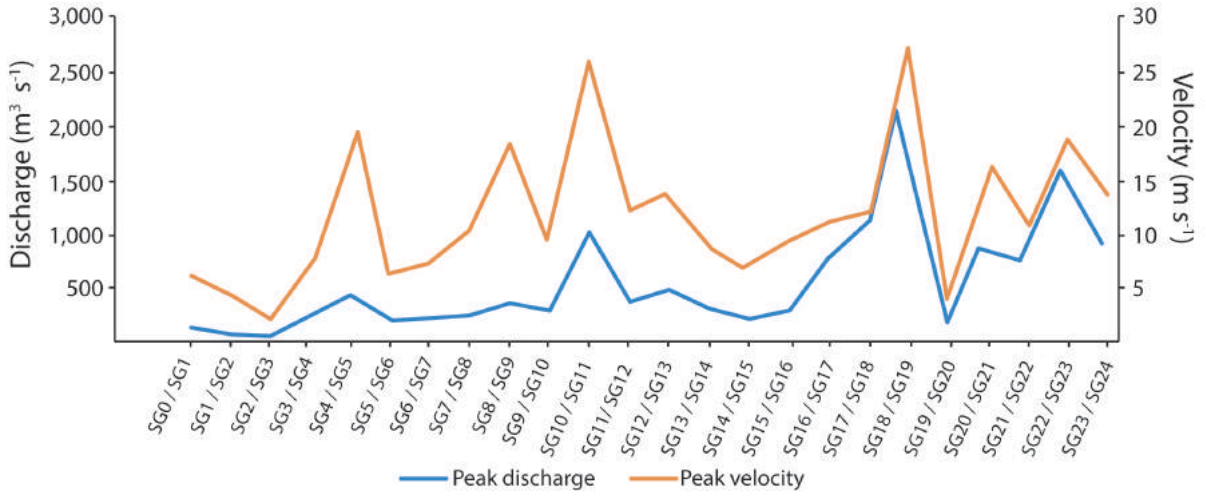

Figure 10: Discharge and flow velocity pattern along the debris flow path.

At the region of the oil pipelines (SG3 and SG4), discharge was approximately 228 m^3 s^{-1} and flow velocity 7.9 m s^{-1}, which can be associated to their preservation due to the relatively weaker and slower flow at that region. It is important to point out, however, that the concurrence of debris flows and debris/flash floods might increase the uncertainty over peak discharge estimations, due to an alteration of the channel cross-section stability with the passage of large sediment volume (Amponsah et al. 2016; Destro et al. 2018).

Discussion

The available rainfall data suggest that the high-intensity precipitation was sharply localized over Pedra Branca hillslopes and had a short duration. Rainfall estimations, however, might be underestimated due to the location of the rain gauges at the valley and not at the hillslopes, where landslides initiate. The estimated return period of the high-intensity rainfall in the region, combined with the large amount of mobilizable on-channel debris at Pedra Branca (ca. 37,000 m^3), suggests that new high magnitude debris flows can potentially occur in the region in the near future (next one or two decades).

The debris flow was triggered by three large landslides, which initiating mechanism is interpreted as loss of suction due to a local rise in the water table by rainfall infiltration. Loss of suction is a common initiation factor at crystalline areas at the Serra do Mar mountain range (Wolle and Hachich 1989; Lacerda 2007) and is attributed to saturation levels reaching depths below the root zone of the soil. Soil saturation level at the hillslope region was already significant due to the antecedent rainfall (23 mm in the previous 48 h) and the sudden rise in the water table, as a result of the high rainfall rates (128 mm h^{-1}), led to slope failure.

Debris flows at Serra do Mar are generally triggered by high precipitation rates accumulated in 72 h, with peak rainfall of > 60 mm h^{-1} (Kanji et al. 1997). The lack of past debris-flow data for the Pedra Branca catchment and the surrounding region is a challenge for the creation of a site-specific rainfall thresholds that could support the development of an Early Warning System (EWS) in the region. Consequently, thresholds developed for different parts of Serra do Mar could preliminarily be adapted and updated for Pedra Branca, such as the one from Kanji et al. (1997). A constant update of these rainfall thresholds is necessary, especially considering the projected increase in the frequency of extreme rainfall events for the south and southeast of Brazil (Marengo et al. 2021) and that these equations were created more than 20 years ago.

Debris-flow initiation is not controlled solely by rainfall, as it also depends on debris supply and recharge rate, which influences the magnitude and the frequency of new events in a catchment. The debris flow in the Pedra Branca catchment had a magnitude of approximately 120,000 m^3, thus a large debris flow. According to Jakob (2005b), such magnitude for a boulder-rich debris flows is atypical, although the statement could be biased due to the general lack of magnitude studies worldwide, especially in mountain areas where debris-flow studies are still incipient. At Serra do Mar, based on the few available magnitude estimates (e.g., Kanji et al. 2007; Kobiyama et al. 2015), 10^5 m^3 debris flows are what is usually reported, probably also due to a bias towards reporting and characterizing only larger events (such as the present study) and the lack of studies aiming at specifically estimating debris-flow magnitude.

The most-suited empirical equation for our study area was the one based on the 98th percentile of the cases analyzed by Marchi et al. (2019) in the Italian alps, indicating that a debris flow with the same magnitude as Pedra Branca has a ca. 2% probability to occur in that region. This could also suggest that at Serra do Mar large debris flows occur less often than smaller ones that tend to go unreported, but such statement is challenging considering the large dataset necessary to establish magnitude-frequency relationships and the differences in geological/geomorphological settings that affect debris-flow dynamics. More magnitude studies at Serra do Mar are recommended and necessary.

We suggest, therefore, that the equations from Marchi et al. (2019) should be tested in future events or in back-analysis studies in Brazil, to attest further its efficacy in representing debris-flow magnitudes in different mountainous areas. Even though the equation shown in Kanji et al. (2007) was created for a catchment at Serra do Mar (based on the 1994 debris flow at Rio das Pedras catchment, in Cubatão), it highly overestimated the magnitude of the Pedra Branca debris flow. This overestimation can be related to the equation's heavy reliance on the physical parameters of the debris flow, which was not tested in our study.

The equation by Marchi et al. (2019) introduces scaling parameters that amplifies the application of the equation when compared to the one presented in Marchi and D'Agostino (2004), which are adjusted according to different debris-flow scenarios and, consequently, can be applied to a wider variety of regions. The simple input parameters are another advantage, which favors it application on mountain regions where few information is available. Moreover, the equation from Chang et al. (2011) also provided approximate results compared to our estimates. While it underestimated the event (24% less than the forensic-based magnitude), the consideration of different parameters that influence the dynamics of a landslide-triggered debris flows (e.g., geology, rainfall, landslide area) can potentially be adequate for Serra do Mar, when a landslide inventory and rainfall data is available.

Forensic geomorphological analyses are fundamental for an accurate depiction of sediment mobilization in a catchment, supporting magnitude estimations and countermeasures dimensioning. Studies that characterize the magnitude of recent debris-flow events are key to support regional scale studies, since they describe how a debris flow develops in a catchment, which characteristics are potential driving factors and quantify the hazard that similar catchments might be susceptible to.

The February 2017 event at the Pedra Branca catchment started as a debris flow at the upper portions of the catchment and, as channel slope decreased, it evolved into a debris flood and, at later stages, a flash flood as it progressed towards the outlet region. This evolution can be attributed to the progressive deposition of debris (especially large rock boulders) along the flow route, especially at the middle portion of the channel. The progressive decrease in discharge and flow velocity can also be attributed to the deposition of material along the channel, a direct result of gentler channel slope from the middle section on and the long length of the channel (2,900 m), decreasing the flow momentum.

Flow momentum decrease is also associated with the entrainment potential of the debris flow, with a progressive reduction in erosion depth towards the debouchment area. Even though the estimation of eroded material is affected by larger uncertainties than the landslides and on-channel debris volume, the debris flow's sediment yield came mostly from the entrainment of material from channel bed and lateral banks, which is a common

characteristic of large debris flows worldwide (e.g., Marchi et al. 2009; Gabet and Sternberg 2008; Bennet et al. 2013; Shen et al. 2020).

Despite the subjectivities and uncertainties related to the forensic-based estimation, it is the most accurate way to describe the hydrodynamic evolution of a debris flow in a channel and is the base for simulation of debris flows using physically-based models. It is also an important pathway for the establishment of F-M relationships, which, so far, are limited to a few selected regions in the world due to the long period of data required to construct meaningful relationships (Stoffel 2010; Huggel et al. 2012). The establishment of magnitude and frequency of debris-flow events is fundamental for accurate risk management.

Several other recent, deadly, debris flows have occurred at Serra do Mar that could have been mitigated if F-M studies and EWS were available, such as at Itaoca (State of São Paulo) in January 2014[3] and in the Teresópolis region[4] (State of Rio de Janeiro) in January 2011. These examples highlight the importance of sediment mobilization analysis in a catchment as well as the need for magnitude studies to quantify the potential damages that could result from debris-flow events and the frequency at which debris flows are expected to occur at Serra do Mar.

Studies on debris-flow frequency are recommended and necessary. Cosmogenic, Optically-Stimulated-Luminescence (OSL) and radiocarbon dating of colluvial deposits are techniques that can be applied in frequency estimation of mass-wasting events in tropical and subtropical regions (Lang et al. 1999; Pánek 2015). Radiocarbon dating, due to lower costs and simpler sampling when compared to the other dating techniques (Pánek 2015), should be attempted in the future at the Pedra Branca catchment, as well in high-hazard catchments at Serra do Mar. The large amount of mobilized LW and organic material by debris flows in the region provide reliable results (Lang et al. 1999). LW can contribute to increase debris-flow hazard (Lucía et al., 2015; Rickenmann, 2016) and, therefore, studies that consider LW mobilization in the densely forested catchments of Serra do Mar are encouraged.

Conclusion

This study characterized a debris flow that occurred at Serra do Mar in February 2017. The event was triggered by a 188 mm rainfall in 3 hours (128 mm h^{-1} maximum intensity), with a return period of 15 years. The debris flow had a total magnitude of 120,195 m^3, with peak discharge of 2,146.7 m^3 s^{-1} and peak velocity of 26.5 m s^{-1}. It was, therefore, a large magnitude stony debris flow triggered by a short to moderate return period precipitation.

[3] Triggered by an accumulated rainfall of 210 mm in two hours, destroying houses and public infrastructures. 25 casualties were reported (Gramani and Martins 2016)

[4] Considered the 8th worst landslide event in world history by the United Nations (Rosi et al. 2019)

The debris flow dammed parts of the Pedra Branca channel, incisively eroded parts of the forest along its path and damaged infrastructures.

The documentation of recent debris-flow events, with magnitude and hydrogeomorphic dynamics characterization, is extremely important for Serra do Mar, where debris-flow studies are still scarce. Magnitude studies for a catchment are important, since they are a pathway for the development of Frequency-Magnitude relationships that can support accurate hazard assessments and reliable monitoring programs. Moreover, the mapping of debris-flow prone catchments throughout Serra do Mar is necessary to identify those that represent greater hazard and to prioritize the implementation of monitoring programs and EWSs.

References

Agência Nacional de Águas – ANA. (2020). Rain gauges "Garuva - 420580301A" and "Estrada Geral Quiriri - 420580302A". Available at http://www.snirh.gov.br/hidroweb/serieshistoricas.

Amponsah W, Marchi L, Zoccatelli D, Boni G, Cavalli M, Comiti F, Crema S, Lucía A, Marra F, Borga M (2016) Hydrometeorological characterization of a flash flood associated with major geomorphic effects: assessment of peak discharge uncertainties and analysis of the runoff response. J Hydrometeorol 17(12): 3063–3077.

Arcement GJ, Schneider VR (1989) Guide for Selecting Manning's Roughness Coefficients for Natural Channels and Flood Plains. U. S. Geological Survey Water-Supply Paper 2339.

Back AJ, Henn JA, Oliveira JLR (2011) Heavy rainfall equations for Santa Catarina, Brazil. Rev Bras Ci Solo 35: 2127-2134.

Beguería S, Van Asch T, Malet J, Gröndahl S (2009) A GIS-based numerical model for simulating the kinematics of mud and debris flows over complex terrain. Nat Hazard Earth Sys 9(6): 1897-1909.

Beniston M (2009) Trends in joint quantiles of temperature and precipitation in Europe since 1901 and projected for 2100. Geophys Res Lett 36: L07707.

Bennett G, Molnar P, McArdell B, Schlunegger F, Burlando P (2013) Patterns and controls of sediment production, transfer and yield in the Illgraben. Geomorphology 188: 68-82

Berger C, McArdell BW, Schlunegger F (2011) Direct measurement of channel erosion by debris flows, Illgraben, Switzerland. J Geophys Res 116: F01002.

Bianco G, Franzi L (2000) Estimation of debris-flow volumes from storm events. In: Wieczorek GF, Naeser ND (Ed) Debris-flow Hazards Mitigation: Mechanics, Prediction and Assessment. Balkema, Rotterdam, pp. 441-448.

Borga M, Stoffel M, Marchi L, Marra F, Jakob M (2014) Hydrogeomorphic response to extreme rainfall in headwater systems: Flash floods and debris flows. J Hydrol 518:194–205.

Centro Nacional de Monitoramento e Alerta de Desastres Naturais – Cemaden. (2020). Rain gauges "Garuva - 420580301A" and "Estrada Geral Quiriri - 420580302A". Available at http://www.cemaden.gov.br/mapainterativo/

Chang C, Lin P, Tsai C (2011) Estimation of sediment volume of debris flow caused by extreme rainfall in Taiwan. Eng Geol 123(1-2):83-90.

Chen NS, Yue ZQ, Cui P (2007) A rational method for estimating maximum discharge of a landslide- induced debris flow: a case study from south western China. Geomorphology 84:44–58.

Church M, Jakob M (2020) What Is a Debris Flood? Water Resour Res 56: e2020WR027144

Destro E, Amponsah W, Nikolopoulos E, Marchi L, Marra F, Zoccatelli D, Borga M. (2018). Coupled prediction of flash flood response and debris flow occurrence: Application on an alpine extreme flood event. J Hydrol 558: 225-237.

de Haas T, Densmore AL (2019) Debris-flow volume quantile prediction from catchment morphometry. Geology 47:791–794.

Gabet E, Sternberg P (2008) The effects of vegetative ash on infiltration capacity, sediment transport, and the generation of progressively bulked debris flows. Geomorphology 101(4): 666-673.

Gaume E, Borga M (2008) Post-flood field investigations in upland catchments after major flash floods: proposal of a methodology and illustrations. J Flood Risk Manag 1(4):175–189.

Giorgi F, Im ES, Coppola E, Diffenbaugh NS, Gao XJ, Mariotti L, Shi Y (2011). Higher hydroclimatic intensity with global warming. J Climate 24:5309–5324.

Gramani MF, Martins VTS (2016) Debris flows occurrence by intense rains on January 13, 2014 at Itaoca City, São Paulo, Brazil: impacts and field observations. Int Symposium Landslides, Napoli, Italy, 8 p.

Gregoretti C, Degetto M, Bernard M, Boreggio M (2018) The Debris Flow Occurred at Ru Secco Creek, Venetian Dolomites, on 4 August 2015: Analysis of the Phenomenon, Its Characteristics and Reproduction by Models. Front Earth Sci 6:80.

Huggel C, Clague JJ, Korup O (2012) Is climate change responsible for changing landslide activity in high mountains? Earth Surf Proc Landf 37: 77-91

Hungr O, Morgan GC, Kellerhals R (1984) Quantitative analysis of debris torrent hazards for design of remedial measures. Can Geotech J 21:663–677.

Hungr O, Leroueil S, Picarelli L (2014) The Varnes classification of landslide types, an update. Landslides 11(2):167–194

Iverson R (2000) Landslide triggering by rain infiltration. Water Resour Res 36(7):1897-1910.

Iverson RM, Reid ME, Logan M, LaHusen RG, Godt JW, Griswold JP (2011) Positive feedback and momentum growth during debris-flow entrainment of wet bed sediment. Nat geosci 4:116-121.

Jakob M (2005a) Debris-flow hazard analysis. In: Jakob M, Hungr O (Ed) Debris-Flow Hazards and Related Phenomena. Springer-Verlag, Berlin, pp. 411–443.

Jakob M (2005b) A size classification for debris flows. Eng Geol 79:151–161.

Kanji MA, Cruz PT, Massad F, Araujo FHA (1997) Basic and Common Characteristics of Debris Flows. Proc 2nd Pan Am Symposium, Rio de Janeiro, v. 10, p. 223-231.

Kanji MA, Cruz PT, Massad F (2007) Debris flow affecting the Cubatão oil refinery, Brazil. Landslides 5(1):71-82.

Kean JW, McCoy SW, Tucker GE, Staley DM, Coe JA (2013) Runoff-generated debris flows: Observations and modeling of surge initiation, magnitude, and frequency. J Geophys Res: Earth Surf 118:2190–2207

Kobiyama M, Michel G, Engster E, Paixão M (2015) Historical analyses of debris flow disaster occurrences and of their scientific investigation in Brazil. Labor e Engenho 9(4):76.

Kronfellner-Kraus G (1985) Quantitative estimation of torrent erosion. Int Symposium Erosion Debris Flow Dis Prev, Tsukuba, Japan, pp. 107–110.

Lacerda W (2007) Landslide initiation in saprolite and colluvium in southern Brazil: Field and laboratory observations. Geomorphology 87(3): 104-119.

Lang A, Moya J, Corominas J, Schrott L, Dikau R (1999) Classic and new dating methods for assessing the temporal occurrence of mass movements. Geomorphology 30(1-2):33-52.

Liu KF, Li HC, Hsu YC (2009) Debris flow hazard assessment with numerical simulation. Nat Hazards 49:137-161.

Lucía A, Comiti F, Borga M, Cavalli M, Marchi L (2015) Dynamics of large wood during a flash flood in two mountain catchments. Nat Hazards Earth Syst Sci 15:1741–1755.

Lucía A, Schwientek M, Eberle J, Zarfl C (2018) Planform changes and large wood dynamics in two torrents during a severe flash flood in Braunsbach, Germany 2016. Sci Total Environ 640-641:315-326.

Luna B, Remaître A, van Asch T, Malet J, van Westen C (2012) Analysis of debris flow behavior with a one-dimensional run-out model incorporating entrainment. Eng Geol 128:63-75.

Maack R (2002) Geografia física do Estado do Paraná. Curitiba, Imprensa Oficial, 440p.

Marchi L, D'Agostino V (2004) Estimation of debris-flow magnitude in the Eastern Italian Alps. Earth Surf Process Landf 29(2): 207-220.

Marchi L, Cavalli M, Sangati M, Borga M (2009) Hydrometeorological controls and erosive response of an extreme alpine debris flow. Hydrol Process 23(19): 2714-2727.

Marchi L, Brunetti M, Cavalli M, Crema S (2019) Debris-flow volumes in northeastern Italy: Relationship with drainage area and size probability. Earth Surf Process Landf 44(4): 933-943.

Marengo J, Camarinha P, Alves L, Diniz F, Betts R (2021) Extreme Rainfall and Hydro-Geo-Meteorological Disaster Risk in 1.5, 2.0, and 4.0°C Global Warming Scenarios: An Analysis for Brazil. Front Clim 3

Massad F (2002) Corridas de massas geradas por escorregamentos de terra: relação entre a área deslizada e a intensidade de chuva. In: XII Congresso Brasileiro de Mecânica dos Solos e Engenharia Geotécnica. São Paulo, São Paulo.

Milne F (2008) Topographic and material controls on the Scottish debris flow geohazard. Thesis, University of Dundee

Mocochinski AY, Scheer MB (2014) Campos De Altitude Na Serra Do Mar Paranaense: Aspectos Florísticos. Floresta 38(4):625–640.

Pánek T (2014) Recent progress in landslide dating. Progress in Physical Geography: Earth and Environment 39(2):168-198.

Pak J, Lee J (2008) A Statistical sediment yield prediction model incorporating the effect of fires and subsequent storm events. J Am Water Resour Ass 44(3):689-699.

Pereira Filho AJ, Vemado F, Reis FAGV, Giordano LC, Cerri RI, Santos CC, Lopes ESS, Gramani MF, Ogura AT, Zaine JE, Cerri LES, Augusto Filho O, D'Affonseca FM, Amaral CS (2018) A Step towards Integrating CMORPH Precipitation Estimation with Rain Gauge Measurements. Adv in Meteorol 2018:1-24.

Petley D (2012) Global patterns of loss of life from landslides. Geology 40:927-930.

Reid ME, Coe JA, Dianne LB (2016) Forecasting inundation from debris flows that grows volumetrically during travel, with application to the Oregon Coast Range, USA. Geomorphology 273:396–411.

Rickenmann D (1999) Empirical relationships for debris flows. Nat Hazards 19(1):47-77.

Rickenmann D, Zimmermann M (1993) The 1987 debris flows in Switzerland: documentation and analysis. Geomorphology 8:175 - 189.

Rickenmann D, Koschni A (2010) Sediment loads due to fluvial transport and debris flows during the 2005 flood events in Switzerland. Hydrol Process 24(8): 993–1007.

Rickenmann D (2016) Methods for the quantitative assessment of channel processes in torrents (steep streams). CRC Press, Taylor and Francis Group, Leiden, Netherlands.

Rosi A, Canavesi V, Segoni S, Dias Nery T, Catani F, Casagli N (2019) Landslides in the Mountain Region of Rio de Janeiro: A Proposal for the Semi-Automated Definition of Multiple Rainfall Thresholds. Geosciences 9:203.

Santi PM, Dewolfe VG, Higgins JD, Cannon SH, Gartner JE (2008) Sources of debris flow material in burned areas. Geomorphology 96(3–4):310–321.

Santi P (2014) Precision and accuracy in debris-flow volume measurement. Environ Eng Geosci 20(4):349-359.

Shen P, Zhang L, Wong H, Peng D, Zhou S, Zhang S, Chen C (2020) Debris flow enlargement from entrainment: A case study for comparison of three entrainment models. Eng Geol 270: 105581.

Steeb N, Rickenmann D, Badoux A, Rickli C, ScheWaldner P (2017) Large wood recruitment processes and transported volumes in Swiss mountain streams during the extreme flood of August 2005. Geomorphology 279:112–127.

Stoffel M (2010) Magnitude–frequency relationships of debris flows - A case study based on field surveys and tree-ring records. Geomorphology 116: 67-76.

Stoffel M, Huggel C (2012) Effects of climate change on mass movements in mountain environments. Progress in Physical Geography 36:421–439.

Surian N, Righini M, Lucía A, Nardi L, Amponsah W, Benvenuti M, Borga M, Cavalli M, Comiti F, Marchi L, Rinaldi M, Viero A (2016) Channel response to extreme floods: insights on controlling factors from six mountain rivers in northern Apennines, Italy. Geomorphology 272: 78-91.

Tabarelli M, Pinto L, Silva J, Hirota M, Bedê L (2005) Challenges and opportunities for biodiversity conservation in the Brazilian Atlantic forest. Conserv Biol 19(3):695–700.

Takahashi T (1991) Debris Flow. A.A. Balkema, Rotterdam.

Takahashi T, Nakagawa H, Harada, T, Yamashiki Y (1992) Routing Debris flows with particle segregation. J Hydraul Eng 118:1490-1507.

Takahashi T (2006) Debris Flows: Mechanics, Prediction and Countermeasures. Taylor and Francis, Balkema, Leiden.

Takei A (1984) Interdependence of sediment budget between individual torrents and a river-system. Proc Int Symp INTERPRAEVENT, Villach, Austria, 2:35–48.

Tang C, Rengers N, van Asch T, Yang Y, Wang G (2011) Triggering conditions and depositional characteristics of a disastrous debris flow event in Zhouqu city, Gansu Province, northwestern China. Nat Hazards Earth Syst Sci 11(11): 2903-2912.

Teixeira MS, Satyamurty P (2011) Trends in the Frequency of Intense Precipitation Events in Southern and Southeastern Brazil during 1960–2004. J Climate 24: 1913-1921.

Varnes DJ (1978) Slope movement types and processes. In: Schuster RL, Krizek RJ (Eds) Special report 176: landslides: analysis and control. Transportation and Road Research Board, National Academy of Science, Washington DC, pp 11–33.

Vieira B, Gramani M (2015) Serra do Mar: The Most "Tormented" Relief in Brazil. In: Migon, P (Ed) World Geomorphological Landscapes. Springer, Berlin, pp. 285-297.

Westra S, Fowler H, Evans J, Alexander L, Berg P, Johnson F, Kendon E, Lenderink G, Roberts N (2014) Future changes to the intensity and frequency of short-duration extreme rainfall. Rev Geophys 52: 522-555

Wilford DJ, Sakals ME, Innes JL, Sidle RC, Bergerud WA (2004) Recognition of debris flow, debris flood and flood hazard through watershed morphometrics. Landslides 1(1): 61-66.

Winter MG, Shearer B (2014) Landslide hazard and risk in a changing climate. In: Sassa K, Canuti P, Yin Y (Ed). Landslide Science for a Safer Geoenvironment, Volume 1: The International Programme on Landslides (IPL). Springer, New York, pp. 281-286.

Wolle CM, Hachich W (1989) Rain-induced landslides in Southeastern Brazil. Proc 12th Int Conf on Soil Mechanics and Foundation Engineering, Rio de Janeiro, Brazil, vol. 3, pp. 1639–1642.

APPENDIX A.3

A multi-step hazard assessment for debris-flow prone areas influenced by hydroclimatic events

Highlights

- Logistic Regression (LR), numerical simulation and rainfall back-analysis are applied
- Simulation determined average runout distances, flow height and velocity
- Short duration (<48h), high intensity (>200mm) rainfall triggers large debris flows
- Very low to very high hazard levels are proposed, based on rainfall and flow parameters

Abstract

Hazard assessment studies are fundamental to identifying disaster-prone areas, especially in locations with high environmental and socioeconomic vulnerability. This study proposes a multi-step debris-flow hazard assessment, based on the combination of Logistic Regression (LR) analysis, numerical simulation and rainfall back-analysis. A landslide-prone area of 84 km^2 is chosen as test-site, including 20 river catchments and one of the largest petrochemical plants in Latin America. Rainfall is the main influencing factor in debris-flow initiation, as highlighted by the LR analysis, followed by soil cover and slope. The analysis also indicated the catchments more susceptible to debris flows and the simulation results show that the average runout distance in these catchments is 470 m, with an average flow height of 5 m and a peak velocity of 23 m s^{-1}. Debris flows are triggered by short duration (<48 h), high-intensity (>200 mm) precipitation, with return periods that vary from 3 to 10 years. Five levels of hazard (very low to very high) are, then, proposed for the study site, based mainly on 48-h accumulated rainfall and flow properties. Industrial and residential areas in the projected debris-flow route generally exhibit the highest overall hazard levels, as many were developed in the depositional area of debris flows and near fluvial courses, where associated floods and flash floods may occur. As pointed out by recent studies, an increase in the frequency of extreme precipitation events is projected in the Serra do Mar region and when the general short return period of the debris-flow triggering rainfall is considered (< 10 years), large magnitude (>10^5 m^3) debris flows are likely to occur in the near future.

Keywords: intense rainstorms, landslides, multivariate statistics, Serra do Mar, Cubatão.

1 Introduction

Sediment transport in mountain regions is mainly initiated by episodic events, such as landslides, debris flows and avalanches (Dietrich and Dunne 1978). Debris flows are especially destructive among the hydrogeomorphic processes, as they are capable of moving sediments very rapidly down steep channels (from organic matter to large rock boulders), representing a major hazard to humans and infrastructures (Corominas et al. 2013). High-intensity precipitation is one of the primary triggering factors and rainfall-triggered debris flows commonly initiate from landslides (Takahashi 2006; Yang et al. 2020).

In Brazil, the Serra do Mar Mountain Range is the main site of landslide and debris-flow occurrence, due to its steep slopes (averaging 25º to 35º) and high rainfall rates (up to 4,000 mm annually) (Vieira and Gramani 2015). Recent projections in the context of global warming have indicated that the Serra do Mar region may experience a surge in the frequency and magnitude of landslide and debris-flow events, particularly in scenarios with a 2.0º C increase in Global Warming Levels (GWLs) (Marengo et al. 2021). Several recent studies have also indicated that global warming may increase the frequency of extreme precipitation events worldwide (e.g., Westra et al. 2014; Deng et al. 2021), which can lead to significant socioeconomic losses, especially in the Global South[5], where little investment is made to prevent natural disasters (Petley 2012; Marengo et al. 2021).

Landslides and debris flows are associated with a high number of fatalities per event in Brazil (Kahn 2005), where 9 out of 100 people live in areas prone to natural hazards (Alvalá et al. 2019). The approach adopted in the country regarding natural hazard management has historically been reactive, relying on measures to cope with the impacts after a disaster has already taken place (Marengo et al. 2021). Even though the National Center of Monitoring and Early Warning of Natural Disasters (*Centro Nacional de Monitoramento e Alertas de Desastres Naturais* - CEMADEN) was created in 2011 and hazard management programs were developed and financed, since 2014 the center has experienced successive cuts in its annual budget, from ca. US$14 million in 2013 to ca. US$ 3.7 million in 2020 (Brasil 2021), challenging a continuous and thorough monitoring of hazards.

Quantitative debris-flow hazard assessments are scarce when compared to other types of hydrogeomorphic processes in Brazil, which can be associated with the lack of investments that lead to poor monitoring, challenging the establishment of realistic estimations of temporal and spatial probability of events (Alvalá et al. 2019). The lack of high-quality data from past-events is another limitation, affecting the implementation of efficacious hazard and risk management programs (Corominas et al. 2013). The foundation of hazard studies that focus on landslide-triggered debris flows commonly relies on a sound landslide inventory, knowledge of the main controlling and

[5] According to the definition of the United Nations Finance Center for South-South Cooperation (UN FCSSC, 2022)

101 triggering factors that influence their occurrence, and the assessment of the elements at hazard (van Westen et al.
102 2008; Corominas et al. 2013).
103 Landslide inventories are a critical first step in hazard and susceptibility studies, applied in the investigation of
104 their distribution patterns in relation to environmental variables, as well as in the validation of hazard scenarios
105 (van Westen et al. 2008; Steger et al. 2021). Moreover, with the association of landslide distribution and temporal
106 probability of a triggering event, it may also be possible to establish frequency-magnitude relationships
107 (Corominas et al. 2013).
108 The influencing factors are associated to the triggering and controlling parameters that lead to debris-flow
109 occurrence, which can vary according to the characteristics of a region (Corominas et al. 2013; Nikolova et al.
110 2020). Since the study of Melton (1958), several attempts have been made to identifying the critical morphometric
111 variables that control debris-flow initiation in a catchment (e.g., Bovis and Jakob 1999; Wilford et al. 2004;
112 Nikolova et al. 2020), including in Brazil (e.g., Dias et al. 2016; Gabelini et al. 2019, among others). Multivariate
113 statistics analyses have traditionally been applied in this regard, due to their objective evaluation of the relationship
114 between a dependent variable (occurrence or not of an event) and a series of independent variables (i.e., the
115 influencing factors) (Corominas et al. 2013).
116 Logistic Regression (LR) is among the most commonly adopted methods in multivariate analyses focused on
117 landslide susceptibility (e.g., Ayalew and Yamagishi 2005; Das et al. 2010). LR has also been applied in recent
118 debris-flow studies (e.g., Wu et al., 2018; Shan et al. 2020), performing satisfactorily in the identification of the
119 main factors that impact debris-flow initiation. LR has shown a lower degree of error when compared to other
120 multivariate analyses in landslide susceptibility studies (Wu et al. 2018), which can potentially be extrapolated
121 for debris-flow studies as well.
122 More recently, numerical and physically-based models have been developed to support hazard and risk analysis,
123 due to their ability to represent important features of the debris-flow dynamics (Hussin et al. 2012). Some
124 examples of dynamic models include DAN-3D (Hungr and McDougall 2009), FLO-2D (Quan Luna et al. 2011)
125 and RAMMS (Frank et al. 2017). Developed by the Swiss Institute for Snow and Avalanche Research (SLF),
126 RAMMS is regarded as the state-of-the-art model in debris-flow simulation (Frank et al. 2017), predicting run-
127 out path, velocity, flow height and impact pressure, as well as entrainment rate (Frank et al. 2017). These
128 parameters are fundamental to estimating hazard intensity that can aid hazard and risk zonation, as well as the
129 dimensioning of protective structures and measures (Hungr and McDougall 2009).

Due to the high environmental and socioeconomic vulnerability of Cubatão (São Paulo state), the largest petrochemical site in Latin America, several studies focused on the susceptibility, hazard and risk to landslides and debris flows have been made in the region (e.g., Wolle and Carvalho 1994; Kanji et al. 2007; Vieira et al. 2010; Cabral et al. 2022). Rainfall thresholds for landslide and debris-flow events have also been developed for the hillslopes of the region by Tatizana et al. (1987), based on the Intensity-Duration (I-D) model first established by Caine (1980).

Debris-flow frequency at Serra do Mar is largely influenced by heavy rain events (Kanji et al. 2007; Lacerda 2007), hence the importance of rainfall thresholds. Accurate limits, thus, are necessary for the quantification of hazards and the implementation of monitoring programs (Caine 1980; Corominas et al. 2013). Due to climate change, a constant assessment and, if needed, updates in these thresholds are necessary to ensure their ability to prevent damage (Chang et al. 2011).

In this context, this study proposes a multi-step hazard assessment for debris-flow prone regions influenced by hydroclimatic events. The central and northeastern hillslopes of Cubatão are chosen as the study site, due to the extensive record of debris-flow events. For the hazard assessment, we first conduct a data-driven Logistic Regression (LR) to identify the main factors that influence debris-flow initiation in the region and the catchments that are more susceptible to the phenomenon, as well as the back analysis of two regional debris-flow events using RAMMS. Based on the outcomes of the simulations, the LR and on the analysis of rain events that led to debris flows in the study site, a hazard matrix is proposed for the creation of a hazard zonation map. Furthermore, an analysis of the rainfall thresholds is performed to verify the current debris-flow curves, as well as the mapping of the infrastructures located in the region to contribute to the hazard zonation.

2 Debris flows and the study area

Cubatão, a municipality with ca. 130,000 habitants in the state of São Paulo, was developed at the foot of the Serra do Mar Mountain Range, a set of steep festooned scarps that borders the Brazilian southern and southeastern coast for about 1,500 km (Fig. 1A) (Vieira and Gramani 2015). Several landslide and debris-flow events have occurred in the region, with the ones from 1985 and 1994 as the most notoriously widespread throughout the hillslopes of Cubatão.

In 1985, the central and northeastern region of the municipality's hillslopes was hit by an intense precipitation between January 23 and 24, triggering more than 1,600 shallow landslides that in some catchments further initiated debris flows (Fig. 1B). The series of debris flows and landslides caused the leakage of ammonia into the Mogi River basin, due to the breakage of a pipe of the petrochemical company Copebrás (Vieira et al. 2010), and the

partial silting of the Mogi River due to the large volume of sediments transported, affecting the operation of Brazil's largest port (Santos) located 20 km away from Cubatão (Gramani 2001).

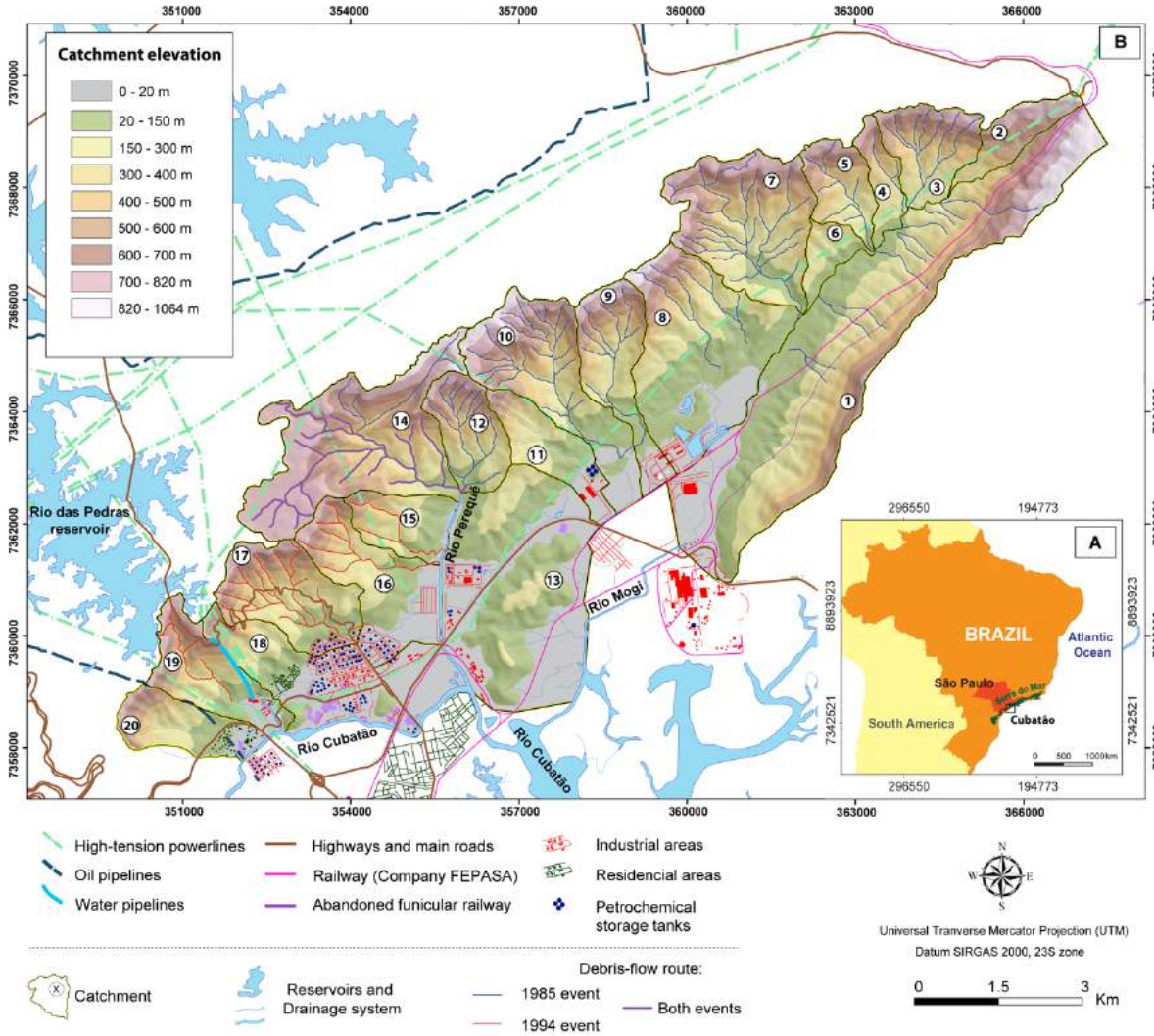

Figure 1: Location of the study area. A) The study area (Cubatão, São Paulo State), located in the Serra do Mar Mountain Range, Brazil. B) Overview of the analyzed catchments (numbers in white circles), located at the central and northeastern hillslopes of Cubatão.

Similarly, on February 6 and 7, 1994, widespread landslides at the hillslopes of the central portion of Cubatão initiated debris flows in some catchments (Fig. 1B), affecting an oil refinery and causing more than U$ 40 million in damages (Kanji et al. 2007). No new regional landslide event of similar magnitude has occurred in Cubatão since then. The municipality is one of the areas in Brazil most prone to Natech[6] disasters, due to the production and storage of petrochemical products and the presence of two important highways (Anchieta - SP 150 and Imigrantes – SP 160) that connect the city of São Paulo to the coast.

[6] When natural hazards affect industrial areas, they can disrupt industrial operations and destroy industrial installations, causing Natech disasters (Natural Hazard Triggering Technological Disasters) (Galderisi et al. 2018).

Figure 1B shows the location of the studied catchments, where, historically, debris flows are more commonly recorded and occur near populated areas. Numbers are adopted to denominate the catchments, due to great controversy on their names. The 20 catchments are characterized by steep slopes (averaging 30º to 35º) and dense rainforest cover. The bedrock is comprised of metamorphic and plutonic rocks of Archean/Proterozoic age (IPT 1986). The vegetation cover map is available as Supplementary Information (SI), as well as the geology and soil cover maps.

The analyzed catchments are supply-limited, and the regolith of the region generally exhibits a well-developed soil layer with a thickness of up to 2m, with structured saprolite layer of up to 10 m (Vieira et al. 2010). Shallow landslides initiate at the most superficial regolith layer (Lacerda 2007), with failure depth varying according to the position of the landslide in the slopes, averaging at 1 m (Cabral et al. 2022). Due to their channelized nature, as well the abundance of stony material on the channels, the debris flows at Serra do Mar can grow volumetrically because of entrainment.

The region is characterized by a subtropical-humid climate (Cfa – Köppen classification), with temperatures that vary from 17º C to 36º C during the year. Annual rainfall can surpass 3,300 mm, reaching up to more than 4,000 mm in some years (Kanji et al. 2007), with summer as the wettest season (December – March). The South Atlantic Convergence Zone (SACZ) and frontal systems are the main synoptic systems responsible for extreme precipitation events over southeastern Brazil (Cavalcanti 2012), enhanced in the Serra do Mar region by orographic effect (Kanji et al. 2007).

3 Material and Methods

3.1 Influencing factors

The selection of the factors that influence debris-flow initiation is based on past studies worldwide and at Serra do Mar (e.g., Wilford et al. 2004; Dias et al. 2016; Wu et al. 2018; Nikolova et al. 2020), as well as on the factors that are assumed to be critical at the study area based on past events. Two assumptions were made in their selection: (1) New debris flows will occur in similar conditions as past ones and (2) the analyzed factors will not change for a long period of time (Wu et al. 2018). The influencing factors are catchment slope, catchment relief, slope aspect, stream power index (SPI), topographic wetness index (TWI), lithology, soil cover, vegetation and 48-h accumulated rainfall (Table 1). The general morphometric characteristics of the studied catchments are shown in Table 2.

A reclassification was conducted to standardize the scale of all the factors and facilitate the statistical evaluation. Frequency ratio was applied in the standardization, as suggested by Chen et al. (2016). The method also highlights

the influence degree of the reclassified factor ($M_{i,j}$, Eq. 1), where the larger the final standard index value ($X_{i,j}$, Eq. 2), the greater the influence on debris-flow initiation (Wu et al. 2018):

$$M(i,j) = s(i,j) / S(i,j) \quad (1)$$

$$X(i,j) = M(i,j) / \sum_{j=1}^{m} M(i,j) \quad (2)$$

Where i = 1, 2, 3…n represents the influencing factor number and j = 1, 2, 3…n is the subclass of the reclassified factor. Each subclass was defined based on the limits defined by the cartographic products (e.g., granite and migmatites are some of the subclasses of lithology). $S_{i,j}$ is the area of each subclass after reclassification (km^2) and $s_{i,j}$ is the area of the actual landslides existing in that subclass (km^2) (Wu et al. 2018). The area of the landslides in the catchments is chosen as the assessing parameter, by comparing the results of catchments where debris flows occur (coded as 1) with those that do not (coded as 0), as the debris flows in the region are landslide triggered.

Table 1: Influencing factors analyzed in this study.

Factors	Symbol	Unit	Description
Catchment relief	H	km	The difference between the highest and the lowest elevation point
Catchment slope	Sl	%	Slope of the catchment
Slope aspect	Sa	-	The compass direction the slope surface faces
Strem Power Index (SPI)	SPI	-	The erosive power of flowing water
Topographic Wetness Index (TWI)	TWI	-	Terrain-driven variation in soil moisture
Lithology	Lit	-	Geology of the catchment's bedrock
Soil	So	-	The soil cover of the catchment
Vegetation	F	-	The type of vegetation cover of the catchment
48-h accumulated rainfall	P	mm	48-h accumulated rainfall prior to the debris flow

3. 2 Landslide inventories and cartographic data

The landslide scars inventories were created from stereoscopic aerial photographs from April 1985 and March 1994, provided by the Geographic and Cartographic Institute of the State of São Paulo (*Instituto Geológico e Cartográfico* - IGC), at a 1:25,000 scale. Aerial photographs from the 1994 event are only available at the central portion of the study area, where landslides were concentrated. These two inventories are available as SI, in online resources. Aerial photographs prior to the 1994 event were also used (October 1992, from IGC), however no photographs prior to 1985 were available and all the scars mapped were assumed to be resulted from this event. The criteria used in the landslide scars' extraction were: lack of vegetation (made easier by the dense tropical forest of the region), characteristic morphology (elongated, length superior to width) and drainage condition of the hillslopes. In total, 1,679 landslide scars were mapped in the 1985 event, with an average area of ca. 338 m^2, whereas 579 were mapped in the 1994 event, with an average area of ca. 500 m^2.

Table 2: Morphometric parameters of the catchments in the study region. Catch. = Catchment, Rr = Relief Ratio; Dd = Drainage Density; Ch. = Channel.

Catchment	Area	Number of landslide scars		Relief ratio	Landslide volume (m^3)		Catch. Relief (km)	Drainage density (km/km^2)	Catch. Length (km)	Channel Slope (%)	Catch. Slope (%)	Landslide scar density		Melton Ratio	Debris-flow event	
		1985	1994		1985	1994						1985	1994		1985	1994
1	15.56	94	14	0.51	68422.3	16028.5	0.98	1.09	1.91	9	51	6.04	N/A	0.25	Y	N
2	1.34	23	N/A	0.21	3061.4	N/A	0.62	0.99	2.912	14	21	17.16	N/A	0.54	N	N
3	2.34	45	N/A	0.34	16678.2	N/A	0.66	2.09	1.92	8	34	19.23	N/A	0.43	Y	N
4	1.07	34	N/A	0.29	8274.8	N/A	0.7	2.24	2.43	10	29	31.78	N/A	0.68	Y	N
5	1.68	90	N/A	0.32	20412.9	N/A	0.71	1.61	2.21	12	32	53.57	N/A	0.55	Y	N
6	0.9	24	N/A	0.43	8588.5	N/A	0.48	1.97	1.12	17	43	26.67	N/A	0.51	N	N
7	5.39	348	N/A	0.23	131737.6	N/A	0.75	2.04	3.33	16	23	65.56	N/A	0.32	Y	N
8	7.18	139	N/A	0.29	33976.8	N/A	0.92	0.82	3.18	10	29	19.36	N/A	0.34	Y	N
9	2.94	100	13	0.33	25740.7	8163.3	0.94	1.42	2.86	9	33	34.01	4.42	0.55	Y	N
10	4.9	184	31	0.28	78865.6	20106.6	0.96	2.34	3.42	13	28	37.55	6.33	0.43	Y	N
11	2.09	46	1	0.30	10234.2	387.7	0.76	1.51	2.57	14	30	22.01	0.48	0.28	N	N
12	2.1	83	37	0.37	32216.1	20474.5	0.8	2.73	2.19	9	37	39.52	17.62	0.53	Y	N
13	9.75	21	32	0.40	8039.8	20782.8	0.4	1.36	1	12	40	2.15	3.28	0.55	N	N
14	7.19	185	121	0.19	53193.2	82632.6	0.75	0.88	3.85	16	19	25.73	16.83	0.13	Y	Y
15	2.75	36	14	0.24	8793.1	8192.9	0.73	1.93	3.06	13	24	13.09	5.09	0.32	N	Y
16	5.3	13	13	0.23	1357.76	429.8	0.74	1.22	3.193	11	23	2.45	2.45	0.44	N	Y
17	3.53	108	143	0.28	17833.2	42702.5	0.8	3.74	2.87	11	28	30.59	40.51	0.43	N	Y
18	3.78	46	85	0.27	9187.6	38969.8	0.8	3.59	2.97	13	27	12.17	22.49	0.41	N	N
19	1.86	12	26	0.35	3763.9	17673.8	0.7	4.72	2.01	12	35	6.45	13.98	0.51	N	Y
20	2.12	1	1	0.43	478.5	478.5	0.76	2.31	1.76	9	43	0.47	0.47	0.52	N	N

A 5m resolution DEM was adopted in this study, created using the *topo to raster* tool in GIS software from 5 m contour topographic maps (the highest resolution available for the area), also provided by IGC. The IGC topographic map is from 1975, before the regional landslide and debris-flow events in the region.

The interpretation of the elements at hazard in the study area is based on the land use map of the Brazilian Institute of Geography and Statistics (IBGE), at a 1:50,000 scale, and high-resolution aerial photographs from 2011 (Ground Sampling Distance of 4 m), provided by the *Empresa Paulista de Planejamento Metropolitano S/A* (EMPLASA). Google Earth aerial photographs were also used as an auxiliary tool, to confirm the most current use of the region's territory.

Vegetation cover information was retrieved from Mattos and Matsukuma (1990), the geological map from IPT (1986), and the soil cover map from Rossi and Pfeifer (1991) and Rossi (2017). The TWI of the catchments was calculated based on Kopecky et al. (2021) using GIS software, being a function of the contribution area of the catchment, flow width and catchment slope. The SPI is based on the contribution area and catchment slope, also calculated in GIS software following de Rosa et al. (2019).

3.3 Field campaigns and geotechnical tests

Three field campaigns were conducted in the study area, in October 2018, October 2019, and May 2022 for field reconnaissance, rock and soil sampling, and investigation of channel morphology and source areas. Eight soil samples were collected and tested, spread at the central and eastern portions of the region, at both metamorphic and granitic regolith (location available as SI, mapped in conjunction with the geology map). Bulk density tests and soil screening carried out indicate that the most superficial soil in the studied region has a bulk density between 1,200 – 1,750 kg m^{-3}, averaging ca. 1,400 kg m^{-3} (Table 3). Stone content is high, increasing rapidly from surface to deeper soil layers, which can increase the bulk density of the slope material that initiates debris flows.

Table 3: Geotechnical test results of the soil samples collected at the study area.

Sample	Lithology	Soil	Collection Depth (m)	Bulk density (kg/m^3)	Porosity (%)	Texture (USDA*)	Cohesion (kPa)	Internal friction angle (Degrees)
1	(Migmatite) PSeMc	Ca3	2	1755	45.05	Sandy loam	10	37
2	(Migmatite) PSeMc	Ca3	1	1284	49.31	Sandy loam	10	37
3	(Migmatite) PSeMc	Ca3	1.5	1400	46.4	Loam	20	35
4	(Migmatite) AcMp	LVa1	1	1200	53.11	Loam	20	35
5	(Migmatite) AcMp	LVa1	1	1274	50.51	Sandy loam	15	32
6	(Migmatite) AcMn	LVa3	2	1450	43.9	Loam	25	34
7	(Migmatite) AcMn	LVa3	1	1360	48.46	Sandy clay	50	29
8	(Migmatite) AcMn	LVa3	1	1216	51.42	Sandy loam	20	37

*Soil classification proposed by the United States Department of Agriculture (USDA)

Screening tests show that the soil has mainly a sandy texture, with sand content ranging between 60% – 80%, and clay between 15% - 40% (Table 3). Shear tests results indicate that the cohesion of the soil ranges from 10 to 50 kPa and the internal friction angle from 29º - 37º. The saturated hydraulic conductivity (Ks) of the soil was not tested in our study, however it is assumed to vary from 10^{-6} m s^{-1} to 10^{-4} m s^{-1} in the region (Wolle and Carvalho 1994).

3.4 Logistic regression (LR)

In a LR model, the dependent variable has two categories, the occurrence (coded as 1) and the absence (coded as 0) of an event (i.e., debris flow). The spatial prediction is modeled by the dependent variable and a number of independent variables (i.e., influencing factors) that are available in a spatially continuous manner across the region. LR fits a s-shaped curve that follows the linear regression:

$$Y = \alpha + \beta X + \varepsilon \quad (3)$$

Where Y is the dependent variable, α is the intercept, β is the regression coefficient representing the variation in Y when X increases (Wu et al. 2018). ε is the stochastic term, representing the error of the model.

The s-shaped curve is a plot of the probability of having a true positive (correctly predicted event response) versus the probability of a false positive (falsely predicted event response) as the cut-off probability varies (Wu et al. 2018). If the probability of an event is denominated P, then log $P/(1-P)$ is the LR of P. The independent variables are assessed (x_1, x_2, …, x_n) to establish the LR equation (Eqs. 4 and 5) (Wu et al. 2018):

$$Logit\ P = Z = B0 + B1\,x1 + B2\,x2 + \cdots + Bn\,xn \quad (4)$$

$$P = \frac{e^{Z}}{1 + e^{Z}} \quad (5)$$

With B_0 as ratio between the probability of occurrence and non-occurrence of the debris flows under the condition of no disaster hazard. B_1, $B_2 \ldots B_n$ are the LR coefficient, which indicates the ratio between the probability of occurrence and non-occurrence of an event when a certain influencing factor changes by a unit volume. B is calculated by solving the sample of the reclassified influencing factors and e is the natural exponential function. The regression analysis was completed using the SPSS software, version 28.0.

Since the influencing factors can potentially show a high to low correlation with each other, a factor combination was made to determine their degree of contribution to debris-flow initiation, as suggested by Wu et al. (2018). In the first round of the LR, the influencing parameters were added one by one, independently, creating a one-factor model. The factor that showed a more positive effect in the model was retained and added in the following round of LR analysis – creating, then, a two-factor model. The process was repeated until all the influencing factors were combined.

To verify the LR results, a Receiver-Operation Characteristic (ROC) analysis was conducted, following Fawcett (2006). The results with a higher Area Under de Curve (AUC) indicate a better prediction of debris-flow initiation, and the order in which each factor is added to the model indicates the influence degree of that factor. For more information on ROC analysis, we refer to Fawcett (2006).

The model obtained with the LR was then applied in the susceptibility assessment of the studied catchments. Three levels of susceptibility are assumed to determine areas most prone to debris-flow initiation: low, when the probability is less than 30%; medium, when the probability is between 30 to 50%; and high, when the probability is greater than 50%. Each catchment was, then, classified with an overall high, medium or low susceptibility, based on the proportion of areas classified with the susceptibility level "high". A catchment is regarded as highly susceptible when over 50% of its total area was classified with the susceptibility level "high", while a catchment is considered with a medium or low overall susceptibility when, respectively, 20-50% or less than 20% of its total area is classified with the susceptibility level "high".

3.5 Debris-flow simulation and calibration

RAMMS uses the Voellmy-fluid friction model for debris flows, based on the Voellmy-fluid flow law (Frank et al. 2017). The Voellmy-fluid flow assumes that a debris flow is a hydraulic-based depth-averaged continuum model and that the flow resistance is divided into a dry-Coulomb friction (μ, dimensionless) and a viscous resistance turbulent friction (ξ, m s^{-2}) (Frank et al. 2017). The flow moves as a plug, with the same mean velocity (u, m s^{-1}) over the height of the flow (h, m). The friction resistance (S, Pa) is given by the Equation 6:

$$S = \mu N + \rho g\, u^2/\xi + 1 - \mu\, N_0 - 1 - \mu\, N_0\, e^{-N/N_0} \quad (6)$$

$$N = \rho h \cos\phi \quad (7)$$

With N as the normal stress in the running surface (Eq. 7) and N_0 as the yield stress of the flowing material, introduced to model ideal plastic materials (Hussin et al. 2012). In the equations, ρ is the bulk density (kg m^{-3}), g is the gravitational acceleration (m s^{-2}), ϕ is the downslope angle of the terrain (degrees). The input parameters of the model are a hydrograph or the initiation volume and the resistance parameters μ and ξ. For further description of the model and its governing equations, we refer to Hussin et al. (2012).

For the calibration of the input parameters, we adopted the landslide scars mapped as the initiation volume, with an average depth of 1m (Cabral et al. 2022), and we assume that all the slope failures at each catchment occurred at the same time due to no information available in this regard. The values for μ and ξ were best matched based on the deposition patterns described in the literature and observed in the aerial photographs, as suggested by Aaron and McDougall (2019).

The simulated and observed deposition areas are compared following Schraml et al. (2015), which uses a coverage index (Ω) as the assessing parameter (Eqs. 8 – 11). The coverage index considers the coincidence between the simulated deposits within the observed deposition (A_x), the area of the simulated deposits outside the observed deposition (A_y), and non-simulated areas within the observed deposition (A_z). The closer the coverage index is to 1, the more accurate the simulation is (Schraml et al. 2015).

$$\chi = \quad A\left(x\right) \; A\left(observed\right) \tag{8}$$

$$\upsilon = \quad A\left(y\right) \; A\left(observed\right) \tag{9}$$

$$\zeta = \quad A\left(z\right) \; A\left(observed\right) \tag{10}$$

$$\Omega = \chi - \upsilon - \zeta \tag{11}$$

Two phases of simulation were adopted: the first one, where ξ is unchanged (ξ = 200) and the μ values vary from 0.03 to 0.2; and the second run with the best matched μ value unchanged, while the ξ values vary from 100 to 1000 m s^{-2}.

3.6 Rainfall analysis

The distribution of the rainfall across the study area during the 1985 and 1994 events was created using interpolation of rain gauge data (kriging technique) in GIS software with a 25 m raster resolution. The rainfall distribution maps are available as SI. In the 1985 event, rainfall was concentrated in the northeastern portion of the study area, where precipitation reached ca. 412 mm in 48 h, with a peak precipitation of 84 mm h^{-1}. In the 1994 event, rainfall was concentrated in the central-west portion of the region, and the 48-h accumulated precipitation reached ca. 452 mm with peak precipitation of 60 mm h^{-1}.

For the rainfall analysis of the 1985 and 1994 events, as well as for the analysis of the rainfall that triggered landslides and debris flows events from 1975 to 2020 (Table 4), rain gauge data was retrieved from the rainfall databases of the Department of Water and Energy of the State of São Paulo (DAEE), the Brazilian National Water Agency (ANA) and CEMADEN. The return period shown in Table 4 is based on the rainfall intensity, duration and frequency (IDF) equation established by Martinez and Magni (1999) for Cubatão (Eq. 12), where *i* is the rainfall intensity (mm $minute^{-1}$), *d* is rainfall duration ($10 < d < 1440$ minutes) and *RP* is the return period (years).

$$i\left(d, RP\right) = 25.1025(d + 20)\left) - 0.7522\right) + 6.4266(d + 20)\left) - 0.705\right) \; - 0.4772 - \tag{12}$$

$$0.9046 \; Ln \;\; RP\left(RP - 1\right)\right)$$

Tatizana et al. (1987) established an I-D threshold in the region, in which four different curves were created based on the intensity of an event: the localized-landslides curve, sparse-landslides curve, regional-landslides curve and debris-flow curve (Fig. 2). These thresholds/curves were established based on the peak hourly intensity of the

rainfall event, combined with the 96-h accumulated rainfall prior to the initiation of the landslide or debris-flow event (Eq. 13):

$$I = K * Ac^{-b} \quad (13)$$

Where I is the hourly peak precipitation (mm h^{-1}), Ac is the 96-h accumulated precipitation (mm) and K and b are geometrical constants that vary according to the climatic conditions and geotechnical characteristics of the study area (Tatizana et al. 1987).

Table 4: Debris flow events recorded in the study region since 1975, updated based on Gramani (2001).

Catchment	Date of the event	24-h accumulated rainfall	48-h accumulated rainfall	96-h accumulated rainfall	Peak rainfall intensity	Magnitude (m^3)	Return period	Losses
1	25/12/1975	247.5 mm	255.5 mm	261.4 mm	N/A	> 10 x 10^6	N/A	N/A
10	29/01/1976	279 mm	315 mm	343 mm	40 mm h^{-1}	1 x 10^5	1.23 years	N/A
1, 2, 3, 4, 5, 6, 7, 8, 9, 10, 12, 14	24/01/1985	242 mm	411 mm	424 mm	84 mm h^{-1}	N/A	10.4 years	Silting of Mogi River, Ammonia leakage
9	24/01/1988	185 mm	186 mm	192 mm	25 mm h^{-1}	N/A	1 year	10 deaths
14, 15, 16, 17, 18, 19	07/02/1994	325 mm	452 mm	452 mm	60 mm h^{-1}	1.7 x 10^5 (Catchment 17)	2.7 years	US$ 40 mi
17	09/04/1996	260 mm	265 mm	265 mm	18 mm h^{-1}	1.6 x 10^4	1 year	No damages
Rio Pilões (West of the study area)	12/12/1999	128 mm	274 mm	274 mm	N/A	3 x 10^5	N/A	N/A
Rio Pilões (West of the study area)	16/02/2000	304 mm	304 mm	304 mm	118 mm h^{-1}	N/A	90.5 years	N/A
Rio Marcolino, Rio Pilões, Ribeirão do cágado (West of the study area)	22/02/2013	312 mm	314 mm	314 mm	118 mm h^{-1}	N/A	90.5 years	1 death, destruction of 45 houses and 01 water treatment plant
17	29/04/2022	169 mm	248 mm	270 mm	35 mm h^{-1}	N/A	1 year	Road blockage

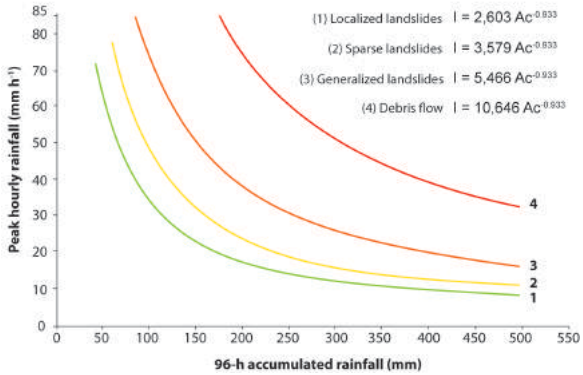

Figure 2: Rainfall thresholds for landslides in the study region, established by Tatizana et al. (1987).

360 *3.7 Hazard zonation*

361 The creation of the hazard zonation map for the study area was based on the simulation of debris flows in the
362 catchments most prone to the phenomenon identified in the LR analysis, calibrated using the two large-magnitude
363 debris-flow events of 1985 and 1994. The simulation results were combined with the analysis of past rain events
364 at the study site, to create a hazard zonation matrix. The information about the land use of the region is also
365 considered in the hazard zonation, by determining the elements at hazard.

366 **4 Results and discussions**

367 *4.1 Debris-flow dynamics, influencing factors and susceptibility*

368 The initiation of rainfall-triggered debris flows in the Serra do Mar region can generally be summarized in three
369 stages, as Lacerda (2007) suggests: (1) rainfall infiltration in the soil that leads to (2) slope failure(s), which further
370 (3) triggers a channelized debris flow. The main process associated with slope failure at the hillslopes of Serra do
371 Mar is loss of suction due to rain infiltration (Lacerda 2007).

372 High- to extreme-precipitation events often occur at catchments at Serra do Mar (Vieira and Gramani 2015), which
373 can trigger large shallow landslides that initiate debris flows in isolated gullies (Fig. 3A), often remaining
374 unreported. An example of such an event is the 1975 debris flow (Table 4) in one of the streams of catchment 1
375 (Fig. 3B), triggered by shallow landslides at the headwater's region. "Shock wave", due to the impact of falling
376 rock boulders, is another mechanism that can trigger debris flows in the study region (Lacerda 2007), as well as
377 dormant landslides, which material can accumulate at upstream reaches and be reactivated by primary landslides
378 or rockfalls in the hillslopes. In the region, there are no reports of debris flows initiated solely by the increase in
379 the discharge of the channel, which leads to the mobilization of in-channel material.

380 Large-magnitude events, such as those in 1985 and 1994, are characterized by multiple source areas, both at
381 upstream and middle reaches of the channel (Fig. 4A). In-channel debris is also an important characteristic of the
382 catchments in the study region (Figs. 3C, 3D, 4B, 4C, 4D), which can contribute to increasing the severity of
383 debris flows. In-channel debris can be observed in upstream (Fig 4C), middle (Fig. 3C) and downstream reaches
384 of the catchments, suggesting that these materials are leftovers from past-debris flows or from recent, localized
385 slope failures along the channel length that were not mobilized.

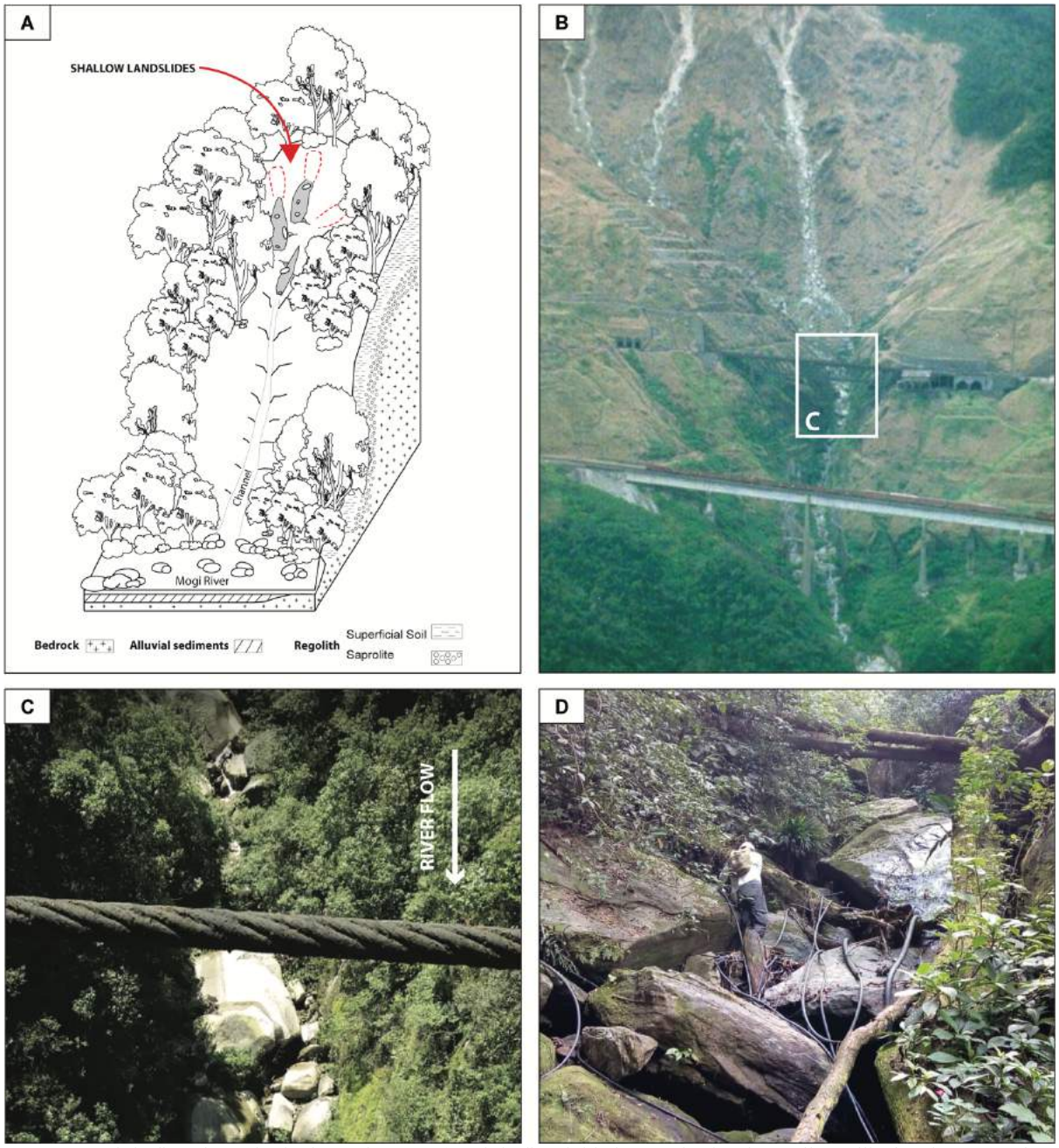

Figure 3: Debris-flow dynamics in the study area. A) Debris-flow initiation mechanism in smaller gullies/catchments at the study area, triggered by shallow landslides at the headwaters' region. B) 1975 debris flow that occurred in one of the streams of catchment 1. Photo from Prof. Dr. Milton Kanji, retrieved from Gramani (2001). C) Overview of the stream where the 1975 debris flow occurred, showing intense accumulation of rock boulders on the channel (Coordinates: 365926.79 m E, 7368058.54 m S). D) Upstream view of catchment 20, showing intense stony debris accumulation on the channel, as well as Large Wood (Coordinates: 350665.03 m E, 7358314.49 m S).

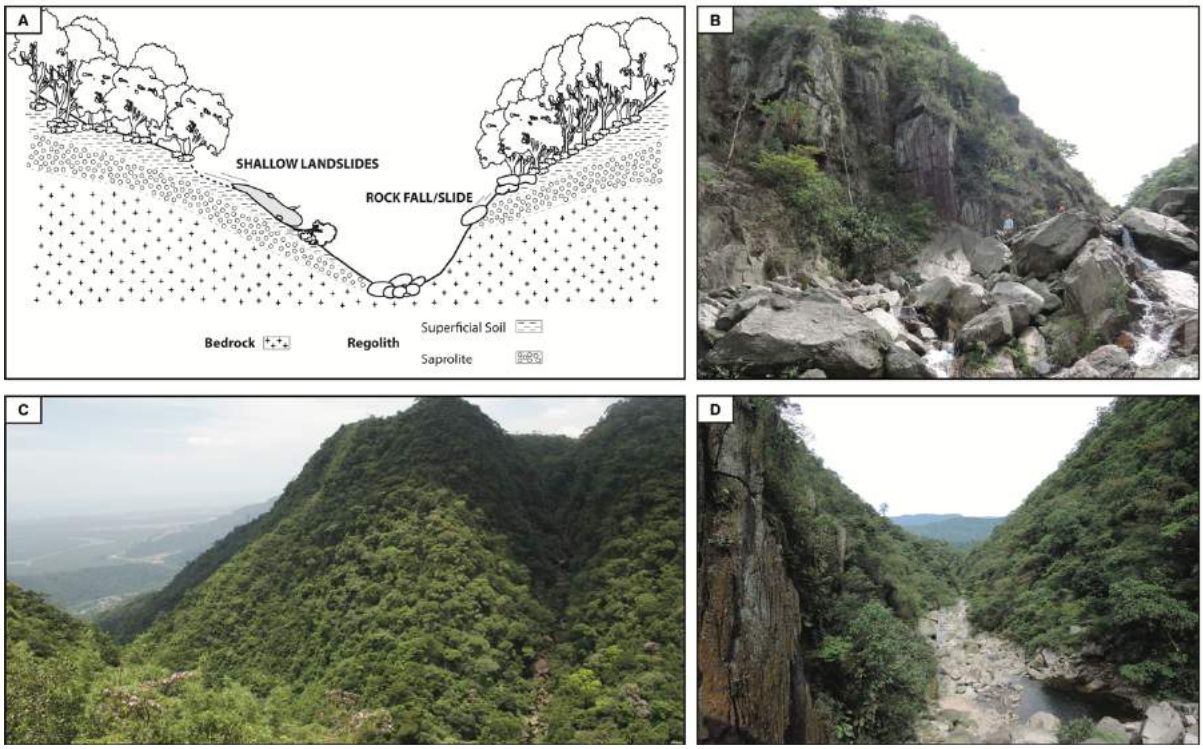

Figure 4: Debris-flow dynamics in the study area. A) Scheme of the initiation mechanism of the 1985 and 1994 debris-flow events, characterized by multiple source areas. B) Upstream view of catchment 7, showing intense stony debris accumulation in the channel, as well as fractured bedrock outcrops at the margins (Coordinates: 360256.69 m E, 7367963.72 m S) C) Overview of the upstream section of catchment 19, showing intense stony debris accumulation on a channel. A strong structural control is observed in the catchment (Coordinates: 350847.96 m E, 7360336.15 m S). D) Downstream view of the upstream section of catchment 7, showing an area with less accumulation of debris in the channel. Areas with intense stony and woody debris deposition are intercalated with areas with few accumulations along the catchment, suggesting that smaller debris-flow might have occurred more recently in small gullies or that slope failures occurred but did not trigger a debris-flow event, accumulating the material in the channel. (Coordinates: 360256.69 m E, 7367963.72 m S).

The standardization procedure of the influencing factors of the catchment that registered debris flows during the events of 1985 and 1994 and the single-factor evaluation, conducted to identify the most impactful subclasses, is shown in Table 5. The lower the rank, the greater its impact on the occurrence of debris flows. The table for the catchments that did not register debris flows is available as Supplementary Information. Based on the optimal model-fitting results (higher AUC) obtained through the LR and on the priority of factors added to the model, the following sequence was established: (1) Rainfall, (2) Soil cover, (3) Basin slope, (4) SPI, (5) TWI, (6) Forest cover, (7) Lithology, (8) Slope aspect, and (9) Basin relief (Table 6).

Several studies at Serra do Mar highlight that rainfall is the main debris-flow initiation factor (Lacerda 2007; Kanji et al. 2007; Vieira et al. 2010, Vieira and Gramani 2015) and our analysis statistically corroborates the statement. 10 rainfall index subclasses were identified across the study area (Table 5), based on the rainfall distribution patterns. For the 1985 events, the subclass 200 – 220 mm is associated with a higher density of debris-flow triggering landslides, while for the 1994 event the subclass 270 – 290 mm is associated with a higher density of landslides. These results potentially indicate that a > 200 mm rainfall accumulated in 48 hours can initiate high-magnitude, multiple-source debris flows.

Table 5: Standardization of the influencing factors and single-factor ranking.

Influencing Parameter	Subclasses	S_{ij} (km^2)		s_{ij} (km^2)		M_{ij}		X_{ij}		Ranking	
		1985	1994	1985	1994	1985	1994	1985	1994	1985	1994
Catchment Slope (%)	0 - 16	11.11	7.564	0.0139	0.0100	0.0013	0.0013	0.0082	0.0089	6	6
	16 - 35	9.11	2.928	0.0546	0.0242	0.0060	0.0083	0.0396	0.0556	5	5
	35 - 53	10.60	3.904	0.1729	0.0747	0.0163	0.0191	0.1075	0.1284	4	4
	53 - 70	10.10	4.636	0.3402	0.1627	0.0337	0.0351	0.2221	0.2357	3	3
	70 - 90	7.07	3.66	0.3383	0.1572	0.0479	0.0429	0.3155	0.2884	1	1
	90 - 172	2.52	1.464	0.1176	0.0617	0.0466	0.0422	0.3072	0.2831	2	2
Lithology	AcMn	14.1	12.46	0.2112	0.1256	0.0150	0.0101	0.1911	0.2455	3	2
	PSeMc	6.6	3.34	0.1295	0.0704	0.0196	0.0211	0.2502	0.5137	1	1
	PSEOM	2.1	0	0.0131	-	0.0062	-	0.0795	-	7	-
	PSEOYt	0.9	0	0.0136	-	0.0151	-	0.1922	-	2	-
	AcMp	6.7	0	0.0218	-	0.0033	-	0.0415	-	6	-
	PSpX	13.23	2.5	0.0779	0.0140	0.0059	0.0056	0.0752	0.1367	5	3
	PSEOY	1.8	0	0.0240	-	0.0134	-	0.1703	-	4	-
	PSpF	0	0.54	-	0.0023	-	0.0043	-	0.1041	-	4
	AcMg	0	0.17	-	0.0000	-	0.0000	-	0.0000	-	5
Rainfall	106 - 130	1.94	0	0.0086	-	0.0044	-	0.0494	-	8	-
	130 - 160	3.13	0	0.0227	-	0.0073	-	0.0807	-	7	-
	160 - 200	4.41	0	0.0630	-	0.0143	-	0.1586	-	2	-
	200 - 240	2.52	0	0.0496	-	0.0197	-	0.2190	-	1	-
	240 - 270	5.30	0	0.0408	-	0.0077	-	0.0854	-	6	-
	270 - 300	8.80	0.46	0.0314	0.0008	0.0036	0.0097	0.0396	0.49900417	9	1
	300 - 330	8.61	6.48	0.0916	0.0620	0.0106	0.0011	0.1181	0.0574785	4	5
	330 - 360	6.64	8.71	0.0936	0.0942	0.0141	0.0016	0.1566	0.08405372	3	4
	360 - 400	9.10	6.92	0.0759	0.0346	0.0083	0.0028	0.0927	0.14608149	5	3
	400 - 420	-	1.85	-	0.0080	0.0900	0.0042	-	0.21338212	-	2
Relief	0 - 20	4.08	4.62	-	-	-	-	-	-	9	9
	20 - 150	10.08	4.35	0.0138147	0.0133	0.0014	0.0030	0.0107	0.0231	8	8
	150 - 300	8.22	2.90	0.05832625	0.0306	0.0071	0.0105	0.0555	0.0798	7	6
	300 - 400	5.25	2.07	0.1025044	0.0178	0.0195	0.0086	0.1526	0.0649	5	7
	400 - 500	5.18	2.00	0.1049369	0.0318	0.0202	0.0159	0.1582	0.1201	4	3
	500 - 600	4.78	1.97	0.1051464	0.0585	0.0220	0.0297	0.1717	0.2244	2	2
	600 - 700	4.34	2.02	0.1048253	0.0779	0.0241	0.0386	0.1886	0.2919	1	1
	700 - 820	6.97	3.79	0.0877866	0.0574	0.0126	0.0152	0.0985	0.1146	6	4
	820 - 930	1.54	0.32	0.03235324	0.0035	0.0210	0.0107	0.1642	0.0811	3	5

Table 5 (Cont.): Standardization of the influencing factors and single-factor ranking.

Influencing Parameter	Subclasses	S_{ij} (km^2)		s_{ij} (km^2)		M_{ij}		X_{ij}		Ranking	
		1985	1994	1985	1994	1985	1994	1985	1994	1985	1994
Slope Aspect	Flat	0	0.0020	-	-	-	-	-	-	10	10
	North	1.18	0.8060	0.0253	0.0194	0.0214	0.0240	0.1418	0.1547	4	1
	Northeast	2.89	3.1152	0.0641	0.0353	0.0222	0.0113	0.1468	0.0730	2	8
	East	5.53	4.5445	0.1264	0.0629	0.0229	0.0138	0.1514	0.0891	1	5
	Southeast	8.55	5.4996	0.1513	0.0826	0.0177	0.0150	0.1172	0.0967	5	3
	South	8.42	5.3920	0.1043	0.0640	0.0124	0.0119	0.0821	0.0764	7	7
	Southwest	4.82	1.7920	0.0752	0.0235	0.0156	0.0131	0.1032	0.0844	6	6
	West	9.93	0.8973	0.0770	0.0131	0.0078	0.0146	0.0514	0.0938	9	4
	Northwest	6.84	1.0694	0.0622	0.0161	0.0091	0.0151	0.0602	0.0971	8	2
	North	1.49	0.5600	0.0329	0.0204	0.0220	0.0365	0.1460	0.2347	3	9
TWI	0 to 4	11.09	4.14	0.3831	0.1537	0.0345	0.0371	0.4627	0.4539	1	1
	4 to 6	22.58	10.12	0.4206	0.2094	0.0186	0.0207	0.2495	0.2532	2	2
	6 to 8	8.63	4.24	0.1182	0.0661	0.0137	0.0156	0.1836	0.1908	3	3
	8 to 11	4.93	2.74	0.0344	0.0182	0.0070	0.0067	0.0934	0.0814	4	4
	11 to 15	4.93	2.17	0.0040	0.0037	0.0008	0.0017	0.0108	0.0208	5	5
	15 to 22	0.29	0.34	-	-	-	-	-	-	-	-
SPI	-9 to -4	1.06	0.38	0.1057	0.0469	0.1002	0.1234	0.4012	0.4547	1	1
	-4 to -2	2.86	1.08	0.1757	0.0612	0.0614	0.0564	0.2457	0.2079	2	2
	-2 to - 0.5	1.50	0.84	0.0211	0.0101	0.0141	0.0120	0.0564	0.0441	6	6
	-0.5 to 0.5	19.90	11.87	0.4036	0.1863	0.0203	0.0157	0.0812	0.0578	5	5
	0.5 to 1.5	18.33	7.29	0.4407	0.1989	0.0240	0.0273	0.0963	0.1005	4	4
	1.5 to 6	6.10	2.60	0.1816	0.0953	0.0298	0.0367	0.1191	0.1351	3	3
Soil cover	LAV3	5.16	14.23	0.0658	0.1638	0.0128	0.0115	0.2115	0.4420	3	2
	CA1	1.4	0	0.0191	-	0.0136	-	0.2263	-	2	-
	LAV1	31.2	0.014	0.3350	-	0.0107	-	0.1780	-	4	-
	CA2	3.2	2.2	0.0250	0.0316	0.0078	0.0144	0.1296	0.5520	5	1
	CA3	2.42	0	0.0372	-	0.0154	-	0.2546	-	1	-
	A	3.12	1.9	-	0.0003	-	0.0002	0.0000	0.0061	6	3
	Others	2.6	3.59	-	-	-	-	-	-	-	-
	Mangrove	0.07	0	-	-	-	-	-	-	-	-
Forest cover	Bare soil	0.2	0.5	0.0007	-	0.0037	0.0000	0.0753	-	6	-
	Others	4.1	3.7	0.0159	0.0049	0.0039	0.0013	0.0800	0.0340	4	4
	Am	6.73	5.6	0.0970	0.0263	0.0144	0.0047	0.2974	0.1192	1	3
	AA	5.25	2.25	0.0587	0.0352	0.0112	0.0156	0.2308	0.3977	3	1
	H	7.65	2.24	0.0296	0.0053	0.0039	0.0024	0.0797	0.0602	5	5
	Ab2	24.06	7.8	0.2760	0.1193	0.0115	0.0153	0.2367	0.3889	2	2

Among the geomorphometric parameters, soil cover shows a higher impact on debris-flow initiation, according to the statistical analysis (Table 7). Cambisols (Ca2 and Ca3) are associated with a higher tendency to trigger

426 debris flows (Table 5), which can be related to the high boulder content that can facilitate rainfall infiltration
427 (Rossi and Pfeifer 1991). Soil samples 1 to 3 were collected in Ca3 type soil, showing bulk density that varies
428 from 1284 – 1755 kg m^{-3}, high sand content (50% to 80%, Sandy Loam/Loam) and high internal friction angle
429 (35º to 37º). The deeper the collection depth, the higher the stone content and bulk density (Table 3). Ferralsols
430 (LVa1 and LVa3) dominate in the study area, as is typical of humid tropical and subtropical regions, and do not
431 show a particularly strong tendency to trigger debris flows, which can be related to a more developed and stable
432 soil profile.
433 Slope angle is another significant morphometric factor that influences debris-flow initiation, due to the direct
434 influence on surface run-off, vegetation and soil cover, loose material accumulation and groundwater infiltration
435 (Lacerda 2007). Slope varies from 0 to 172 % in the catchments, with the range of 70 to 90% (35º to 40º) the most
436 prone to trigger debris flows at the study area, followed by the range of > 90% (> 40º). In general terms, the higher
437 the slope the greater the tendency to slope failure, although in very steep slopes (>40º) the accumulation of
438 mobilizable material might not be sufficient to initiate debris flows.
439 The SPI is another strong indicator of debris-flow triggering areas, as it influences the transport and erosion
440 potential of the river/stream (de Rosa et al. 2019). SPI can be used to characterize debris-flow initiation (Low
441 SPI), transport (High SPI) and deposition areas (Low SPI) (Chen et al. 2017), and, as we can see in our results
442 (Table 5), areas with a low SPI are more prone to debris-flow initiation due very low stream flow in the hillslopes.
443 Areas with a high SPI index (1.5 to 6) can also contribute to debris-flow development, which can be associated
444 with the erosion of lateral slopes as a result of stronger flow power. Moreover, the catchments in the region have
445 a moderate/high drainage density (Table 2), which suggests a fairly impermeable substratum that results in
446 overland flow that can acquire high erosive power – contributing, thus, to debris-flow entrainment.
447 The relationship of Topographic Wetness Index (TWI) with debris flows has been demonstrated by other studies
448 (e.g., Nikolova et al. 2020), with high TWI areas having the ability to collect more surface water, i.e., associated
449 to debris-flow deposition in flatter areas. In the study region, the lower the TWI the higher susceptibility to debris
450 flows initiation, since the main initiation areas are in steep portions at higher altitudes in the hillslopes.
451 Based on the LR model results, rainfall, soil, SPI and TWI are the most relevant parameters (Eq. 14) that should
452 be used in the prediction of debris flow in the region, due to a higher AUC (0.892, Table 6) in the output ROC
453 curve and high-significance of all the variables ($p < 0.05$) in the statistical evaluation of the model (Table 7). An
454 LR model with all the influencing factors produced a similar AUC (0.892) in the ROC analysis (Table 6), although

not all of the variables showed significance in the statistical evaluation (Table 7). For susceptibility studies in the region, therefore, we suggest the use of Equation14.

$$Z = 1.98 + 1.54\,TWI + 4.6SPI + 6.47Sl - 4.39So - 15.4P \quad (14)$$

Although with a weaker statistical significance in predicting debris-flow initiation in the study area, vegetation is the sixth most influencing factor and is associated with a strong control over the strength of the superficial soil layer, representing a slope-stabilizing factor since it can affect surface runoff and create obstacles for flow propagation (Liu et al. 2021). Am (Medium-height broadleaf vegetation), AA (Broadleaf and bush vegetation) and Ab2 (Broadleaf vegetation) are associated with a higher tendency to initiate debris-flow and are characterized by medium-height broadleaf vegetation, weakly (Ab2) to strongly (Am, AA) degraded by the pollution of the region (especially acid rain) (Mattos and Matsukuma 1990). The effect of pollution on vegetation may contribute to weakening their support of the soil, leading more easily to slope failures.

Table 6: Results of the ROC analysis of the validation tests of the LR models, according to the Area Under the Curve (AUC) of the ROC Curve.

Factors	1 factor model	2 factor model	3 factor model	4 factor model	5 factor model	6 factor model	7 factor model	8 factor model	9 factor model
Rainfall	**0.853**	-	-	-	-	-	-	-	-
Lithology	0.755	0.768	0.863	0.859	0.876	0.882	**0.882**	-	-
Slope	0.595	0.853	**0.879**	-	-	-	-	-	-
Relief	0.641	0.752	0.837	0.84	0.882	0.879	0.869	0.879	**0.892**
Soil	0.709	**0.876**	-	-	-	-	-	-	-
Vegetation	0.598	0.859	0.863	0.866	0.873	**0.886**	-	-	-
TWI	0.605	0.853	0.878	0.876	**0.892**	-	-	-	-
SPI	0.503	0.846	0.876	**0.889**	-	-	-	-	-
Slope aspect	0.536	0.683	0.866	0.856	0.882	0.885	0.881	**0.886**	-

Lithology is intrinsically associated with the soil type and vegetation of a region, especially in areas with well-developed regolith such as Serra do Mar. Even though a more explicit relationship between lithology and debris-flow initiation is not observed in our analysis, Proterozoic stromatic migmatites (PSeMc), occurring at higher elevations in the catchments, are more prone to debris-flow initiation, accompanied by the other migmatites types (AcMn, AcMp, AcMg) and granitoid rocks (PSEOY) (Table 5). Schists (PSpX) and Phyllites (PSpF) show a lower tendency, which can be related to a more developed and stable regolith, as a result of a weaker strength to weathering.

Slope aspect and relief are the two least relevant factors to debris-flow initiation among the selected influencing parameters (Table 6). In the study region, the slope direction most prone to debris-flow initiation varied according to the event, with the eastern and northeastern slopes associated with a higher tendency to initiate debris flows in

the 1985 event, and in the 1994 event the northern and northwestern slopes. This is directly related to the rainfall direction of these events: eastern-northeastern in 1985 and western-northwestern in 1994.

The relative relief can control the type of vegetation in the hillslopes, as well as influence both SPI and TWI. In study region, however, relief did not play a prominent role in debris-flow initiation, with the 600 – 700 elevation range showing a higher tendency to trigger slope failures that can lead to debris flows. This elevation range is associated with stromatitic migmatites (PSeMc) and the 70 – 90% slope range, which shows a stronger influence on debris-flow initiation.

Table 7: Statistical validation of the LR models, showing the regression coefficients (B) and relevant statistical parameters.

	Factor	B	Standard Error	Wald test	Degrees of Freedom	P-value
9-Factor model	Rainfall	-27.758	10.622	6.829	1	0.009
	Soil	-1.117	4.652	0.058	1	0.081
	Basin slope	14.851	9.501	2.443	1	0.011
	SPI	0.214	6.068	0.001	1	0.097
	TWI	2.332	3.667	0.404	1	0.053
	Forest	-17.270	8.846	3.811	1	0.051
	Geology	-3.434	4.994	0.473	1	0.049
	Slope aspect	3.249	8.618	0.142	1	0.071
	Elevation	-6.832	10.188	0.450	1	0.050
	Constant (B_0)	7.282	3.630	4.025	1	0.045
5-factor model	Rainfall	-15.379	6.195	6.163	1	0.013
	Soil	-4.39	3.596	1.491	1	0.022
	Basin slope	6.468	6.962	0.863	1	0.035
	SPI	4.594	4.332	1.125	1	0.029
	TWI	1.537	2.783	0.305	1	0.048
	Constant (B_0)	1.978	1.679	1.388	1	0.024

Furthermore, applying the LR model to assess the areas with a high susceptibility to debris-flow initiation at the study site, catchments 20, 19, 17, 16, 15, 14, 12, 10, 9 and 7 are those most susceptible overall (Fig. 5). The northeastern portion of catchment 1 also shows a high percentage of highly susceptible areas (Fig. 5), which can be related to steeper slopes and the more widespread occurrence of Cambisols in the headwaters' region. The statistical results of the debris-flow susceptibility assessment are available as Supplementary Information.

4.2 Debris-flow simulation

Based on the LR susceptibility analysis, catchments 20, 19, 17, 16, 15, 14, 12, 10, 9, 7 and 1 are simulated using RAMMS. The model was calibrated based on the debris-flow event of 1985 in catchments 14, 12, 10, 9, 8, 7 and 1, while catchments 14, 15, 16, 17 and 19 were calibrated based on the 1994 event. Catchment 20 was not modeled as no debris flow was recorded both in 1985 and 1994. The initiation areas were determined according to the landslide inventories, and a bulk density of 1,900 kg m^{-3} was assumed for the source areas and the entrainment

zone, according to past debris flow studies in bedrock channels (Takahashi 2006), as well as based on our geotechnical sampling and tests (Table 3).

The volume of the landslides that initiated the debris flows in each catchment is shown in Table 5. Considering the whole study area, the magnitude of the 1985 landslide event is estimated at ca. 540,900 m^3, while the magnitude of the 1994 landslide event is estimated at ca. 227,000 m^3. The magnitude of the debris flows (i.e., volume of sediments mobilized) at each catchment is estimated based on magnitude equations from Marchi et al. (2019), as suggested by Cabral et al. (2021) for catchments at Serra do Mar (Table 8).

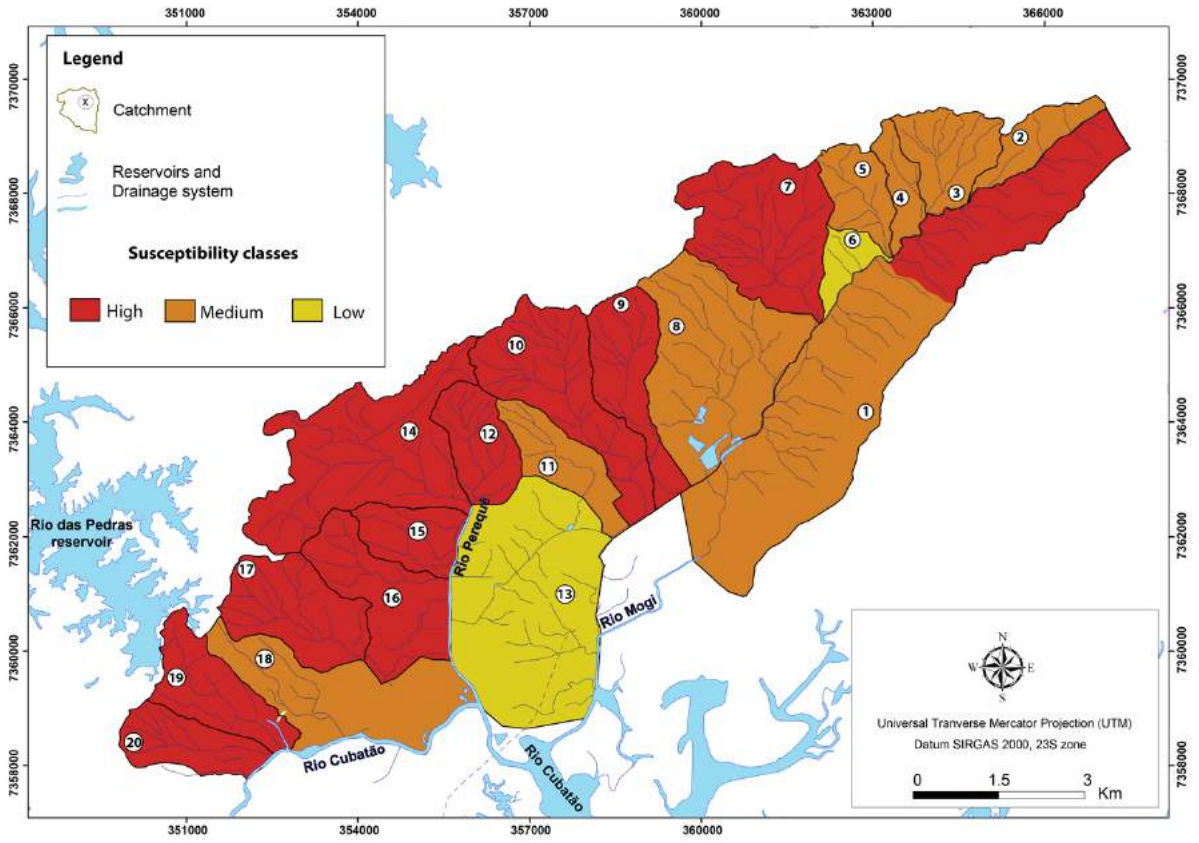

Figure 5. Map showing the overall susceptibility to debris-flow initiation of the 20 catchments at the study area, based on the LR model.

Figure 6 shows the calibration results based on the coverage index (Ω), which aided the identification of the best-matched simulations (Fig. 7 and 8), based on the comparison of the runout distances observed and those modeled by RAMMS. One of the parameters subjected to most uncertainties during modeling is erosion depth, as no comprehensive information for any of the modeled catchments was available. In our simulations, we adopted for all the catchments two maximum erosional depths: 3 m at upper and intermediate reaches, and 0.5 at lower reaches of the catchments. A 3 m erosion depth was reported by Kanji et al. (2007) in catchment 17 (1994), which we extrapolated for all the other catchments in the study region.

Another limitation was the lack of available information about catchments 19, 14, 12, 7 and 1, since no deposition pattern could be interpreted from aerial photographs. Even though we performed calibrations in these catchments in the same manner as the others, the best matched parameters adopted were those of with μ equal to the channel slope of the downstream portion of the catchment and ξ was assumed to be similar to the general trend of the area ($\xi = 200$ m s^{-2}). The lack of depositional fan at these catchments, and at most of the catchments in the study region, is related to the debouchment into the rivers Mogi, Perequê and Cubatão, which receive most of the sediments of the 20 studied catchments, as reported by Tatizana et al. (1987) and Kanji et al. (2007).

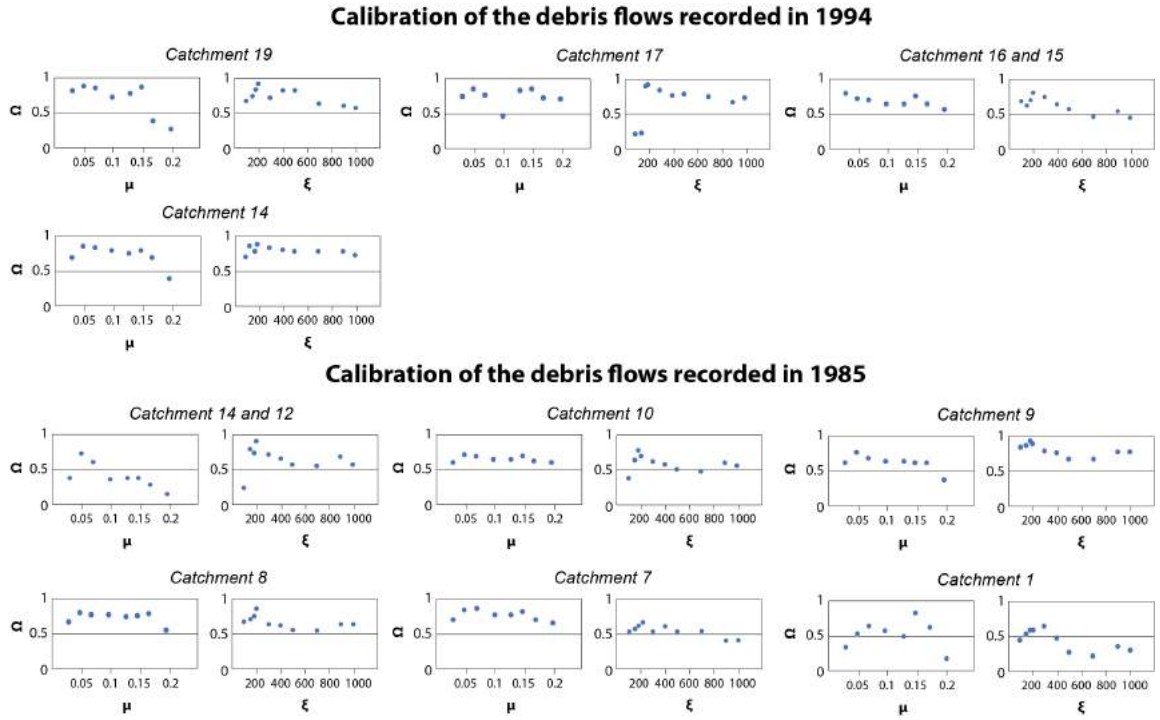

Figure 6: Calibration using the coverage index (Ω) of the debris-flow simulations for the selected catchments at the study area. The closer the coverage index is to 1, the more representative the simulation.

Table 8 RAMMS-2D results and characteristics of the debris flows. Est. = estimated, Max. = maximum.

Catchment	Year of the event	Initiation volume (m^3)	Est. Magnitude (m^3)	Runout	Flow parameters					
					μ	ξ (m s^{-2})	Max. Flow height	Max. erosion depth	Max. velocity	Max. Impact pressure
1	1985	68,422.3*	2.5 x 10^4	N/A*	0.1	300	3.2 m	0.88 m	30.96 m s^{-1}	1917.55 kPa
7	1985	131,737.6	2.5 x 10^5	N/A*	0.05	200	8.6 m	3.67 m	23.62 m s^{-1}	1115.38 kPa
8	1985	33,976.8	1.1 x 10^5	480 m	0.05	200	5.5 m	1.3 m	24.25 m s^{-1}	1175.73 kPa
9	1985	25,740.7	1.3 x 10^5	270 m	0.05	180	4 m	0.74 m	14.04 m s^{-1}	354.74 kPa
10	1985	78,865.6	2 x 10^5	700 m	0.05	180	4.7 m	1.74 m	14.25 m s^{-1}	406.1 kPa
12,14	1985	85,409.3	2.4 x 10^5	N/A*	0.05	200	5.4 m	1.59 m	30.87 m s^{-1}	346.35 kPa
14	1994	82,632.1	2 x 10^5	N/A*	0.05	200	5.6 m	1.8 m	32.93 m s^{-1}	550.87 kPa
15, 16	1994	10,150.7	0.8 x 10^5	510 m	0.03	200	4.7 m	2.11 m	16.75 m s^{-1}	561.26 kPa
17	1994	43,702.46	1.7 x 10^5	400 m	0.05	200	5.3 m	2.84 m	12.48 m s^{-1}	296.13 kPa
19	1994	17,673.8	0.8 x 10^5	N/A*	0.05	200	2.9 m	1.45 m	30.98 m s^{-1}	1919.98 kPa

* Direct discharge in the drainage system of the region. Indirect effects of debris flows include floods and silting.

Moreover, even though the debris flows at the study area exhibit a very high content of stony debris, most of the larger boulders (>1 m) are interpreted to deposit along the debris flow route and are not carried for long distances. Most of the damage in the downstream areas of the catchments is due to the smaller boulders (< 1 m), fine sediments and woody debris. These interpretations are supported by witnesses of the 1985 and 1994 events and the field campaigns that were conducted in the study area, where voluminous boulder deposits in areas with gentler slopes at upper/intermediate reaches of channel were observed (Fig. 4D). Moreover, the geomorphic characteristics of the studied catchments are similar to others at Serra do Mar, where comprehensive characterizations of recent debris flows have been made (e.g., Cabral et al. 2021).

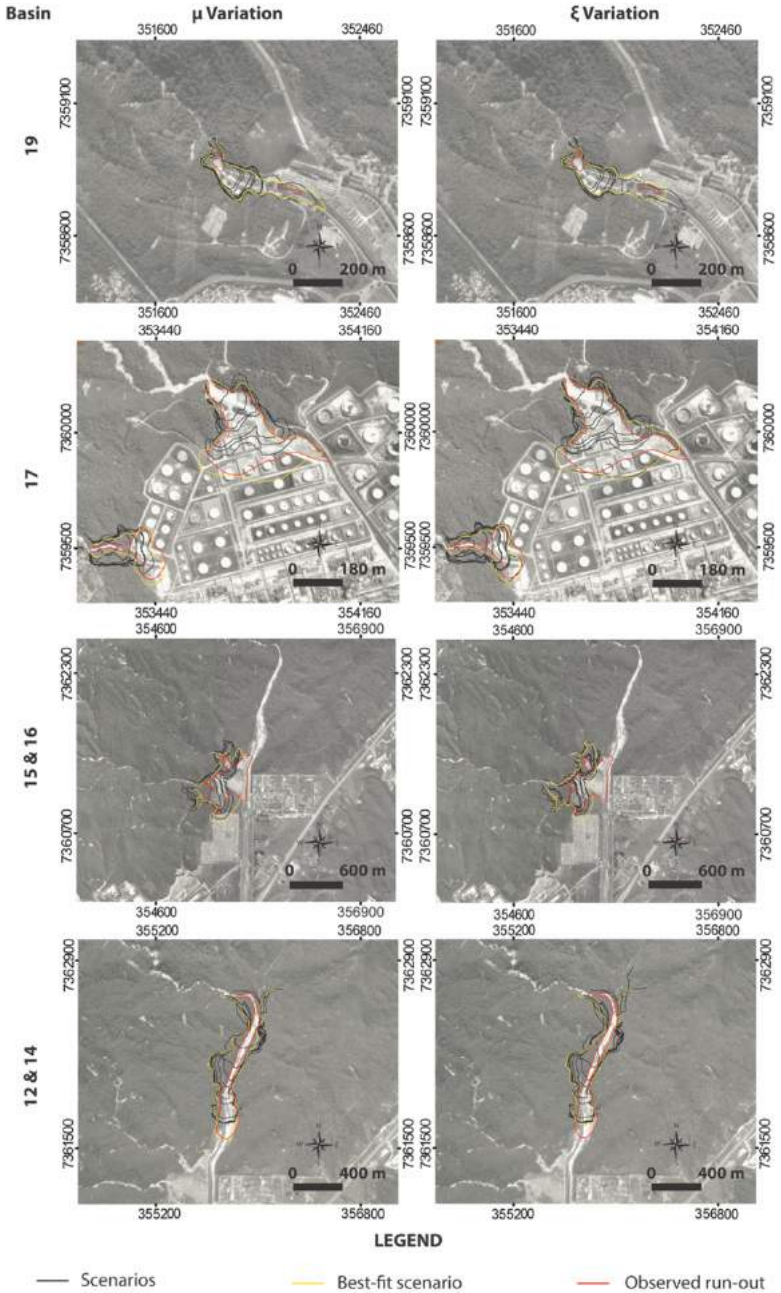

Figure 7: Comparison between modeled and observed run-out distance of the 1994 debris-flow event for the selected catchments.

The average runout distance, according to the simulations, is ca. 470 m, with the largest distance observed in catchment 10 (700 m) and the shortest in catchment 9 (270 m). Maximum flow heights (Fig. 9 and 10) are observed in catchment 7 (8.6 m, 1985) and in catchment 14 (5.6 m, 1994), where initiation volume is higher. Overall, flow height in the studied catchments averages 5 m. The average peak velocity of the debris flows is 23.1 m s^{-1}, with the highest velocities observed in catchment 14 (30.87 m s^{-1}) and catchment 1 (30.96 m s^{-1}). Maximum impact pressures are observed in catchments where steep knickpoints are observed (catchments 19, 1, 7 and 8).

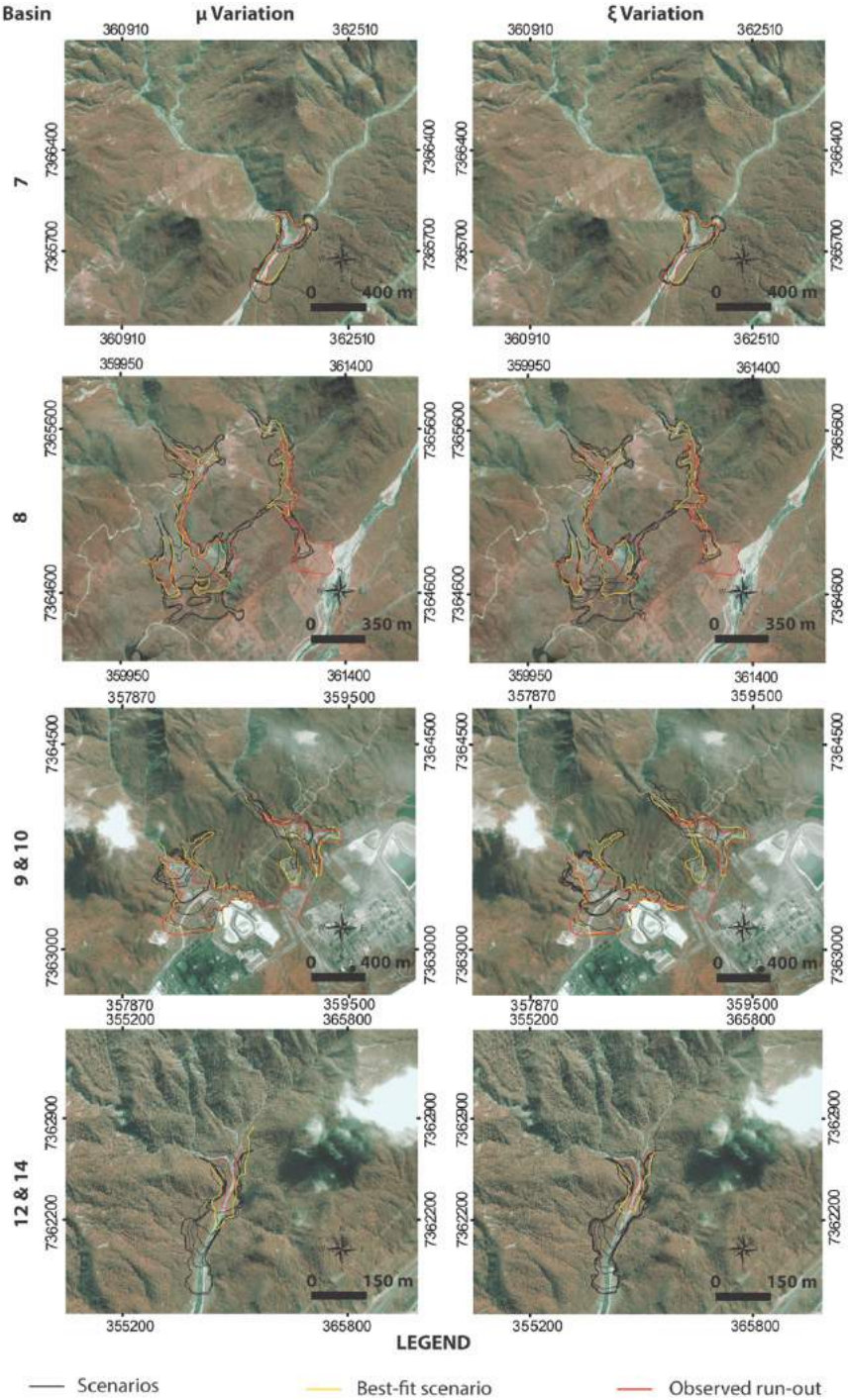

Figure 8: Comparison between modeled and observed run-out distances of the 1985 debris-flow event for the selected catchments.

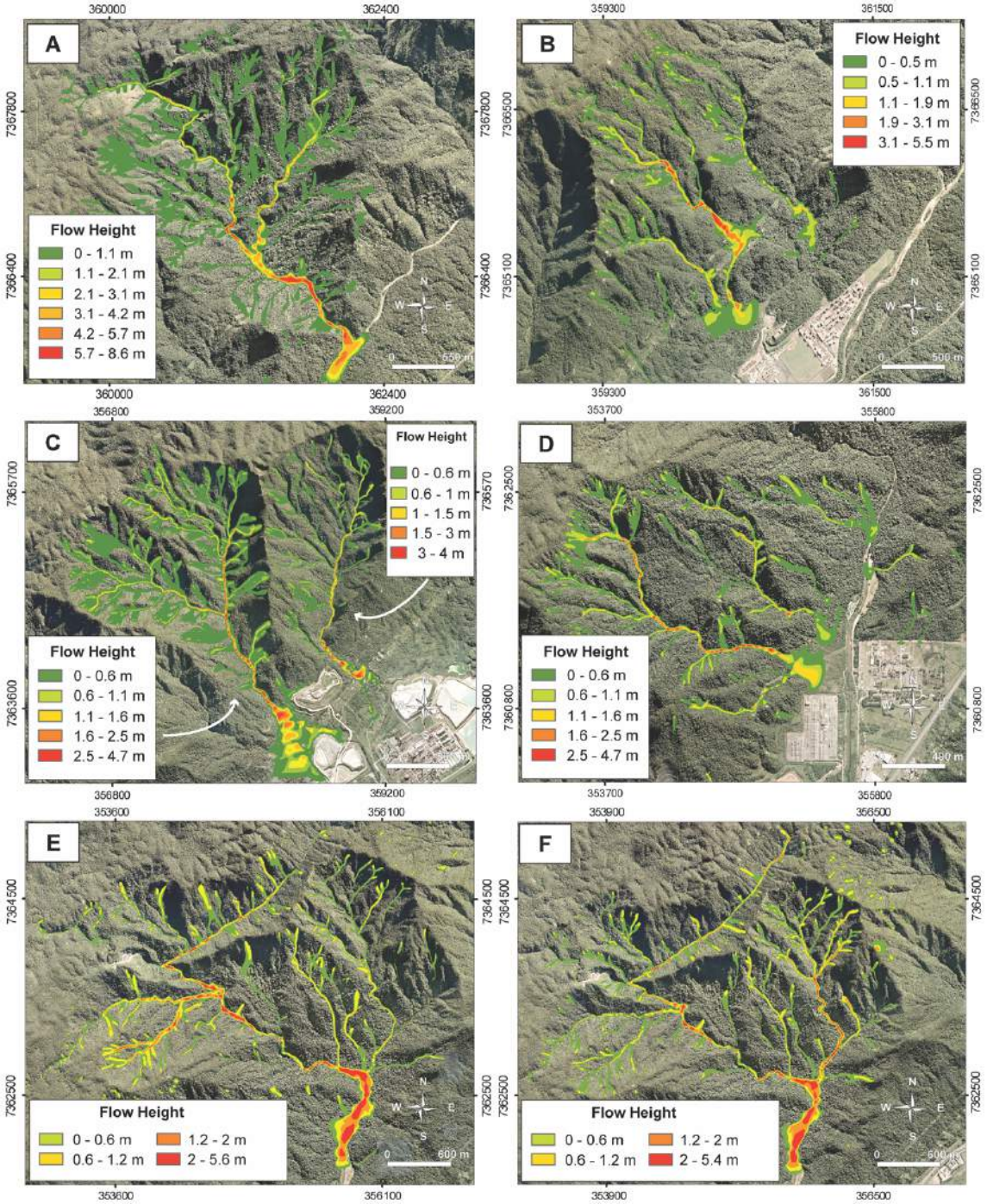

Figure 9: RAMMS modeling results showing maximum flow height. A) Catchment 7 (1985). B) Catchment 8 (1985). C) Catchments 9 and 10 (1985). D) Catchment 15 and 16 (1994). E) Catchment 14 (1994). F) Catchments 14 and 12 (1985).

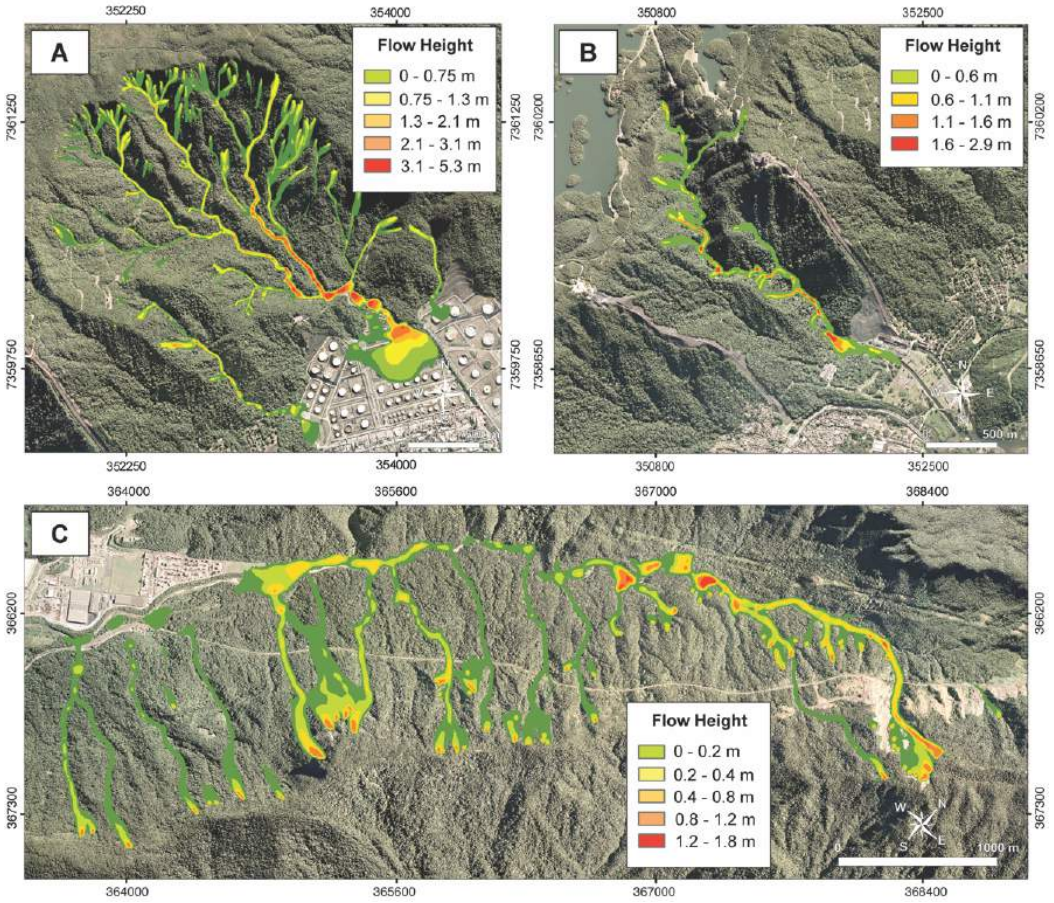

Figure 10: RAMMS modeling results showing maximum flow height. A) Catchment 17 (1994). B) Catchment 19 (1994). C) Catchment 1 (1985).

4.3 Rainfall analysis

The rainfall patterns that have historically triggered debris flows in the study area show that the phenomena are mainly initiated by high-intensity, short-duration rainfall, as also highlighted by other studies in the region (e.g., Tatizana et al. 1987; Kanji et al., 2007), with the rainfall accumulated 48 h prior to an event suggested as the most critical by our analysis (Fig. 11). Such pattern of short-duration/ high-intensity precipitation is also observed in other parts of the world (e.g, Taiwan, Chang et al. 2011; Japan, Fukuoka 1980; New Zealand, Selby 1976).

The short return periods (<10 years) of the rainfall events that have initiated debris flows (Table 4), including the very large ones from 1985 and 1994, indicates that large events (>10^5 m^3) can potentially occur every decade in the study site. However, as table 4 highlights, the number of debris-flow events has been declining in Cubatão in the past two decades (2000 – 2020) when compared to the previous ones (1980 – 2000), including in magnitude and, consequently, damage. Studies in the region have suggested that the environmental recuperation of the region during the 1990s has helped to stabilize the vegetation of the hillslopes (e.g., Massad 2002), which may assist in the stabilization of the soil and lead to fewer occurrences of slope failures and debris flows. However, such an

effect is challenging to determine, especially considering that, in our statistical analysis, vegetation cover does not play a very strong effect on debris flow initiation at the study area.

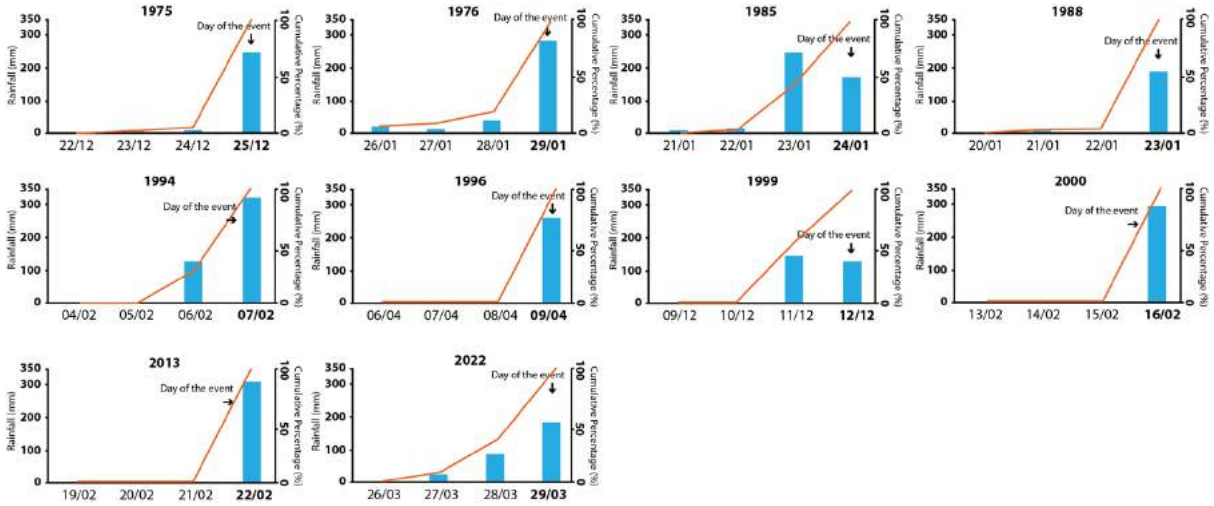

Figure 11: Daily rainfall indices up to 4 days (96 hours) prior to debris-flow events in the study region (blue bars). The phenomenon's initiation is more strongly influenced by the rainfall accumulated 48 hours prior to an event, as highlighted by the cumulative percentage graph (orange lines).

Due to this lack of recorded events in the last two decades, the rainfall thresholds established by Tatizana et al. (1987) are still relevant for the study region, even though it fails to classify the 1999 and 1976 events as debris flows. As pointed out by Segoni et al. (2018), rainfall thresholds should not be interpreted in an absolute manner, especially in complex and large areas. These two specific debris-flow cases were localized and triggered by landslides, falling above the localized landslide curve, highlighting how geomorphic characteristics also control the debris-flow development in a catchment.

The effect of the geomorphic aspects on debris flow development can also be observed when rainfall is correlated with the volume of the landslides that initiated the event and the estimated debris-flow magnitudes. Considering the effect of the 48-h accumulated rainfall on the volume of material mobilized in the slopes a positive Spearman correlation between rainfall and landslide magnitude is observed for both 1985 (0.62) and 1994 (0.81) events, highlighting the direct effect of rainfall over slope failure. However, when the effect of rainfall on debris-flow magnitude is considered, such relationship is weaker, showing a low positive Spearman correlation index both for the 1985 event (0.3) and for the 1994 event (0.51). These results can potentially indicate the strong influence of entrainment on debris-flow magnitude in the study region. The graphs with the correlation analysis are available as Supplementary Information.

Even though the region is covered by at least 13 rain gauges, the lack of hourly rainfall data for events before 2013 is a shortcoming that challenges an accurate analysis and correlations. Hourly data is available only for restricted locations, mostly in the oil refinery region (Catchment 17). A suggested update in the rainfall thresholds

would be the adoption of 48-h accumulated rainfall instead of 96 h, as our analysis demonstrate. Moreover, in a possible implementation of an Early Warning Systems in the region, field information about the catchments should also be considered, due to the intense in-channel debris accumulation in virtually all of them, which can be remobilized in future events – even by localized landslide events if the rainfall is intense enough.

The main question raised from our analysis is why debris-flow events were more frequent during the 1980s and 1990s, and, since the year 2000, few isolated debris flows occurred, but not to such extent as the 1985 and 1994 events. Climate studies focused on the area of Cubatão have indicated that the broader region will experience more extreme conditions, with drier conditions in the dry season (winter) and wetter conditions in the rainy season (summer), with a projected increase of heavy rain events (Marengo et al. 2021). An increase in dry periods has already been starkly identified in the Brazilian southeast, due to the increased warming in the region since 1961 that led to the intense drought of 2014 (Nobre et al. 2016) and a more recent one in 2021.

4.4 Hazard zonation

As rainfall is identified as the most influencing factor in debris-flow initiation at the study area, a hazard zonation matrix is thus proposed based on rainfall accumulated in 48 h, as well as the depositional areas and flow behavior patterns modeled by RAMMS.

Five levels of hazard are interpreted: very high, high, medium, low, and very low (Table 9). Very high-hazard areas are those where the model simulated a > 1 m flow height and velocity of > 1 m s^{-1}, as also proposed by Hürlimann et al. (2006), and humans and infrastructures are directly affected. High hazard areas are those where the debris flow runout can reach up to 1 m in height and velocity of up to 1m s^{-1}, and infrastructures may be directly impacted. Medium hazard areas are those that are not directly impacted by the sediments transported in a debris flow, but can exhibit flooding or silting that may impact infrastructures. Areas with low hazards are those that can experience some kind of side impacts of the debris flows, such as floods, but are inhabited, or areas with retention structures installed, as is the case of catchment 19. Areas with very low hazard are those where no impacts of any sort are expected.

Based on the hazard level matrix and on the infrastructures at hazard in each catchment (Table 10), a hazard zonation map was created for the 20 catchments (Fig. 12). The map shows the zonation based on a rainfall of over > 200 mm in 48 h, which can be adapted to different hazard levels according to rainfall indices. Catchments 19, 16, 15, 11, 10 and 9 exhibit an overall higher hazard in the region (Table 10), due to a higher probability of debris-flow related damages to humans and infrastructures. Retention structures in such catchments could potentially decrease their hazard level.

Table 9: Hazard level matrix developed for the study area, based on different rainfall indices and the impacts on infrastructures and population.

			Rainfall index in 48 hours		
			> 200 mm	< 200 mm, > 150 mm	<150 mm, >100 mm
Severity	Direct impacts	flow height ≥ 1m; velocity ≥ 1 m s^{-1}	Very high	Very high	High
		flow height < 1m; velocity < 1 m s^{-1}	High	High	Medium
	Indirect impacts	floods or silting	Medium	Medium	Low
		Areas with retention structures installed; Remote areas	Medium	Low	Very low
	No impacts	-	Very low	Very low	Very low

Table 10: Infrastructures, both public and private, at hazard in each catchment and overall hazard level, for a 200 mm rainfall in 48 h.

Catchment	Elements at hazards	Overall Catchment Hazard level
1	Railways from the company MRS Logistica; Fertilizer company "Yara Cubatão", Container storage company "Rodopark"	Medium
2	-	Low
3	-	Low
4	-	Low
5	-	Low
6	-	Low
7	Container storage company "Depotce"	Medium
8	-	High
9	Fertilizer company "Mosaic Fertilizantes do Brasil"	High
10	Petrochemical company "Copebras"; industrial gas company "White Martins"	High
11	Chemical plant "Birla Carbon Brasil"	High
13	Petrochemical company "Braskem", Logistic company "Brado Logistica", Chemical industry "Hidromar", Carbocloro Oxypar Chemical Industries; Industrial gas company "Messer Gases", Three transportation companies	Low
12, 14, 15, 16	Electrical substation	High
17	Petrobras oil refinery	Medium/Low
18	Vila Light (Residential area with approximately 140 houses, 60 of which have residents), FAFEN (Oil refinery), Thermoelectric Plant "Euzébio Rocha"; Fertilizers company "Yara Brasil"	High
19	Hydropower plant "Henry Boden", with electrical subestations	High
20	Anchieta and Imigrantes Highway, Vila Fabril (residential area with more than 400 houses), oil pipelines	High

Areas that have not shown any history of debris-flow occurrence since 1975, such as catchment 20, were classified as high hazard areas in the context of >200 mm rainfall in 48 h, based on the LR susceptibility analysis. These catchments exhibit voluminous in-channel deposits of stony material (Fig. 3D), which contribute to increasing their potential hazard to residential areas and infrastructures that are located within their limits. The average runout distance with a 470 m radius was assumed as a very high hazard area, in catchments where no debris flows were recorded.

Catchment 17, which has an extensive history of debris flows, is classified as a medium/low hazard level, due mainly to the retention structures installed and the removal of in-channel debris deposits promoted after the 1996 debris flow.

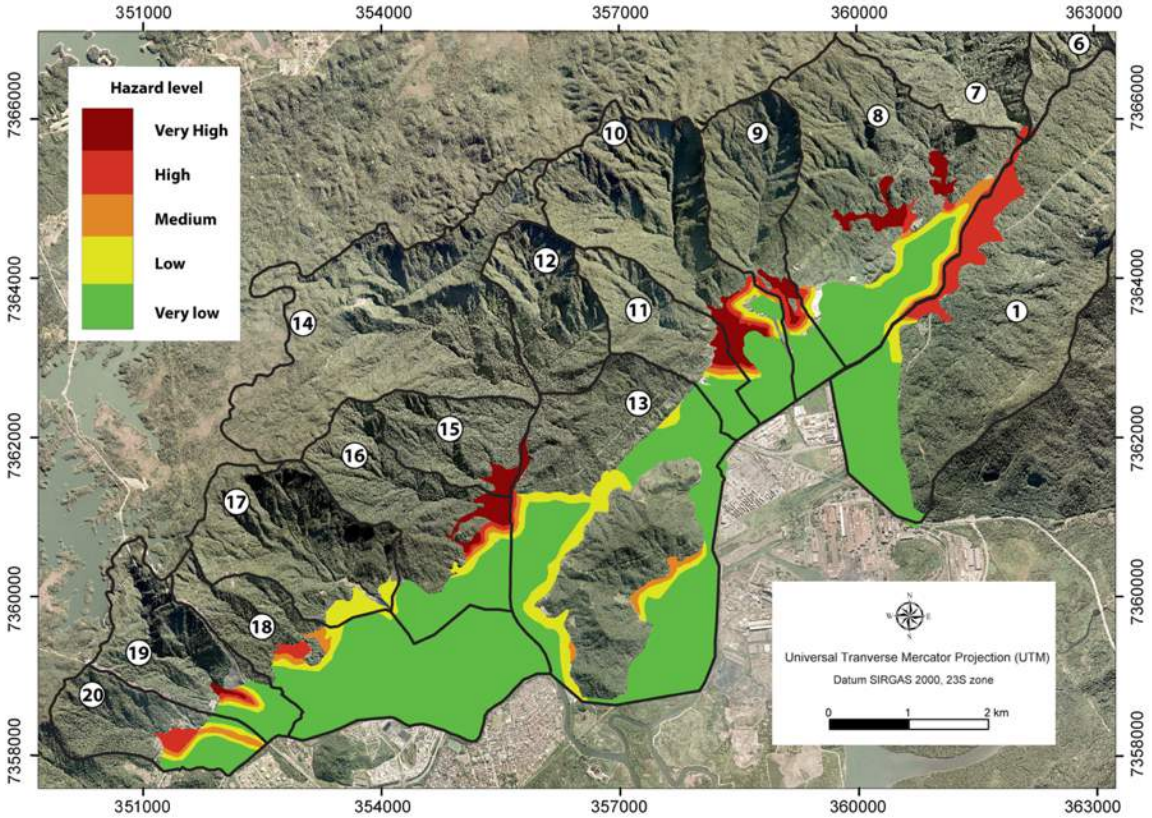

Figure 12: Debris-flow hazard zonation of the study area, based on the runout distances of the debris flows that occurred in the study simulated using RAMMS, on rainfall intensity (200 mm in 48 h), as well as on the elements at hazard.

As DeBortoli et al. (2017) point out, the mapping of vulnerability of the community is necessary in risk analyses, since it is critical to prevent and reduce the risk to which communities/industries are exposed. Such mapping, however, demands a more in-depth and multidisciplinary approach. Moreover, the expansion of the city towards mountain areas, especially by socially vulnerable communities, can increase the risk of new events, even those with smaller magnitudes.

The multi-step hazard assessment here proposed and applied in the hazard zonation of Cubatão joins other studies that aimed at creating new methodologies that can help to mitigate future landslide-related damage, such as the works of Cardinali et al. (2002), Hürliman et al. (2006; 2008), Wu et al. (2018), Huangfu et al. (2021), among many others. When assessing debris-flow hazard, especially in areas where the initiation factor is landslides, it is necessary to combine analysis of all the factors that can lead to the initiation of the phenomena (Steger et al. 2021), as well as aspects of their dynamics, represented mainly by the runout distance (Corominas et al. 2013; Frank et al. 2017). The transition from landslides to debris flows occurs especially during periods of heavy rainfall,

654 although, as demonstrated in our analysis and other studies (e.g., Takahashi 2001; Corominas et al. 2013; Hungr
655 1997), rainfall intensity is not always directly related to the magnitude of an event.
656 The combination, therefore, of different, data-driven methodologies is fundamental to ensuring the reliability of
657 the hazard evaluation, focusing on the different aspects related to a phenomenon. As pointed out by Wu et al.
658 (2018), LR is considered one of the most reliable methods in landslide susceptibility assessment, identifying the
659 main characteristics that influence the phenomenon in a particular region. When combined with the state-of-the-
660 art, numerical model RAMMS, which provides concrete, physically-based results (Frank et al. 2017), the hazard
661 evaluation can reliably represent the potential impact of future debris-flow events in a region. Moreover, the
662 inclusion of rainfall analysis provides good indication of future events probability and the different associated
663 hazard levels.

664 **5 Conclusions**

665 Our study proposed a multi-step hazard assessment, applied in 20 river catchments located in the municipality of
666 Cubatão, Latin America's largest petrochemical site. The LR analysis highlighted that rainfall is the main
667 influencing factor on debris-flow initiation, and the back-analysis of rain events suggests that the precipitation
668 accumulated 48 h prior to an event plays a more significant role in debris-flow deflagration than the current 96-h
669 model proposed in the rainfall thresholds developed for the region. The numerical simulation in the most
670 susceptible catchments further showed the different flow behavior patterns and runout distances that supported
671 the creation of a hazard zonation matrix with five levels of hazard (very low to very high).
672 The rainfall thresholds established for landslides in the region are considered generally efficient in the
673 representation of the precipitation patterns that can lead to debris-flow initiation. A suggested update in the rainfall
674 thresholds would be the adoption of 48-h accumulated rainfall instead of 96 h, as our analysis demonstrates.
675 Moreover, in a possible implementation of an Early Warning Systems in the region, geomorphic information of
676 the catchments should also be considered, due to the voluminous in-channel debris deposits that occur in most
677 catchments, which can be remobilized by future debris-flow events.
678 Hazard zonation maps, in conjunction with vulnerability studies, can subsidize the creation of risk management
679 programs, establishing the guidelines that should be followed during emergency situations. Even though there is
680 an observed decrease in the number of recorded debris-flow events in the study area (from 6, between 1980-2000,
681 to 2, between 2001-2022), the projected increase in the frequency of extreme precipitation events due to climate
682 change in the Serra do Mar region can mean that, in the near future, large magnitude debris-flows events ($>10^5$

683 m^3) may occur in the study area. The region, therefore, should be prepared for the negative effects of this natural
684 hazard.

685 **Acknowledgments**

686 The authors would like to thank Prof. Masato Kobiyama, from the Universidade Federal do Rio Grande do Sul,
687 and Prof. Tiago Martins, from the Universidade Federal de São Paulo, for their comments during the development
688 of this research. The authors would also like to thank the Engineering Geology Editor Dr. Janusz Wasowski and
689 the two anonymous reviewers for their comments, which significantly contributed to improve the manuscript.

690 **Funding**

691 This study was financed in part by the Coordenação de Aperfeiçoamento de Pessoal de Nível Superior—Brasil
692 (CAPES —Finance Code 001) and the National Council for Scientific and Technological Development (CNPq
693 Brasil, 311962/2018-1)

694 **Conflicts of interests**

695 The authors declare no competing interests

696 **References**

697 Aaron JB, McDougall SD (2019) Rock avalanche mobility: the role of path material. Eng Geol 257: 105126.
698
699 Alvalá RS, Dias MA, Saito S, Stenner C, Franco C, Amadeu P. et al. (2019). Mapping characteristics of at-risk population to
700 disasters in the context of Brazilian early warning system. International Journal Of Disaster Risk Reduction 41: 101326. Doi:
701 10.1016/j.ijdrr.2019.101326
702
703 Ayalew L, Yamagishi H (2005) The application of GIS-based logistic regression for landslide susceptibility mapping in the
704 Kakuda-Yahiko Mountains, Central Japan. Geomorphology 65:15–31.
705
706 Bovis MJ, Jakob M (1999) The role of debris supply conditions in predicting debris flow activity. Earth Surf Process
707 Landforms 24:1039–1054.
708
709 Cabral VC, Reis FAGV, Mendoza CM, Oliveira A. (2022) Model-based assessment of shallow landslide susceptibility at a
710 petrochemical site in Brazil. Revista Brasileira de Geomorfologia 23(2): 1394-1419.
711
712 Cabral VC, Reis FAGV, D'Affonseca FM, Lucía A, Corrêa CV, Veloso V, Gramani MF et al. (2021) Characterization of a
713 landslide-triggered debris flow at a rainforest-covered mountain region in Brazil. Natural Hazards 108: 3021-3043. Doi:
714 10.1007/s11069-021-04811-9
715
716 Caine N (1980) The Rainfall Intensity: Duration Control of Shallow Landslides and Debris Flows. Geografiska Annaler 62:
717 23 – 27. Doi: 10.2307/520449
718
719 Cardinali M, Reichenbach P, Guzzetti F, Ardizzone F, Antonini G, Galli M, Cacciano M, Castellani M, Salvati P (2002) A
720 geomorphological approach to the estimation of landslide hazards and risks in Umbria, Central Italy. Nat Hazards Earth Syst
721 Sci 2: 57–72. Doi: 10.5194/nhess-2-57-2002
722
723 Cavalcanti IFA (2012) Large scale and synoptic features associated with extreme precipitation over South America: a review
724 and case studies for the first decade of the 21st century. Atmospheric Research 118: 27-40. Doi:
725 10.1016/j.atmosres.2012.06.012.
726
727 Chang C, Lin P, Tsai C (2011) Estimation of sediment volume of debris flow caused by extreme rainfall in Taiwan. Eng
728 Geol 123(1–2): 83 – 90.
729
730 Chen J, Li Y, Zhou W, Iqbal J, Cui ZJ (2016) Debris-flow susceptibility assessment model and its application in semi-arid
731 mountainous areas of the southeastern Tibetan plateau. Nat Hazards Rev 18(2): 05016005
732

Chen W, Xie X, Wang J, Pradhan B, Hong H, Bui DT, Duan Z, Ma J (2017) A comparative study of logistic model tree, random forest, and classification and regression tree models for spatial prediction of landslide susceptibility. Catena 151: 147–160.

Corominas J, van Westen C, Frattini P, Cascini L, Malet JP, Fotopoulou S, Catani F et al. (2014) Recommendations for the quantitative analysis of landslide risk. Bulletin of Engineering Geology and the Environment 73: 209 – 263. Doi: 0.1007/s10064-013-0538-8

Dias VC, Vieira BC, Gramani MF (2016) Parâmetros morfológicos e morfométricos como indicadores da magnitude das corridas de detritos na Serra do Mar Paulista. Confins 29. Doi: 10.4000/confins.11444

Das I, Sahoo S, van Westen C, Stein A, Hack R (2010) Landslide susceptibility assessment using logistic regression and its comparison with a rock mass classification system, along a road section in the northern Himalayas (India). Geomorphology 114:627–637

Debortoli NS, Camarinha PIM, Marengo JA et al (2017) An index of Brazil's vulnerability to expected increases in natural flash flooding and landslide disasters in the context of climate change. Nat Hazards 86:557–582. Doi: 10.1007/s11069-016-2705-2

De Rosa P, Fredduzzi A, Cencetti C (2019) Stream Power Determination in Gis: An Index to Evaluate the Most 'Sensitive'points of a River. Water 11(6): 1145. Doi: 10.3390/w11061145

Deng YC, Hwang JH, Lyu YD (2021) Developing Real-Time Nowcasting System for Regional Landslide Hazard Assessment under Extreme Rainfall Events. Water 13: 732. Doi: 10.3390/ w13050732

Dietrich W, Dunne T (1978) Sediment budget for a small catchment in mountainous terrain. Zeitschrift für Geomorphologie 29: 191-206.

Fawcett T (2016) An introduction to ROC analysis. Pattern Recognition Letters 27(8): 861–874. Doi: 10.1016/j.patrec.2005.10.010

Frank F, McArdell BW, Oggier N, Baer P, Christen M, Vieli A (2017) Debris-Flow Modeling at Meretschibach and Bondasca Catchments, Switzerland: Sensitivity Testing of Field-Data-Based Entrainment Model. Natural Hazards and Earth System Sciences 17(5): 801–15. Doi: 10.5194/nhess-17-801-2017.

Fukuoka M (1980) Landslides associated with rainfall. Geotechnical Engineering 11: 1–29.

Gabelini BM, Corrêa CV, Cerri RI, Reis FAGV, Zaine JE, Giordano LC (2019) Avaliação da suscetibilidade a escorregamento na Serra do Mar pela aplicação da compartimentação fisiográfica. Geologia USP. Série Científica 19(1): 193 – 211. Doi: 10.11606/issn.2316-9095.v19-138528

Galderisi A, Ceudech A, Pistucci M (2008) A method for Natech risk assessment as supporting tool for land use planning mitigation strategies. Nat Hazards 46: 221e241.

Gramani MF. Caracterização geológica-geotécnica das corridas de detritos ("*Debris Flows*") no Brasil e comparação com alguns casos internacionais. Dissertation, Universidade de São Paulo, 372 p.

Huangfu W, Wu W, Zhou X, Lin Z, Zhang G, Chen R, Song Y, Lang T, Qin Y, Ou P et al (2021) Landslide Geo-Hazard Risk Mapping Using Logistic Regression Modeling in Guixi, Jiangxi, China. Sustainability 13: 4830. Doi: 10.3390/su13094830

Hungr O, McDougall S (2009) Two numerical models for landslide dynamic analysis. Computers & Geosciences 35(5): 978-992. DOI: 10.1016/j.cageo.2007.12.003

Hussin HY, Quan Luna B, van Westen CJ, Christen M, Malet JP, van Asch T (2012) Parameterization of a Numerical 2-D Debris Flow Model with Entrainment: A Case Study of the Faucon Catchment, Southern French Alps. Natural Hazards and Earth System Sciences 1(10): 3075-90. https://doi.org/10.5194/nhess-12-3075-2012.

Hürlimann M, Copons R, Altimir J (2006) Detailed debris flow hazard assessment in Andorra: A multidisciplinary approach. Geomorphology *78*(3–4): 359–372. Doi: 10.1016/j.geomorph.2006.02.003

IPT (1986) Programa Serra do Mar – levantamentos básicos nas folhas de Santos e Riacho Grande, Estado de São Paulo. Publicação IPT nº 23.394(2), 120p.

Kahn ME (2005) The Death Toll from Natural Disasters: The Role of Income, Geography, and Institutions. The Review of Economics and Statistics 87(2): 271–284.

Kanji MA, Cruz PT, Massad F (2007) Debris flow affecting the Cubatão oil refinery, Brazil. Landslides 5(1): 71-82. Doi: 10.1007/s10346-007-0110-3

Kopecký M, Macek M, Wild J (2021). Topographic Wetness Index calculation guidelines based on measured soil moisture and plant species composition. Science Of The Total Environment 757: 143785. Doi: 10.1016/j.scitotenv.2020.143785

Lacerda WA (2007) Landslide Initiation in Saprolite and Colluvium in Southern Brazil: Field and Laboratory Observations. Geomorphology 87(3): 104–119. Doi: 10.1016/j.geomorph.2006.03.037.

Liu Q, Jian W, Nie W (2021) Rainstorm-Induced Landslides Early Warning System in Mountainous Cities Based on Groundwater Level Change Fast Prediction. Sustainable Cities and Society 69(2):102817. Doi: 10.1016/j.scs.2021.102817.

Marchi L, Brunetti M, Cavalli M, Crema S (2019) Debris-flow volumes in northeastern Italy: Relationship with drainage area and size probability. Earth Surf Process Landf 44(4): 933-943.

Marengo JA, Camarinha PI, Alves LM, Diniz F, Betts RA (2021) Extreme Rainfall and Hydro-Geo-Meteorological Disaster Risk in 1.5, 2.0, and 4.0°C Global Warming Scenarios: An Analysis for Brazil. *Frontiers in Climate* 3, no. 13 (2021-March-03 2021). https://doi.org/10.3389/fclim.2021.610433. https://www.frontiersin.org/article/10.3389/fclim.2021.610433.

Mattos IFA, Matsukuma CK (1990) Mapeamento evolutivo da vegetação da Serra do Mar-Cubatão-SP. In: 6º Congresso Florestal Brasileiro, 1990, Campos do Jordão. Florestas e meio ambiente: conservação e produção, patrimônio social 3: 330-342.

Melton MA (1958) Correlation Structures of Morphometric Properties of Drainage Systems and Their Controlling Agents. Journal of Geology 66: 442-460. Doi: http://dx.doi.org/10.1086/626527

Nikolova V, Kamburov A, Rizova R (2020) Morphometric Analysis of Debris Flows Basins in the Eastern Rhodopes (Bulgaria) Using Geospatial Technologies. Natural Hazards 105(1): 159-75. Doi: 10.1007/s11069-020-04301-4.

Nobre CA, Marengo JA, Seluchi ME, Cuartas LA, Alves LM (2016) Some Characteristics and Impacts of the Drought and Water Crisis in Southeastern Brazil during 2014 and 2015. Journal of Water Resource and Protection 8: 252-262. Doi: 10.4236/jwarp.2016.82022

Petley D (2012) Global Patterns of Loss of Life from Landslides. Geology 40(10): 927-30. Doi: 10.1130/g33217.1.

Quan Luna B, Blahut J, van Westen CJ, Sterlacchini S, van Asch TWJ, Akbas SO (2011) The application of numerical debris flow modelling for the generation of physical vulnerability curves. Nat Hazards Earth Syst Sci 11: 2047–2060. Doi: Doi: 10.5194/nhess-11-2047-2011

Rossi M (2017) Mapa pedológico do Estado de São Paulo: revisado e ampliado. São Paulo: Instituto Florestal 1: 118.

Rossi M, Pfeifer RM (1991) Pedologia do Parque Estadual da Serra do Mar. I. Levantamento de reconhecimento de solos. Revista do Instituto Florestal 3(1): 1–44.

Schraml K, Thomschitz B, McArdell BW, Graf C, Kaitna R (2015) Modeling Debris-Flow Runout Patterns on Two Alpine Fans with Different Dynamic Simulation Models. Natural Hazards and Earth System Sciences 15(7): 1483 – 1492. Doi: 10.5194/nhess-15-1483-2015.

Segoni S, Piciullo L, Gariano S (2018) A review of the recent literature on rainfall thresholds for landslide occurrence. Landslides 15(8): 1483-1501. Doi: 10.1007/s10346-018-0966-4

Selby MJ (1976) Slope erosion due to extreme rainfall: a case study from New Zealand. Geografiska Annaler 58A:131–138.

Shan Y, Chen S, Zhong Q (2020) Rapid Prediction of Landslide Dam Stability Using the Logistic Regression Method. *Landslides* 17(12): 2931 – 2956. Doi: https://doi.org/10.1007/s10346-020-01414-6.

Steger S, Mair V, Kofler C, Pittore M, Zebisch M, Schneiderbauer S (2021) Correlation Does Not Imply Geomorphic Causation in Data-Driven Landslide Susceptibility Modelling - Benefits of Exploring Landslide Data Collection Effects. Sci Total Environ 776: 145935. Doi: https://doi.org/10.1016/j.scitotenv.2021.145935.

Takahashi T (2006) Debris Flows: Mechanics, Prediction and Countermeasures. Taylor and Francis, Balkema, Leiden.

Tatizana C, Ogura AT, Cerri LE, Rocha MCM (1987) Análise de Correlação entre Chuvas e Escorregamentos - S. do Mar, Mun. Cubatão. .. Proc Braz Congr Eng Geol 2:225–236 Terzaghi K (1947) Memorandum concerning the slide area at the power plant. In from theory to practice in soil mechanics, 1967, 2nd edn. Wiley, New York, pp 410– 415

van Westen CJ, Castellanos E, Kuriakose SL (2008) Spatial Data for Landslide Susceptibility, Hazard, and Vulnerability Assessment: An Overview. Engineering Geology 102(3-4): 112 – 131. Doi: https://doi.org/10.1016/j.enggeo.2008.03.010.

Vieira BC, Fernandes NF, Filho OA (2010) Shallow landslide prediction in the Serra do Mar, São Paulo, Brazil. Nat Hazards Earth Syst Sci 10: 1829 – 1837. Doi: 10.5194/nhess-10-1829-2010, 2010.

Vieira BC, Gramani M (2015) Serra do Mar: The Most "Tormented" Relief in Brazil. In: Migon, P (Ed) World Geomorphological Landscapes. Springer, Berlin, pp. 285-297.

Yang Z, Wang L, Qiao J, Uchimura T, Wang L (2020)Application and Verification of a Multivariate Real-Time Early Warning Method for Rainfall-Induced Landslides: Implication for Evolution of Landslide-Generated Debris Flows. Landslide*s* 17(10): 2409 – 2419. Doi: https://doi.org/10.1007/s10346-020-01402-w.

Westra S, Fowler HJ, Evans JP, Alexander LV, Berg P, Johnson F, Kendon EJ, Lenderink G, Roberts NM (2014) Future Changes to the Intensity and Frequency of Short-Duration Extreme Rainfall. Reviews of Geophysics 52(3): 522 – 555. Doi: 10.1002/2014rg000464.

Wilford DJ, Sakals ME, Innes JL, Sidle RC, Bergerud WA (2004) Recognition of Debris Flow, Debris Flood and Flood Hazard through Watershed Morphometrics. Landslides 1(1): 61 – 66. https://doi.org/10.1007/s10346-003-0002-0.

Wolle CM, Carvalho CS. Taludes Naturais. In: FALCONI, F.F.; JUNIOR, A.N. (Org.) Solos do Litoral de São Paulo. ABMS, São Paulo: 1994, p. 180-203.

Wu S, Chen J, Zhou W, Iqbal J, Yao L (2018) A Modified Logit Model for Assessment and Validation of Debris-Flow Susceptibility. Bulletin of Engineering Geology and the Environment 78(6): 4421-38. Doi: https://doi.org/10.1007/s10064-018-1412-5.